

# **Silica fouling in coal seam gas water in reverse osmosis desalination**

By

Lyudmila (Lucy) Lunevich

Master of resource and environmental planning – Massey  
University – New Zealand

Master of sanitation engineering – Riga Technical University –  
Latvia

Bachelor of process engineering – Polytechnic Institute – Belarus

A thesis submitted to Victoria University, Melbourne – Australia  
for the degree of Doctor in Philosophy

The Institute for Sustainability and Innovation at Victoria  
University

Melbourne Australia

May 2015





## Abstract

Silica precipitation and silica scale formation on membrane surfaces in RO desalination present a significant operational challenge in water purification. Silica scale formation on the membrane surface leads to flux decline, RO system productivity lost, membrane degradation, and increased cost of chemicals. In spite of the apparent simplicity of silica's composition and scale formation on the membrane surface, fundamental questions and empirical knowledge persist about the formation, solubility and behaviour of silica species during the silica polymerisation, precipitation and scale formation.

The broad objective of the present study was to define conditions and factors affecting silica polymerisation and precipitation in coal seam gas (CSG) waters in Australia. The scope of the problem was narrowed to focus on dissolved silica species studied by  $^{29}\text{Si}$  NMR spectroscopy, removal of silica by coagulation as pre-treatment step for RO desalination and silica fouling patterns in RO desalination for a range of salinities in both synthetic and CSG waters to develop a conceptual model of silica precipitation and deposition on the membrane surface.

The CSG industry in Australia generates significant quantities of CSG water, especially during the first 3-5 years of reservoir development when the hydraulic pressure needs to be released to extract the gas from coal seam. To avoid high cost of brine treatment and residual disposal frequently requires high recovery RO desalination to treat CSG water to level acceptable for further re-use. Furthermore, CSG waters in Australia have all four critical parameters, which potentially lead to silica precipitation prior it reached the solubility limit. These parameters include medium to high salinity, medium silica concentrations, high alkalinity at pH9 and slightly elevated aluminium concentrations.

Practical field, theoretical and laboratory research works have been undertaken to study industry's concerns and bring fundamental and practical solutions to the problem. In this research the author developed a conceptual model of dissolved silica polymerisation, silica fouling and its implication for RO desalination. The key findings from this study include: (1) precipitated silica was not found on the membrane surface

in various synthetic, salinity waters in the absence of aluminium likely as a result of sodium ions serving as barrier preventing deposition of dissolved silica species and colloidal silica structures; (2) effect of sodium ions on dissolved silica species studied by  $^{29}\text{Si}$  NMR showed that sodium shield dissolved silica species and at the same time stimulate release of monomeric silicic acid as a result of close interaction between sodium ions and water shell; (3) effect of aluminium on dissolved silica species studied by  $^{29}\text{Si}$  NMR and coagulation by ACH coagulant in various salinity coal seam gas waters demonstrated a significant impact of aluminium on silica polymerisation path and structural changes within dissolved silica species. Based on the results of coagulation studies the new hypothesis proposed potential substitution of sodium ions by aluminium ions in the sodium binding layer created by sodium around silica in relatively high salinity waters ( $> 8\text{g/L}$ ). Overall it was found that the cumulative effect of sodium and aluminium ions on silica precipitation involves complex reactions. Sodium ions depress silica solubility at the same time preventing silica from deposition on the membrane surface. The majority of dissolved silica polymerised in the bulk solution and was discharged in the reject stream of the RO system. To conclude practical silica solubility or the solubility defined empirically is a key for prevention of silica polymerisation in RO desalination systems.

## Declaration

‘I, Lyudmila (Lucy) Lunevich, declare that the PhD thesis entitled **Silica fouling in coal seam gas water in reverse osmosis desalination** is no more than 100,000 words in length including quotes and exclusive of tables, figures, appendices, bibliography, references and footnotes. This thesis contains no material that has been submitted previously, in whole or in part, for the award of any other academic degree or diploma. Except where otherwise indicated, this thesis is my own work’.

Signature

Date 8<sup>th</sup> May 2015

## Acknowledgement

The contents of this volume are based on more than three and a half years of part-time and full-time research work. During this time the author has been a member of the team of PhD students at the Institute for Sustainability and Innovation, College of Engineering and Science, Victoria University, Melbourne. During the PhD research the author has also spent 10 months working for a major coal seam gas operator in Queensland, Australia. Experimental works such as water quality testing, analysis, pre-treatment studies were performed on coal seam gas fields and their respective laboratory. The majority of the experimental works were performed at Victoria University, Werribee Campus and  $^{29}\text{Si}$  NMR experimental works were performed at Victoria University, Footscray Campus.

The references listed in this volume are intended as references only. The list is not a complete literature review of the topics covered. Much more literature was reviewed during the course of research, especially in the first year of the PhD. This is in part due to the novelty of the material, and, in part, its breadth covering many fields.

The thesis covers three major studies:  $^{29}\text{Si}$  NMR dissolved silica species studies, removal of silica by coagulation before RO desalination and silica fouling (precipitation) in a RO bench-scale system after the water was pre-treated with coagulant and ultrafiltration. A range of salinity synthetic and CSG waters were studied. Dissolved silica species, which have particular impact on silica scale formation, were studied under impacts of sodium and aluminum ions and pH conditions by  $^{29}\text{Si}$  NMR spectroscopy.

The  $^{29}\text{Si}$  NMR study, outlined in chapter 4, reported in this volume cannot be considered comprehensive. The impact of other cations on dissolved silica species can be studied to identify silica precipitation processes involving dissolved silica species. The  $^{29}\text{Si}$  NMR silica species dilution method is only a beginning for what the author hopes will eventually evolve. The immediate purpose of this chapter is to stimulate interest in this approach to predicting interactions among chemical elements and the

shielding effect of different impurities on the silica species, in the hope that others can reach a stage where direct practical application is possible within the industries dealing with the dissolved silica species.

Professor Stephen Gray, head of the Institute for Sustainability and Innovation, has been responsible for arranging this study, providing the necessary financial support and approval for the author the freedom to work in different areas of this project. He has also provided laboratory space as well as initially suggesting that a study in the area of salinity impact of silica solubility be conducted thus resulting in the process leading to this thesis. Dr Peter Sanciolo significantly contributed to development of the initial method of silica fouling studies in RO system. Later this method was re-designed by the author.

The author wishes to sincerely thank Professor Stephen Gray and Doctor Peter Sanciolo for unconditional support and interest for these endeavors. Thank you for putting up with me and being so supportive of this research. Thanks are also extended to Professor Andrew Smallridge for the considerable time invested in  $^{29}\text{Si}$  NMR spectroscopy studies, for providing advice on the techniques, time and expertise. Thank you to Professor Raphael Semiat at the Technion, Israel Institute of Technology, Haifa for encouragement to research with Professor Stephen Gray at Victoria University.

The author would also like to acknowledge the assistance rendered from other institutions - the consultations on the chemistry of colloidal silica by Professor Thomas Healy (retired) at the University of Melbourne. Thanks to Professor Jeremy Joseph (retired) at the Royal Holloway University of London and my ex-colleague from URS Corporation Ltd, Melbourne, who kindly accepted to mentor me over this journey and for sharing a wealth of his research expertise generally and, in particular, in CSG water management and treatment.

The majority of the financial support for this study has been provided by the Commonwealth Government Fund for Research Training Scheme (RTS), while natural CSG waters were supplied by a number of CSG operators in Queensland, Australia.

My thanks also go to the following people that either share wealth of their academic expertise or industry experience, or helping to collect data on field and laboratory, organizing field trips in Queensland:

- Professor Johanna Rosier at the University of Sunshine Coast for encouragement and the motivation to work towards a PhD;
- Professor Ron Adams for his excellent lectures on research conceptualization, and sharing his academic experience during the PhD coursework;
- Dr Ludovic Dumeé at Deakin University for assistance with EDS electronic microscope membrane examination works, SEM training and considerable SEM works and for making himself available whenever it was required;
- Dr Nicholas Milne for sharing publications on silica chemistry, helping set up RO experimental system and sourcing parts and equipment;
- Dr Malene Cran for training with many experimental techniques at VU, providing technical support on the quality of seawater and brackish water membranes and for wise and timely advice;
- Mr Noel Dow for technical advice on experimental equipment, training, and providing assistance when needed;
- Dr Jianhua Zhang for helping to maintain RO equipment during the experimental works and for sharing his research experience;
- Mrs Catherine Enriquez for the administration support and for helping to follow the University procedures;
- Mr Peter Warda, Chief Engineer at Shell Global Solutions for reviewing technical publications and taking incredible interest in my PhD research;
- Dr Jeuron Van Dillewijn, Liquid Natural Gas Water Manager at Shell Global Solutions for providing access to CSG waters on fields, access to the comprehensive water quality database, the opportunity to perform pre-treatment of CSG water in the laboratory and for presenting it to Shell Global Engineering panel (Canada) for cross examination and review;
- Mrs Yvonna Driessens Principal Upstream Process Consultant at Shell Global Solutions, India for the review of CSG water studies, providing advice and recommendations during my work in Brisbane;

- Mr Nikolai Lunevich, my husband for support, patience, and relocation for 10 month to Brisbane while I was working there, without him I would not be able to fully focus on this interesting and life challenging project;
- My children Catherine and Eugene for their financial support, allowing me to focus on the research for a considerable period of time, for their interest in my experimental works, debate at home about the uniqueness of the silica science and its significant variety of industrial applications.

The author would like to thank you the administration staff at the Institute for Sustainability and Innovation, Victoria University, Werribee for working hard to ensure the research laboratory is safe and in good working condition, and for your professionalism. It is very much appreciated.

To the Creator, for providing for me with a life of fulfilment and so many wonderful opportunities to grow, discover, and learn from others.

## Conference and presentations

Lunevich, L., Sancio, P., Gray, S., Silica polymerisation and its effect on RO desalination, Institute for Sustainability and Innovation, Victoria University 3030, Melbourne, Australia, **International Membrane Science and Technology Conference 2012** (IMSTEC2013), Brisbane, November 24 - 28, Membrane Society of Australasia (MSA).

Lunevich, L., Milne, N., Sancio, P., Gray, S., Coal seams gas water environmental management practice in Australia, Victoria University 3000, Melbourne, Australia, **Student Conference Melbourne**, July 21 – 22, 2012.

Lunevich, L., Sancio, P., Smallridge, A., Gray, S., On the Silica Edge – Silica Polymerization, Institute for Sustainability and Innovation, Victoria University 3030, Melbourne, Australia, **International Membrane Science and Technology Conference 2013** (IMSTEC2013), Melbourne, November 25-29, Membrane Society of Australasia (MSA).

### Oral presentations

November 2012 Brisbane, Queensland – Australia – **International Membrane Science and Technology Conference**, talk on a Silica polymerisation and its effect on RO desalination, Institute for Sustainability and Innovation, Victoria University 3030, Melbourne, Australia, International Membrane Science and Technology Conference 2012 (IMSTEC2013), Brisbane, November 24 - 28, Membrane Society of Australasia (MSA).

July 2012 Melbourne, Victoria – Australia – **Victoria University Student Conference**, talk on RO desalination of coal seam gas water and brine concentrate, Victoria University, Melbourne.

May 2014 Melbourne, talk on Water and brine management strategy in coal seams gas water industry in Australia, Victoria University 3000, Melbourne, Australia, **Student Conference Melbourne**, July 21 – 22, 2012.

July 2015 Singapore – **2<sup>nd</sup> International Conference in Desalination using Membrane Technology**, talk on The Silica Edge – RO Desalination: Silica Fouling, Institute for Sustainability and Innovation, Victoria University 3030, Melbourne, Australia, Singapore, 26 – 29 July 2015, Desalination using Membrane Technology, (the abstract accepted for oral presentation).

## Table of Contents

Abstract.....	i
Declaration.....	iii
Acknowledgement.....	iv
Conference and presentations.....	viii
List of Tables.....	xv
List of Figures.....	xvi
List of common abbreviation.....	xxii
Chapter 1 Introduction.....	1
1.1 Background.....	1
1.2 Problem statement.....	3
1.3 Significance.....	4
1.4 Objectives.....	4
1.5 Approach.....	5
Chapter 2 Literature review.....	8
2.1 RO system.....	8
2.1.1 Overview.....	8
2.1.2 RO technology.....	8
2.1.3 RO process.....	10
2.2 Membrane fouling.....	11
2.2.1 Colloidal fouling.....	14
2.2.2 Organic fouling.....	16
2.2.3 Inorganic fouling and silica solubility.....	16
2.2.4 Concentration polarisation (CP).....	19
2.2.5 Chemical precipitation.....	21
2.2.6 Fouling models.....	21
2.3 Silica chemistry and its effect on RO desalination.....	24
2.3.1 Aqueous silica.....	24
2.3.2 Dissolved silica species.....	26
2.3.3 Colloidal silica.....	28
2.3.4 Silica polymerisation.....	29
2.3.5 Kinetics of silica polymerisation.....	32
2.3.6 Silica scale formation.....	34
2.3.7 Silica in salinity waters.....	35
2.3.8 Silica and aluminium precipitation.....	36

2.4 Coal seam gas water (CSG) in Australia .....	39
2.4.1 What is coal seam gas water .....	39
2.4.2 Physical and chemical properties .....	41
2.4.3 CSG water desalination .....	43
2.4.4 Silica removal by coagulation .....	47
2.5 Conclusion .....	49
2.6 Objectives .....	50
Chapter 3 Experimental method .....	51
3.1 Introduction .....	51
3.2 Experimental design .....	51
3.2.1 Bench-scale RO system .....	55
3.3 RO feed experimental solutions .....	61
3.3.1 Synthetic solutions .....	61
3.3.2 CSG waters .....	62
3.4 Analytical methods .....	65
3.4.1 Measurement of pH and conductivity .....	65
3.4.2 Inductive coupled plasma (ICP) spectrometry .....	66
3.4.2.1 Standard preparation .....	66
3.4.2.2 ICP calibration .....	66
3.4.2.3 Sample preparation .....	66
3.4.3 Silico-molybdate method .....	67
3.5 Coagulation experiments .....	68
3.5.1 Chemicals and reagents .....	68
3.5.2 Solution compositions .....	69
3.5.3 Apparatus and procedures .....	70
3.5.4 Coagulation process and salinity .....	74
3.6 Membrane examination .....	74
3.6.1 Scanning Electron Microscopy (SEM) .....	75
3.6.2 Energy Dispersive Spectroscopy (EDS) .....	75
3.7 <sup>29</sup> Si Nuclear Magnetic Resonance ( <sup>29</sup> Si NMR) .....	76
3.7.1 Experimental design .....	77
3.7.2 <sup>29</sup> Si NMR acquisition parameters .....	79
3.7.3 <sup>29</sup> Si NMR samples .....	79
3.7.4 <sup>29</sup> Si NMR equipment and sampling tubes .....	79
3.7.5 Sodium silicate environment .....	80
3.7.6 Limitations .....	81

Chapter 4 <sup>29</sup> Si NMR study of dissolved silica species .....	83
4.1 Introduction .....	83
4.1.1 Concentration polarisation (CP) .....	84
4.1.2 Sample preparation .....	86
4.2 <sup>29</sup> Si NMR baseline solution .....	87
4.3 Effect of dilution with H <sub>2</sub> O .....	88
4.4 Effect of sodium .....	91
4.4.1 Quantitative composition.....	92
4.5 Effect of aluminium.....	98
4.5.1 Quantitative composition.....	98
4.6 Effect of pHs.....	102
4.6.1 High pH (9 – 11.5).....	102
4.6.2 Low pH (2 – 3) .....	104
4.6.3 pH (5 – 8).....	107
4.7 Discussion.....	107
4.8 Conclusion.....	112
Chapter 5 Silica removal by coagulation.....	114
5.1 Introduction .....	114
5.1.1 Objectives of experiment.....	114
5.1.2 Rational for salinity investigation .....	115
5.2 Results of jar tests.....	117
5.2.1 Coagulants and best doses .....	117
5.2.1.1 Turbidity removal (groundwater) .....	117
5.2.1.2 Effect of pH on turbidity removal .....	120
5.2.2 DOC removal (groundwater).....	121
5.2.2.1 Effect of pH on DOC removal.....	123
5.2.3 Metals removal (groundwater) .....	124
5.2.4 Silica removal (groundwater) .....	125
5.2.5 Turbidity removal (storage dam water) .....	128
5.2.6 Silica removal (storage dam water) .....	130
5.2.7 Aluminium residual .....	132
5.2.8 Effect of salinity .....	133
5.2.8.1 Experimental.....	133
5.2.8.2 Effect of sodium .....	133
5.3 Discussion.....	137
5.4 Conclusion.....	143

Chapter 6 RO silica fouling .....	145
6.1 Introduction .....	145
6.1.1 Experimental.....	145
6.2 Data analysis.....	145
6.2.1 Types of silica fouling .....	145
6.2.2 Normalised flux .....	147
6.3 Results .....	149
6.3.1 Stable and maximum silica concentrations .....	149
6.3.2 Practical silica solubility.....	151
6.3.3 SiO <sub>2</sub> – HO <sub>2</sub> system .....	153
6.3.3.1 Silica precipitation at pH3, pH9 and pH11.....	153
6.3.3.2 Membrane surface examination .....	156
6.3.4 Synthetic water .....	157
6.3.4.1 RO residual silica concentration.....	157
6.3.4.2 Effect of salinity .....	160
6.3.4.3 Effect of pH .....	161
6.3.4.4 Membrane surface examination .....	164
6.3.5 CSG water .....	167
6.3.5.1 RO residual silica concentration.....	167
6.3.5.2 Effect of salinity .....	171
6.3.5.3 Effect of pH .....	173
6.3.5.4 Membrane surface examination .....	175
6.3.6 Effect of aluminium.....	176
6.3.6.1 Flux decline .....	176
6.3.6.2 Aluminium-silicate fouling .....	178
6.3.6.3 Membrane surface examination .....	180
6.4 Discussion.....	181
6.5 Conclusion.....	188
Chapter 7 Conclusion and future research.....	191
7.1 Summary.....	191
7.2 Conclusion.....	191
7.4 CSG water .....	195
7.5 Significance .....	197
7.5 Recommendation for future research .....	198
Reference.....	202
Appendix A – CSG water quality typical parameters .....	215



## List of Tables

Table 2.1	Silica solubility vs pH values.	24
Table 2.2	Silica solubility vs temperature.	24
Table 3.1	Experimental conditions for synthetic waters.	51
Table 3.2	Experimental conditions for CSG waters.	53
Table 3.3	RO operating parameters and maximum operation limits.	55
Table 3.4	Dow Filmtec SW30HRLE membrane characteristics.	57
Table 3.5	CSG water quality.	61
Table 3.6	Water quality analysis for composite samples.	67
Table 3.7	<sup>29</sup> Si NMR shift observed for the initial concentrated sodium silica solution and corresponding relative quantities of silicon in each Q <sup>n</sup> type surrounding.	74
Table 3.8	<sup>29</sup> Si NMR experimental solutions and pH conditions.	76
Table 3.9	<sup>29</sup> Si NMR acquisition parameters by a Bruker DPX300 Spectrometer.	77
Table 3.10	<sup>29</sup> Si chemical shifts, $\delta$ of silicate anions identified in sodium silicate solutions in accordance with (Stoberg, 1996).	80
Table 4.1	<sup>29</sup> Si NMR chemical shift observed for the mother sodium silicate solution (baseline sample).	86
Table 5.1	The measurement of the sludge height between the top of the sludge and the bottom of the breaker. (Measurements of floc size during coagulation of CSG water (2013) with 50 mg/L ACH at pH8.23).	117
Table 5.2	Summary of the coagulation by ACH, ferric chloride and aluminium sulphate for CSG water collected in 2014 (initial total silica =22.68 mg/L, initial dissolved silica = 11.88 mg/L).	126
Table 5.3	Summary of silica (as SiO <sub>2</sub> ) removal by coagulation using ACH, ferric chloride and aluminium sulphate for dam water at 200, 400 and 600mg/L doses at initial total silica concentration 25mg/L and dissolved silica 20mg/L.	130
Table 5.4	Residual aluminium recorded in raw CSG waters and in post-coagulated treated CSG waters at various coagulation doses by ACH and aluminium sulphate.	131
Table 6.1	Recovery rate vs concentration factors.	146
Table 6.2	Salinity vs normalised flux.	148
Table 6.3	RO feed compositions, flux and permeate recovery, stable and maximum residual silica solubilities.	152
Table 6.4	Summary of silica precipitations for synthetic waters.	158
Table 6.5	Summary of silica precipitations for CSG waters.	169
Table 6.6	Summary of silica precipitations in different salinity CSG waters.	173
Table 6.7	Maximum and stable residual silica concentration for different salinity waters at pH9 (20°C).	182

## List of Figures

Fig. 2.1	Representation of the resistant encountered by flow through a fouled membrane.	22
Fig. 2.2	Structure of two typical $\text{Si}_7\text{O}_{18}\text{H}_4\text{Na}_4$ molecules present in the initial concentrated sodium silicate mother solution.	26
Fig. 2.3	Silica species in equilibrium with amorphous silica, Diagram computed from equilibrium constants (25°C). The line surrounding the shaded area gives the maximum soluble silica. The mononuclear wall represents the lower concentration limit, below which multinuclear silica species are not stable. In the natural waters the dissolved silica is present as monomeric silicic acid.	27
Fig. 2.4	Dissolved silica species polymerisation ( $Q^0 < Q^1 < Q^2 < Q^3$ aggregation) path into amorphous silica structure (mechanism proposed by Iler (1976).	28
Fig. 2.5	CSG water and gas gathering network and water treatment infrastructure and gas compression station.	39
Fig. 2.6	Indicative CSG water and brine management infrastructure.	41
Fig. 2.7	Process flow diagram of CSG water treatment.	45
Fig. 3.1	RO system – experimental arrangement and main equipment used.	56
Fig. 3.2	RO experimental apparatus at the Victoria University, Melbourne.	58
Fig. 3.3	Synthetic waters with different salinity and silica concentrations outlined SW1 – TDS=6g/L, SW2-TDS=7.5g/L, SW3-TDS=12.5g/L, SW4=30g/L and SW5-TDS=60g/L.	60
Fig. 3.4	(a) CSG water sourced from the field, (b) – raw and filtered CSG waters via 0.45µm filter.	62
Fig. 3.5	Coagulation experimental equipment (Stuart Scientific): mixers.	68
Fig. 3.6	Coagulation of CSG water (2013) in the flocculator SW1 (Stuart Scientific) with ACH at doses of 0, 10, 20, 30, 40, and 50 mg/L after 15 minutes of experiment.	69
Fig. 3.7	Coagulation of CSG water (2013) in the flocculator SW1 (Stuart Scientific) with aluminium sulphate at doses of 0, 10, 20, 30, 40, and 50 mg/L after 10 minutes from the start of experiment.	69
Fig. 3.8	Coagulation of CSG water (2013) in the flocculator SW1 (Stuart Scientific) with aluminium sulphate at doses of 0, 10, 20, 30, 40, and 50 mg/L after 20 minutes from the starts of experiment.	70
Fig. 3.9	Coagulation of CSG water (2013) in the flocculator SW1 (Stuart Scientific) with aluminium sulphate at doses of 0, 10, 20, 30, 40, and 50 mg/L after 45 minutes from the starts of experiment.	70
Fig. 3.10	Coagulation of CSG water (2013) by 50 mg/L ACH, 500 mg/L ferric chloride and 45 mg/L ACH at pH 6.5 for silica and DOC removal after 45 minutes from the start of experiment.	71
Fig. 3.11	$^{29}\text{Si}$ NMR system includes Bruker DPX300 spectrometer and server and $^{29}\text{Si}$ NMR spectrum of a sodium silicate solution in D2O with Si/M molar ratio 1.7.	78
Fig. 4.1	Fully polymerised silicate anion $[\text{Si}_8\text{O}_{18}(\text{OH})_6]^{6-}$ adopted from	

	Smolin (1987). Coupling points (-OH groups) may link the silicate to RO membrane surfaces.	83
Fig. 4.2	<sup>29</sup> Si NMR spectrum of the initial concentrated sodium silicate solution (baseline sample) at Si/M molar ratio 1.7.	85
Fig. 4.3	Consolidated results of <sup>29</sup> Si NMR spectrum (Q <sup>0</sup> , Q <sup>1</sup> , Q <sup>2</sup> , Q <sup>3</sup> type surroundings) of the samples for the range of diluted silicate solutions with H <sub>2</sub> O (at Si/M molar ratio 1.7, 1.55, 1.41, 1.31, 1.21, 0.85, 0.68, 0.29, 0.14, 0.11).	87
Fig. 4.4	Consolidated results of <sup>29</sup> Si NMR spectrum (Q <sup>0</sup> , Q <sup>1</sup> , Q <sup>2</sup> , Q <sup>3</sup> type surroundings) for a range of diluted silicate solutions with NaCl (1000mg/L) (at Si/M molar ratio 1.7, 1.14, 0.85, 0.68, 0.43).	90
Fig. 4.5	(a) <sup>29</sup> Si NMR spectrum of sodium silicate diluted with H <sub>2</sub> O at Si/M molar ratio 1.14 (upper) and <sup>29</sup> Si NMR spectrum of sodium silicate diluted with NaCl (1000mg/L) at Si/M molar ratio 1.14 (lower), 4.5(b)- <sup>29</sup> Si NMR spectrum of sodium silicate diluted with H <sub>2</sub> O at Si/M molar ratio 0.85 (upper) and <sup>29</sup> Si NMR spectrum of sodium silicate diluted with NaCl (1000mg/L) at Si/M molar ratio 0.85(lower), 4.5 (c) - <sup>29</sup> Si NMR spectrum of sodium silicate diluted with H <sub>2</sub> O at Si/M molar ratio 0.67 (upper) and <sup>29</sup> Si NMR spectrum of sodium silicate diluted with NaCl (1000mg/L) at Si/M molar ratio 0.67(lower).	92
Fig. 4.6	<sup>29</sup> Si NMR spectrum of sodium silicate diluted with AlCl <sub>3</sub> (130mg/L) at Si/M molar ratio 0.85 (lower); <sup>29</sup> Si NMR spectrum of sodium silicate diluted with NaCl (1000mg/L) at Si/M molar ratio 0.85 (middle); <sup>29</sup> Si NMR spectrum of sodium silicate diluted with H <sub>2</sub> O at Si/M molar ratio 0.85 (upper).	93
Fig. 4.7	The experimental solutions after 24 hours of <sup>29</sup> Si NMR experiment: tubes “1” and “2” show the samples diluted with sodium chloride (at the 1.14 and 0.68 Si/M molar ratio respectively). Tube “3” is the sample diluted with deionised water at the 0.68Si/M molar ratio.	95
Fig. 4.8	Consolidated results of <sup>29</sup> Si NMR spectrum (Q <sup>0</sup> , Q <sup>1</sup> , Q <sup>2</sup> , Q <sup>3</sup> type surroundings) of the samples for the range of diluted silicate solutions with AlCl <sub>3</sub> (130mg/L) (at Si/M molar ratio 0.68, 0.85, 1.14, 1.41, 1.55, 1.61, 1.7).	97
Fig. 4.9	<sup>29</sup> Si NMR spectrum of baseline sample Si/M molar ratio 1.7 and of the sample diluted with AlCl <sub>3</sub> (130mg/L) at Si/M molar ratio 1.61.	98
Fig. 4.10	The experimental solutions after 48 hours of <sup>29</sup> Si NMR experiment: “1” is dilution with aluminium chloride at the 1.61 Si/M molar ratio and “2” is dilution with H <sub>2</sub> O at the 1.61Si/M molar ratio.	99
Fig. 4.11	<sup>29</sup> Si NMR spectrum of the sodium silica solution diluted with H <sub>2</sub> O at 0.5 Si/M molar ratio at adjusted pH9.	100
Fig. 4.12	<sup>29</sup> Si NMR spectrum of the sodium silica solution diluted with H <sub>2</sub> O at 0.5 Si/M molar ratio at adjusted pH10.	101
Fig. 4.13	<sup>29</sup> Si NMR spectrum of the sodium silica solution diluted with H <sub>2</sub> O at 0.5 Si/M molar ratio at adjusted pH2.	102
Fig. 4.14	<sup>29</sup> Si NMR spectrum of the sodium silica solution diluted with H <sub>2</sub> O	

	at 0.5 Si/M molar ratio at adjusted pH3.	103
Fig. 4.15	The experimental solution at pH3 at Si/M molar ratio 0.5, “1” is the solution at pH3 immediate after pH adjustment, and “2” is the solution after 24 hours of <sup>29</sup> Si NMR experiment, gel was observed at the bottom of sample 2.	104
Fig. 4.16	Gelling solutions during the preparation of sodium silica solution at pH5, pH7 and pH8.	105
Fig. 4.17	Dissolved silicate polymerisation in CP layer on the membrane surface in medium and high salinity waters without presence of aluminium.	106
Fig. 4.18	Polymerised silicate under effect of aluminium and final deposition on the RO membrane surface.	108
Fig. 5.1	Conceptual diagram of coagulation mechanism of silica (as SiO <sub>4</sub> ) removal using ACH (Al <sup>13+</sup> species) in low (0-8g/L), medium (12g/L) and high (30g/L) salinity waters.	114
Fig. 5.2	Turbidity removal from groundwater composite samples (CSG water 2013) following coagulation with different doses of ACH, Al <sub>2</sub> (SO <sub>4</sub> ) <sub>3</sub> and FeCl <sub>3</sub> pH =8.4 at initial turbidity 81.9NTU.	115
Fig. 5.3	Turbidity removal from the supernatant after sub-samples(groundwater composite) were treated with 35mg/L of ACH (as Al <sup>3+</sup> ), 50 mg/L of Al <sub>2</sub> (SO <sub>4</sub> ) <sub>3</sub> (as Al <sup>3+</sup> ) and 60 mg/L of FeCl <sub>3</sub> , ( as Fe <sup>3+</sup> ) respectively at initial turbidity 81.9 NTU.	119
Fig. 5.4	DOC removal from groundwater composite samples treated at different doses of ACH (as Al <sup>3+</sup> ) at pH6 and pH8.4, Al <sub>2</sub> (SO <sub>4</sub> ) <sub>3</sub> (as Al <sup>3+</sup> ) and FeCl <sub>3</sub> (as Fe <sup>3+</sup> ) at pH 8.4 for initial DOC=19mg/L.	123
Fig. 5.5	DOC removal from the supernatant after sub-samples(groundwater composite) were treated with 45mg/L of ACH, 50 mg/L of Al <sub>2</sub> (SO <sub>4</sub> ) <sub>3</sub> and 60 mg/L of FeCl <sub>3</sub> , respectively at initial DOC=19mg/L.	122
Fig. 5.6	Metals removal from the supernatant after sub-samples (groundwater composite 2013) were treated at various doses ACH.	123
Fig. 5.7	Dissolved silica removal from the supernatant (groundwater composite CSG water collected in 2013 initial dissolved silica = 16 mg/L) at different doses of ACH, FeCl <sub>3</sub> , Al <sub>2</sub> (SO <sub>4</sub> ) <sub>3</sub>	125
Fig. 5.8	Turbidity removal from dam water composite treated with different doses of ACH, Al <sub>2</sub> (SO <sub>4</sub> ) <sub>3</sub> and FeCl <sub>3</sub> .at initial turbidity 60mg/L.	127
Fig. 5.9	Total silica (as SiO <sub>2</sub> ) removal from storage dam water treated at different doses of ACH, Al <sub>2</sub> (SO <sub>4</sub> ) <sub>3</sub> or FeCl <sub>3</sub> . at initial total silica concentration 25mg/L.	129
Fig. 5.10	Total (TS) and dissolved (DS) silica removal by ACH, ferric chloride and alum at 45mg/L dose and for various salinity waters at initial total silica concentration 21mg/L and dissolved silica 16.8mg/L	133
Fig. 5.11	Sodium binding layer surrounding silica species and substitution of sodium ions from these binding layers by aluminium (Al <sup>13+</sup> species) in solutions with NaCl concentrations of < 8g/L.	135

Fig. 6.1	Four types of RO silica fouling in the initial range of salinity 12.5g/L (0.4mol/L) to 30g/L to final salinity 59.6g/L (1Mol/L) plotted against silica concentrations vs water recovery.	145
Fig. 6.2	Flux decline trends for low(6g/L), medium(12.5g/L) and high(30g/L) salinity waters vs water recovery at initial silica concentrations ( $\text{SiO}_2=70\text{mg/L}$ ) at pH9 condition. (Low salinity RO runs were 8 – 9.5hours, medium salinity RO runs were 14 – 18 hours, high salinity RO runs were 36 – 42 hours).	147
Fig. 6.3	Dissolved silica (as $\text{SiO}_2$ ) concentrations (RO residual silica concentrations in the recycled stream) vs water recovery - maximum and stable residual silica concentrations recorded in medium salinity ( $\text{NaCl}=12.5\text{g/L}$ ) synthetic waters with initial silica concentration 70mg/L at pH9.	149
Fig. 6.4	Stable residual silica (as $\text{SiO}_2$ ) concentrations at pH 8.5-9 (sodium chloride concentration for synthetic water 1 - $\text{NaCl}=59.6\text{g/L}$ , synthetic water 2 – $\text{NaCl}=29.5\text{g/L}$ , synthetic water 3 – $\text{NaCl}=17.5\text{g/L}$ ) and the Hamrouni et al (2001) silica solubility plotted against salt concentration.	151
Fig. 6.5	Dissolved silica concentration vs water recovery in deionised water for an initial silica concentration of 84mg/L at pH3, pH9 and pH11 (Figure 6.6).	153
Fig. 6.6	Flux decline trends vs water recovery in deionised water at an initial silica concentration 84mg/L at pH3, pH9 and pH11 (Figure 6.5).	154
Fig. 6.7	(a) Silica scale deposit on the RO membrane surface at initial concentration $\text{SiO}_2=84\text{mg/L}$ diluted in deionised water, pH9 and (b) EDS membrane surface elemental analysis.	155
Fig. 6.8	Silica fouling trends in synthetic water at pH3, pH9 and pH11 vs water recovery in low salinity feed ( $\text{NaCl}=6\text{g/L}$ ). Initial RO feed dissolved silica concentration = 50mg/L.	156
Fig. 6.9	Silica fouling trends in synthetic water at pH3, pH9 and pH11 vs water recovery in medium salinity feed ( $\text{NaCl}=12.5\text{g/L}$ ). Initial RO feed dissolved silica concentration = 50mg/L.	157
Fig. 6.10	Silica fouling trends in synthetic water at pH3, pH9 and pH11 vs water recovery in high salinity feed ( $\text{NaCl}=30\text{g/L}$ ). Initial RO feed dissolved silica concentration = 50mg/L.	157
Fig. 6.11	Effect of salinity on stable residual silica concentrations plotted against silica solubility by Hamrouni (2001) in synthetic waters at pH 8-9.	159
Fig. 6.12	Effect of salinity on maximum residual silica concentrations plotted against silica solubility by Hamrouni (2001) in synthetic waters at pH8-9.	160
Fig. 6.13	Stable residual silica concentrations for medium, high salinity synthetic waters at pH3 and silica solubility at pH3 (Gorrepati (2010)) vs salinity.	160
Fig. 6.14	Effect of pHs on stable residual silica concentrations in medium (12.5g/L) and high (30g/L) salinity synthetic waters.	162

Fig. 6.15	Effect of pH on maximum silica solubility in medium and high salinity synthetic waters.	162
Fig. 6.16	Membrane surface EDS examination (a) low salinity synthetic water SiO <sub>2</sub> =50mg/L at pH9, (b) medium salinity synthetic water SiO <sub>2</sub> =50mg/L at pH9, (c) high salinity synthetic water SiO <sub>2</sub> =50mg/L at RO feed at pH9, (d) EDS elemental analysis of the membrane surface (high salinity).	164
Fig. 6.17	(a), (b) SEM images of the RO membrane surface at 76% water recovery in medium salinity CSG water with an initial silica concentration (as SiO <sub>2</sub> ) of 50mg/L and aluminium concentration (as Al <sup>+3</sup> ) of 27.5mg/L at pH9 (c) SEM image of the RO membrane surface at different magnification and (d) EDS elemental mapping of the RO membrane surface.	166
Fig. 6.18	Silica fouling and turbidity results measured in the recycle stream in medium salinity (12.5g/L) CSG water, initial silica concentration SiO <sub>2</sub> =70mg/L at pH9 vs water recovery.	167
Fig. 6.19	Silica fouling and turbidity results measured in the recycled stream in medium salinity (12.5g/L) CSG water, initial silica concentration SiO <sub>2</sub> =50mg/L at pH3 vs water recovery.	167
Fig. 6.20	Silica fouling trends in CSG water at pH3, pH9 and pH11 vs water recovery in low salinity (NaCl=6g/L) RO feed and dissolved silica concentration 50mg/L.	168
Fig. 6.21	Silica fouling trends in CSG water at pH3, pH9 and pH11 vs water recovery in medium salinity (NaCl=12.5g/L) RO feed and dissolved silica concentration 50mg/L.	168
Fig. 6.22	Silica fouling trends in CSG water at pH3, pH9 and pH11 vs water recovery in high salinity (NaCl=30g/L) RO feed and dissolved silica concentration 50mg/L.	169
Fig. 6.23	Effect of salinity on stable residual silica concentrations in CSG waters.	170
Fig. 6.24	Effect of salinity on maximum residual silica concentration in CSG waters.	171
Fig. 6.25	Effect of pH on stable solubility in medium and high salinity CSG waters.	172
Fig. 6.26	Effect of pH on maximum solubility in low, medium and high salinity CSG waters	172
Fig. 6.27	Membrane surface of RO experiment with CSG water spiked with sodium chloride (30g/L) and silica (50mg/L) at pH9.2 - SEM (7000 x magnification) and EDS elemental analysis of the membrane surface.	174
Fig. 6.28	Flux decline and turbidity results at silica concentration SiO <sub>2</sub> =40mg/L, medium salinity (12.5g/L) CSG water and Al=27.7mg/L at pH9.	176
Fig. 6.29	Aluminosilicate scale deposition on the RO membrane surface at 55% water recovery in medium salinity CSG with an initial silica concentration (as SiO <sub>2</sub> ) of 80mg/L and aluminium concentration (as Al <sup>+3</sup> ) of 27.7mg/L at pH9. (Blue is silicate, Green is aluminosilicate).	177

Fig. 6.30	Aluminium-silicate fouling at silica concentration $\text{SiO}_2=40\text{mg/L}$ , $80\text{mg/L}$ and $120\text{mg/L}$ in medium salinity ( $12.5\text{g/L}$ ) CSG water and $\text{Al}=27.7\text{mg/L}$ at $\text{pH}9$ .	178
Fig. 6.31	Aluminium-silicate fouling at silica concentration $\text{SiO}_2=40\text{mg/L}$ , $80\text{mg/L}$ and $120\text{mg/L}$ in medium salinity ( $12.5\text{g/L}$ ) synthetic water and $\text{Al}=27.3\text{mg/L}$ at $\text{pH}9$ .	178
Fig. 6.32	SEM images and EDS elemental mapping of the RO membrane surface at $76\%$ water recovery in medium salinity CSG water with an initial silica concentration (as $\text{SiO}_2$ ) of $50\text{mg/L}$ and aluminium concentration (as $\text{Al}^{+3}$ ) of $27.5\text{mg/L}$ at $\text{pH}9$ .	180
Fig. 6.33	Maximum and stable residual silica concentrations at initial RO silica concentrations $50 - 70\text{mg/L}$ and silica solubility by Hamrouni (2001) vs salinity at $\text{pH}9$ .	186

## List of common abbreviation

American Water Work Association	AWWA
Derjaguim-Landau-Verwey-Overbeek	DLVO
Coal seam gas	CSG
Concentration polarisation	CP
Reverse osmosis	RO
Ultra-filtration	UF
Micro-filtration	MF
Mechanical vapour compressor (brine concentrator)	MVC
Brine concentrator (vertical or horizontal)	BC
Silicon-29 nuclear magnetic resonance	<sup>29</sup> Si NMR
Scanning Electron Microscopy	SEM
Energy Dispersive Spectroscopy	EDS
Electrical conductivity	EC
Inductively Coupled Plasma	ICP
Total dissolved solids	TDS
Dissolved organic carbon	DOC
Department of Environmental Resource Management	DERM
Environmental Protection Authority	EPA
Environmental Protection Act 1971	EPA 1971
Powder activated carbon	PAC
Multi-effect distillation	MED
Mechanical vapour compressor	MVC
Total organic carbon	TOC

Aluminium chlorohydrate	ACH
High	HDPE
Magic-angle-spinning	MAS
Tetramethylsilane	TMS
Second electrons	SE
Backscattered electrons	BE
Energy Dispersive X-ray	EDX

## Chapter 1 Introduction

### 1.1 Background

Silica removal processes are critical in desalination of coal seam gas (CSG) water by reverse osmosis (RO) technology as silica can deposit on the membrane surface of RO systems. As a result of silica deposition, the quantity and quality of portable water produced by RO system will be reduced. Deposition of silica also reduces the lifetime of RO membranes. The silica scaling compounds, (amorphous silica and/or metal silicates) can form in the bulk solution, leading to the formation of colloidal silica which can later foul the membrane during the filtration process. These scaling compounds can also form directly on the membrane from soluble silica species during filtration (Sanciolo and Gray 2014, Ning 2005). One of the main complicating elements is the effect of various cations and anions, and in particular aluminium ions, in the water on silica polymerisation and scale formation. The use of anti-scalants is seldom effective for silica scale mitigation as most anti-scalants target the crystallised deposition on the membrane surface and are not effective for amorphous silica deposition (Gabelich 2005, Semiat 2003). Adding a commercial antiscalants does not improve the ability to control for aluminium silicate fouling, and also can be a contributing factor in aluminium-based scalant formation.

Removal of colloidal silica from RO feedwater is typically accomplished by coagulation, assuming that the coagulation is optimised for no elevated concentrations of aluminium residual present in the RO feed (Healy 1994). The aluminium residual may interact with ambient silica within the membrane system to cause unexpected fouling with aluminium silicates.

Silica is one of the major foulants in desalination of CSG water in Australia. Its presence limits water recovery, increases the cost of pre-treatment, and increases the cost of chemicals. Silica present in CSG water is also a problem for brine treatment and residual recovery. Silica accumulated in the reject stream of RO can contaminate commercial products such as sodium chloride and sodium bicarbonate. CSG industry in

Australia produces million gallons of CSG water with medium to high silica concentrations. The management of CSG water is a key effective business operation for all CSG operators in Queensland. RO desalination is frequently necessary to manage the purified water in a sustainable manner.

To reduce fouling in RO membranes the feed water is pre-treated for removal of foulants. This removal process is almost always preceded by coagulation which is designed to destabilize the particles and change the particle size distribution. The degree of destabilization and the size distribution are the principal determinants of removal efficiency. Within coagulation, particle destabilization is typically accomplished through the addition of chemicals that change the surface chemistry and aid particle attachment. The particle size distribution is then changed by providing gentle mixing to keep particles in suspension and promote particle-particle collisions, or flocculation. Silica has “anomalous behaviour” mechanisms during coagulation, which has not been very well understood.

The removal of colloidal silica from the feedwater, however, does not prevent silica scale formation from the remaining soluble silica species, which may be present in relatively small quantities in the feedwater, but which can exceed the solubility limit of the silica-scaling compound(s) in the concentrate stream of the RO at high water recovery. The solubility limit of the scaling compounds is difficult to reliably predict as it depends on the combined effect of solution conditions such as pH, salinity and the presence of multivalent cations (Semiati 2001, Demakis 2006).

Over the past 20 years, increased understanding of both the mechanisms of membrane fouling and silica scale formation on the membrane surface that improve the membrane performance and economic life of the RO systems has been gained. For example, Semiati (1996), El-Manharawy (2001), and Yong (1993) developed practical tools to study silica scale formation on the membrane surface that accounts for pH, silica concentrations, and silica solubility in a particular water matrix. Analysis of different approaches to silica polymerisation and scale formation studies showed that silica fouling needs to be studied empirically, for each specific water matrix.

## 1.2 Problem statement

Desalination of CSG waters has become increasingly important because of their potential for beneficial use as a recycled water resource and for aquifer recharge. Desalination technologies, both thermal and non-thermal, require pre-treatment to prevent fouling and to enhance the proportion of water recovered. For source water of poor quality such as CSG water, pre-treatment processes can form a significant proportion of the water treatment plant. The selection of a suitable desalination technique depends primarily on a combination of influent salinity level and silica content, and the output water quality required.

Silica scale formation on the membrane surface during RO desalination has been problematic for CSG and some mining industries in Australia. Demand for reduction of concentrated RO waste stream (brine) and higher production of purified water puts even more pressure on the industry to investigate sustainable ways to increase productivity of RO systems. The silica fouling mechanism in the case of RO systems is not well understood due to silica solubility limit variations in different water matrices and pre-treatment applied to RO feed prior to RO processing. The threshold limits for silica deposition are rather uncertain, and the complex silica hydrolysis and condensation (polymerisation) processes are not well understood. Comparisons of predictions from currently available silica solubility data and experimental research and operation of RO treatment plants reveals that the current data are inadequate to explain silica precipitation for some waters with relatively low silica concentrations. Although mitigation of silica precipitation is attempted, most techniques are ineffective or lead to even higher silica scale formation on the RO membrane surface (Semiati 1996, 20012, 2003, Demakis 2003). Presently, there is no reliable way to predict silica scale formation.

This research work is a contribution to the effort of developing new design criteria for an environment-centred model of RO technology to achieve good environmental outcomes for humans and ecosystems.

### **1.3 Significance**

The role of RO technology in desalination of CSG water and other mining waters is changing dramatically. Tightened requirements for increased efficiency, high permeate recovery; reduction of energy consumption, reduction of chemicals for membrane cleaning, and reduction of unit cost of purified water have led to increased emphasis on silica scale mitigation.

Optimisation of the RO pre-treatment processes for prevention of RO silica fouling remains a key design consideration. Currently the pre-treatment processes for CSG water account for 70% of RO plant, because of the need for 92 – 94% water recovery. The pre-treatment process frequently consists of coagulation, clarification, filtration, microfiltration, ultra-filtration and ion-exchange for micro-particle removal and reduction of cations and anions acting as nucleation sites for further fouling. The pre-treatment process requires optimisation to reduce cost and at the same time improve water recovery by RO. Prevention of silica polymerisation and better understanding of silica polymerisation and silica scale formation can lead to development of an operational management strategy to prevent silica fouling. In light of these changes, an improved coagulation regime should result in improved design and operation not only of coagulation facilities but of these downstream processes. Improved understanding of silica polymerisation within the RO system will provide a potential optimisation of the current expensive pre-treatment process, and a significant reduction of chemicals used in the RO plants.

### **1.4 Objectives**

The broad objective of the present study follows from the comprehensive literature review and communication with the industry partners conducted over the course of this research and which is mainly summarised in chapter 2 of this thesis. The general objective was to define conditions affecting silica polymerisation in CSG waters in RO desalination. The specific objectives of the research were to:

- I. Develop a conceptual silica polymerisation model using  $^{29}\text{Si}$  NMR data and silica solubility results to explain silica polymerisation on RO membrane surfaces.
- II. Review potential silica removal efficiency of coagulation and the influence of salinity on silica removal by a range of coagulants;
- III. Identify CSG water components and coagulation residuals that influence silica solubility, and in particular lowering of silica solubility, using synthetic and field CSG waters;
- IV. Develop relationships between pH, silica concentration, and silica species present for the polymerisation of silica (silica scale formation).

## 1.5 Approach

The stated objectives were achieved by undertaking (I) studying dissolved silica species using  $^{29}\text{Si}$  NMR spectroscopy (described in chapter 4 of this research), (II) removal of total and dissolved silica by coagulation as the coagulation is a common pre-treatment used by coal seam gas industry to reduce silica content prior to RO process, and (III and IV) finally RO experiments were performed to study silica fouling trends in various salinity and pH conditions synthetic and CSG waters. Several coagulation experiments were performed in the laboratory environment investigating the effect of pH, coagulant type, coagulant dose and impact of salinity on the coagulation rate. The effect of different parameters on silica polymerisation and scale formation was studied by conducting bench scale RO experiments using synthetic simulated CSG waters with different compositions and field CSG waters as feedwaters. The extent of silica polymerisation was assessed by measuring the permeate flux and the soluble silica concentration as a function of water recovery in constant pressure RO experiments. The water composition variables investigated were pH, silica concentration, salinity, and cations (aluminium) present in the RO feed. This data was used to gain further insight into the chemistry of silica and its effect on RO desalination, the silica scale formation mechanism, the role of the water matrix in silica polymerisation, and our current understanding of a chemical model for RO physical-chemical separation. Specifically: silica solubility limits in high recovery RO filtration for a range of water matrix.

Furthermore, the silica polymerisation mechanism was studied by  $^{29}\text{Si}$  NMR spectroscopy for a range of silica concentrations. The objective of the  $^{29}\text{Si}$  NMR experimental work was to develop a method to study five dissolved silica species identified in sodium silicate solutions and then develop this method to investigate effect of pH, sodium chloride and aluminium concentrations on these dissolved silica species. The effects on these silica species were evaluated through the collection of  $^{29}\text{Si}$  NMR spectrum across the studied solutions and peak area of each silica species present. Concentration polarization leads to high local silica concentrations near the membrane surface to condensation of some silica species. The relative proportion of oligomeric silica decreases as the oligomers associated and form sol particles as a result of silica polymerization (formation of amorphous silica) on the membrane surface. For supersaturated conditions, the nucleation process will in principle be governed by interacting silanol groups that polymerise via Si-O-Si bonds (Iler 1976). Under these conditions, the probability of interactions between neighboring silanol groups to form Si-O-Si bonds is high, and therefore intramolecular nucleation is favored (Dietzel 1998). During silica precipitation the monomer group,  $[\text{SiO}_6]^{4-}$ , rapidly polymerise by random packing of  $[\text{SiO}_4]^{4-}$  units, which results in non-periodic structures and the formation of amorphous silica or silicate in the presence of different cations (Dietzel 1993). To date,  $^{29}\text{Si}$  NMR has not been used to investigate the impact of sodium and aluminum ions, and pH conditions on dissolved silica species and applied it to RO silica fouling mechanisms because it is problematic to obtain silicon spectra at the silica concentrations and pH values where RO fouling occurs (typically up to  $\sim 120$  ppm  $\text{SiO}_2$ , pH less than 9). To overcome this limitation, commercial sodium silicate solutions were used to identify trends what might be happening at lower concentrations described in details in chapter 4.

The remainder of this thesis is divided as follows: Chapter 2 contains general background regarding coal seam gas water properties, RO process models, and a review of pertinent literature related to the experimental portions of the research. Chapter 3 describes the experimental methods and analytical techniques. Chapter 4 presents the results obtained on dissolved silica species and the impact of sodium and aluminium ions on silica polymerisation. Chapter 5 reports the results of silica reduction by

coagulation and the impact of salinity on silica removal. Chapter 6 presents the results of silica fouling of RO system after the feed was pre-treated by coagulation and ultrafiltration. The coagulation pre-treatment applied to all CSG water samples and some synthetic waters. Chapter 7 concludes the key findings and discusses potential future research and development necessary to mitigate silica scale formation in high recovery RO systems and implication for industries.

## **Chapter 2 Literature review**

### **2.1 RO system**

#### **2.1.1 Overview**

As outlined in chapter 1, the aim of the present work is to prevent silica scale formation on RO membrane surfaces in desalination of CSG water. This study focuses on first reduction of silica in CSG water by coagulation prior to RO processing. Then silica fouling was studied in different water matrices to understand silica precipitation patterns. During multiple RO experiments various residual silica concentrations in the recycled stream were recorded to analyse silica solubility limits and the phenomena of silica precipitation to identify various pseudo - solubility residual concentrations. In parallel dissolved silica species were studied by  $^{29}\text{Si}$  NMR spectroscopy.

The literature review follows a general overview of RO desalination technology, reviews a number of physical – chemical models explaining super-saturation conditions on RO surface, then membrane fouling is discussed in greater detail followed by the chemistry of silica with emphasis on silica precipitation, dissolved silica species and silicate scale formation. The literature briefly discussed the properties of CSG water in Australia as silica precipitation has frequently occurred on the membrane surface.

#### **2.1.2 RO technology**

RO is considered the most cost effective technique for purification of medium (6 – 8g/L) and relatively high (20 – 30g/L) salinity waters compare to other desalination technologies (Cohen 2007, Sheikholeslami 2002). Along with a remarkable development of the technology, however, there is increasing concern over membrane fouling and silica scale deposition (Baoxia 2013, Brant 2012, Barger 1991). Membrane fouling significantly reduces productivity of the RO technology and increases the unit cost of purified water.

Increasing productivity of the RO desalination by increasing permeate recovery to 94 – 96% leads to reduced brine volume and provides higher overall efficiency for the

system. One of the main difficulties when operating at high recovery, however, is the greater possibility of colloidal fouling and silica scale formation as silica concentration is increased (Brant 2012, El-Manharawy 2000, Parekh 1988). While much research effort has been undertaken to gain a better understanding of silica scaling mechanisms, silica scaling remains a major unsolved problem facing membrane desalination (Sanciolo and Gray 2014, Semiat 2001, Rautenbach 1989). Operating near the silica solubility limit leads also to scaling (Coronell 2006, Demadis 2005). Besides fouling and scaling there are other causes of flux decline in membrane processes, including both membrane ageing and degradation of the membrane material (Brant 2012, Semiat 1996). Recent research suggests that the chemical and physical properties of the membrane materials may be the primary controlling parameters for membrane fouling in all membrane separations (Cob 2012, Wood 2011).

Following review of thermal desalination technology development, it is easy to see how RO science inherited many theories and some problems from thermal desalination models. One of those that came into RO science from thermal distillation is the Langelier model (El Manharawy and Hazaf 2003, 2002). This model is based on the thermally related behaviour of the pH and hardness of water, where the fouling of calcium carbonate is determined on the basis of its saturation value at ambient temperature, known as the Langelier Saturation Index (LSI). Accordingly, DuPont introduced an accurate model and monographs for the prediction of formation of other common scales (Ca, Mg, Ba, Sr and silica) based on their thermal specific solubility at high temperatures (El Manharawy and Hazaf 2003, 2002). A number of researchers are critical of this approach because this thermal model was established many years prior to the use of RO, and developed with respect to the concept of super-saturation of dissolved salts in heat exchangers at elevated temperature and with sufficient contact time. For instance El-Manharawy and Hazaf (2002) warn that in the application of the thermal model to RO science for prediction of scale formation in membrane separation many serious errors can occur. This is due to the basic differences between thermal desalination and RO desalination techniques, the latter being a high pressure driven process under normal temperature while thermal desalination uses heat exchange. Furthermore, most thermal systems (multi-effect distillation (MED), BC, boiler) are

designed to operate for 10 or 11 months per year to allow time for them to stop for seasonal maintenance, because of the scale accumulation on the internal walls, which increases proportional energy consumption in the system. Silica scale formation is a significant and complex problem in these thermal systems (Braun 2012, Demadis 2005, 2009), which seems has been inherited by modern RO technology.

The growing popularity of RO in many municipal and industrial applications significantly increased design throughputs, RO systems become environmentally unsustainable, especially in inland applications, mainly because of the need to discharge RO concentrate in relatively high volume (Malaeb 2010, Katarachi 2005). Cumulative impact on local ecosystems of an RO plant (assuming concentrate discharges to evaporation and crystallisation ponds) over its life cycle could be quite significant. Buhrs (1993) and Moroni (2004) characterise these environmental problems as highly complex (ie, they are ‘science intensive’), comprehensive (having ecological and economic dimensions). In such circumstances (characterised by a high degree of uncertainty and disagreement) it is difficult, if not impossible, to formulate ‘good’ environmental policy and good practice. Not surprisingly, perhaps, CSG water and brine management policies, in Queensland, have continued to be developed without adequate consideration being given to environmental implication (Steven 2013, Anderson 2010).

### **2.1.3 RO process**

RO is a physical-chemical separation process in which only water molecules pass through a semi-permeable membrane. Salt ions are rejected, i.e., they do not pass through the membrane. By applying pressure in excess of the osmotic pressure in RO, water (acting as a solvent) is forced from a region of high solute concentration through a membrane to a region of relatively lower solute concentration.

The osmotic pressure,  $P_{osm}$ , of a solution can be determined experimentally by measuring the concentration of dissolved salts in solution:

$$P_{osm} = 1.19 (T + 273) * \Sigma(mi) \quad (1)$$

where  $P_{\text{osm}}$  = osmotic pressure (in psi),  $T$  is the temperature ( $^{\circ}\text{C}$ ), and  $\Sigma(m_i)$  is the sum of the molar concentrations of all constituents in the solution. An approximation for  $P_{\text{osm}}$  may be obtained by assuming that 1,000 mg/L of total dissolved solids (TDS) yields about 10 psi (0.72 bar) of osmotic pressure.

It is believed that the mechanism of water and salt separation by RO is not fully understood (Cob 2012, Semiat 1996). The theory suggests that the chemical nature of the membrane is such that it will absorb and pass water preferentially to dissolved salts at the solid/liquid interface. This may arise from weak chemical bonding between the water and the membrane surface, or by dissolution of water within the membrane structure (Cohen 2006, Barger 1991). Either way, a salt concentration gradient is formed across the solid/liquid interface leading sometime to membrane fouling (Brant 2013, Cob 2012).

It has been said that various diagnostic models for membrane fouling have not yet proven successful to predict this phenomena (Semiat, 1997, Gill 1993). Uncertainties regarding membrane fouling arises from different pre-treatments processes, water matrix or water composition and permeate recovery targets in each RO system (Brant 2012, Cohen 2006, Barger 1991). Most research in this area comes from pilot plants and bench scale studies performed with various natural water qualities. Natural waters which serve as feeds to RO systems are obviously complex chemical systems consisting of many soluble constituents as well as suspended colloidal, chemical and biological species (Coronell 2006, Barger 1991). Some believe that geochemical modelling of the feedwater's chemical composition needs to be done to accurately predict the fouling potential (Demadis 2007, Rowe 1973). No model so far has been developed to explain silica fouling and silica scale deposition on the membrane surface. Nevertheless, a number of models were developed to explain some set of conditions which potentially could explain silica scale deposition.

## **2.2 Membrane fouling**

Membrane fouling is simple accumulation of deposits on membrane surfaces and within the porous membrane structure. Eyecapm (2003) has described this broad mechanism as

the following: “*fouling is a condition in which a membrane undergoes plugging or coating by some element in the stream being treated, in such a way its output or flux is reduced and in such a way the foulant is not in dynamic equilibrium with the stream being ultra-filtrated*”. According to Brant (2012) there are four different categories of membrane fouling, including (1) inorganic, (2) organic, (3) biological, and (4) colloidal fouling. Fouling occurs when rejected, dispersed or dissolved solids are not transported from the membrane surface back into the bulk solution. This accumulation of solid or dispersed layer on the membrane surface reduce the permeate flux through the membrane by providing an additional hydraulic resistance to mass transport. This solid or suspended layer can block membrane material, creates concentration polarisation (CP), provides a favourable environment for aggregation of varieties of colloidal matters, and eventually cake formation and growth as well as a gel layer on the membrane surface occurs (Brant 2012, Safari and Phipps 2005).

Substantial effort in current RO science has focused on investigating fouling mechanisms in order to mitigate the many negative consequences of fouling through careful membrane material selection, system design, and process operation. This improved understanding has resulted in dramatic improvements in membrane materials, new pre-treatment processes, modification of RO stages into more flexible arrangements, and improved selection of cleaning agents (ASTM 1989). Nevertheless, fouling may occur as a result of many factors, sometimes an unpredictable combination of RO feed and operating conditions (ASTM 1989). Fouling generally depends on the following most significant factors:

- Feed water quality and composition
- Salinity (TDS)
- Physical and chemical characteristics of the membranes and foulants
- Operation pressure
- Membrane process design and operation
- Membrane configuration.

Of these factors, the TDS of the water and other specific elements accelerating fouling (such as Ca, Mg, Ba, Sr, Al) and permeate recovery required are the most critical factors

(Brant 2012, Semiat 2003, Safari and Phipps 2005). Understandably, then more complex the source water, the more challenging RO desalination is likely to be. The chemistry and composition of colloidal structures of the feed water determine the fouling mechanism that will be expected. Therefore, there are numerous interaction pathways in complex solutions, such as CSG water, that influence each other. In particular particle size distribution, organic content, RO configuration, particle hydrophobicity and charge can influence the formation of complex membrane foulants. Currently there is no reliable physical chemical model which could predict the nature of membrane fouling (namely foulant-foulant interactions) (Cob 2012, Brant 2012).

It is believed that membrane fouling is a two-step process involving nucleation and growth (Cob 2012, Cohen 2007). As in crystallisation, it has been observed that an initial nucleation phase is followed by a growth phase. Nucleation was found to be a function of product water flux, particle size, and the number of nucleation sites (Brant, 2012, Ning 2010, Semiat 1996). The rate of growth was controlled by the product flux, the rates of metal and silica polymerization, and shear forces in the bulk flow. Regardless of the mechanism, growth only occurs close to the surface because of a number favourable factors present simultaneously, such as elevated concentrations of cations and anions due to CP. When fouling follows this nucleation-growth mechanism minor increases in cations and anions effect precipitation patterns. pH is a significant factor in the prediction of membrane fouling by metal hydroxides and silica that can be hydrolysed (Hafez 2002, Amjad 1992). These species have their lowest fouling potential at their respective isoelectric points (the pH where the species concerned is neutral) (Ning 2010, Bremere 2000). Colloidal particles at this point aggregate to form large, discrete and coagulated particles. Because they are discrete entities like precipitated salts, such particles settle according to Stoke's Law – i.e. the settling velocity is proportional to the diameter and density of the particles (Bremere 2000). Most coagulated particles are too large to nucleate successfully on the membrane surface. Instead, they collect on the surface but do not flocculate, and therefore, allow for good permeate flow because they are not closely packed (Brant 2012, Coronell 2006). Coagulated particles can be removed relatively easily by increasing the Reynolds number of the feedwater. If the pH is some distance from the isoelectric point, colloidal

metal hydroxide particles are generally stable with regard to aggregation. Stabilization of any colloidal particle results in its behaviour being controlled by its surface charge density (Coronell 2006). The stabilized particles remain small and independent as they are carried by the flow to the membrane surface and can easily nucleate at active sites there. Metal hydroxide particles are generally attached to the membrane surface by van der Waal's forces, the mechanical forces delivered by the water flux push them onto the membrane surface. After sufficient colloids have attached to the surface, growth via polymerization begins (Healy 1994). Once attached, the stable metal (or other hydrolyzable ion) colloidal particle can form many polymeric hydroxide bridges to other similar particles. Ultimately, a flocculated solid phase builds up with some of the particles attached to the membrane. These attached flocs cause serious loss of permeate flux and, effectively, permanent retention of the metal species on the membrane. As discussed above, a number of other physical and chemical factors such as system hydraulics, pressure, CP and colloidal silica present in the solution can affect membrane fouling.

### **2.2.1 Colloidal fouling**

Substantial research and modelling has also been carried out in relation to colloidal fouling by unreactive particles in ultrafiltration (Kleinstreuer and Belfort 1984). Colloids can include any type of materials or aggregate of different materials, including organics (fats, oils, carbohydrates, DOC) (Boerlage 2001, Chen 2006, Laborie 1997). Colloids are categorised according to their most prevalent parent material and particular type, including high silica concentrations (Chen 2006). The most common inorganic colloids in membrane process are composed of materials like silica, aluminium silicate clays, iron and aluminium (Yiantsios 2005). Some inorganic colloids, such as in the case of CSG water are already present in raw water. Colloids may form as the feed water passes through the treatment plant as a result of increased concentration, for instance silica concentrated in RO reject stream, or a result of chemical addition, complexation between dissolved ionic species and organic matter, and nucleation and growth of sparingly soluble salts (Brant 2012, Yiantsios 2005).

Silica is of primary concern for colloidal matter in natural CSG water in Australia (DERM 2010, Stevenson 2013). Silica is usually represented as  $(\text{SiO}_2)_n$ , to represent the different crystalline and amorphous forms in which this compound may exist (Ning and Troyer 2007). Colloidal silica results from the polymerisation of silica containing particles and as a result of elevated silica concentrations. In the presence of carbonic acid ( $\text{H}_2\text{CO}_3$ ), silica has two acid-base characters that affect the characteristics of the silica and its membrane interaction (Brant 2012). Some other factors that influence the solubility and form of silica in solution include pH, ionic strength, ionic composition, and temperature (Hamrouni and Dhahbi 2001).

The chemistry of silica dioxide was first described by Lomonosow in Russia in 1763 (Bergna 1994). The concept of the colloidal state as a highly dispersed state of a given phase in a dispersion medium was developed by Borshov in Russia in 1869. Mendeleev suggested in 1871 that the general colloidal state of a substance depends on the complexity of its composition and the size of the particle. This concept continues to be researched in current time by Legrand in France (Legrand 2010). After these major discoveries, large-scale, systematic research in colloidal chemistry began in the Soviet Union in the 1920s (Iler 1976). The mechanism of silica polymerisation, the dependence of adsorption and the energy of adsorbent surface and on the properties of the adsorbed substances (amorphous silica) were studied by Kiselev (Institute of Physical Chemistry, Academy of Sciences, Moscow) and colleagues (Bergna 1994). Kiselev made notable contributions to the study of amorphous silica and silicates, 600 monographs and textbooks written by him and colleagues. In the 1930s, studies of the condensation processes of silicic acids showed that hydroxyl (silanol) groups  $\text{Si-OH}$ , should be present on the surface of silicates and silicas. Nonetheless, as more new technologies are introduced and developed such as RO technology, more research is required on silica chemistry and silica solubility limits within specific environments and operations conditions. Sanciolo and Gray (2014), Semiat (1996), Brant(2012) and others point out that research is needed in this area as the form of silica determines the most appropriate technique for removing the foulant from the membrane system feed water.

### **2.2.2 Organic fouling**

Organic fouling seems to occur through a variety of mechanisms, including adsorption, attachment, pore blockage, and cake or gel layer formation. As discussed previously, organic fouling depends upon the characteristics of the organic matter (composition, size, hydrophobicity, and charge), the membrane characteristics, the water chemistry, and the hydrodynamics of the membrane system. Problem arises when the membrane surface adsorbs organic matter and the membrane surface is altered, normally becoming more attractive for other organic compounds, cations and anions to deposit. According to Darton and Fazel (2001) organic fouling occurs prior to any other type of fouling because NOM, organic macromolecules, organic colloids, biopolymers are always present in the RO feed in minor quantity depositing on the membrane surface. Organic fouling remains a significant problem for groundwater RO desalination plants including CSG water. Mallevalle (1989) and Brant (2012) highlight the ability of organics to interact with other materials to enhance membrane fouling adds to the complexity of this problem. Silica, and particularly colloidal silica, deposit easily on the surface of organic materials creating colloidal aggregates (Ning 2010). For instance, humic acid represents almost 50% of dissolved organic carbon in CSG water. Residual humic acid following coagulation can pass through clarification and microfiltration treatment and deposit on the RO membrane surface creating a favourable environment for silica deposition and other inorganic matter.

### **2.2.3 Inorganic fouling and silica solubility**

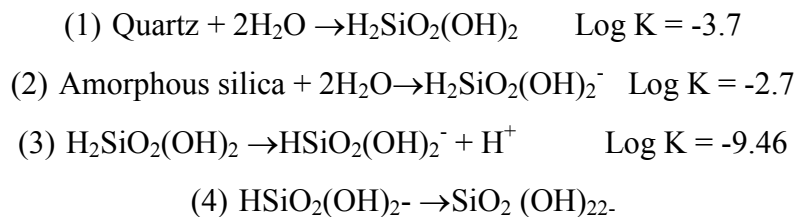
Extreme silica concentrations arising on the membrane surface and overall supersaturation conditions can affect silica solubility limits (Sanciolo and Gray 2014, Ning 2010, Semiat 1996). Various industries developed their own engineering code of practice for management of elevated silica concentrations to avoid exceeding silica solubility limits leading to silica scale deposition. For instance, indicative silica solubilities at 25°C in deionised water for a range of pHs was developed by the US boiler industry and are summarised in Table 2.1.

Table 2.1 – Silica solubility vs pH values

pH	Solubility of SiO <sub>2</sub> (mg/L)
6 to 8	120
9	138
9.5	180
10	310
10.5	876

However, silica solubility limits could vary generally from 120mg/L to 140mg/L as a result of water chemistry, as recorded in different research (Ning 2010, Semiat 1999, 2000). Pseudo-solubility silica limits at residual silica concentrations 200 – 240 mg/L were also observed by a number of authors probably due to a rapid increase in silica concentrations and slow kinetics (Bartman 2010, Baes 1976).

Solubility of silica can be characterised by the following equilibria at 25°C (AWWA 2010). Monosilicic acid has been written as H<sub>2</sub>SiO<sub>2</sub>(OH)<sub>2</sub>, rather than Si(OH)<sub>4</sub> or H<sub>4</sub>SiO<sub>4</sub> in order to emphasize its diacidic character, and the tendency of silicon, like other metalloids, to coordinate with hydro and oxo-ligands (Stumm and Morgan 1976).



Stumm used these equilibria to describe the speciation of silica in aqueous solution. His data indicated that at normal environmental pH values (pH9) dissolved silica exists exclusively as mono-silicic acid. This conclusion is supported by the finding that soluble silica has a diffusion coefficient of 0.53 indicating a molecular size about equivalent to monosilicic acid. Below about pH = 9.4 the solubility of amorphous silica is about 120 ppm. Quartz has a solubility of only about 6 ppm, but its rate of crystallization is so slow at ordinary temperatures and pressures that the solubility of

amorphous silica represents the upper limit of dissolved silica concentration in natural waters.

The solubility of aqueous silica depends on monomer silica concentrations, pH, salinity (cations and anions present) in the solution, pressure and temperature (Hamroni and Dhahbi 2001). Analytical aspects of silica solubility limits in saline waters have been investigated by Hamroni and Dhahbi (2003, 2001), who point out that the efficiency of the RO desalination process was limited by the solubility of silica.

The code and practice developed by AWWA (2001) for the RO industry in the US, table 2.2, recommends that if a silica scaling potential exists, aluminium and iron must be removed by 1µm cartridge filtration if possible. Since the solubility of silica increases below a pH of approximately 7.0 and above a pH of about 7.8, the actual solubility of SiO<sub>2</sub> in a concentrated stream can be affected by the pH of that stream.

Thus the silica solubility can be obtained by multiplying the pH7 SiO<sub>2</sub> solubility at the specific temperature by the pH correction factor to give the corrected solubility (SiO<sub>2cor</sub>) (AWWA, 2001). A comparison of the silica solubility (SiO<sub>2cor</sub>) of the RO system with the pH corrected silica solubility (SiO<sub>2c</sub>) (AWWA 2001) can be made. If SiO<sub>2c</sub> is greater than SiO<sub>2cor</sub> silica scaling can occur and adjustment is required. Because silica chemistry is quite complex, this practical way is currently adopted by the RO membrane industry (AWWA 2001).

Table 2.2 - Silica solubility vs temperature

Temperature (°C)	Solubility of SiO <sub>2</sub> (mg/L)
5	85
10	96
15	106
20	118
25	128
30	138
35	148

While an extensive body of data exists describing the dependence of SiO<sub>2</sub> solubility on temperature, the effect of pressure on the solubility of silica has never been measured. It is a widely held view, mostly from past research in the geothermal field, that pressure has little effect on the solubilities of amorphous silica below about 300 degree (Fourier 1988). Contrary to this proposition, a recent report from marine research claims that the solubility of the silica decreases by about 10% after each ~200 bar of increase of pressure (Mauni, 2014).

Aluminium and iron oxides are a commonly encountered inorganic colloidal foulants, as evidenced by their frequent appearance in membrane autopsies (Nghiem and Schafer, 2006). Other metal oxides, such as those of aluminium and manganese, are also a source of fouling in membrane systems. Dissolved manganese may be present in anoxic brackish groundwater sources, whereas aluminium is encountered in systems using aluminium salts as a coagulant. Both of these types of metal oxides are encountered as a membrane foulants far less frequently than iron (Brant 2012, Healy 1994). Iron fouling can occur when the soluble form of iron (Fe<sup>2+</sup>) is oxidised to insoluble forms allowing precipitation out of solution onto a membrane surface (Kenneth 1987). The solubility of iron (III) is governed by the solubility of Fe(OH)<sub>3</sub>, which is less than 0.1mg/L in freshwater over a pH range of approximate 5 - 9. The solubility of iron (III) is higher in more-saline waters as a result of ionic effects. It is, therefore, critical that dissolved metals like iron, aluminium and manganese be removed before reaching RO membranes, as these materials may foul and perhaps oxidize or catalyse the oxidation of the membrane material (Brant 2012, Sheikholeslami and Lee 2002).

#### **2.2.4 Concentration polarisation (CP)**

CP occurs at the membrane surface when ions are rejected and the concentration cations and anions increases in a layer at the membrane surface. CP could arise in various severities and could limit the membrane performance. A major impact of CP is a significant decline of flux because of the elevated osmotic pressure, and fouling due to solute-membrane interaction and increasing solute concentrations above their solubility limit (Koo 2001). CP is also referred to as the build-up of any material on a membrane surface. A variation of the osmotic pressure model indicates that decreasing the

thickness of the CP boundary layer should result in an increase in the mass transfer coefficient for a membrane system. Because CP is a function of the system hydrodynamics, it can be reduced by controlling the flow (Cohen 2007, 2003). One way to reduce CP is to keep the horizontal feed flow turbulent. It appears increased cross flow reduces the thickness of the laminar boundary layer, thereby increasing the relative amount of back diffusion of solute to the feed stream.

Yet, the effect of CP resulting from specific water matrices is better to obtain empirically by monitoring RO performance (Sheikholeslami and Lee 2001). Complex physical chemical processes arise in the CP zone that can significantly depress the silica solubility limit and as a result increase silica scale deposition on the membrane surface.

Increased concentration of a solute next to the membrane surface can have several effects such as reduction of permeate water quality, and silica and/or salt precipitation on the membrane surface (Gabelich 1993, Brant 2012). According to theory, CP increases from the value of the bulk stream at the edge of the boundary to an elevated concentration next to the membrane surface. Furthermore, CP is function of many variables including water quality, hydrodynamics, diffusivity of the solute, and the thickness of boundary layer. CP seems to be an important cause of membrane fouling, especially for high flux RO systems (AWWA 2001, ASTM 1989).

The main methods to moderate CP are reduced permeate flux or improved pre-treatment of the RO feed water by removal of metals or ions, and removal of particulate matter and DOC that lead to fouling and cake enhanced osmotic pressure. For CSG water desalination, reduction of permeate recovery lead to a dramatic increase in brine production, for which additional treatment and residual recovery is necessary by complex thermal technologies such as BC or MED or both depending on the quality of residual required (commercial or industrial grades). Improved pre-treatment of CSG water is a way to reduce the impact of CP on the membrane surface and improve the efficiency of RO systems. In fact, an effective pre-treatment frequently allows achievement of 92 – 94 % permeate recovery without significant scaling problems (Sheikholeslami 2002, AWWA 2001, Hann 1994, 1997).

### 2.2.5 Chemical precipitation

Formation of a cake layer on the membrane surface will depend on the physiochemical properties of the solution and physiochemical property of specific foulant such as silica. However, the rate of growth of the cake layer depends on many variables in this system, including the super saturation conditions, hydrodynamics of the flow, and pH conditions (AWWA 2001, Brant 2012). In the case of silica deposition, two major factors affect the rate of deposition: silica super-saturation and pH (Ning and Lee 2010, 2008). Frequently, to mitigate precipitation of one particular foulant creates favourable conditions for precipitation of other foulants – this is true when various anti-scalants are added to the RO feeds (Demakis 2001, 2005). Nucleation was found to be a function of the product water flux, particles size, and the number of nucleation sites available for polymerised silica to deposit (Cob 2010, Ning and Lee 2010). For instance at pH values away from the isoelectric point, colloidal aluminium particles stabilised and their aggregation behaviour was controlled by their surface charge (Barger 1991). These particles can easily nucleate on membrane surfaces providing a favourable environment for silica to precipitate as aluminium-silicate.

Chemical precipitation can be sometimes be avoided by selecting the right pH condition that silica for instance, remains in solution at relatively high concentrations (Sanciolo 2014, Gray 2006, Semiat 1996). For instance, very high pH conditions (pH10 to pH11) frequently help to mitigate chemical precipitation. However, these pH conditions are not always practical and acceptable for large commercial RO systems.

### 2.2.6 Fouling models

Fouling prediction in RO processes have been reviewed by a number of authors (El-Manharawy 1999, Barger 1991). Barger and Carnahan (1991) described three fouling models – the gel-polarization model, resistance – in – series approach, and transport – accumulation approach. Each model takes into account a set of criteria to explain fouling, but none of them are based on comprehensive criteria. For instance, the gel-polarization model considers a layer of molecules of constant concentration, which aggregate into a gel deposit that is formed at the membrane surface. Gel concentration, in this model, depends on the morphological, physical, and chemical properties of the

feed water, but not on feed concentration, operating pressure, membrane materials, or the hydraulic conditions in the system (Rautenbach 1989, Barger 1991). As a result, the model has reduced connection with the fluid dynamics of colloid particles, and cannot explain cake formation.

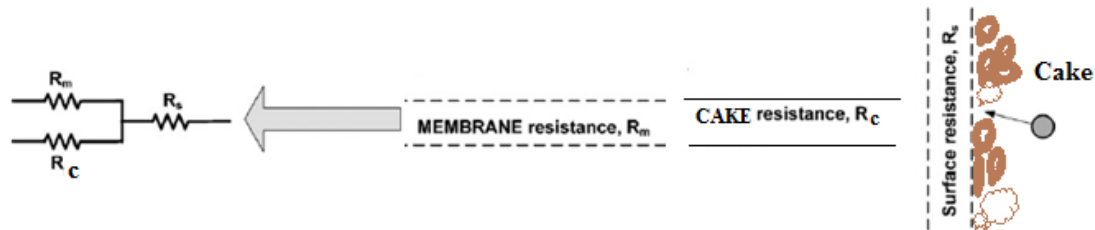


Figure 2.1 - Representation of the resistant encountered by flow through a fouled membrane.

Ho and Zydney (2001) have developed a fouling model that accounts for simultaneous pore blockage and cake formation, with the cake layer only forming over those regions of the membrane that have first been blocked by an initial deposit. This model assumed that the initial flux decline arises from pore blockage by the physical deposition of large aggregates on the membrane surface and that this is incorporated into a cake layer (Ho and Zydney, 2001). The filtrate flux through the blocked pores was evaluated using Darcy’s law assuming a resistance in series model:

$$J_{\text{blocked}} = \frac{-P}{\mu} \cdot (R_m + R_c) \quad (1)$$

where  $-P$  is the transmembrane pressure,  $\mu$  the solution viscosity,  $R_m$  the membrane resistance, and  $R_c$  the resistance of the filter acid cake that forms over the membrane surface.

The resistance-in-series model assumes that the water flux is proportional to the change in pressure. The gel concentration model uses the proportionality constant, originally developed for UF system, and is then interpreted as the system's resistance to product water flow instead of the permeation coefficient (Rautenback 1989). The model sometimes applies to the fouling potential of low (<70%) recovery RO system, which is a major limitation of the model. While the resistance-in-series model can also help with

understanding of silica scale formation, overall it is more applicable to crystal deposit on the membrane surface and less to amorphous silica.

The individual components of these feedwaters will affect each other's solubility, growth kinetics, and concentration polarization. These essential factors would have to be experimentally determined for each feedwater to provide any basis at all for an accurate analysis by this method. For natural CSG waters it will be difficult to apply this approach as the RO feed can slightly change over the life time of the CSG project as a result of water quality changes (Whitehouse 1995). The presence of dissolved silica species in relatively high salinity natural CSG water and practical silica solubility will be more important. Nevertheless, the model is useful for understanding the concept of silicate deposit formation on the membrane surface.

The transport – accumulation approach model is based on a numerical solution of the governing field equations for a fouling system. This equation is often simplified to:

$$Q_w = A * (NDP)$$

Where  $Q_w$  is the rate of water flow through the membrane,  $A$  represents a unique constant for each membrane material type, and  $NDP$  is the net driving pressure or net driving force for the mass transfer of water across the membrane. The model includes an accumulation term in the equation for the mass balance at the membrane surface. For instance, for slightly soluble salts, this term requires knowledge of the salt's solubility, crystallization growth parameters, adsorption characteristics, and particle trajectory in the flow channel (Rautenbach 1989, Semiat 1996). According to Cohen (2006), a velocity profile must be developed for the defined channel geometry and flow regime, and this is then used to solve the continuity equation. At this point, the solution scheme uses the mass of the particles formed to calculate its velocity and trajectory towards the membrane. Once a particle reaches the membrane, its mass is added to that of any existing fouling layer. The pure water flux is calculated from an updated cake resistance, and the entire scheme is checked using a new mass balance calculation. While one particle may reach the membrane surface, the model also allows for simultaneous formation, growth, and transport of other particles. This dynamic model can be credited with variable success for soluble, slightly soluble, and organic solutes,

as well as for colloidal suspensions, when compared to related experimental results. This model seem to be supported by experimental results obtained by many (Exley 1993, Gabelish 2005, El-Manharawy 2000), especially for the batch processing of designated feedwaters and for the continuous flow of highly soluble salts such as sodium chloride.

Regardless of the model used, experimental work is necessary to verify the silica scaling conditions including the silica solubility limit in a range of water matrices, impact of salt, salt concentrations, and presence of other cations such as aluminium in particular. Any form of modelling chosen to explain fouling and/or scale formation mechanisms for a particular water matrix would depend on the completion of sufficient experimental work to define chemical precipitation fouling of RO membranes, so that some insight into the physical and chemical interactions involved could be gleaned from the experimental data.

## **2.3 Silica chemistry and its effect on RO desalination**

### **2.3.1 Aqueous silica**

A major observation was made by Gabelish (2005), El-Manharawy (2000) about silica scale deposition in RO desalination for different water matrix (Gabelish (2005), El-Manharawy (2000)). In desalination of groundwater silica tends to precipitate on the membrane surface, but in desalination of seawater silica is precipitates to a lesser extent (El-Manharawy (2000)). This phenomenon of silica chemistry can be explained by presence of various silica species, which frequently define silica solubility and physicochemical reactions (Iler 1976, Kiselev 1956). For seawater the composition is relatively balanced; though, this might not explain low silica precipitation in seawater desalination.

Dissolved silica is supplied to the environment by chemical and biochemical weathering processes which involve ion substitution and chelate forming reactions which remove mineral lattice cations. The concentration of dissolved silica in natural waters is controlled by a buffering mechanism which is thought to involve the sorption and desorption of dissolved silica by soil particles and sediment (Stumm and Morgan 1996).

The dissolution process of silica and silicates from rocks into water is mainly due to hydrolysis of silica-oxygen-silica bonds, resulting in the liberation of silicic acid ( $\text{Si}(\text{OH})_4$ ) and silicates into aqueous phase (Marshall 1979, Davis 1964). It is difficult to define precisely the term “aqueous silica” as there is an array of silica species possible (Bergna 2005, Healy 1994). Temperature, pH and ionic strength have a substantial influence on the solubility of amorphous silica and forms of silica present in a solution (Ning 2010, Bergna 1992, Hamrouni 2001). Silica may occur in natural waters in different forms linked to special terminology as follows:

- “Soluble” or “dissolved” silica containing monomers, dimers and polymers of silicic acid.
- “Insoluble” or “colloidal” silica, which results from polymerisation of silicic acid forming particles and three dimensions gel networks.
- “Reactive” silica containing monomers and dimers forms that react with ammonium molybdate within 10 min. The other forms are referred to as “non-reactive” silica (Hamrouni 2001, Sjöberg 1996).

Silica polymerisation is a structural growth process. This process leads to the formation of “colloidal silica”, which is a complex and amorphous product (Healy 1994, Bergna and Roberston 2005). When silicate ions polymerize, they form rings of various sizes, cross-linked polymeric chains of different molecular weights, and oligomeric structures. The arrangements of  $[\text{Si}(\text{O}_4)]^{4-}$  and  $[\text{SiO}_6]^{8-}$  and the tendency of these units to form a three-dimensional framework structure are fundamental to silica crystal chemistry (Bergna 1994, Sjöberg 1996).

Aqueous silica sols are of particular interest in colloidal science because their coagulation-dispersion behaviour is said to be “anomalous”, that is, their stability in terms of electrolyte – pH control does not follow the pattern followed by almost all other oxide and colloidal materials (Healy 1994). To date, there has been little agreement on what constitutes stability for aqueous silica. One of the unexpected properties of silica is that silica, unlike other oxides, will not regulate charge during the approach of two surfaces (Healy 1994). An explanation for the “anomalous” behaviour

of silica sols can be related to steric stabilization effects that require oligomeric or polymeric silica species be present at the silica-water surface and that steric repulsion results during overlap of such layers (Kiselev 1998, Healy 1994). Early works by Sjöberg (2008, 2007), and Marsmann, Engelhardt, Harris, and Newman (1996) have shown the existence of a variety of silica species in aqueous environments and their role in silica polymerization and precipitation patterns. Aqueous silica species and equilibrium in sodium silicate (“water glass”) solutions were studied by Svenson using combined pH and  $^{29}\text{Si}$  NMR data. At high  $\text{SiO}_2/\text{Na}_2\text{O}$  ratios, polymerisation leads to the formation of polysilicate species containing silica polymerised structures which includes 6-8 silicon atoms and consisting of predominately dissolved silica groups ( $\text{Q}^0$ ,  $\text{Q}^1$ ,  $\text{Q}^2$ ,  $\text{Q}^3$ ,  $\text{Q}^4$  type surroundings). Most research on silica species conducted so far was to identify as many silica species as possible (Dietzel, Stober, Iler, Marsmann, Silver). To date, there is no study of the effect of cations on silica species in aqueous silica solutions

### 2.3.2 Dissolved silica species

Aggregation (polymerisation) of dissolved silica species into more complex networks under various physical and chemical conditions leading to silica precipitation might be considered a key to understanding of silica scale deposition on the RO membrane surface. Past results from others on silica structural evolution obtained by  $^{29}\text{Si}$  NMR show that structural control of silica polymerisation processes is complicated because many and diverse variables affect concurrent reactions differently (Sjöberg 1996, Dove 1994). Inductive and steric factors contribute to the reaction rates (Cob 2012, Iler 1979). pH is probably the single most important variable in these reactions. Markides (1987) demonstrated by  $^{29}\text{Si}$  NMR that for all pH values from 2.5 to 11.5, the smallest particles were of a similar size being only a few nanometers in diameter, but the rate of formation of such particles drastically increased with pH (from pH2.5 to pH11.5). This agrees with literature models of particle nucleation and growth by Iler (1976) and Baldyga (2012). The effect of pH, sodium chloride concentration and presence of other cations show a different connection between the rates of aggregation, precipitation and gelation (Gorrepati 2010, Smolin 1976, Ostirikov and Gleim 1955). None of these arguments are

definitive, although assignments to monomer, dimer, ect have been made and speculations put forward regarding other sub-species present by a number the researchers (Sjöberg, 2001, 1983, Dietzel 1999).

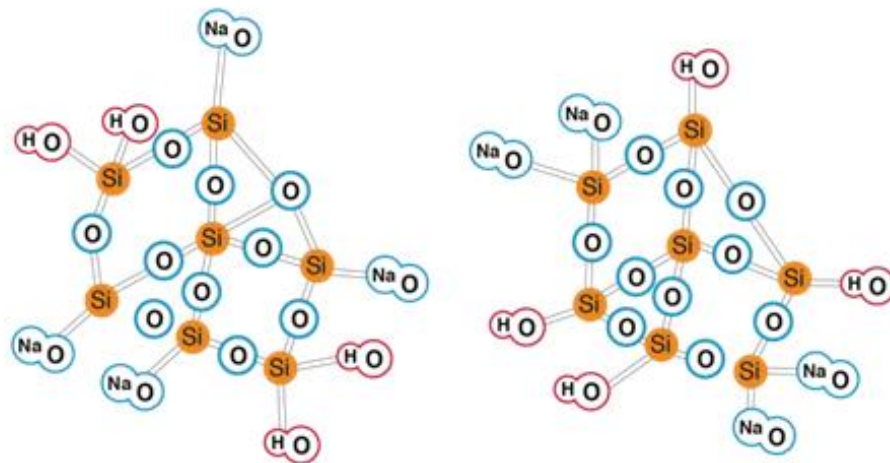


Figure 2.2 – Structure of two typical  $\text{Si}_7\text{O}_{18}\text{H}_4\text{Na}_4$  molecules present in the initial concentrated sodium silicate mother solution.

Dissolved silica species can be found in commercial sodium silicate solutions, Figure 2.2. Moreover, sodium silicate solutions consist of two domain states of silica – the colloidal domain (amorphous  $\text{SiO}_2$ ), Figure 2.3, illustrates two silica conditions - the dissolved silica species (mononuclear domain) and colloidal (amorphous silica – insolubility domain) silica. Mononuclear sodium silicate solutions contain a network of  $[\text{SiO}_4]^{4-}$  species, shown in Figure 2.3, which exist in the sodium silicate solution in equilibrium with amorphous silica.

Figure 2.3 shows that the mononuclear wall follows the line characterizing  $[\text{Si}(\text{OH})_4]$  up to a pH of approximately 9, and then ionisation of dissolved silica species dramatically increases as soon as the pH9 value is past. The concentration of mononuclear silica then increases with increasing pH from pH9 to pH11.5. One domain in the concentration-pH diagram is important for the study dissolved silica species (aqueous silica) by  $^{29}\text{Si}$  NMR in particular: the monomeric domain where mononuclear Si species  $[\text{Si}(\text{OH})_4]$ ,  $[\text{Si}(\text{OH})_3^-]$  and  $[\text{Si}_2(\text{OH})_2^{2-}]$  prevail thermodynamically.

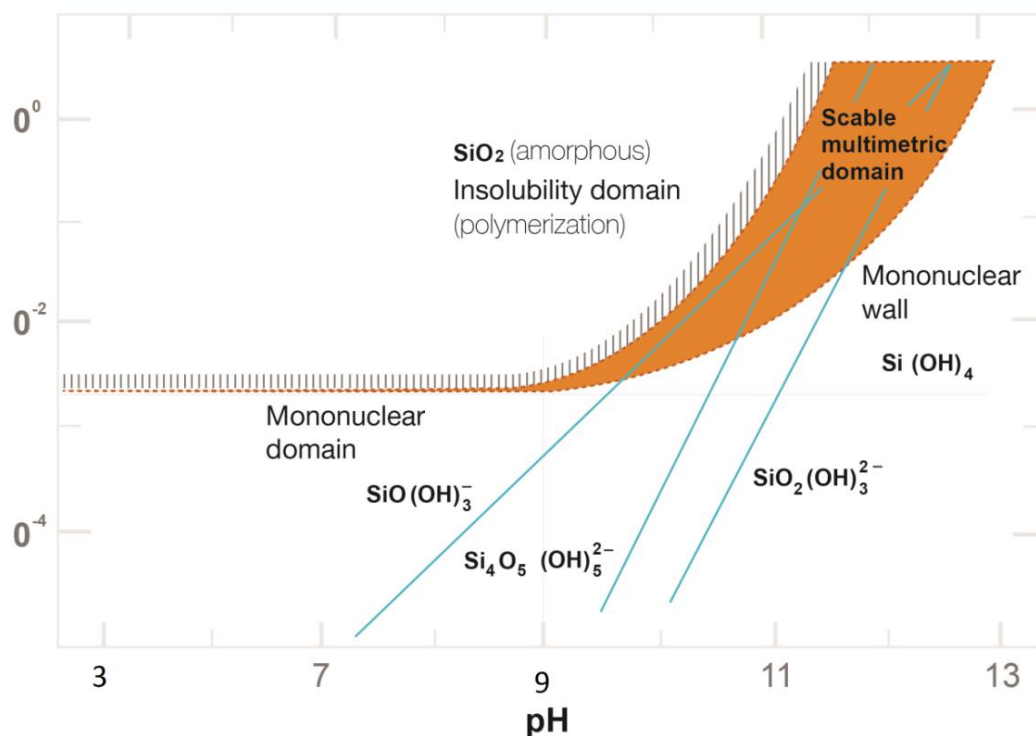


Figure 2.3 – Silica species in equilibrium with amorphous silica. Diagram computed from equilibrium constants (25°C). The line surrounding the shaded area gives the maximum soluble silica. The mononuclear wall represents the lower concentration limit, below which multinuclear silica species are not stable, adopted from “Aquatic Chemistry” by Stumm and Morgan (1996).

### 2.3.3 Colloidal silica

Silica is a primary cause of concern for fouling RO membranes in desalination systems (Sanciolo and Gray 2014, Semiat, 2003, El-Manharawy 2000). In the presence of carbonic acid ( $\text{H}_2\text{CO}_3$ ), silica has two acid-base characters that affect the characteristics of the silica and its interaction with membrane surfaces. First, the complexation of silica with hydrated forms of heavy elements (calcium, aluminium, magnesium and iron) creates colloids that grow through polymerisation and bridge with organic and inorganic matter to form gel-like layers on membrane surfaces (Wang 2010, Sheikholeslami et. al., 2002). Second, reactive silica is known to consist of low ionised forms (such as monomeric silica acid) at pHs of 6 to 9 and to form an essentially all-silica gel or cake

structure (Brand 2012, Wang 2010). These silica structures cause flux decline and higher TMPs. Research has shown that colloids can be composed of any number of different materials; the mostly commonly encountered inorganic colloid is silica ( $\text{SiO}_2$ ) (Ning 2010, Demakis 2010). Colloidal silica results from the polymerisation of silicic acid containing particles and three-dimensional gel networks (Hamrouni and Dhahbi 2001). Silica may also form amorphous silica deposits especially in the presence of calcium carbonate and calcium sulphate (Ham 2014, Sheikholeslami et. al., 2002). Colloidal silica is the most stable product of the silico-oxygen acid polymerisation process (Brant 2012). Colloidal silica can form in bulk solution or RO feed when dissolved silica solubility exceeds the silica solubility limit. Colloidal silica or non-reactive silica groups can form in low pH conditions such as pH 2.5 – 3.5 when silica polymerisation skips the colloidal silica precipitation step and directly forms a gel (Iler 1976).

In CSG waters, silica exists as either colloids or as un-dissociated (ortho-) silicic acid ( $\text{H}_4\text{SiO}_4$ ) when the pH is between 8.5 and 9.2. A second form of silica foulant is silicates, which are complex forms of silica in which hydroxides of other elements copolymerize with silicic acid (Brant 2012, Hawkis 2013). Therefore, silica fouling may be mitigated to some extent through pre-treatment of the raw water by coagulation. Ideally, coagulation should leave no aluminium, no silica, and no ferric ions in the pre-treated water for RO feed (Demadis 2009, Healy 1994).

#### **2.3.4 Silica polymerisation**

Silica polymerisation and deposition, on the RO membrane surface, has been researched experimentally (Semiat and Hasson 1996, 1999, 2003, Gill 1996, Bowen 1979) and more recently computational simulations have been performed (Jianjun, et al, 2006), where the molecular mechanism and rate of hydrolysis have been explored through calculation of the reaction barriers and pathways. Both studies showed that the main factors influencing silica polymerisation are pH, temperature, saturation, impurities present in the solution, and the autocatalysis effect of already precipitated silica that accelerates further precipitation. Total silica surface area in solution is also a factor determining the rate of silica polymerisation. Carbonate hardness also accelerates

further polarisation and precipitation as does magnesium. The presence of magnesium enhances silica polymerisation and also depresses silica solubility when calcium was present.

Computational simulations found that the siloxane bond, often presented on silica surfaces, is difficult to hydrolyse because of the high reactivation energy barrier, especially with the aid of hydrolysis (Jianjun et al., 2006). However, monomers of silicic acid condense to form larger oligomers, which link together to produce primary particles (nucleation). Depending on process conditions, these particles can either grow by reaction with monomers or grow by aggregation (Iler 1976). Aggregation can lead to gelation of the colloidal suspension, but not necessarily to silica deposition on the membrane surface (Bergna 2006).

The research by Bergna (2006, 1994), Sjoberg (2008, 2001), Iler (1979), Kiselev (1978), Baldyga (2009) and others provide insight into the physical and chemical processes involved. The experimental data are rather debatable, and there is no general agreement about silica hydrolysis and condensation in aqueous solutions and complexation to cations and anions at the particle – water interface. Healy (1994) referred to the behaviour of colloidal silica as “anomalous silica sols” because the Derjaguin-Landau-Verwey-Overbeek (DLVO) theory seem to be unable to cope with silica hydrolysis while it explains satisfactory the behaviour of all other colloidal systems. For example, it is well known that the silica sols are stable at their point of zero charge and that they also coagulate in alkaline solutions, in which their electrical surface charge is high and where their stability should increase. Such behaviour is very unusual. Yates (2000) proposes a thermodynamic approach to replace the failing DLVO theory. According to Healy (1994), on other hand, the DLVO theory should give a coherent description of the aqueous silica behaviour on the condition that all the forces that play a role in the interaction are introduced in the model. Stability of silica at the point of zero charge may be explained by steric stabilisation from oligomers on the surface of the silica sols (Healy 1994) that prevent aggregation.

Membrane scaling phenomena are governed by the silica solubility limit prevailing in the CP layer on the membrane surface (Semiati 2003, 2001, 1996). According to Semiati (2003), the rate of change in the silica scale formation during the course of RO processing is dictated by two opposing trends: the concentration effect due to permeate withdrawal which acts to increase the silica scale formation, while the decline in permeate flux due to scaling and osmotic effects acts as to decrease the rate of silica scale deposition. Permeability decline data provides a more accurate characterisation of the silica scaling process (chapter 5 of this thesis). What is not yet clear from the experimental silica studies by Semiati (2003) is the impact of dissolution (hydrolysis) on existing silica deposits and on colloidal silica present in the concentration polarization zone (i.e., close the membrane surface) and how on-going processes of hydrolysis and condensation effect silica polymerisation in this zone. Will silica deposit on the membrane surface as a result of monomer silica groups concentration exceeding the practical solubility limit or will it remain in dispersion and why?

Baoxia and Elimelech (2012) tried to explain silica scaling reversibility in RO process by proposing three steps of both homogeneous and heterogeneous nucleation processes on the membrane surface. However, mechanisms of silica precipitation leading to two different nucleation processes are conflicting to what can be expected for homogeneous silica nucleation. The diagram, figure 2.3, describes indicative silica species distribution in different silica solubility zones, for various pH and concentrations. These silica species arise from published light-scattering experiments and help to define the pH-concentration domain in which multiple ions are present as precursors to silica polymerisation (Stumm and Morgan 1987).

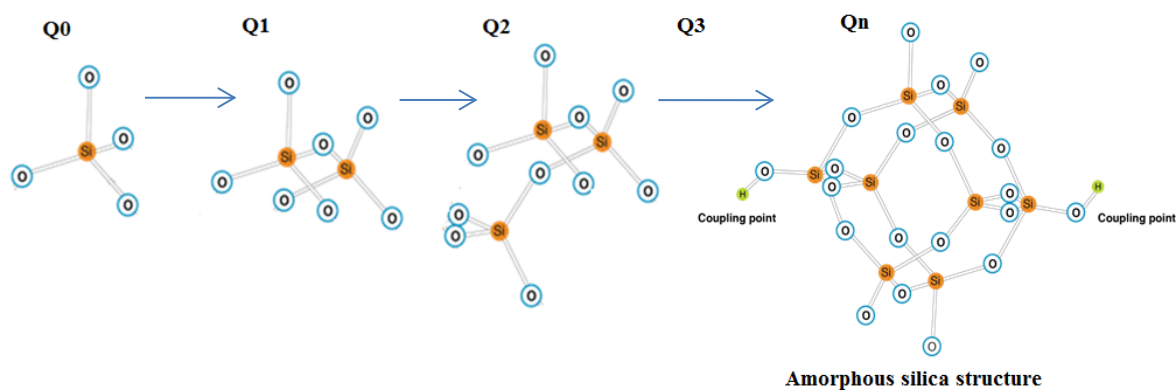


Figure 2.4 – Dissolved silica species polymerisation ( $Q^0 < Q^1 < Q^2 < Q^3$  aggregation) path into amorphous silica structure (mechanism proposed by Iler (1976)).

According to Iler's (1976) description of silica chemistry and dissolved silica polymerisation pathways (Figure 2.4), increasing dissolved silica concentration well above solubility limit in the CP layer will initiate silica precipitation likely firstly by aggregation of monomeric silica acid in bulk solution before deposition on the membrane surface. This is contrary to what was proposed by Baoxia and Elimelech (2012), who claimed in their RO research that monomeric silicic acid could attach to the membrane surface without the presence of nucleation coupling points. Dietzel (2003, 2001, 1997) also illustrated in his analytical study of dissolved silica polymerisation pathways that dissolved silica species in the polymerisation process follows as  $Q^0 < Q^1 < Q^2 < Q^3$  aggregation path until they react with other impurities. It is possible, however, the work completed by Baoxia and Elimelech (2012) considered the presence of other potential coupling points on the membrane surface such as  $-OH$ ,  $-COOH$  groups and coupling points that are a function of the water chemistry from precipitates such as  $Al(OH)_n$ ,  $Fe(OH)_n$  leading to monomeric silicic acid coupling to the membrane surface.

### 2.3.5 Kinetics of silica polymerisation

A considerable amount of study has been devoted to the polymerisation of silicic acid, but little work has been done on the understanding of kinetics involved in the process of polymerisation of silica on RO membrane surface. Goto (2001) and Sheikholeslami

(2001, 2003) have studied RO feed solutions and precipitation of silica in concentrations approaching those found in natural system. In an examination of an aqueous solution of silicic acid in the pH range 7 – 10, the rate of disappearance of monomeric silicic acid was found to follow third order kinetics. The third order kinetic behaviour of silica polymerisation has also been noted by Marshall (1982) in acid solutions, but as the pH of the system is increased there was a noticeable change in mechanism. But then again, the mechanism of polymerisation of silica systems of low concentrations is not completely understood (Semiati 2003, Bishop and Bear 1970). It seems in different silica concentration ranges, the silica polymerisation rate is quite different. For instance, the polymerisation reaction of monomeric silicic acid in the presence of base was found to follow second order kinetics. Iler (1976) and Kiselev (1978) have reported that the polymerisation process follows second order kinetics in basic solution, but both studied silica in the concentration 1.8 - 3.0%. Semiati (1996) and Ning (2010) studied silica in the relatively lower concentration range 0.2 - 0.5% and reported that the reaction was first order with respect to  $\text{SiO}_2$  and first order with respect to hydroxide. All authors seem to be agreed that the two species necessary for the polymerisation reaction to take place in a reasonable length of time are a silicic acid anion and a neutral silicic acid molecule. As the two reactants approach each other in the solution, it is possible the first reaction involves the formation of a hydrogen-bonded intermediate. The hydrogen bond formed would allow the reactants to be held in close proximity, so that the splitting out of a hydroxyl with subsequent formation of a silicon-oxygen bond can occur. This mechanism is controlled, as would be expected, by the ionisation of silicic acid which in turn depends on the pH of the system. Bishop (1972) and Greenberg (1958) confirmed that the polymerisation occurs through one oxygen bridge and the system appears to form only in linear chains (Bishop 1972, Iler 1979).

The kinetics of silica polymerisation in dilute aqueous solutions was also studied by Weres (1981), Bauman (1959), Engelhardt (1977), Marshall (1980), and Matijevic (1971). They all found that the state of ionisation of the silica surface controls the rate of polymerisation. The rate of deposition of dissolved silica on the surface of amorphous silica is proportional to the surface density of ionised silanol groups. The extent of surface ionisation also determines the value of the surface tension, and this

also the rate of homogeneous nucleation. Bauman (1959) found that the “polymerisation rate” increased rapidly with increasing dissolved silica concentration, and also that it increased with increasing dissolved salt concentration at pH3.

### **2.3.6 Silica scale formation**

Silica scale formation can occur when dissolved silica becomes super-concentrated on the membrane surface and/or in the bulk solution and exceeds its solubility limit (She 2003, Wiesner 1992). Generally the properties of the silica scale depend on the chemistry of the RO solution. Silica scale formation as mineral scale formation is in most cases initiated within the CP boundary layer because of the elevated ion concentrations in the CP relative to those in the bulk solution (Elimelech 1998). Though the chemistry of silica scaling appears to be straightforward, it has proven to be particularly challenging and remains poorly understood, because of the many different forms of silica species involved and the complex interactions that occur between scale-forming compounds and other foulants (Semiat 2003, Sheikholeslami and Bright 2002). A minimum of four stages of scale formation have been identified: (1) attainment of super-saturation, (2) nucleation, (3) colloidal aggregation and (4) particle growth around the nucleus (Hasson and Semiat 2006, Tzotzi 2007). Initially silica deposits as a gel or amorphous composite before it ages and forms the cake (Baoxia 2012, Ning 2010). Similar to mineral scale formation, silica deposit is likely to cause an increase in pressure drop and permeate flux decline across a membrane element.

Several investigations on high recovery membrane systems have been carried out (Cob 2012, Rahardianto 2007, Bond 2008) and reported that after the 96 and 98% recovery was achieved the fouling layer was much thicker than for instance at 91% recovery. At 96 and 98% recovery the membrane surface was completely covered with Si, Al, Fe and O, most likely due to the presence of silica and aluminium and iron hydroxides (Cob 2012, Rahardianto 2007, Bond 2008). As the recovery of RO system is increased further, the propensity for fouling from the higher concentrations increases and the concentration of ions within the CP layer is increased dramatically at the membrane surface leading to fouling and scale depositing (Gray 2014, Bartman and Cohen 2010).

Leading RO desalination technology companies (Veolia, GE, Saur, ect) propose diverse approaches to mitigate silica scale formation. For instance, a system composed of two RO stages in which the primary concentrate was treated to reduce its scaling potential and then the concentrate was treated again in the second RO has been proposed. Other common RO arrangements to avoid critical silica concentrations on the RO membrane surface is the removal of silica between second and third or between third and fourth RO stages, especially when very high permeate recovery and system reliability are expected (Personal communication with GE and Veolia Water Australia). However, while different approaches allow some flexibility for high recovery RO desalination, silica scale formation on the membrane surface, as a result of depressed solubility in the super-saturation zone on the membrane surface, remains unresolved. The risk of silica fouling is the biggest limiting factor in maximizing recovery for brackish water RO systems (Brant 2012, Cob 2012, Semiat 2003).

### **2.3.7 Silica in salinity waters**

Rothbaum and Rohde (1979) studied the polymerisation of silica over the broad temperature range of 5°C to 180°C, mostly using un-buffered, very low salinity media (monosilicic acid and sodium silica only). Adding small amount of sodium chloride to the solution was found to have little effect. They also developed a simple model of the polymerisation process which postulates that the rate-limiting step is the formation of dimers, which is then followed by relatively rapid polymer growth.

Added salts seem to accelerate both molecular deposition and homogeneous nucleation by increasing the extent of surface ionisation and decreasing solubility of silica. It is also important to note that sodium in small concentrations slightly increased silica solubility (El Manharaw 1999) and in higher concentration depressed silica solubility (Healy 1994). In comparing the effects of concentrations of different salts, Baumann found that sodium chloride and bromide strongly accelerated both polymerisation and depolymerisation, but to different degrees. Salts decrease the rate of solubility and increase the rate of nucleation. They also found that a small amount of fluoride greatly increased the polymerisation rate at pH 4 - 5 and attributed this to a powerful, specific

catalytic effect (Mitra 2008). Overall, it was concluded that the accelerating effect of added salts was due to specific catalysis by the anions.

Whether heterogeneous or homogeneous silica scale is the predominate mechanism of silica scale formation in membrane systems remains an unknown effect of salinity, and other cations and anions on silica scale formation and why in some cases silica in relatively high concentration does not deposit on the membrane surface but in some cases at relatively low concentration it precipitates on the membrane surface and could lead an irreversible membrane damage. These potential conflicting data highlights the need for continued research on silica chemistry and its implication for RO desalination.

### **2.3.8 Silica and aluminium precipitation**

Aluminium frequently presents along with silica in natural waters (Stoberg 1985, Marshall 1997). There is particular affinity between the oxides of aluminium and silicon (Iler 1976). It may be present as silt, clay, and algae skeletons (Farooque et al, 2004). Feed water pre-treatment can prevent clays from loading onto the membranes but can be ineffective if large amounts of clay are present, especially in very fine, stable, dispersed forms are present (Nirielle and Carnahan 2006), as for example in CSG waters. For instance, if kaolinite is introduced into pure water it dissolves incongruently. While the existence of  $\text{Al}(\text{OH})_4^-$  and its formation constant have been well established, there is a great deal of uncertainty about the composition and stability of other aluminium hydrolysis species (Baes 1976, Stumm and Morgan 1962). Aluminium silicates are frequently found deposited onto RO membrane surfaces (Demadis 2006, Yates 1975). This phenomenon may result from the ‘post-precipitation’ of soluble aluminium and silica that pass through a treatment plant or, alternatively, by the deposition of colloidal aluminium silicates that pass through a treatment. It has been recognised that better understanding of the effect of residual aluminium on silica polymerisation is necessary to develop appropriate pre-treatment and monitoring strategies.

Iler (1976) points out that more research is necessary to better understand effect of aluminium on silica and silica on aluminium. Iler (1979) identified that monomeric silica is strongly adsorbed onto the surface of hydrous aluminium oxides.



There is a reaction between  $\text{Si}(\text{OH})_4$  and aluminium hydroxides  $\text{Al}(\text{OH})_3$  by which several reaction layers of  $\text{SiO}_2$  are built up, with simultaneous decrease in pH of the suspension (Iler 1976, Bergna 2006). Formation of the first layer is rapid, but the second and third layers form progressively more slowly. It would seem that diffusion of  $\text{Al}^{3+}$  or  $\text{AlO}_2^-$  from the surface of the crystal must be involved, with the formation of a silica-rich aluminosilicate. A relatively low content of aluminium ion in the  $\text{SiO}_2$  layer greatly reduces its solubility, thus explaining the deposition of  $\text{SiO}_2$  from a solution unsaturated with respect to pure amorphous silica (Bergna 2006, Iler 1979). Baumann (1976) found that when different amounts of aluminium ion were added to a solution of monomeric silica (420mg/L  $\text{SiO}_2$ ), more silica remained in the molybdite reactive state than when no aluminium was present. With no aluminium present, after 4 days there remained 130 mg/L of molybdite-reactive silica as monomer in equilibrium with 290mg/L of relative inactive high polymer (Stoberg 2005). But when aluminium was present in the Al:Si atomic ration of 1:7, there remained about 200mg/L of molybdite-reactive silica. It can be interpreted that the alumina had combined with silica to form an aluminosilicate that later was decomposed by the alumina had combined with silica to form an aluminosilicate that later was decomposed by the strongly acidic molybdite reagent liberating additional active silica that appeared as monomer (Stoberg 2005).

If the silica surface is completely covered with a layer of alumina even as thin as one two molecules in thickness, for example, it then acts as though it were a solid alumina particle, bearing a positive charge and stable at low pH (Iler 1979). A monolayer of chemisorbed hydrocarbon groups makes the particle act as through it were a large hydrocarbon molecule. An important modification of the silica surface is with aluminate ions. As evidenced by the exceedingly low solubility of aluminosilicate minerals, such as clays, there is a strong specific interaction between the oxides of aluminium and silicon (Iler 1979). The peculiar relationship between aluminium and silicon is probably because both can, under suitable circumstances, assume a coordination number of 4 or 6 toward oxygen, and because both have approximately the same atomic diameter. Since the aluminate ion  $\text{Al}(\text{OH})_{4-1}$  is geometrically similar to  $\text{Si}(\text{OH})_4$ , the ion can be inserted

or exchanged into the SiO<sub>2</sub> surface, thus creating an aluminosilicate site having a fixed negative charge (Iler 1979).

The anionic nature of aluminium, when substituted for silica in the 4-coordinated state, was first recognised by Pauling in crystalline minerals and soon thereafter in alumina-silica cracking catalysts (Iler 1979). Milliken et al. (1976) showed that the anion is stable only in the presence of a cation other than hydrogen, the free acid being unstable, and that excess silica must be present. The pH is thus an important factor and only about 15% alumina in silica was stabilized in the adsorbed anionic form at pH 6 when the stabilizing cation was ammonium. Below pH3, in the hydrogen form, the aluminium reverted to the 6-coordinate state. This behaviour of aluminium is used in modifying the surface of colloidal silica so the particles will remain negatively charged down to pH 3 in contrast to very pure silica, which is negatively charged by the adsorption of hydroxyl ions above pH7 but loses the charge in acid solution (Iler 1976, Bergna 2006). Iler prepared a series of silica sols modified with various amounts of aluminate. Stabilization by aluminate ion in the particle surface requires that each aluminium atom be surrounded by three oxygen atoms each linked to silicon, which means that no more than 25% of the surface silicon sites can be replaced by aluminium atoms. This assumes, of course, that the underlying silica is nonporous and not accessible to reaction with Al(OH)<sub>4</sub><sup>-</sup> ions.

The coverage was titrated with a cationic surfactant which was adsorbed more strongly as more anionic sites are present at pH3.5. With the above series of modified sols, Iler demonstrated that with higher surface charge, the particles became less reactive with hydrogen bonding agents. The alumina-modified sols were more stable toward gelling in the pH range 4-6 where unmodified sols gelled most rapidly and were less sensitive to salt (Iler 1979).

## 2.4 Coal seam gas water (CSG) in Australia

### 2.4.1 What is coal seam gas water

Coal seam gases, mostly methane, are absorbed into the coal seam geological formation (solid matrix), found in abundance in some regions of Australia. The pores and the open fractures in the coal contain the gas which in many circumstances is saturated with water (Hamawand and Yusaf 2014, 2013). The process of extracting the gas from the coal seam begins with reducing the pressure within the matrix of the coal. This not only results in release of the trapped gases but also involves extracting a large amount of water which is called CSG water (Hamawand and Yusaf 2014, 2013).

Figure 2.5 illustrates gas and water gathering systems for collection and separation of gas and water released from the underground, and water treatment infrastructure and gas station for gas compression.

Generally the quality of the water collected as a result of CSG extraction ranges from relatively low salinity (~ 1g/L) to medium (8 – 12g/L) and high (30-45g/L) salinity, and may be rich in other constituents that make it unsuitable for many beneficial uses as defined by Department of Environment Resources Management (DERM), Queensland, Australia <http://www.ehp.qld.gov.au/management/non-mining/csg-water.html>. See Appendix A for typical water quality data from CSG fields in Australia.

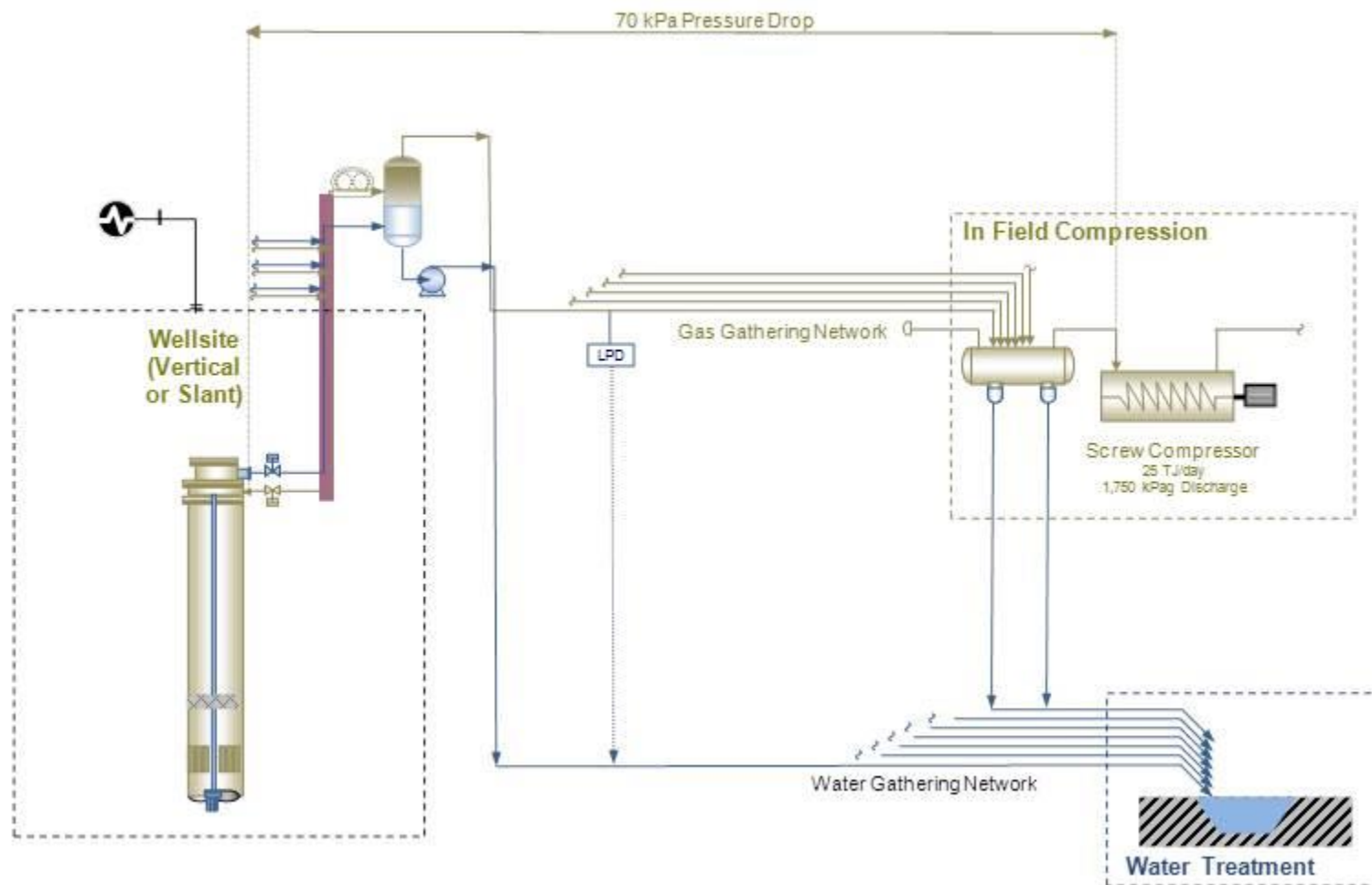


Figure 2.5 – CSG water and gas gathering network and water treatment infrastructure and gas compression station.

### 2.4.2 Physical and chemical properties

Physical and chemical parameters of CSG water depend on coal seam reservoir geology, and also the design and physical installation of water gathering network. CSG water can contain a substantial amount of salt and high sodium, low calcium and low magnesium concentrations, and very minor barium and strontium concentrations (Hamawand and Yusaf 2013). As the water table within the aquifer decreases overtime, the salinity and silica concentrations increase (Wiener and Klute 1997, Hamawand and Yusaf 2013). Depending on the construction of production wells, specifically the casing and design of gas and water gathering systems, the suspended solids can vary from as low as 0 mg/L to 800 - 1000mg/L. Generally, these suspended solids consist of much dispersed fine clays particles, silicates, metal oxides, and many other minerals (Taulis 2012, Wiener and Klute 1997).

Suspended solids contain highly dispersed fine particles of clays, which do not readily settle (DERM, Queensland). These clays frequently contain colloidal and dissolved silica and aluminium that falls within the broad classification of silicates (Hamawand and Yusaf 2013). Clay particles are primarily in the size range of 0.3 to 1.0  $\mu\text{m}$ . These clays enter CSG water as a result of erosion processes. Common examples of clays are aluminium silicates ( $\text{Al}_2\text{O}_3\text{SiO}_3$ ), kaolinite [ $\text{Al}_2\text{Si}_2\text{O}_5(\text{OH})_4$ ], feldspar ( $\text{KAlSi}_3\text{O}_8$ ), mullite ( $3\text{Al}_2\text{O}_3 \cdot 2\text{SiO}_2$ ), and andalucite ( $\text{Al}_2\text{OSiO}_2$ ), and kaolinite [ $\text{Al}_2\text{Si}_2\text{O}_5(\text{OH})_4$ ]. These aluminium silicates have proven to be especially difficult to remove from RO members using conventional acid and alkaline cleaners (Chesters, 2009). Particulate materials and dissolved solids in CSG waters can be categorized into four main groups: settleable solids  $>100 \mu\text{m}$ , supra-colloidal solids 1 – 100  $\mu\text{m}$ , colloidal solids 0.001 – 1  $\mu\text{m}$ , and, dissolved solids  $<0.001 \mu\text{m}$  (Hamawand and Yusaf 2013, Brant 2012). Ultimately, disposal is facilitated by temporary evaporation ponds, prior to pumping of CSG water for RO desalination. The temporary storages are costly due to their size, the associated land costs and the cost of later remediation.

The CSG water has some residual colour and a slight methane odour, Figure 3.4 (b), chapter 3. Dissolved organic carbon (DOC) is present in concentrations of between 5

and 30 mg/L, and often incorporates a significant proportion of humic acid (Taulis 2012, Moran 2012). This compares to surface fresh-waters with typical ranges from 0.1 to 50mg/L as DOC and for ocean waters the content varies from 0.5 to 5mg/L at the surface (Duan 2002). The humic content of CSG waters in Australia varies from 7 – 20 mg/L (DERM, Queensland). Humic substances in the CSG water are often described as amorphous, brown coloured, acidic polyelectrolytes with anionic functional groups (Edzwald and Benschoten 1990). With RO membrane filtration processes, humic substances have been regarded as a serious foulant that may lead to irreversible membrane fouling and membrane degradation (Duan 2002, Brant 2013).

The salinity of the CSG waters in Queensland, across the Surat and Bowen basins is very variable and can be between 1,000 mg-TDS/L (Dalby, Moone, Chinchilla) and 45,000 mg-TDS/L (Emerald, Blackwater, Springsure) (Klohn Crippen Berger, 2012). It has been reported that using such water for irrigation may reduce water availability for crops, as a result of its effect on crop growth (Hamawand and Yusaf 2013). High sodium, low calcium and low magnesium concentrations can significantly reduce water infiltration rate through soil (Taulis, Milke 2012).

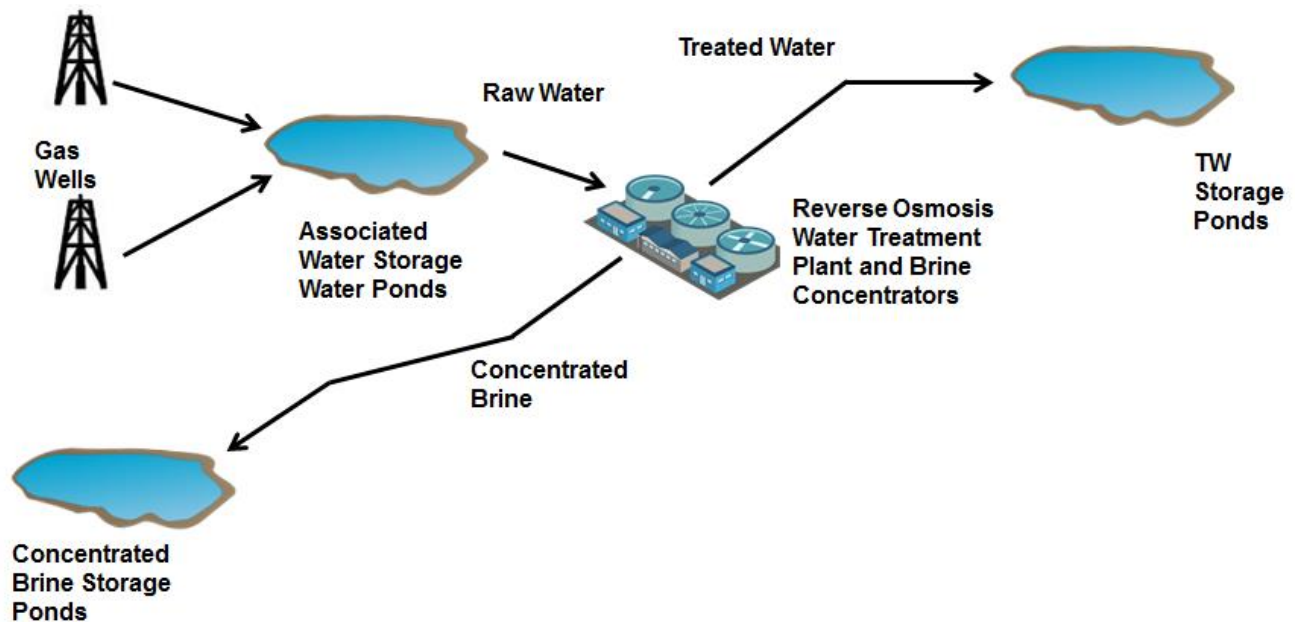


Figure 2.6 – Indicative CSG water and brine management infrastructure.

The Queensland government adopted minimum CSG water quality suitable for irrigation: as conductivity (EC) of <math><950\text{ms/cm}^3</math> as a 95<sup>th</sup> percentile over a one-year

period, sodium adsorption ration (SAR) of 6 or less for heavy soils as a 95<sup>th</sup> percentile over a one-year period; or 12 or less for light soils as a 95<sup>th</sup> percentile over a one-year period, pH within the 6.0 – 8.5. (<http://www.ehp.qld.gov.au/management/non-mining/documents/general-bua-irrigation-of-associated-water.pdf>)

Samples collected for this research, by the author, for coagulation studies discussed in chapter 5 were from CSG production wells across the Surat and Bowen basins in Queensland, show that the dominant anions are sodium, bicarbonate and chloride. The pH is typically high at around 8.4 (mean of 20 samples from 5 boreholes) and the alkalinity is relatively high (420mg-CaCO<sub>3</sub>/L). The concentrations of calcium and magnesium are low, at 1 to 10 mg/L, and sulphate is even lower (0.5 - 1 mg/L) (Steven 2007). The concentration of strontium is low between 0.5 and 2.5 mg/L, while that of barium is typically between 1 and 6 mg/L (Steven 2007), and boron, fluoride, iodide and bromide levels can also be at 1 to 5 mg/L. Total silica concentration in CSG waters is between 20 and 80 mg/L (Samuel 2011, Klohn Crippen Berger, 2012). These concentrations arise from dissolution from the local rock formations, and are often relatively high if the water has been in contact with plagioclase (Samuel 2011, Steven 2007).

### **2.4.3 CSG water desalination**

Desalination of CSG waters has become increasingly important because of the potential for beneficial use of the desalted water as a recycled water resource and for aquifer recharge (DERM Queensland). Desalination technologies, both thermal and non-thermal, require pre-treatment to prevent fouling and to enhance the proportion of water recovered. For source water of poor quality such as CSG water, pre-treatment processes can form a significant proportion of the water treatment plant. The selection of a suitable desalination technique depending on primarily on a combination of influent salinity level and the content of scaling compounds, usually silica, and the product water quality required (GE, 2010).

Medium and high salinity CSG water in Australia undergoes RO desalination to reduce TDS of the water and remove some undesirable contaminants. Additionally the reject

stream (or brine) generated by the RO system will require treatment via a set of brine concentrators and crystallisers (GE, 2010). The overall treatment train is site specific, depending on quality and quantity of CSG water produced, existing infrastructure and community needs, but generally a relatively big scale plant consists of (figure 2.7):

- Pre-treatment by coagulation, this is required to mitigate the upstream variability associated with suspended solids, DOC, metals and silica concentrations. It must be noted that coagulation is frequently used again prior to brine treatment via brine concentrators.

It is well understood principle that the operation of downstream membrane process depend on the efficiency and type of pre-treatment technologies. Figure 2.7 illustrates typical water treatment infrastructure used for CSG water treatment and residual management.

There are many factors that can influence the operating recovery of a membrane plant and cleaning of the membranes (AECOM 2012). Of particular note in the raw water design basis results are total calcium, barium, magnesium, silica, aluminium and dissolved organics which can be in concentrations that contribute significantly to solids loading and should be reduced before microfiltration. In absence of clarification process, consideration of settling time in holding ponds and the design of a floating intake structure may allow some reduction of solids and hardness concentrations, however, the dissolved organics concentrations need to be reduced to < 5 mg/L, preferably < 3mg/L after microfiltration. This can only practically occur through a combination of the following typical process steps:

- Direct coagulation & microfiltration.
- Enhanced coagulation & powder activated carbon & clarification.
- Granular activated carbon.
- Dissolved air flotation or similar.

The use of the upstream clarification processes provides /more stable operation for the MF/UF processes that is designed to protect the upstream IX and RO operations. The use of anti-scalant is not typical for MF/UF, however, with the calcium carbonate

precipitation potential and alkalinity buffering capacity of these feed waters; the use of any acid for reducing pH and therefore reducing carbonate scale potential is impractical.

A silica specific anti-scalant is a good option for the MF/UF feed allowing the MF/UF membrane technology to focus on insoluble organics and suspended solids removal with minimum carbonate scale that can be rectified during the daily and monthly cleans. A drawback of anti-scalant used to mitigate silica scaling can be increased of residual aluminium.

The use of IX has shown merit on CSG associated raw water, particularly with the legislative drivers around the phasing out the use of evaporation ponds for the purposes of RO reject/brine storage management. It should be noted, however, that the selection of resin and appropriate design parameters are critical to the success of the IX operation and more importantly the RO membrane plant. The affinity for individual ions varies for different resin types, a factor which relies on the type of acid and from which monomer the resin has been synthesised, as well as the feed pH and prevailing cations in the feedwater. Some silica removal by IX will be also an important consideration in the CSG plant. With a reliable and efficient ion exchange process upstream, it is possible to maintain between 92 to 94% RO recovery on a well-designed three stage RO system (CSG water treatment, AECOM 2013). However, monitoring of silica scale formation is key for successful high recovery operation.

Elevated silica concentrations (150 – 250 mg/L), in particular for salt recovery from RO reject streams, are undesirable and required pre-treatment prior to brine processing via brine concentrators (BC). Different technology provider companies like GEA, GE, Veolia – HDP use slightly different treatment processes for silica removal including coagulation and clarification of BC, chemical treatment, dilution of feed stream to control silica concentrations. The brine treatment process generally consists of extracting and purifying the salt and soda ash from the brine relying primary on cooling, addition of carbon dioxide, and evaporation to selectively crystallize sodium bicarbonate and sodium chloride (salt).

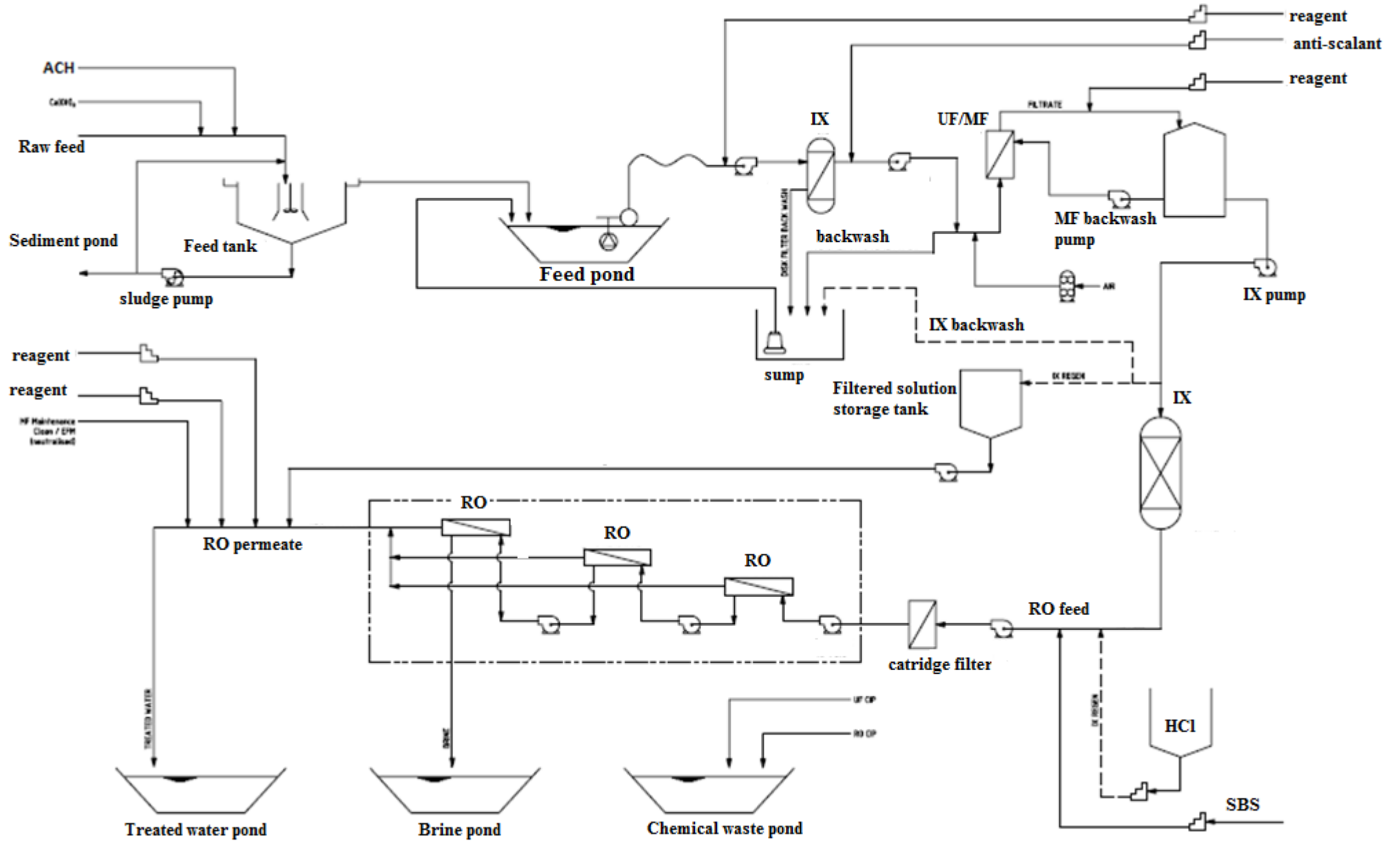


Figure 2.7 illustrates conceptual process flow of CSG water treatment

The presence of undesirable minerals in the brine such as fluoride, potassium, boron, lead, dissolved organic material and silica requires additional processing steps to keep the sodium bicarbonate and salt within specification. The primary processing operations are:

- Brine treatment for the removal of suspended solids, organics, some silica, and heavy metals, including, powdered activated carbon (PAC), redissolving of mixed salts, redissolving of secondary sodium bicarbonate, coagulation, clarification and filtration.
- Primary carbonation for the extraction of sodium bicarbonate crystals including saturation with carbon dioxide and sodium bicarbonate washing & filtration.
- Evaporation processing for extraction of clean water, sodium chloride crystals and mixed salts including de-carbonation, BC, salt crystallization and mixed salt.
- Fluoride treatment for the precipitation of fluoride and purging of boron, potassium, nitrates and other soluble impurities including a secondary carbonation step.

Of course the treatment steps described above will depend on the purity of product (final commercial product) required from the concentrated brine. Elevated silica concentrations remain a problem for all thermal desalination technologies including MED, mechanical vapour compression (MVC), BC (vertical and horizontal). Standard equipment specification requires < 50mg/L silica concentration in the feed brine. The presence of silica in the feed brine can contaminate the product salts and can cause fouling in the evaporators which would decrease the overall system efficiency and may also accumulate to levels affecting product quality. In order to reduce the amount of silica that advances into the main section of the plant, MgO usually will be added to precipitate the silica (Veolia, 2010).

#### **2.4.4 Silica removal by coagulation**

Coagulation is an effective process because of its simplicity and low cost (Healy 1994). It enables physical and chemical contaminants to be removed at an early stage of the water treatment process. Nevertheless, the introduction into the desalination sequence of

pre-treatment by coagulation could create a major new waste stream. In its untreated form, this sludge is rarely suitable for discharge into the natural environment. It is essential, therefore, that this waste stream be properly managed and the coagulation process optimised by minimising inputs of the coagulant and minimising the volume of sludge requiring additional treatment. Understanding the properties of CSG waters and selecting an effective coagulant for a particular water matrix is a key consideration for an effective pre-treatment process. It is also important to study the compatibility between the selected coagulants the membrane material (AWWA 2006, Zhao and Taylor 2007). Residual coagulant species, either aluminium or iron, may cause severe fouling of downstream membranes if not controlled (Brant 2012, Healy 2002). Proper coagulant dosing has been identified as a critical parameter for minimizing membrane fouling (Brehant et al 2002). Minimising the coagulation dose, while still achieving adequate particle aggregation, can significantly reduce fouling of downstream membranes (Healy 2001, Brehant 2002). Overdosing can result in a high residual coagulant concentration that will deposit on, and subsequently foul membranes (Brant 2012, Farahbakhsh 2004). Furthermore, coagulant overdosing may result in the generation of colloidal materials that can severely foul the downstream membranes.

A study (Gabelich 2002) reported that aluminium residuals cause colloidal fouling of RO membranes through interactions with silica to form aluminium silicates, a finding also supported by more-recent research (Howe 2006). In conjunction with microfiltration, coagulant carryover has been a problem reported in previous studies (Burashid and Hussian 2004, Gabelich 2002). Brant (2012) points out that further research is needed on the impacts of chemical addition on the generation of foulants in aqueous systems. This research may lead to the development of new agents that resist forming colloidal foulants after the coagulation process is complete.

In most industrial applications, especially in the oil and gas industry, silica will be removed by coagulation first regardless of downstream processes. Generally coagulation is a relatively effective and cheap treatment to remove silica and in particular colloidal silica (Healy 1994). The precipitation and adsorption of silica by magnesium hydroxide is also used for pre-treatment of water. Coagulation has been

considered to be the result of van der Waals attraction which draws two particles together at the moment of collision, unless opposed by a hydration barrier or by the electrostatic repulsion forces between the similarly charged particles, or both. There are, therefore, two factors that retard coagulation of silica: one being the “hydration” of the surface of the particles by a layer of water molecules hydrogen-bonded to the SiOH groups and the surrounding cloud of positive counter ions such as  $\text{Na}^+$ , forming a double layer” (Bergna 2005, Healy 1994). Coagulation aids silica removal. However, silica is “hydrophobic”, although under some conditions where salts cause coagulation it has become classed as somewhat hydrophobic (Sheikholeslami 2002). When coagulating agents are adsorbed onto the surface on membranes, the surface becomes hydrophobic. These metastable characteristics of silica affect coagulation efficiency.

Studies have reported different efficiency results for silica removal particularly from brackish ground waters, which can be similar to CSG water. Den *et al* reported using coagulants for high salinity waters (brine) ( $\text{NaCl}=11\text{g/L}$ ) containing silica, with a silica removal efficiency of up to 80%. They concluded that the optimum dose depended on both the silica concentration and the background mix in the solution, as well as the proportional removal of silica required. For higher silica concentration, higher removal efficiency can be expected (Den 2007, Stumm and Morgan 1996). They demonstrated that coagulants were particularly effective for removing colloidal silica because the colloidal particles carry strong negative charges in the neutral pH range. Cheng *et al* used a jar test to show that colloidal silica and soluble silica can be effectively removed with alum –  $\text{Al}_2\text{O}_3$  – at a rate of 30 mg/L for a 30 mg/L  $\text{SiO}_2$  feed removal was up to 50% for silica at pH 7.1 (Cheng, 2009). This indicates that it is feasible to remove both colloidal silica and dissolved silica using coagulation.

## 2.5 Conclusion

High water recoveries in RO treatment are feasible if the scaling salts are removed in pre-treatment steps. This seems to be feasible for iron and multi-valent ion scale precursor ions, but silica remains and its presence then limits water recovery. Residual aluminium concentrations in raw CSG water and post-coagulation quality can also contribute to silica precipitation as aluminosilicate. Further research is needed to define

silica residual concentrations for different water matrix in particular for CSG water in Australia, which is produced in a significant quantity in Australia, as a result of CSG development.

The present study has been designed to determine the effect of silica chemistry of silica residual concentrations in RO desalination of synthetic and CSG waters. No previous study has investigated cumulative effects of parameters such as pH, and the effects of sodium concentrations and aluminium concentrations, which present in coal seam gas water and some mining waters in Australia.

## 2.6 Objectives

The broad objective of the present study was to define factors affecting silica fouling in RO desalination of CSG waters in Australia. The scope of the problem was narrowed to focus three aspects: silica removal by coagulation, silica fouling in RO process, and structural evolution (hydrolysis and condensation processes) of dissolved silica species such as  $Q^0$ ,  $Q^1$ ,  $Q^2$ ,  $Q^3$  type surroundings by  $^{29}\text{Si}$  NMR spectroscopy.

The specific objectives of the research were to:

- (1) Develop a conceptual silica polymerisation model using  $^{29}\text{Si}$  NMR data and silica solubility results to explain silica polymerisation on RO membrane surfaces;
- (2) Review potential silica removal efficiency of coagulation and the influence of salinity on silica removal by a range of coagulants;
- (3) Identify CSG water components and coagulation residuals that influence silica solubility, and in particular lowering of silica solubility, using synthetic and field CSG waters;
- (4) Develop relationships between pH, silica concentration, and silica species present for the polymerisation of silica (silica scale formation).

## Chapter 3 Experimental method

### 3.1 Introduction

The objective of this experimental work was to develop an understanding silica polymerisation (silica precipitation) in the RO process, and in particular for RO desalination of CSG waters. Data on silica solubility was collected for a range of water compositions and pH conditions. The effects of several variables (salinity, silica concentration, pH and aluminium residual) on flux decline, water recovery, silica scale formation, and precipitation growth on the membrane surface were evaluated through the collection of RO desalination data during approximately 180 bench-scale RO silica precipitation experiments. Data was collected on synthetic and CSG waters to evaluate different water matrices and their effect on silica polymerisation. In parallel, five dissolved silica species were studied in sodium silicate solutions by  $^{29}\text{Si}$  NMR spectroscopy to gain a better understanding of the impact of sodium, aluminium and pH conditions.

This chapter describes the main analytical methods and experimental techniques used to obtain the project objectives. Additionally, sampling and analysis procedures are described for the different experiments. Limitations of each technique applicable to this research work have been also discussed at the end of each subsection.

### 3.2 Experimental design

All RO silica fouling (silica precipitation) experiments were performed with the same RO operation pressure, temperature, and membrane type. First, a set of experiments were performed with deionised water then on synthetic waters with different sodium chloride and silica concentrations, and pH values. Second, similar RO bench scale experiments were performed with CSG water. Each experiment recorded the flux decline, silica concentration in the concentrate, and conductivity rejection, turbidity was also measured. The experimental conditions for RO experiments are shown in Tables 3.1 and 3.2. For the same experimental conditions a minimum of three to a maximum of five RO runs were performed to obtain the common trends before the experimental conditions were changed. Overall one hundred and eighty one RO runs were performed.

Table 3.1 – Experimental conditions for synthetic waters

Nominal RO feed composition			Feed pH
NaCl (g/L)	SiO <sub>2</sub> (mg/L)	Al <sup>+3</sup> (mg/L)	
-	20	-	7
-	50	-	7
-	120	-	7
-	20	-	3
-	50	-	3
-	120	-	3
-	20	-	11
-	50	-	11
-	120	-	11
3	20	-	7
3	50	-	7
3	70	-	7
3	20	-	3
3	50	-	3
3	70	-	3
3	20	-	11
3	50	-	11
3	70	-	11
6	50	-	7
6	60	-	7
6	70	-	7
6	50	7	7
6	60	7	7
6	70	7	7
6	50	-	3
6	60	-	3
6	70	-	3
6	50	-	11
6	60	-	11
6	70	-	11
12.5	50	-	7
12.5	60	-	7
12.5	70	-	7
12.5	50	-	3
12.5	60	-	3
12.5	70	-	3
12.5	50	-	11
12.5	60	-	11
12.5	70	-	11
17.5	50	-	9

Nominal RO feed composition			Feed pH
NaCl (g/L)	SiO <sub>2</sub> (mg/L)	Al <sup>3+</sup> (mg/L)	
17.5	60	-	9
17.5	70	-	9
30	50	-	9
30	60	-	9
30	70	-	9
30	80	-	9
30	60	7	9
30	70	7	9
30	80	7	9
30	50	-	3
30	60	-	3
30	70	-	3
30	50	-	11
30	60	-	11
30	70	-	11
12.5	40	27.7	9
12.5	80	27.7	9
12.5	120	27.7	9

Table 3.2 – Experimental conditions for CSG waters

RO feed composition			Feed pH
NaCl (g/L)	SiO <sub>2</sub> (mg/L)	Al <sup>3+</sup> (mg/L)	
6	20	7	9
6	20	7	3
6	20	7	11
6	50	7	9
6	60	7	9
6	80	7	9
6	50	7	3
6	60	7	3
6	80	7	3
6	50	7	11
6	60	7	11
6	80	7	11
30	60	7	9
30	60	7	3
30	60	7	11
30	80	7	9
30	60	7	3
30	60	7	11
6	20	9	9
6	20	11	9
6	20	15	9
12.5	40	27.5	9
12.5	80	27.5	9
12.5	120	27.5	9

In the RO experiments silica precipitation (membrane fouling) was initiated from initially particle-free solutions. Samples collected from the recycled stream were immediately filtered through a 0.20µm filter to separate the dissolved component of silica. All samples were diluted to a final volume of 14 mL in volumetric flasks using distilled deionized water. Deionized water for dilutions was stored in 5 – 10L plastic containers over the period of the experiments to maintain the same dilution background matrix and to avoid any leakage of silica from glassware. The same deionized water was used for the preparation of standard solutions. The silica fouling trend for each experimental condition (Tables 3.1 and 3.2) was assessed by collecting stable and maximum residual (dissolved) silica concentrations results for a minimum of three to a maximum of five RO experiments. Approximately 1 – 2 % variation in the stable residual silica concentrations was allowed. Once consistent results for silica precipitation patterns were obtained, the silica concentration was slightly increased

holding all other experimental conditions constant in order to test the RO concentrate stream silica concentrations maximum and stable readings for a particular salinity water. These results are described in chapter 6. In addition, the impact of aluminium concentration (post-coagulation water quality) on silica precipitation solubility limits was also studied, and the results discussed in chapter 6.

### **3.2.1 Bench-scale RO system**

A Sterlitech CF042 laboratory scale, cross flow, membrane filtration unit was used. It was arranged with over 2.0 litres of feed storage. The feed stream was pumped from the feed storage tank to the feed inlet, figure 3.1. The feed inlet was located on the cell bottom. Flow continues through a manifold into the membrane cavity. Once in the cavity, the solution flows tangentially across the membrane surface. A portion of the solution permeates the membrane and flows through the permeate carrier, which is located on top of the cell. The permeate flows to the center of the cell body top, is collected in a manifold and then flows out the permeate outlet connection into permeate collection glassware, figure 3.2. The concentrate stream, which contains the material rejected by the membrane, continues sweeping over the membrane and collects in the manifold. The concentration then flows out the concentrate tube into the feed storage. The operational pressure was maintained at 45 bar in all runs as per Table 3.3 using a pressure regulating valve on the feed line which constant pressure feed to be maintained when the osmotic pressure increased as result of TDS increase in the recycled stream. The temperature of the water, after the main pump, was controlled to 15.5 degree by a cooling system shown in figure - 3.2.

A seawater membrane element (SW30) was sourced from DOW Chemical Company. The element was cut and accurately opened to disassemble the membrane itself from protective materials. Then the membrane sheets were cut from the permeate tube and then stored with sodium meta-bisulphate (0.1% concentration) and in plastic bags. The plastic bags were stored in the laboratory fridge at approximately 4°C. During this time the plastic bags and sodium meta-bisulphate were replaced with the new bags each two-three weeks to keep the membrane samples in good condition. Any detected oxidised membrane samples were removed from the plastic bags and disposed. Prior to each RO

experiment, 4 x 8 cm of membrane sample was cut and installed in the base of the RO test cell. The new membrane was compressed for 1 hour with deionised water at the operational pressure of 45 bar prior to each RO experiment. To avoid any abrupt pressure or cross-flow variations during start-up, so as to prevent possible membrane damage, the feed flow was increased gradually over 30-60 second time frame. The specified cross-flow velocity was achieved gradually over 20-30 seconds.

Table 3.3 – RO operating parameters and maximum operation limits.

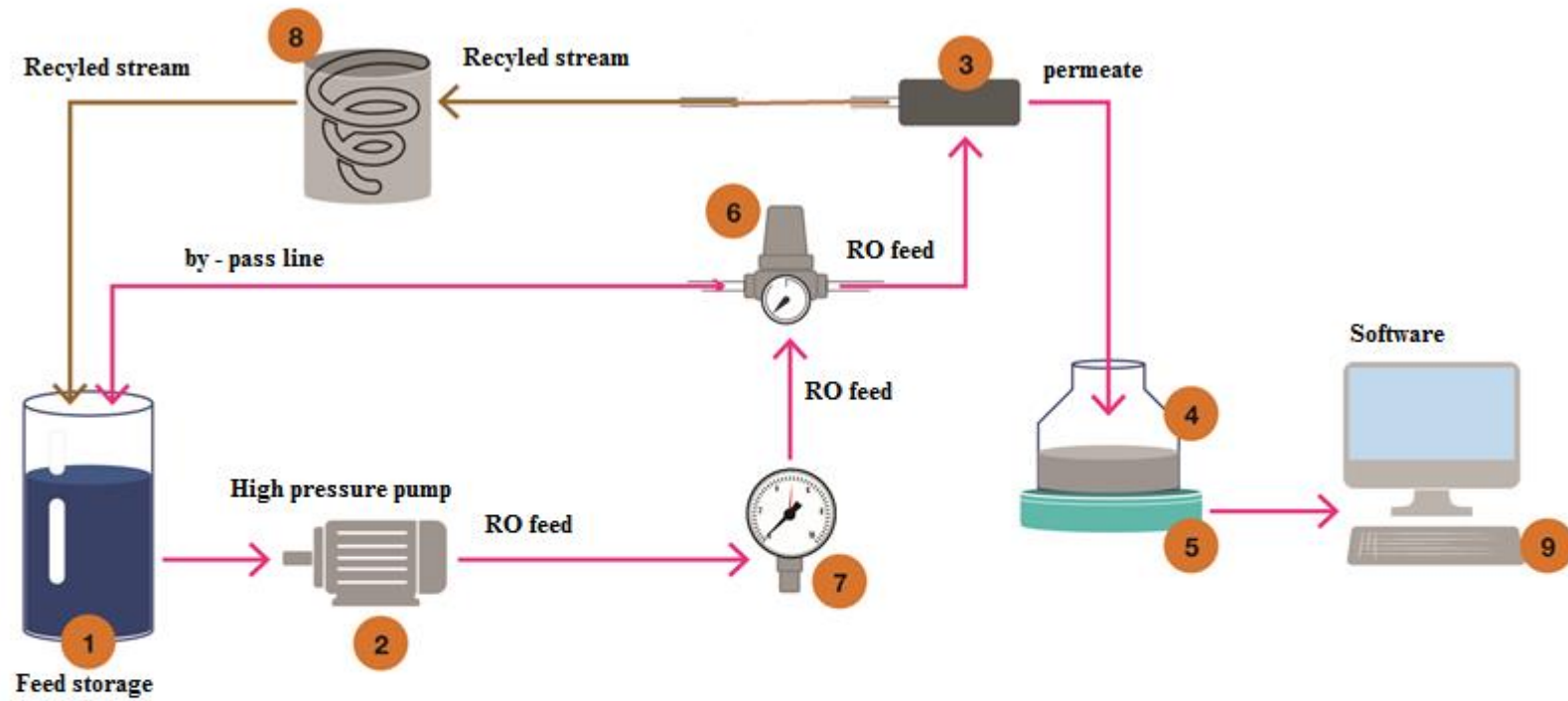
Parameter	Operation	Operation limits
Effective Membrane Area	42 cm <sup>2</sup>	-
Maximum feed turbidity (the feed was filtered with 0.45µm filter or similar UF filters)	< 1 NTU	1 NTU
Maximum pressure	45 bar	69 bar
Maximum operating temperature	15.5°C	45°C
pH range, continuous operation	3 - 11	2 - 11
Flow range	1 – 6 L/m <sup>2</sup> /h	3.6 m <sup>3</sup> /h
Flux range	10 – 60 L/m <sup>2</sup> /h	-

The RO system, figure 3.1, includes a high pressure pump, frequency controller to vary the pump speed, cooler and feed tank storage. The system also included a check valve for pressure control allowing smooth operation and constant pressure over the period of the experiment. All experiments were conducted in a continuous flow pilot system with concentrate recycling and continuous removal of the permeate. A sharp decline in permeate flow rate denoted the solubility limits and scaling thresholds had been reached and this was confirmed by chemical analysis of the recycled concentrate stream. ROSA software was used to estimate the osmotic pressure increase across the experiments so that the required experimental pressure could be estimated. The required operating pressure was set at 45 bar as a result of these estimates. The experimental RO system was designed to enable unattended overnight operation with constant withdrawing of permeate and recycling of concentrate.

Analyses of flux decline results, caused by silica deposition and scaling processes, and based on examination of the decay in permeability at various silica concentrations

prevailing on the membrane surface. Reinforcing data for the on-set of silica fouling (polymerisation and precipitation) was gathered from dissolved silica concentrations (declined dissolved silica concentrations) in the recycling stream with data obtained from ICP spectroscopy and/or silica molybdenum method (Hatch) and later by scanning electron microscopy (SEM) membrane examination. The experimental silica concentration data was compared to the theoretical silica concentration in the concentrate recycling stream. The theoretical concentrations we calculated using the initial feed silica concentration and assuming 100% rejection of silica and no scaling. When the theoretical and experiment values were no longer consistent, with the experimental values being lower than the theoretical values, scaling was assumed to occur.

All experiments reported in this study were conducted at constant pressure and with subsequent flow rates in the range of 1.3 – 1.7 L/h (flow velocity ~ 2.5m/s) given by the Hydro-cell M-03 pump installed in the system. The feed flow to the RO unit was set by the constant pressure and resistance across the cell. The filtration times varied between 8 and 36 hours due to the large variation in osmotic pressure between experiments with low and high salinity that effected the operational flux, and because all experiments were run until the water recovery reached approximately >70%.



- |   |   |
|---|---|
| 1. Feed Tank                                      | 6. Pressure Control Valve                     |
| 2. High Pressure Feed Pump                        | 7. Pressure Gauge with 'T' 3/8 Tube connector |
| 3. RO Unit  | 8. Cooler                                     |
| 4. Permeate Collector                             | 9. Computer                                   |
| 5. Electronic Balance for measuring permeate mass |   |

Figure 3.1 – RO system – experimental arrangement and main equipment used

During filtration significant scaling formation was sometimes observed from the operating conditions, when pressure dropped quickly and the experiment was terminated. The membrane was carefully removed from the RO unit for examination for any silica scale formation. SW30 high salt rejection commercial seawater RO membrane by DOW Film Tec was used throughout all the experiments, and characteristics of the 4” membrane that was dissected are listed in Table 3.4.

Table 3.4 – Dow FilmTec SW30HRLE membrane characteristics

DOW Filmtec SW30HRLE	Membrane permeability (L/m <sup>2</sup> /hr/bar)	Stab. salt rejection for standard feedwater conditions (%)	Min salt rejection for standard feedwater conditions (%)	Max feed flow rate (m <sup>3</sup> /h)
Seawater	1.16 – 1.32	99.7	99.4	2.5

All total dissolved solids (TDS), electrical conductivity (EC), temperature and pH values were measured with a Hach model H2500 combined conductivity-pH-temperature meter. Conversion of conductivity to TDS was undertaken using the internally calibrated conversion within the portable Hach meter based on standardised NaCl solutions. For quality control TDS measurement for selected samples was analysed using standard method described in section 3.4.

The total concentrations of cations (Na<sup>+</sup>, Mg<sup>2+</sup>, Ca<sup>2+</sup>, Sr<sup>2+</sup>, Ba<sup>2+</sup>, Al<sup>3+</sup>) and silica were determined by inductively coupled plasma (ICP) spectroscopy (OES). Reactive silica concentrations were determined by the silico-molybdate method using a Hach spectrophotometer DR 2000/2010 as described in details in 3.4.3 of this chapter.

To perform total and dissolved silica analysis, samples were taken from the recycling stream storage (RO feed storage) at each 2.0 - 2.5% of permeate recovery, depending on the experimental conditions, and in particular the flux.



Figure 3.2 – RO experimental apparatus at the Victoria University, Melbourne (Figure 3.1)

### 3.3 RO feed experimental solutions

Synthetic water prepared in the laboratory and natural CSG waters sourced from CSG production fields in Queensland, Australia were used for RO experiments. Specific details and results obtained on synthetic and CSG waters are described in chapter 6.

#### 3.3.1 Synthetic solutions

Ten litre batches of various sodium chloride concentration solutions were prepared by dissolving sodium chloride in deionised water (Milli-Q, Millipore Corp.). Waters were spiked with silica and aluminium chloride as required. Sodium silica (water glass,  $\text{Na}_2\text{SiO}_3$ , composition ratio - water 62.9% and silicic acid/sodium salt 37.1%) from STAR<sup>TM</sup> Sodium silicate solution PQ Corporation, US was used. Analytical grade sodium chloride and analytical grade aluminium chloride ( $\text{AlCl}_3 \cdot 6\text{H}_2\text{O}$ ) were obtained from the Sigma-Aldrich Chemical Co, China. pH adjustments were made using 0.1% HCl and 0.1% NaOH. De-ionised water was obtained from a laboratory reverse osmosis unit (conductivity < 1  $\mu\text{S}/\text{cm}$ ). The RO feed solution was filtered via a 0.45 $\mu\text{m}$  filter (cellulose acetate; ADVANTEC<sup>®</sup> Membrane filter, Toyo Roshi Kaisha, Ltd, Japan). The inorganic content of all synthetic solutions were confirmed by ICP analysis (Shimadzu ICP5000).

The procedure for preparing 10 litres of synthetic water solutions was as follows:

- Dissolve 5, 15, or 30 g of laboratory grade sodium chloride into 10 litres of deionized water.
- Vacuum filter solution successively through 0.2 $\mu\text{m}$  filter (cellulose acetate; ADVANTEC<sup>®</sup> Membrane filter
- Dissolve sodium silicate solution into deionised water to obtain a silica concentration of 90,000 mg/L.
- Add a calculated volume of concentrated dissolved silica into a freshly prepared sodium chloride solution to achieve the desired silica concentration.
- Prepare aluminium chloride solution of 130mg/L for addition of necessary amount to sodium chloride solutions for aluminium studies.

- Confirm & verify the final concentration of silica, sodium chloride and aluminium by ICP analysis.

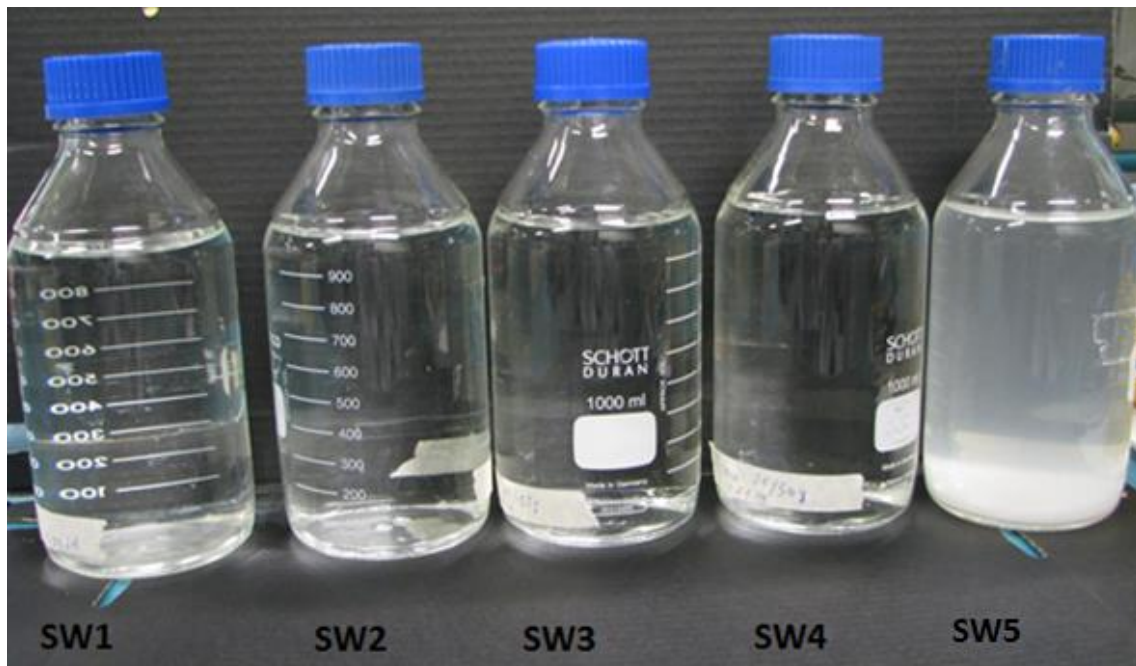


Figure 3.3 – Synthetic waters with different salinity and silica concentrations outlined SW1 – TDS=6g/L, SW2-TDS=7.5g/L, SW3-TDS=12.5g/L, SW4=30g/L and SW5-TDS=60g/L.

The water shown as SW5 in figure 3.3 prepared for visual observation of the highest concentrated final solution, which occurred after 50% permeate recovery with RO of SW4 feedwater.

### 3.3.2 CSG waters

The CSG water was twice sourced from the production fields in Queensland during this research work. CSG water was sampled on the production fields in Queensland during January to May 2013 and used for coagulation studies in Brisbane, described in chapter 5. In July 2014 CSG water was sourced from Queensland and delivered to Victoria University, Melbourne for coagulation and RO experiments. Both waters were from the Surat basin. On the fields in 2013, CSG water samples were collected from six production wells near Dalby, Tipton and Kogan North in Queensland, Australia. Further samples were collected at the same time from a storage dam holding CSG water from a

number of production wells prior to treatment. This was to make a combined sample representative of what might be delivered to any “full-scale” water treatment plant.

The wells were pumped for 30 minutes before sample collection to ensure, as far as possible, that the water was representative of local conditions. Both the ball valve and connecting PVC tube were flushed thoroughly with the well water prior to sampling. Low density polyethylene containers were used as they can be sealed tightly without any other material making contact with the sample. Three 25 litre drums were collected from each well using this technique. The samples themselves were then mixed in the laboratory to form a single “grand” composite. The pH, conductivity and water temperature were recorded on site immediately after extraction. The water from the storage dam was collected as grab samples from three different points in the dam, 1m from the edge and the samples then mixed in the laboratory. All of the samples were delivered to the laboratory within 24 hours of collection and no form of chemical preservation was undertaken. All of the samples were refrigerated at between 4 and 5°C while stored.

Table 3.5 – CSG water quality

Parameter	Unit	CSG groundwater composite (2013)	CSG storage dam water composite (2013)	CSG groundwater composite (2014)
Suspended solids	mg/L	340	120	102
Turbidity	NTU	81.9	60	36.5
Temperature	°C	25	26	20.5
Conductivity	µS/cm	7200	14200	8100
Total Calcium	mg/L	8.4	9.0	11.75
Dissolved Calcium	mg/L	3.4	4.2	9.3
Total Magnesium	mg/L	4.2	5.0	5.3
Dissolved Magnesium	mg/L	3.6	3.2	3.2
Total Barium	mg/L	1.2	2.3	0.05
Dissolved Barium	mg/L	0.9	1.1	0
Total Strontium	mg/L	2.1	2.1	0.44

Table 3.5 – CSG water quality (continue from page 13)

Parameter	Unit	CSG groundwater composite (2013)	CSG storage dam water composite (2013)	CSG groundwater composite (2014)
Dissolved Strontium	mg/L	1.3	1.2	0
Total Silica (SiO <sub>2</sub> )	mg/L	21.0	25.0	22.7
Dissolved Silica (SiO <sub>2</sub> )	mg/L	16.8	20.0	11.9
TOC	mg/L	31	280	115
DOC	mg/L	19	205	7.1
pH	-	8.43	9.40?	9.15
DO	mg/L	-	0.7	-
Alkalinity ( as CaCO <sub>3</sub> )	mg/L	1123	1200	1211



(a)

(b)

Figure 3.4 (a) – CSG water sourced from the field, (b) – raw and filtered CSG waters via 0.45µm filter.

Typical CSG water composition find in Australia included in Appendix A.

### 3.4 Analytical methods

The analysis of synthetic and CSG waters for its dissolved and colloidal components were part of the research described in this volume. Conductivity, alkalinity, major cations and anions, turbidity, DOC and TOC, temperature and pH were measured as per Standard Methods. pH and temperature were also measured on field. TDS was measured by a Hach conductivity meter (H2500) at constant temperatures. Then correlation graphs for sodium chloride were used to confirm TDS. For quality assurance, selected samples were measured by drying the water sample in a pre-weighing container (as per standard method) and weighing the container after evaporation of the sample. However, in this measurement the CO<sub>2</sub> of the bicarbonates has come off and correction must add the bonded CO<sub>2</sub> to initial alkalinity. Alkalinity analysis was performed by NATA accredited laboratory (ALS Environmental in Canberra, Australia). Alkalinity is measured by the sum of alkaline (Na, K) or alkaline-earth (Ca, Mg) bicarbonate, carbonate and hydroxide anions. When the pH is greater than 8.3 as the case for CSG water, there may be a simultaneous presence of carbonates and even alkaline hydroxides. Two measurements were made in succession.

The organic content of the raw waters was determined by a combustion TOC (DOC) analyser (Shimadzu TOC5000). This is the measurement of the carbon contained in organic matter. It was obtained by burning the organic matter and measuring the of CO<sub>2</sub> produced. Other specific instruments and techniques used discussed in the subsequent sections.

#### 3.4.1 Measurement of pH and conductivity

Solution pH was measured using a Hach pH meter, electrode (Model 8175) automatic temperature correction probe (Model 917005). The probe was calibrated daily using standard pH3, pH7 and pH10 buffer solutions. Conductivity of solutions was measured with the same Hach meter. The probe was calibrated weekly using standard conductivity solutions for low and high range conductivity measures. Following each analysis the pH and conductivity probes were washed with clean water to remove any silica gel and salt deposition, which was frequently observed on glassware and laboratory equipment.

### **3.4.2 Inductive coupled plasma (ICP) spectrometry**

Inductively coupled plasma optical emission spectrometry (ICP-OES) is an analytical technique, which was specifically used to determine the concentration of silicon ( $\text{Si}^{2+}$ ) and metals and metalloids at trace, minor and major concentrations in CSG and synthetic waters.

The main principle of the technique is that an aqueous sample is converted to aerosols via a nebulizer. And then the aerosols are transported to the inductively coupled plasma which is a high temperature zone (8,000 – 10,000°C). The analytes are heated (excited) to different (atomic and /or ionic) states and produce characteristic optical emissions (light). These emissions are separated based on their respective wavelengths and their intensities are measured using spectrometry. The intensities are proportional to the concentrations of analytes in the aqueous sample.

#### **3.4.2.1 Standard preparation**

Multi-element working standard solutions were prepared for Ca, Mg, Ba, Al, Si, Na, and Sr by transferring different amounts of primary standards into 5 volumetric flasks. Multi-element working standards were prepared in the range 0.01mg/L to 60mg/L. The ICP standards were prepared approximately once per two weeks.

#### **3.4.2.2 ICP calibration**

Prior to each sampling run, the ICP was calibrated with 5 different strength standard solutions, starting with a deionised water sample. The standardisation was carried out each day prior to performing ICP analysis.

#### **3.4.2.3 Sample preparation**

After collection of samples, the samples were filtered through 0.2 $\mu\text{m}$  filters and diluted with deionised water to ensure the concentrations were within the calibration range of the ICP. Then the diluted sample was spiked with a drop of HCl (0.1% concentration). ICP analysis was performed with and without HCl addition (0.1% HCl) to compare the result on dissolved silica concentrations determined by ICP. The general ICP protocol included:

- 1.5 - 2ml sample was collected each time from the RO recycling solution, then the sample was filtered through 0.2µm filter and 0.5 or 1ml of filtered sample was discharged to 14 mil plastic tubes for ICP analysis. This volume was diluted with the required volume of deionised water.
- Dilution factors, to bring more concentrated analytes into the ICP specified range, were used in the range of 10 to 50 depending on the solution analysed (total dissolved solid (TDS) must not exceed 0.1 g per 100ml of solution);
- Minimum 10 ml sample was prepared for ICP run to allow the system to analyse it twice;
- Samples were measured with standardization blanks, drift control samples, and quality control samples;
- After a batch of samples was measured, the data were downloaded to an Excel spreadsheet for analysis.

The major limitation of this method was that dilution of samples could introduce an error into a final calculation. To reduce the significance of errors arising from dilution, the samples were analysed with different dilution factors to verify the results. The maximum predicted error was calculated to be < 10%. Therefore, the errors do not affect the trends in the data nor the overall conclusions presented in the thesis. In the remainder of this research, the error is only mentioned where is considered to be useful for helping to explain trends in the data.

### **3.4.3 Silico-molybdate method**

The silicomolybdate method developed by HACH Company (US) was used to analyse “soluble or reactive silica” in the solutions. Soluble or reactive silica represented by the monomer silica groups react with molybdate reagent within 10 minutes. Silica and phosphate in the sample react with molybdate ion (ammonium molybdite) under acidic conditions to form yellow silicomolybdic acid complex and phosphor-molybdic acid complexes. Oxalic acid is added to destroy the molybdophosphic acid leaving silicomolybdate intact, and thus eliminating any colour interference from phosphates. Silica is then determined by measuring the remaining yellow colour at 452 nm. It must

be mentioned, however, that this method measures “soluble silica” and this term includes not only the monomer silicic acid but also oligomer species such as dimers, trimers, tetramers, etc. The detectable concentration range of this system is 0 - 100 ppm.

A limitation of the method is that it is not sensitive in the pH range 9 to 15. According to the Stumm’s diagram (Stumm and Morgan 1976) a number of monomer silica species dramatically increases from pH9. Other disadvantage of this method is the detection range limit. If a sample requires dilution because the silica concentration exceeds the detection limit, then colloidal silica present in the sample could release monomeric silica groups and thereby influence the accuracy of the result.

### **3.5 Coagulation experiments**

Pre-treatment by coagulation is an important process to reduce total and dissolved silica concentrations before RO systems. Coagulation at the optimal dose can effectively remove suspended solids, turbidity, colloidal matters, DOC, total and dissolved metals and silica. Coagulation was performed with three coagulants (aluminium chlorohydrate (ACH), ferric chloride and alum sulphate) and an extensive range of doses were explored both in the field and in university laboratories. The impact of salinity on coagulation efficiency was studied using synthetic waters as described in chapter 5, while field tests used CSG water.

#### **3.5.1 Chemicals and reagents**

The coagulants used in the tests were aluminium chlorohydrate (ACH) –  $\text{Al}_2\text{Cl}(\text{OH})_5 \cdot 2\text{H}_2\text{O}$  – aluminium sulphate ( $\text{Al}_2(\text{SO}_4)_3 \cdot 18\text{H}_2\text{O}$ ) and ferric chloride ( $\text{FeCl}_3 \cdot \text{FeCl}_3 \cdot 2\text{H}_2\text{O}$ ). All chemicals used were of analytical reagent grade and were obtained from the Sigma-Aldrich Chemical Co, China. The ACH reagent comprised 23 to 24% w/w Al, the ferric chloride 14 to 15% w/w Fe (III) or 39 to 47% w/w  $\text{FeCl}_3 \cdot 2\text{H}_2\text{O}$ , and the aluminium sulphate 7.5 to 8% Al or 49 to 52% w/w  $\text{Al}_2(\text{SO}_4)_3$ . pH adjustments were made using 10% HCL and 10% NaOH. Laboratory reagent grade “DARCO” powdered activated carbon (PAC) was supplied by Chem-Supply, and had a nominal grain size of 45  $\mu\text{m}$ .

### 3.5.2 Solution compositions

The three synthetic saline CSC waters were prepared based on typical CSG water quality (groundwater composite). De-ionised water was obtained from a laboratory reverse osmosis unit (conductivity < 1  $\mu\text{S}/\text{cm}$ ). Humic acid was obtained as a commercial grade solid (Aldrich Chemical Company). Stock humic acids solutions were prepared from 1 g of dry humic acid product dissolved into 1 L deionised water. Calcium, magnesium, barium and strontium reagents were analytical grade (Merck), and these components were added to mimic the CSG water quality. A batch of low salinity water was prepared and spiked with humic acid and metals then the volume was divided into three equal volumes. Medium and high salinity waters were prepared by addition of sodium chloride to the required concentrations. The organic content of the raw saline waters was determined by a TOC analyser (Shimadzu TOC5000). Specific volumes of stock humic acid solution were added to produce “synthetic water” with a TOC of 31mg/L. The solution was then further filtered using a 0.45  $\mu\text{m}$  membrane and analysed for DOC concentration. ICP (Shimadzu E-9000) was used for total metals and silica analysis. Dissolved metals were determined by ICP following filtration through a 0.2  $\mu\text{m}$  filter. The water quality of the composite samples used in the tests are summarised in Table 3.6.

Table 3.6 – Water quality analysis for composite samples

Parameter	Unit	CSG synthetic Low salinity	CSG synthetic Medium salinity	CSG synthetic High salinity
Suspended solids	mg/L	335	330	333
Turbidity	NTU	73.7	68.6	76
Temperature	$^{\circ}\text{C}$	19	19	19
Conductivity	$\mu\text{S}/\text{cm}$	1800	6880	45100
Total Calcium	mg/L	8.4	8.4	8.4
Total Magnesium	mg/L	4.2	4.2	4.2
Total Barium	mg/L	1.2	1.17	1.2
Total Strontium	mg/L	2.1	2.1	2.1
Total Silica	mg/L	21.0	21.0	21.0
Dissolved Silica	mg/L	16.8	16.8	16.8

TOC	mg/L	31	31	31
DOC	mg/L	20	20	20
pH	-	7.8	9.6	9.7
Alkalinity (CaCO <sub>3</sub> )	mg/L	1227	1227	1227

*\* Temperature of the water measured in the fields (January 2013)*

### 3.5.3 Apparatus and procedures

Six 1 litre beakers were each filled with sample water and placed in a flocculator (SW1 Stuart Scientific, Figure 3.5), as shown in Figures 3.6 to 3.10. Initially, the solutions were stirred at 150 rpm for 2 minutes while coagulant was added, in order to cause flash mixing. They were then stirred at 30 rpm for 13 minutes, before mixing was stopped. After 30 minutes of settling, 500 ml of supernatant was siphoned into 500 ml HDPE bottles for testing.

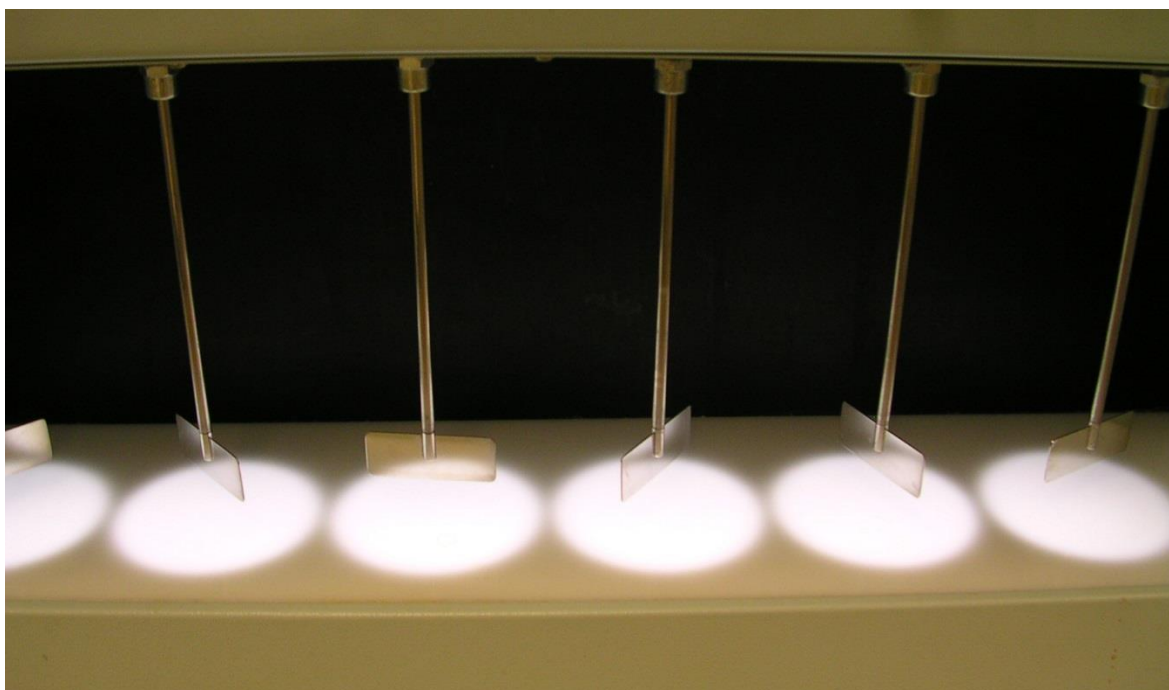


Figure 3.5 – Coagulation experimental equipment (Stuart Scientific): mixers

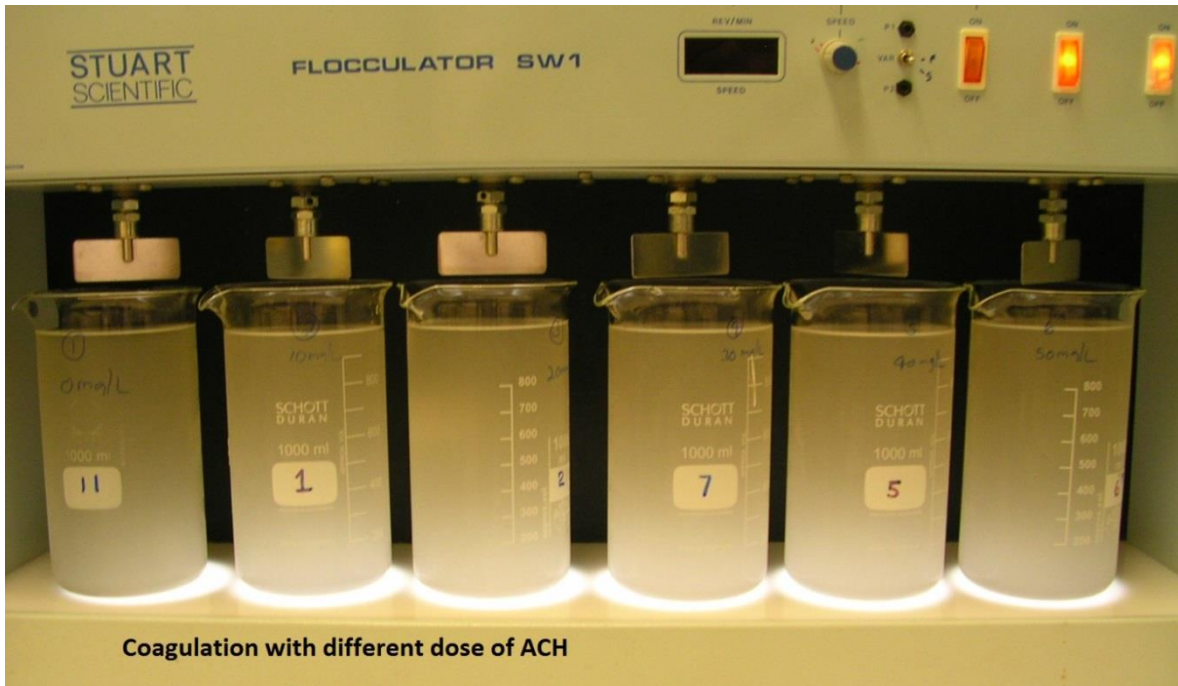


Figure 3.6 – Coagulation of CSG water (2013) in the flocculator SW1 (Stuart Scientific) with ACH at doses of 0, 10, 20, 30, 40, and 50 mg/L after 15 minutes of experiment



Figure 3.7 – Coagulation of CSG water (2013) in the flocculator SW1 (Stuart Scientific) with aluminium sulphate at doses of 0, 10, 20, 30, 40, and 50 mg/L after 10 minutes from the start of experiment.



Figure 3.8 – Coagulation of CSG water (2013) in the flocculator SW1 (Stuart Scientific) with aluminium sulphate at doses of 0, 10, 20, 30, 40, and 50 mg/L after 20 minutes from the start of experiment.



Figure 3.9 – Coagulation of CSG water (2013) in the flocculator SW1 (Stuart Scientific) with aluminium sulphate at doses of 0, 10, 20, 30, 40, and 50 mg/L after 45 minutes from the start of experiment.

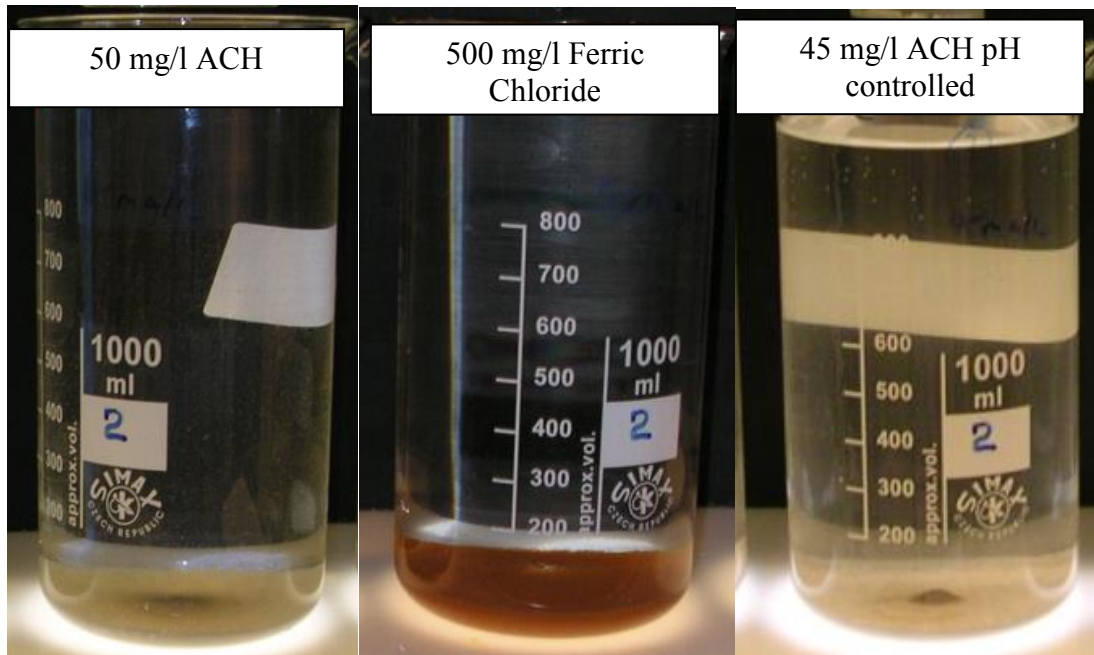


Figure 3.10 – Coagulation of CSG water (2013) by 50 mg/L ACH, 500 mg/L ferric chloride and 45 mg/L ACH at pH 6.5 for silica and DOC removal after 45 minutes from the start of experiment.

The samples were dosed with coagulant at concentrations of between 10 and 100 mg/L, in order to determine the best dose. As neither visible floc formation nor substantial turbidity removal occurred when using ferric chloride at the initial set of coagulant dosing concentrations, the concentration range investigated for this species was subsequently increased to 100 to 800 mg/L.

The first coagulation experiments were conducted at the “natural” pH (8.4) over a range of coagulant doses with the aim of investigating coagulation efficiency at raw water pH and determining the best process chemical concentration in that circumstance. During these trials, the concentrations of suspended solids, turbidity, DOC, total Ca, Ba, Sr, Mg, and Si, were recorded for both the feed and treated waters. ICP technique was used to analysis total and dissolved metals and silica concentrations.

For the pH controlled tests, an appropriate volume of sample was chosen to lower the pH at once using hydrochloric acid to ensure consistency between jars. pH controlled testing was carried out at pH 6.5. To improve DOC removal, powdered activated carbon

(PAC) slurry was added to 500 ml of supernatant water after coagulation. The PAC was boiled in deionised water to ensure that it was fully dispersed before use, and weighed doses of carbon slurry (0.5, 1.0, 2.0 and 3.0 g) were mixed into 500 L of supernatant sample by stirring at 140 rpm for 2 minutes.

#### **3.5.4 Coagulation process and salinity**

Coagulation processes can be studied by two common methods – jar testing and zeta potential. An advantage of the jar test method compared to zeta potential measurements is the ability to visually observe the physical-chemical processes during each stage of the process - mixing, settling, and decanting, and to observe changes in dispersion, colour removal, clarification and floc formation during these stages. This is especially important for natural CSG water as it has a slightly yellow colour and included very fine dispersed clay-like particles.

The current understanding of particle aggregation in coagulation processes derives from the work of Smoluchowski (1978) and Stumm and Morgan (1976). Coagulation of turbidity in water treatment by iron and alum salts occurs predominantly by two mechanisms: (1) adsorption of hydrolysis species on the colloid causing charge neutralisation, and (2) sweep coagulation where particles are enmeshed with the precipitating hydroxide. For example the reactions that precede charge neutralisation with alum are extremely fast and occur within microseconds without formation of Al(III) hydrolysis polymers and within 1s if polymers are formed. The formation of aluminium or iron hydroxide precipitate before sweep coagulation commences is slower and occurs in the range of 1 to 7s (Smoluchowski 1978). An analysis of two modes of coagulation implies that for charge neutralisation, rapid dispersion (less than 0.1 s) of the coagulants in the source water stream is imperative so that the hydrolysis products that develop in 0.01 to 1 s will cause destabilisation of the colloid.

#### **3.6 Membrane examination**

All RO membranes were examined to evaluate the level of fouling. Scanning electron microscopic (SEM) (Cambridge Instrument model 360, Leo Electron Microscopy, Thornwood) was conducted at the Victoria University and Deakin University, Institute for Frontier Materials, Geelong. Energy-dispersive spectroscopy (EDS) (Model

QX2000, Oxford Instrument, Concord, Mass) was conducted in concert with the SEM at the Deakin University, Institute for Frontier Materials, Geelong.

### **3.6.1 Scanning Electron Microscopy (SEM)**

Scanning electron microscopy (SEM) was used to examine membrane surface morphology and silica scale formation. Membrane samples were air dried in clean plastic lab ware for at least 48 hours priority to analysis. Membrane samples (8 x 8 mm square) were prepared for top surface views by cutting a small piece of membrane and then attaching it to an aluminium mount with double sided sticky tape. Prior to the examination of the membrane surface, samples were coated with a thin, gold film with a thickness ranging from a few to 10 nm.

The sample of the membrane under examination was placed within a specially designed copper holder. When a primary electron beam scans over specimens, secondary electrons (SE) and backscattered electrons (BE) are emitted from the specimen. Intensity of SE or BE is converted into brightness on the monitoring display and shows the morphology of the specimen surface. SEM images have two advantages over the optical microscope - very high magnifications are possible and a large depth of focus can be obtained. The main structures of SEM are an electron gun, lenses, specimen chamber, which are evacuated to high vacuum with the evacuation system. Electron beam generated with an electron gun is focused on the specimen. Specimen surface is scanned with the electron beam in X-Y directions. By the scanning of an incident electron beam on the specimen, secondary electrons (SE) and backscattered electrons (BE) are emitted from the specimen surface. SE and BE are detected as a signal and the morphology of the specimen surface is converted in to an image on the monitor display.

### **3.6.2 Energy Dispersive Spectroscopy (EDS)**

EDS is an analytical technique used for the elemental analysis of the chemical elements deposited on the RO membrane surface. This technique is based on X-ray fluorescence spectroscopy which relies on the interactions between electromagnetic radiation and matter.

The analysis of the X-ray emission spectra by the matter will change according to the elements present in the sample. EDS gives an elemental composition of the surface deposition and was used extensively in this research.

The following EDS detector and detector conditions were used: “FEI Quanta 3D FEG FIB-SEM, fitted with an Energy Dispersive X-ray (EDX): Apollo detector. The beam voltage and current were 20 kV and 1.2 nA during EDS spectra acquisition respectively, for a working distance of 10 mm. The data were analysed on the EDAX Genesis software. Electron micrographs were acquired on the same apparatus but at a beam voltage of 5 kV and a beam current of 0.2 nA at the same working distance. This was performed to minimize charging on the surface of the materials.

The limitation of this technique is that if a surface has a complicated morphology, too thin a coating may cause charging because the coating film loses its continuity. If a coated film is thick, this hides fine structures on the specimen surface; therefore, a thin conducting film is desirable. In general, a coated film is prepared to be a few to 10 nm in thickness. Multiply samples of the same membrane were examined to confirm consistent surface images and results across the membranes.

### 3.7 <sup>29</sup>Si Nuclear Magnetic Resonance (<sup>29</sup>Si NMR)

Table 3.7 – <sup>29</sup>Si NMR shift observed for the initial concentrated sodium silica solution and corresponding relative quantities of silicon in each Q<sup>n</sup> type surrounding.

Silica species (type surrounding)	Q <sup>0</sup>	Q <sup>1</sup>	Q <sup>2</sup>	Q <sup>3</sup>	Q <sup>4</sup>
Formula & name group	SiO <sub>4</sub> Monomer “Neso”	(SiO <sub>4</sub> ) <sub>2</sub> O Dimmer	(SiO <sub>4</sub> ) <sub>3</sub> Dimmer	(SiO <sub>4</sub> ) <sub>n</sub> Trimmer	(SiO <sub>4</sub> ) <sub>n</sub> Tetramer “Glasberg”
Chemical shift (ppm)	-67.37	-80.12	-88.32	-97.31	-108.21

Given that RO scaling involves precipitation-dissolution (condensation-hydrolysis) reactions of dissolved silica species, metals and inorganic constituents in water, <sup>29</sup>Si

NMR spectroscopy was used to study dissolved silica species. The technique is useful to gain an understanding of the behaviour of dissolved silica species identified in sodium silicate solutions, under the studied effects influencing silicate precipitation on the membrane surface. The sodium silicate environment provides a homogeneous distribution of colloidal silica. Silica in the sodium chloride environment presents in two domains - colloidal and dissolved groups. Moreover, silicon spectra of dissolved silica species in the sodium silicate system can be extracted without shielding of them by other chemical elements. Table 3.7 shows formulas and chemical shifts of each dissolved silica species studied, namely  $Q^0$ ,  $Q^1$ ,  $Q^2$ ,  $Q^3$  and  $Q^4$ . The main information derived from  $^{29}\text{Si}$  NMR spectra is the chemical shift, the intensity (peak area) or proportion of each species. The  $^{29}\text{Si}$  chemical shift is determined by the number and type of tetrahedral framework of atoms connected to tetrahedral silicon atoms, Table 3.7. The spectrum thus allows the detection of the number of structurally equivalent kinds of silicon atoms of various Si-O units in silicates. Meaningful trends of different silica polymerisation paths could be constructed as a result of these studies.

### **3.7.1 Experimental design**

Four types of studies were performed and are summarized in Table 3.8 - effect of dilution with deionised water, dilution with 1000 mg/L sodium chloride, dilution with 130 mg/L aluminium chloride and the effect of pH at pH3, pH9 and pH10-11.5.

Table 3.8 – <sup>29</sup>Si NMR Experimental solutions and pH conditions

Effect of dilution SiO <sub>2</sub> :Na <sub>2</sub> O:H <sub>2</sub> O x H <sub>2</sub> O		Effect of sodium chloride SiO <sub>2</sub> :Na <sub>2</sub> O:H <sub>2</sub> O x NaCl (1000mg/L)		Effect of aluminium SiO <sub>2</sub> :Na <sub>2</sub> O:H <sub>2</sub> O x Al <sub>2</sub> Cl <sub>3</sub> (130mg/L)		Effect of pH (pH3, pH9, pH11) SiO <sub>2</sub> :Na <sub>2</sub> O:H <sub>2</sub> O x H <sub>2</sub> O	
<i>Experimental solutions silica concentration (Si/M molar ratio) &amp; pH of the solution</i>							
Si/M molar ratio	pH	Si/M molar ratio	pH	Si/M molar ratio	pH	Si/M molar ratio	pHs
1.7	11.56	1.7	11.48	1.7	11.48	-	-
-		-	-	1.61	10.67	-	-
1.55	11.55	-	-	1.55	10.63	-	-
1.41	11.54	-	-	1.41	10.23	-	-
1.31	11.53	-	-	-	-	-	-
1.21	11.53	-	-	-	-	-	-
1.14	11.52	1.14	11.53	1.14	10.14	-	-
0.85	11.50	0.85	11.51	0.85	10.16	-	-
-	-	-	-	0.77	10.13	-	-
0.67	11.49	0.67	11.49	0.67	10.13	0.67	2,3, 9,9.5, 10.5
-	-	-	-	-	-	0.5	2,3, 9,9.5, 10.5
-	-	0.49	11.48	-	-	0.4	2,3, 9,9.5, 10.5
-	-	0.43	11.48	-	-	0.25	2,3, 9,9.5, 10.5
0.29	11.39	-	-	-	-	-	-
0.24	11.38	-	-	-	-	-	-
-	-	-	-	-	-	0.2	2,3, 9,9.5, 10.5
0.19	11.37	-	-	-	-	-	-

### 3.7.2 <sup>29</sup>Si NMR acquisition parameters

The <sup>29</sup>Si NMR aqueous silica species acquisition conditions were selected based on dissolved silica concentrations and references available from the literature (Stoberg 1999, Marsmann 1999, Bergna 1994).

Table 3.9 – <sup>29</sup>Si NMR acquisition parameters by a Bruker DPX300 Spectrometer

Conditions	Selected value
Measuring time of each sample	~ 1.5 hrs
Pulse length	8 sec
Acquisition time	0.8 msec
Waiting period	20 sec

### 3.7.3 <sup>29</sup>Si NMR samples

The starting commercial sodium solution had the following characteristics: relative density = 1.33, pH = 11.56; Si/M molar ratio = 1.7. Diluted solutions were prepared by adding distilled water to this concentrated solution at room temperature.

### 3.7.4 <sup>29</sup>Si NMR equipment and sampling tubes

NMR experiments were performed using a Bruker DPX300 Spectrometer at Victoria University, Footscray, Melbourne, operating with a 4.7T magnetic field (<sup>29</sup>Si Larmor frequency 39.7MHz). Despite the liquid nature of the initial solution, Magic Angle Spinning (MAS) was necessary to obtain resolved spectra and the 1D experiment was conducted at room temperature under MAS conditions at 5kHz.

The spectrum shows the resonance of the principal building units of a polysilicate. This and all other spectra were run on a Bruker DPX300. Conditions: measuring time 1.5h, 8 second pulse length, 0.8 second acquisition time. Single pulse spectra were obtained using 90° pulse angle (8μs) and a recycled delay of 20s. Chemical shift are externally referenced (calibrated) to tetramethylsilane (TMS) <sup>29</sup>Si at 0ppm. Although TMS is an

inert substance, has a low boiling point and a rather short relaxation time, its chemical shift is in the middle of the shift range of other organo-silicon compounds.

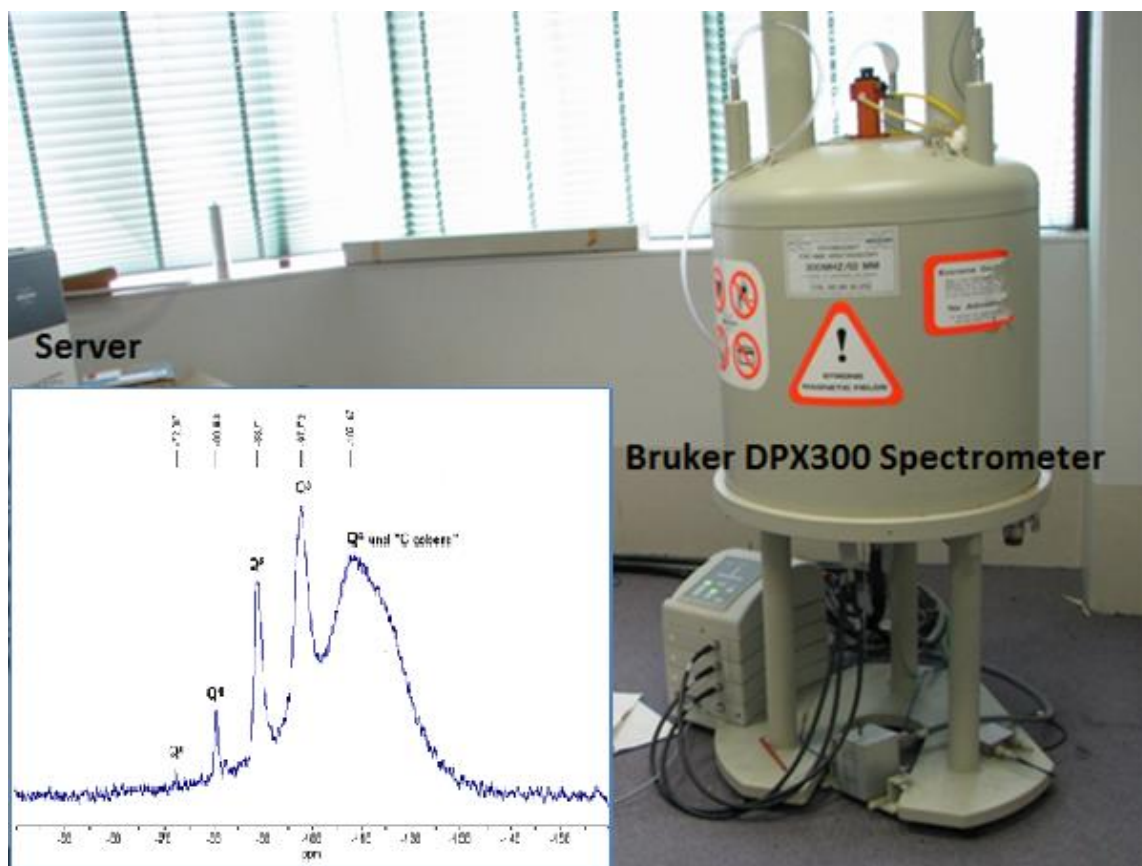


Figure 3.11 –  $^{29}\text{Si}$  NMR system includes Bruker DPX300 spectrometer and server and  $^{29}\text{Si}$  NMR spectrum of a sodium silicate solution in  $\text{D}_2\text{O}$  with Si/M molar ratio 1.7.

Sample solutions were injected into five millimetre diameter Pyrex tubes, (see figure 3.12) and inserted into the NMR sampling channel at the top of the equipment,(see figure 3.12)  $^{29}\text{Si}$  NMR spectra were collected over approximately 1.5 hours.

### 3.7.5 Sodium silicate environment

$^{29}\text{Si}$  NMR spectroscopy can be a very valuable technique for the study of the species present in aqueous solutions. However, firm deductions about the chemical structure of such species can only be made using systems enriched in  $^{29}\text{Si}$ . Sodium silica solutions provide a suitable environment to study silica species once their spectra are identified.

### 3.7.6 Limitations

One of the limitations of the technique is that the large number of structurally different silicate species observed by  $^{29}\text{Si}$  NMR spectroscopy contributes to the fact that the observed resonance lines of commercial sodium silica solutions are rather broad. Table 3.10 shows a number of subspecies recorded for instance for Mono-substituted cyclic trimer (86.2, 86.4, 94.7, 97.3, 97.4). However all these species have similar number of silicon atoms, overlapping and small difference in resonance frequency of the different lines cause substantial line broadening. The second important limitation of the technique is that the five millimetre diameter Pyrex tubes used by  $^{29}\text{Si}$  NMR Spectroscopy were made of borosilicate glass containing approximately 80% silicon dioxide and 12% Boron Oxide. The resonance of the tube material contributes mainly to  $\text{Q}^4$  spectra. Because silica species  $\text{Q}^4$  is very much a gel, for accuracy of interpretation of the results  $\text{Q}^4$  species were disregarded in all  $^{29}\text{Si}$  NMR experiments discussed in chapter 4. Quartz glass is essentially 100% silicon dioxide. Because quality NMR sample tubes are made from Pyrex, they often contribute substantial and broad signals in  $^{29}\text{Si}$  NMR Spectroscopy. The insert of most broad band probes is made from Quartz, which can also contribute background signals to  $^{29}\text{Si}$  spectra. These background signals can make important spectral features of the sample impossible to discern. Overcoming them adds another challenge to NMR, particularly  $^{29}\text{Si}$  NMR, because of the low abundance and relative sensitivity of this spin 1/2 nucleus. To overcome these, all spectra obtained during the  $^{29}\text{Si}$  NMR work were calibrated with background spectra obtained from the original silica species (five species present in Table 3.7).

Table 3.10 summarises all silica species and sub-species recorded during the experimental works with  $^{29}\text{Si}$  NMR technique. For accuracy of the results all subspecies recorded were integrated into relevant silica species.

Table 3.10 – <sup>29</sup>Si chemical shifts, δ of silicate anions identified in sodium silicate solutions in accordance with (Stoberg, 1996).

Silica species	Q <sup>n</sup> site	- δ(ppm)
Monomer	Q <sup>0</sup>	49.9
		51.9
		55.7
		58.4
		65.1
		66.4
		67.6
	Q <sup>0</sup>	69.2
		69.4
	Q <sup>0</sup>	71.9
Dimer	Q <sup>1</sup>	73.6
		78.0
	Q <sup>1</sup>	76.1
		76.9
Linear trimer	Q <sup>1</sup> Q <sup>1</sup> Q <sup>2</sup> Q <sup>2</sup>	79.9
		80.1
		88.1
		90.6
Cyclic tetramer	Q <sup>1</sup>	77.4
Linear tetramer	Q <sup>1</sup> Q <sup>2</sup>	88.3
		88.4
Cyclic tetramer	Q <sup>2</sup>	88.7
Mono-substituted cyclic trimer	Q <sup>1</sup> Q <sup>2</sup> Q <sup>3</sup>	86.2
		86.4
		94.7
		97.3
		97.4
Bridge cyclic tetramer	Q <sup>2</sup> Q <sup>3</sup>	93.8
		96.3
		97.3
Mono-substituted cyclic tetramer	Q <sup>1</sup> Q <sup>2</sup> Q <sup>3</sup> Q <sup>3</sup>	95.6
		95.3
		97.1
Tricyclic hexamer I	Q <sup>2</sup>	95.6
Tricyclic hexamer II (cisoid)	Q <sup>3</sup>	101.0

## Chapter 4 $^{29}\text{Si}$ NMR study of dissolved silica species

### 4.1 Introduction

The objective of this experimental work was to study dissolved silica species and the effect of sodium and aluminium ions, and pH conditions on silica species to identify chemical pathways that may explain silica precipitation and silica scale formation on RO membrane surfaces. Structural changes of silica species were evaluated through the collection of  $^{29}\text{Si}$  NMR spectrum, chemical shift and peak areas, using  $^{29}\text{Si}$  NMR spectroscopy for aqueous silica.

$^{29}\text{Si}$  NMR spectroscopy is a valuable technique to obtain further insights into the mechanisms of hydrolysis and condensation of silica species present in super-saturated (colloidal) silica environments. Nevertheless, knowing the distribution of  $Q^n$  ( $Q^0$ ,  $Q^1$ ,  $Q^2$ ,  $Q^3$ ,  $Q^4$ ) species within the solution is obviously not sufficient to uniquely identify the multitude of possible polysilicate trimers, tetramers, pentamers, hexamers, etc, that may form during the course of precipitation and gelation on the RO membrane surface. Yet,  $^{29}\text{Si}$  NMR spectroscopy is useful in the determination of structural trends, affecting dissolved silica species that result under varying conditions such as the effect of salinity, pH, and aluminium ions.

In the current experiments, a method was developed to investigate the hydrolysis and condensation processes of dissolved silica species present in sodium silica solutions. Through this thesis the  $Q^n$  notation is used, as introduced by Engelhardt (1977), to specify NMR silica spectrum. The superscript  $n$  denotes the number of equivalent  $Q$  groups (the number of silicon atoms connected to a central silicon atom via oxygen) within the same silica species. In case no strict assignments can be made, the superscript  $n$  will not be referred to since the (broad) NMR line originates from several different silicon chemistries. As described in chapter 3,  $Q^0$  type refers to a silicon atom with zero connections to another silicon species,  $Q^1$  type refers to a silicon atom connected to one silicon species,  $Q^2$  type refers to a central silicon atom connected to two silicon species,  $Q^3$  refers to a central silicon atom connected to three silicon species and  $Q^4$  is a central

silicon atom connected to four silicon species. A description of the experimental design, experimental conditions, and apparatus are outlined in chapter 3. A description of the sample preparation and data analysis are presented here and in chapter 3.

#### 4.1.1 Concentration polarisation (CP)

It follows from the field results that clay is an actual source of total and dissolved silica and aluminium in CSG waters in Australia, which lead to silicate scale formation on the membrane surface in the RO desalination process especially if a high permeate recovery (> 94%) is required (Brant 2012). Under certain conditions, silicic acid may be deposited on the membrane surface in the form of silicates or it may serve as cementing material (glass-like structures) for setting particles of different composition. Deposition of silica or silicate on the RO membrane surface could occur when the dissolved silicate exceeds its solubility limit. The solubility limit, however, is moderated by cations and anions in the specific water matrix and the pH condition of the RO feed due to their effects on silicate solubility.

The composition of the water matrix, especially the concentration and types of cations present in the CP zone on the membrane surface, may be seen as the main source of variations in the structure of silicate deposited on membranes. As such, knowledge of the deposition and dissolution of dissolved silicate species under the effect of different cations may thus lead to new insights in silicate deposition. Especially in the field of osmotic membrane separation, it has been noted that only small amounts of cations impurities may impose different deposition structures (Sheikholeslami, 2002, Cob 2012). Moreover, there has been considerable speculation on the role of aluminium in aluminosilicate deposition (Chappex 2012, Iler 1976, Bergna 1994).

Super-saturation conditions arising on RO membrane surfaces can lead silicate to aggregate into colloidal structures and deposit on the surface. Typical fully polymerised silicate structure is demonstrated in Figure 4.1. Figure 4.1 shows the silicon – oxygen anion, which in the given structure also consists of two rings, each being built out of four silicon – oxygen tetrahedra,  $Q^3$  type surroundings. This structure of silicate is commonly present in gelling phase (Stoberg 1997). However, hydrolysis (separation) of

monomeric silica acid ( $Q^0$  type) can occur after addition of  $H_2O$  (Tognonvi, 2010). During growth of the structures shown in Figure 4.1, the relative proportion of oligomeric silica gradually decreases as the size of the sol particles is increased (Bergna and Roberts 2006). Particle growth may thus arise from the condensation of monomers and oligomers at particulate surfaces in accordance with the mechanism proposed by Iler (1979). Aggregation of these structures on the RO membrane surface leads to amorphous silicate deposits. Characterisation of the structure of these compounds, Figure 4.1, is of considerably interest for the crystal chemistry of silicates.

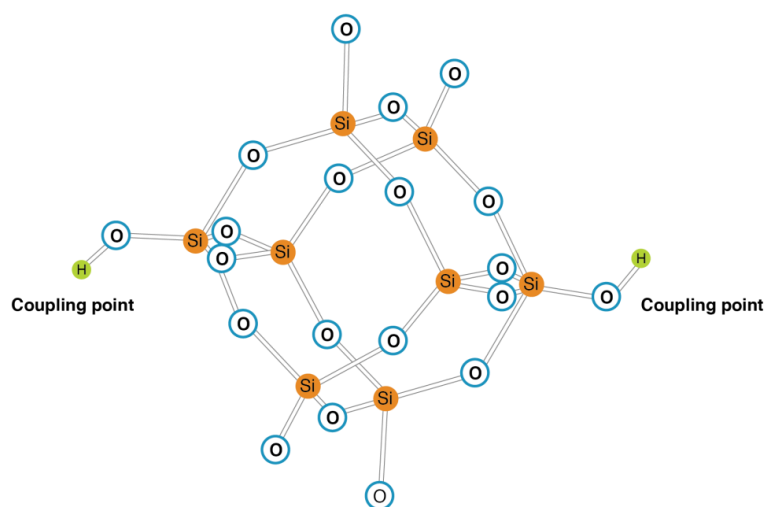


Figure 4.1 – Fully polymerised silicate anion  $[Si_8O_{18}(OH)_2]^{-6}$  adopted from Smolin (1987). Coupling points (-OH groups) may link the silicate to RO membrane surfaces.

The speciation of polysilicate solutions was originally investigated in basic, aqueous systems by Engelhard and co-workers (1977). According to their  $^{29}Si$  NMR results, a common condensation sequence is monomer, dimer, trimer, cyclic trimer, cyclic tetramer, and then higher-order rings. They also observed an equilibrium distribution of species at long reaction times that was independent of the starting materials (mono-, di- or trisilic acids), indicating that complete restructuring occurs under these conditions. A similar reaction pathway was proposed by Iler (1976) for the formation of aqueous silicate colloids: highly condensed cage structures form the pre-critical nuclei for subsequent colloidal growth. The  $^{29}Si$  NMR spectra of aqueous silicate systems are quite complex, because of the many polysilicates that can be formed from  $SiO_4$  and

because hydrolysis and condensation reactions occur concurrently (Marsmann 1987, Dietzel 2002). For example, depending on the extent of hydrolysis, a total of 48 chemically different linear trimers and 81 chemically different cyclotetramers are possible (Sjöberg 1996, Engelhardt 1987).

In order to study different effects on dissolved silica species, the species were studied in alkaline sodium silicate solutions. Dilution of sodium silicate with H<sub>2</sub>O liberates monomeric silica (Q<sup>0</sup> type surroundings), which subsequently leads to oligomerisation into larger silicate anions (Q<sup>1</sup>, Q<sup>2</sup>, Q<sup>3</sup>, Q<sup>4</sup> type). In this way, polymerisation of monomeric silicate anions can be studied in situ using <sup>29</sup>Si NMR.

#### 4.1.2 Sample preparation

Firstly, the experimental solutions were prepared by adding a relevant volume of deionised water into the mother sodium silicate solution (1.7Si/M molar ratio). For the effect of sodium ions on silicate species, sodium chloride (as NaCl=1000mg/L) was added to the mother sodium silicate solution. Similarly for the effect of aluminium ions, aluminium chloride (as AlCl<sub>3</sub>=130mg/L) was added to the mother sodium silicate solution. The proportions of the experimental solutions used are described in chapter 3, Table 3.8. The ratio of silicon to water is expressed as Si/M in molar ratio, where M is the molarity of water (for the reference sodium silicate solution the Si/M ratio was 1.7). The experimental solutions were prepared 8 – 6 hours prior to each <sup>29</sup>Si NMR experiment. Secondly, a single sample was prepared from the relevant experimental solution 10 - 15 minutes prior to each <sup>29</sup>Si NMR experiment. Approximately 5mL of the experimental solution was injected into a ~5 mm diameter Si NMR tube, then ~0.2mL of D<sub>2</sub>O solution was injected into the tube. Then the sample was inserted into the NMR sample chamber for <sup>29</sup>Si NMR analysis for approximately 1.5 hours. Acquisition of NMR data was undertaken for 1.5 hours by a Bruker 2500 <sup>29</sup>Si NMR. The <sup>29</sup>Si NMR acquisition parameters designed for all experiments are outlined in Table 3.9, chapter 3.

#### 4.2 Results.

## 4.2 $^{29}\text{Si}$ NMR baseline solution

$^{29}\text{Si}$  NMR of aqueous silicate solutions exhibit several resonances corresponding to structurally different associations with the  $^{29}\text{Si}$  atom. The difference in resonance frequencies is caused by the local environment of the atoms, and depends on the number of adjoining bound silicon atoms (Marsmann 1987). Several configurations for  $\text{Q}^1$  to  $\text{Q}^4$  associations are possible, with linear, cyclic or cubic species possible, which all give slightly different resonance bands for  $\text{Q}^1$  to  $\text{Q}^4$ .

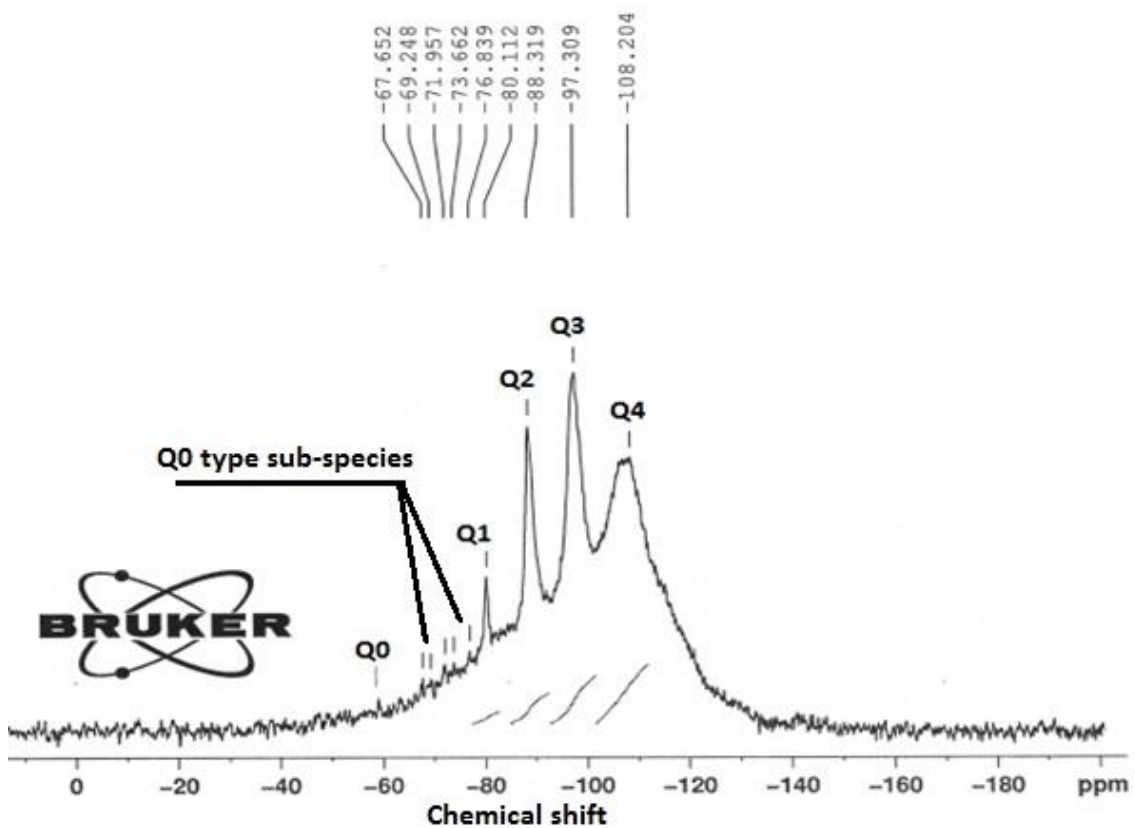


Figure 4.2 –  $^{29}\text{Si}$  NMR spectrum of the initial concentrated sodium silicate solution (baseline sample) at Si/M molar ratio 1.7.

The resonance bands may broaden more or narrow proportionally to the number of different structures belonging to each resonance group ( $\text{Q}^1$ ). The more silicon atoms present in the silica species, the more negative is the  $^{29}\text{Si}$  the chemical shift, Figure 4.2 and table 4.1.

Table 4.1 –  $^{29}\text{Si}$  NMR chemical shift observed for the mother sodium silicate solution (baseline sample)

Silica species	$Q^0$	$Q^1$	$Q^2$	$Q^3$	$Q^4$
Assignment	monomer	dimmer	dimer	trimer	tetramer
$^{29}\text{Si}$ Chemical shift (ppm)	-67.37	-80.12	-88.32	-97.31	-108.21
$Q^0$ relative proportions (%) (area under the peak)	2.5	13.5	33.5	52.9	-

The  $^{29}\text{Si}$  NMR spectra of the initial concentrated sodium silicate sample (baseline sample) (solution Si/M atomic ratio = 1.7) is plotted in Fig 4.2. The five signals observed correspond to the following chemical shifts – 67.37, -80.12, -88.32, -97.31 and -108.21ppm that are characteristic of  $Q^0$ ,  $Q^1$ ,  $Q^2$ ,  $Q^3$  and  $Q^4$  species respectively. The fraction of each  $Q^n$  species has been determined by dividing the integrated intensity of the corresponding signal by the sum of all signal intensities except  $Q^4$ . This is after the background was subtracted, and is summarised in Table 4.1. Because the majority of  $Q^4$  spectrum is silica glass from the NMR tube and  $Q^4$  silica is corresponds to amorphous silica, the  $Q^4$  spectrum was disregarded in the following results.

In order to confirm the reproducibility of these spectra, (figure 4.2), a set of three experiments were performed with samples of mother sodium silicate (non-diluted solutions). The results of three samples gave the same spectra with chemical shifts for the silicate species peaks within  $\pm 0.01$ ppm of each other. The obtained average relative integrated intensities of the different  $Q^n$  species present in the original solutions are reported in figure 4.2 and table 4.1. As can be seen from Table 4.1, the relative proportions of each species were:  $Q^0=2.5\%$ ,  $Q^1=13.5\%$ ,  $Q^2=33.5\%$  and  $Q^3=52.9\%$ . “ $Q^0$  Subspecies” shown in Figure 4.2 and in other results were integrated into the total  $Q^0$  silicate species for accuracy of the results.

### 4.3 Effect of dilution with $\text{H}_2\text{O}$

Figure 4.3 shows consolidated results of  $^{29}\text{Si}$  NMR spectra recorded for dilution with deionised water. The results are arranged such that the front diagram presents the chemical shifts for the baseline sample (1.7 Si/M molar ration) and the last diagram

shows the chemical shift for the most diluted sample (0.11Si/M molar ratio). Figure 4.3 illustrates the chemical shift for each silica species for the range of experimental solutions.

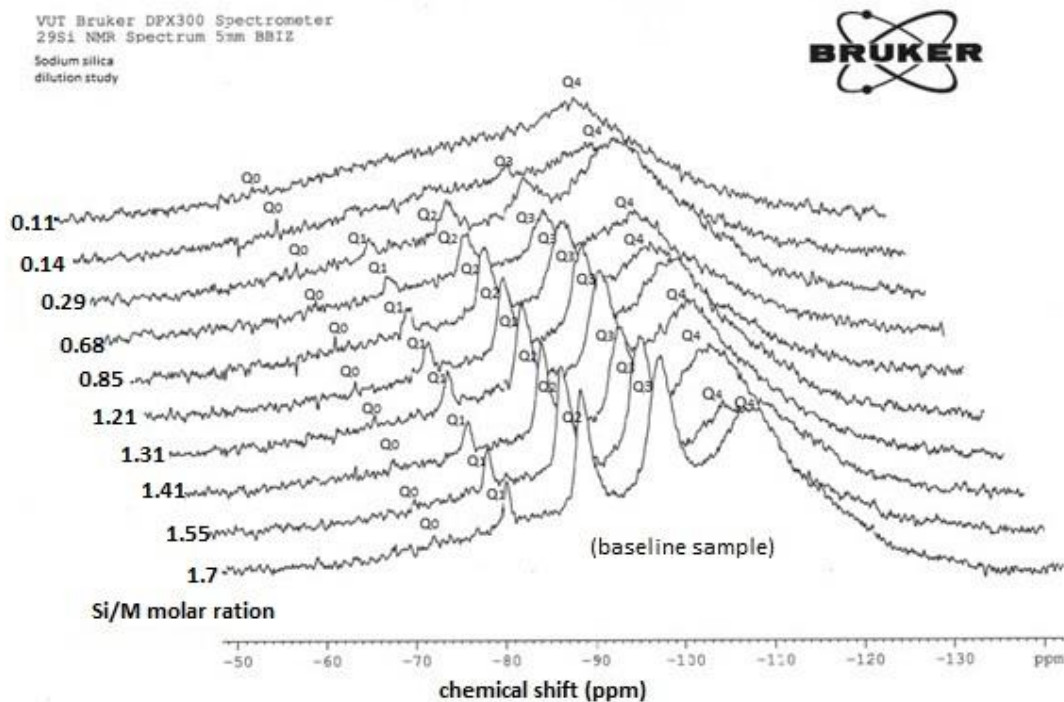


Figure 4.3 – Consolidated results of  $^{29}\text{Si}$  NMR spectrum ( $\text{Q}^0$ ,  $\text{Q}^1$ ,  $\text{Q}^2$ ,  $\text{Q}^3$  type surroundings) of the samples for the range of diluted silicate solutions with  $\text{H}_2\text{O}$  (at Si/M molar ratio 1.7, 1.55, 1.41, 1.31, 1.21, 0.85, 0.68, 0.29, 0.14, 0.11).

As can be seen from Figure 4.3, each further dilution slightly reduces the peaks for  $\text{Q}^1$ ,  $\text{Q}^2$ ,  $\text{Q}^3$  type surroundings until these three silicate species disappeared at the 0.11Si/M molar ratio. The last sample shows that only  $\text{Q}^0$  type surroundings present at this silicate concentration. It was observed that each further dilution generates slightly higher concentrations of monomer silicic acid  $\text{Q}^0$  silicate species, probably due to relatively fast hydrolysis processes affecting this type of silicate species.

For instance, the relative proportion of  $\text{Q}^0$  type surrounding was 2.5% at the 1.7Si/M molar ratio and gradually increased with dilutions up to ~8% at the 0.11Si/M molar ratio. As can be seen,  $\text{Q}^0$  (the smallest building block of silicate species or called monomeric silica acid ( $\text{Si}(\text{OH})_4$ )) can be relatively easy hydrolysed from the more

complex species perhaps due to the lower activation energy required to break the –O-Si-O- bonds, compare to formation (hydrolysis and condensation) of the Q<sup>2</sup> and Q<sup>3</sup> type species (Dietzel 1996). A slight increase of Q<sup>0</sup> type was expected as each dilution results in the release of Q<sup>0</sup> type as a consequence weak –O-Si-O- bonds.

Figure 4.3 also illustrates that Q<sup>1</sup> type surroundings were obtainable across all dilution ratios at about 10 to 12% until they disappeared for the 0.11Si/M molar ratio. Similarly, Q<sup>2</sup> type surroundings presented across all dilution ratios at ~ 30% for low dilutions until they disappeared at high dilutions. Q<sup>3</sup> type surroundings can also be seen across all dilution ratios at approximately 50 - 60% at low dilution and disappearing at high dilution. The dilution results suggest that Q<sup>1</sup>, Q<sup>2</sup>, Q<sup>3</sup> type surroundings might be less mobile and according to Stumm and Morgan (1979) are less ionised species.

Figure 4.3 shows that relative proportions of all four silica species was relatively constant until the disappearance of Q<sup>1</sup>, Q<sup>2</sup> and Q<sup>3</sup> at high dilution ratios, possibly indicating equilibrium between species. The experiment was terminated at the 0.11Si/M molar ratio when Q<sup>1</sup>, Q<sup>2</sup>, Q<sup>3</sup> species disappeared as complete hydrolysis was likely to have occurred. It is also possible that the designed <sup>29</sup>Si NMR acquisition parameters were not suitable to study lower concentrations of silica species.

These results were consistent with the hypothesis developed by Sjöberg (1993), who stated that while each solution has some equilibrium for silica species present, the tendency of silanol groups of a silicate molecule to ionise increases in the order: Q<sup>0</sup> > Q<sup>1</sup> > Q<sup>2</sup> > Q<sup>3</sup>. According to Zhang (2012), the polymerization of silicic acid is a condensation reaction, and requires ionized SiO(OH)<sub>3</sub> groups and unionised silica Si(OH)<sub>4</sub>. This requirement implies that the rate of silicate polymerisation depends on the extent of silicate ionization. The position of the Q<sup>0</sup> peak over all range of dilutions undoubtedly, Figure 4.3, shows gradual increase of Q<sup>0</sup> surrounding, which is difficult to conclude about others monomeric silica species (Q<sup>1</sup>, Q<sup>2</sup>, Q<sup>3</sup>).

Q<sup>0</sup> type surrounding silica species plays a key reaction in hydrolysis and condensation (oligomerisation) of other monomeric species such as Q<sup>1</sup>, Q<sup>2</sup>, Q<sup>3</sup> and silicate precipitation reactions. Smolin (1985) points out that during dilution weaken oxygen – silicon bonds as a result of attack by water molecules, with the extent of weakening

related to the number of siloxane bridges (Si-O-Si). For instance, during dilution, colloidal sodium silicate ( $\text{Si}_2\text{O}_{18}\text{H}_4\text{Na}_4$ ) will release  $\text{Na}^+$  ions and replace it with -OH. OH groups will weaken Si-O bonds leading to potential hydrolysis or dissolution of monosilicic acid ( $\text{Q}^0$ ) from polymerised species.

Using  $^{29}\text{Si}$  NMR it was also possible to observe dissolved silica species present as monomeric silicate ( $\text{Q}^0$ ) as isolated molecules and as linked molecules ( $\text{Q}^1$ ,  $\text{Q}^2$ ,  $\text{Q}^3$ ), referred to as polysilicic acid. The influence of hydrolysis on the structural evolution of silicate polymers was studied by Pouxviel (1987) and Coltrain (2005). Coltrain (2005) demonstrated that higher amounts of water enhance hydrolysis and under acid conditions nearly complete hydrolysis occurs. The simplified study of the reaction involving additional water molecules, as was undertaken in this section, is very useful to gain a basic insight into the Si-O-Si bridging mechanisms of the hydrolysis process. Similar processes can occur in the CP zone on the membrane surface, where hydrolysis and condensation of silica species occur simultaneously, particularly if there is a shift of super-saturation occurs towards lower concentrations for instance.

The effect of dilution with water demonstrated that higher dilution ratios enhance hydrolysis rates, mainly due to hydrolysis of Si-O-Si bonds, resulting in liberation of monomeric silica groups -  $\text{Q}^0$  type surroundings. Nevertheless, an understanding of the reaction variables affecting hydrolysis and condensation processes is needed to compare other relevant impacts on silicate precipitation, such as the effect of sodium and aluminium ions, and pH conditions to explain why in some cases silicate deposits on membranes and in other cases silicate does not deposit on the membrane surface.

#### **4.4 Effect of sodium**

Limited references are available on the impact of sodium chloride on dissolved silicate species. Generally  $\text{Na}^+$  acts as a stabilising agent, as it decelerates the condensation of hydrolysed monomer and dimer species (Healy 1994). Sodium ions in solution concentrations  $> 8\text{g/L}$  (as NaCl) tend to create a binding layer around silicate species preventing access of water molecules into polymeric silicate structures (Healy 1994). However, dissociated sodium ions attract water molecules according to their charge,  $z$  to ionic radius,  $r$  (El-Manharawy 2002). Low ( $z/r$ ) ions (such as  $\text{Na}^+$  and  $\text{Cl}^-$ ) surrounded

with a single water shell of 4 to 6 water molecules. These 4 to 6 water molecules could weaken Na-O-Si-O- bonds so Q<sup>0</sup> type could redissolve into the solution unless Na-O-Si-O-Si-O-Si-O-Si-O- bonds (sometime double ring structure exist, Figure 4.1) will prevent Q<sup>0</sup> type from dissolution from the silica polymeric structure, Figure 4.1.

A detail not found in any previous work, the results described in this chapter show that addition of sodium chloride substantially increases the release of monomeric silicic acid (Q<sup>0</sup>) and impacts hydrolysis and condensation processes of Q<sup>1</sup>, Q<sup>2</sup>, Q<sup>3</sup> type surroundings silicate species compared to similar dilutions with deionised waters, Figures 4.4, 4.5 and 4.6. The results are demonstrated in the following sections.

#### 4.4.1 Quantitative composition

Figure 4.4 illustrates the chemical shift collected for silicate species for the range of experimental alkaline sodium silicate solutions with addition of sodium chloride (as NaCl=1000mg/L).

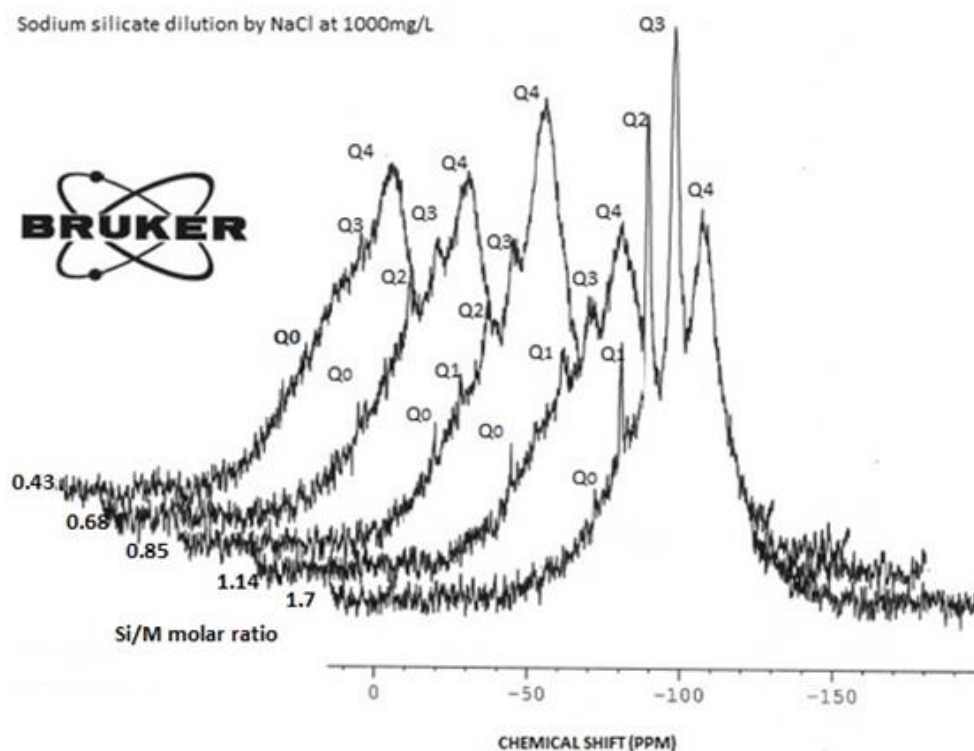
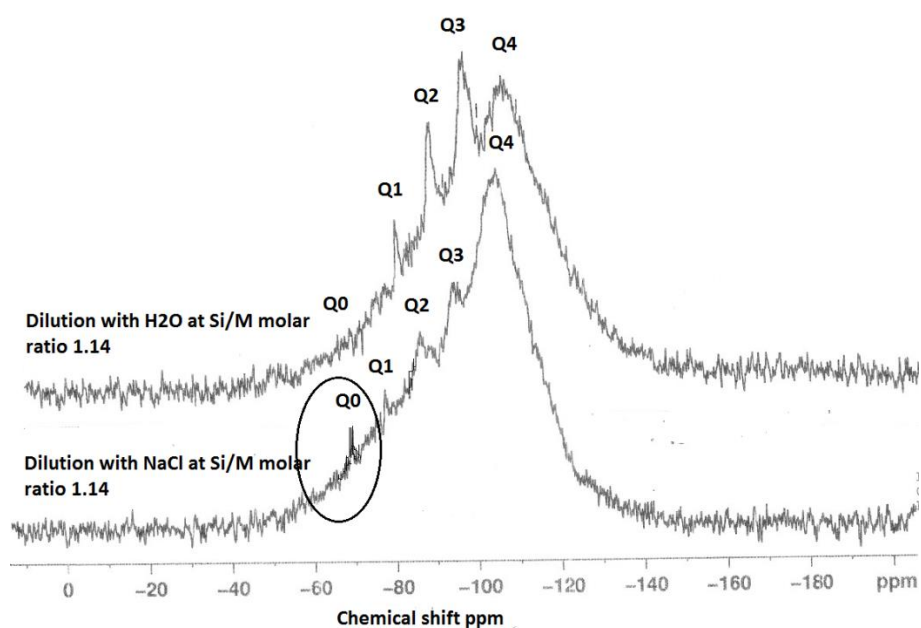


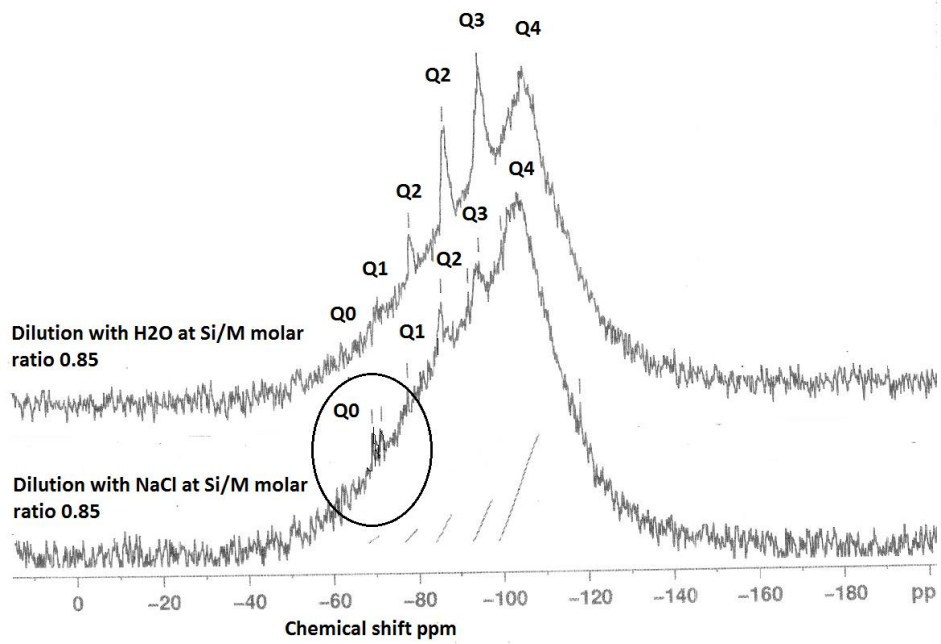
Figure 4.4 – Consolidated results of <sup>29</sup>Si NMR spectrum (Q<sup>0</sup>, Q<sup>1</sup>, Q<sup>2</sup>, Q<sup>3</sup> type surroundings) for a range of diluted silicate solutions with NaCl (1000mg/L) (at Si/M molar ratio 1.7, 1.14, 0.85, 0.68, 0.43)

It can be seen that addition of sodium chloride solution leads to the loss of the  $^{29}\text{Si}$  NMR spectra and that the spectra intensity for  $\text{Q}^1$ ,  $\text{Q}^2$ ,  $\text{Q}^3$  species at the 1.14 Si/M molar ratio decreases, Figure 4.6. The relative proportions of  $\text{Q}^2$  and  $\text{Q}^3$  type surroundings at the 1.14Si/M molar ratio dramatically reduced, probably due to the shielding effect of sodium ions on these silica species. These results are consistent with the hypothesis proposed by Healy (1994) in which he discussed sodium ions acting as binding layers surrounding oligomer silica species. This effect was observed for  $\text{Q}^1$ ,  $\text{Q}^2$  and  $\text{Q}^3$  type surroundings. As can be seen from Figure 4.4, further addition of sodium chloride leads to the disappearance of  $\text{Q}^1$  type at the 0.68 Si/M molar ratio and the disappearance of  $\text{Q}^2$  type at the 0.43 Si/M molar ratio. This probably is due to a combination effects; first the binding effect of sodium ions on these species and second polymerisation of small species  $\text{Q}^1$  and  $\text{Q}^2$  type into  $\text{Q}^3$  type.

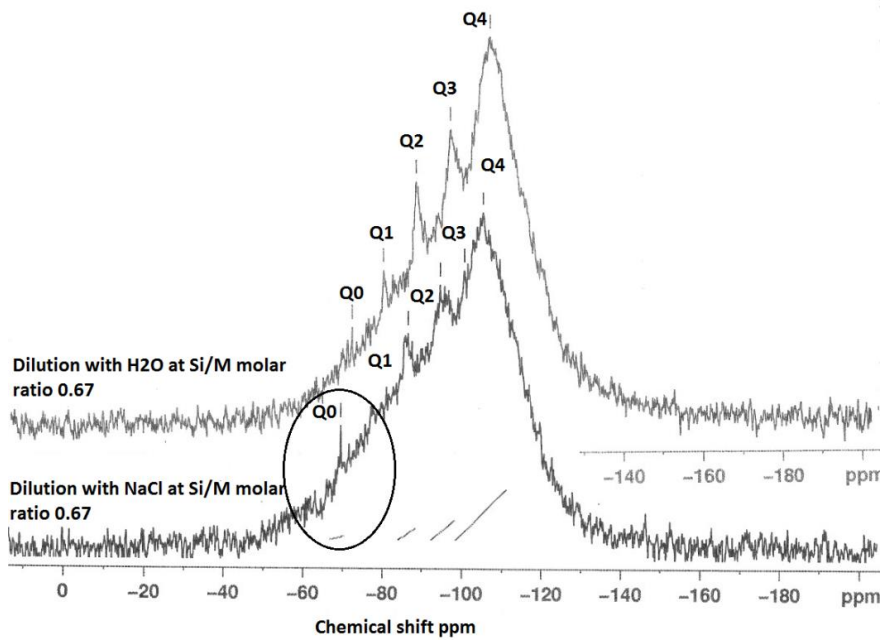
Figure 4.5 (a), (b) and (c) shows the  $^{29}\text{Si}$  NMR spectrum for various Si/M molar ratios demonstrating effect of sodium on monomeric silica species ( $\text{Q}^0$  type surroundings) compare to the same dilutions with  $\text{H}_2\text{O}$ . As can be seen, a much higher proportion (at least twice) of monomeric silica acid ( $\text{Q}^0$ ) was shown with the dilution with sodium chloride compare to the dilutions with  $\text{H}_2\text{O}$ .



(a)



(b)



(c)

Figure 4.5 (a) -  $^{29}\text{Si}$  NMR spectrum of sodium silicate diluted with  $\text{H}_2\text{O}$  at Si/M molar ratio 1.14 (upper) and  $^{29}\text{Si}$  NMR spectrum of sodium silicate diluted with NaCl (1000mg/L) at Si/M molar ratio 1.14 (lower), 4.5(b)-  $^{29}\text{Si}$  NMR spectrum of sodium silicate diluted with  $\text{H}_2\text{O}$  at Si/M molar ratio 0.85 (upper) and  $^{29}\text{Si}$  NMR spectrum of sodium silicate diluted with NaCl (1000mg/L) at Si/M molar ratio 0.85(lower), 4.5 (c) -  $^{29}\text{Si}$  NMR spectrum of sodium silicate diluted with  $\text{H}_2\text{O}$  at Si/M molar ratio 0.67 (upper)

and  $^{29}\text{Si}$  NMR spectrum of sodium silicate diluted with NaCl (1000mg/L) at Si/M molar ratio 0.67(lower).

Figure 4.6 illustrates silicate spectrum for dilution with  $\text{H}_2\text{O}$  and dilution with sodium chloride at the Si/M molar ratio 0.85. The results clearly demonstrate a reduction of proportions of  $\text{Q}^1$ ,  $\text{Q}^2$  and  $\text{Q}^3$  type surroundings, but  $\text{Q}^0$  type was present in slightly higher proportion than in the baseline sample. When mother sodium silicate solution is diluted, more monomer  $\text{Q}^0$  type surrounding is released into the solution. With dilution by NaCl, liberation of monosilicic acid ( $\text{Q}^0$ ) from silica polymorphs, such as  $\text{Q}^2$ ,  $\text{Q}^3$  types, was slightly higher. This might suggest that negatively charged surface of silanol groups ( $\text{Si-O}^-$ ), neutralised by hydrated cations  $\text{Na}^+$ , are attacked by hydroxyl anions ( $\text{OH}^-$ ) by which the coordination number of the silicon atom is increased to more than four.

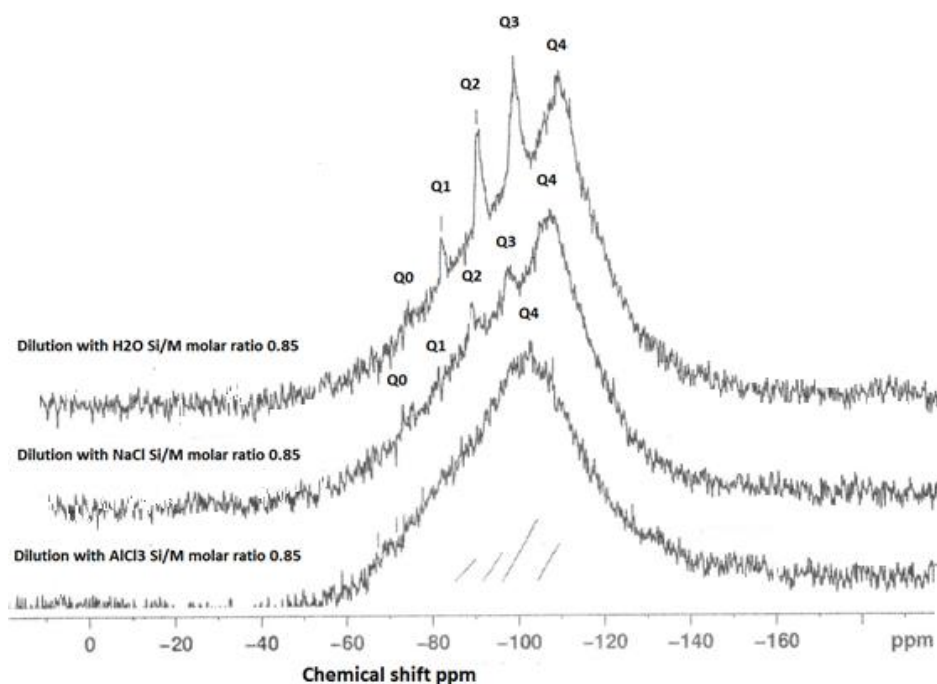


Figure 4.6 –  $^{29}\text{Si}$  NMR spectrum of sodium silicate diluted with  $\text{AlCl}_3$  (130mg/L) at Si/M molar ratio 0.85 (lower);  $^{29}\text{Si}$  NMR spectrum of sodium silicate diluted with NaCl (1000mg/L) at Si/M molar ratio 0.85 (middle);  $^{29}\text{Si}$  NMR spectrum of sodium silicate diluted with  $\text{H}_2\text{O}$  at Si/M molar ratio 0.85 (upper).

As a result, the underlying silicon bonds are weakened and monomeric silicate anions are released from the other silicate groups, including from colloidal silicate present in the solution. It is likely a similar mechanism applies to  $Q^1$  and  $Q^2$  species when these species disappeared from the spectrum.

Other potential interpretations for the loss of sensitivity of silicate species under the effect of sodium ions is that destabilisation of the  $-O-Si-O-$  bonds by  $Na^+$  occurred to the extent that some silicate species precipitated in the sample (Si NMR tube) or were transferred into  $Q^4$  type surroundings. This hypothesis is demonstrated in Figure 4.7, where silica precipitation is shown within the  $^{29}Si$  NMR tubes numbered “1” and “2”. As can be seen, silica precipitation occurred in tubes “1” and “2” probably due to the destabilisation effect of sodium ions on dissolved silica species. No visible silica precipitation was observed in the tube “3”. The precipitation occurred after 48 hours of  $^{29}Si$  NMR experiment.

Sodium silicate mother solution is already stabilised with NaOH, Figure 2.2, and the majority of the silanol groups on the surface of silicate sol are covered with  $Na^+$  ions.  $Na^+$  ions are strongly adsorbed onto the silanol group, and this condition is expressed as Si-ONa, Figure 2.2. However, addition of extra sodium chloride seems to shift the equilibrium between dissolved silicate and amorphous silicate domains resulting in silicate polymerisation and precipitation as shown in Figure 4.7.  $Na^+$  ions liberated as a result of dilution generate a silicate steric layer (Healy 1994) surrounding oligomer silicate such as  $Q^2$ ,  $Q^3$  species, which leads to further binding of  $Na^+$  to the stabilizing layer. According to Healy (1994), the presence of increasing amounts of bound  $Na^+$  must switch off the electro steric contribution of the adsorbed polysilicate structures. This suggests that the effect of sodium ions is to attract  $-OH$  groups to  $Q^0$  type silica species and also to prevent  $-OH$  groups forming into  $Q^2$ ,  $Q^3$  type forcing silica to precipitate. Both effects play a major role in sodium – silicate interactions.



Figure 4.7 – The experimental solutions after 24 hours of  $^{29}\text{Si}$  NMR experiment: tubes “1” and “2” show the samples diluted with sodium chloride (at the 1.14 and 0.68 Si/M molar ratio respectively). Tube “3” is the sample diluted with deionised water at the 0.68Si/M molar ratio.

The results shown in Figure 4.4, 4.5, 4.6 and 4.7 suggest that sodium ions not only shield silicate species but also sustain monomeric silica acid (possible speed up hydrolysis of weak connected monomeric silica acid) and depress hydrolysis and condensation processes of  $\text{Q}^1$ ,  $\text{Q}^2$ ,  $\text{Q}^3$  types by preventing access of water molecules into polymeric silica species. The trend is to either shield  $\text{Si}-(\text{O}-\text{Si})_4$  bonds ( $\text{Q}^4$ ) or to hydrolyse  $\text{Si}-(\text{O}-\text{Na})_x$  bonds. This means for  $\text{Q}^0$  type surrounding,  $\text{Si}-\text{OH}$  is the preferred bond over  $\text{Si}-\text{O}-\text{Na}$ . Instead for  $\text{Q}^1$  and  $\text{Q}^2$  type surroundings,  $\text{Si}-\text{O}-\text{Na}$  is preferred over  $\text{Si}-\text{OH}$ . For  $\text{Q}^3$  type silicates with  $\text{Na}^+$  and  $\text{OH}^-$  associations occurring in some combination and depending on pH, leads to ionisation of silicate species and more complex physical structures of silicate species. The mechanism is consistent with the disappearance of  $\text{Q}^1$  before  $\text{Q}^2$  before  $\text{Q}^3$  and an increase in  $\text{Q}^0$  type species. Legrand (1999) and Lerman (1988) propose that the physical structure of silicate species is

defined by the probability of chemical reactions that occur and can influence chemical behaviours of silicate.

## 4.5 Effect of aluminium

Hydrolysing aluminium salts are used most widely for coagulation, including for CSG waters in Australia. In particular, aluminium chlorohydrate (ACH) is used for CSG water treatment. The effect of residual aluminium on silicate scale formation is less known, and concerns have been expressed by many practitioners and researchers (Iler (1979), Bergna (1994), Healy (1994) that aluminium might have a significant impact on dissolved silicate species. Iler (1979) has remarked that there is a peculiar affinity between the oxides of aluminium and silicon. This affinity results from the nature of  $(\text{SiO}_4)^{4-}$  and  $(\text{AlO}_4)^{5-}$ , which is responsible for the vast range of natural aluminosilicates (Bergna 1994).  $\text{Al}^{3+}$  ions appear to slow down hydrolysis of silicate species (Stoberg 2001). It was therefore; appropriate to investigate further the effect of aluminium on monomeric (reactive) silica species. The results of aluminium addition on hydrolysis and condensation of silica species are presented.

### 4.5.1 Quantitative composition

Figures 4.8 and 4.9 illustrate the results of  $^{29}\text{Si}$  NMR spectrum recorded for five dilutions with aluminium chloride (130mg/l). Figure 4.6 shows a comparison of the effects of sodium and aluminium on dissolved silicate species. Figure 4.8 shows that silicate species disappeared at Si/M molar ratio is 0.85, while all silicate spectra were observable at similar dilutions with  $\text{H}_2\text{O}$  and sodium chloride.

As can be observed from Figures 4.8 and 4.9, the impact of a minor addition of aluminium (as  $\text{AlCl}_3=130\text{mg/L}$ ) at the 1.61 Si/M molar ratio was quite substantial. Relative proportions of  $\text{Q}^0$ ,  $\text{Q}^1$ ,  $\text{Q}^2$  and  $\text{Q}^3$  type reduced to nearly background spectra, Figure 4.9. For instance,  $\text{Q}^1$  type surroundings disappeared immediately after the first addition of aluminium, presumably indicating shielding of  $\text{Q}^1$  type surroundings or rearrangement into  $\text{Q}^0$  type. It is known that aluminium ions can break silicate bonds (Dietzel 2003, Marshmann 2002). The  $\text{Q}^0$  species spectrum was observably low, and the amount of the monomeric species was less than 2.5% of the total spectra at very low

initial dilutions and then disappeared from the  $^{29}\text{Si}$  NMR spectrum at higher dilutions as can be seen in Figure 4.8. Figure 4.6 also illustrates that at a dilution ratio of 0.85, all dissolved silicate species disappeared probably as a result of silicate precipitation as aluminium silicate.

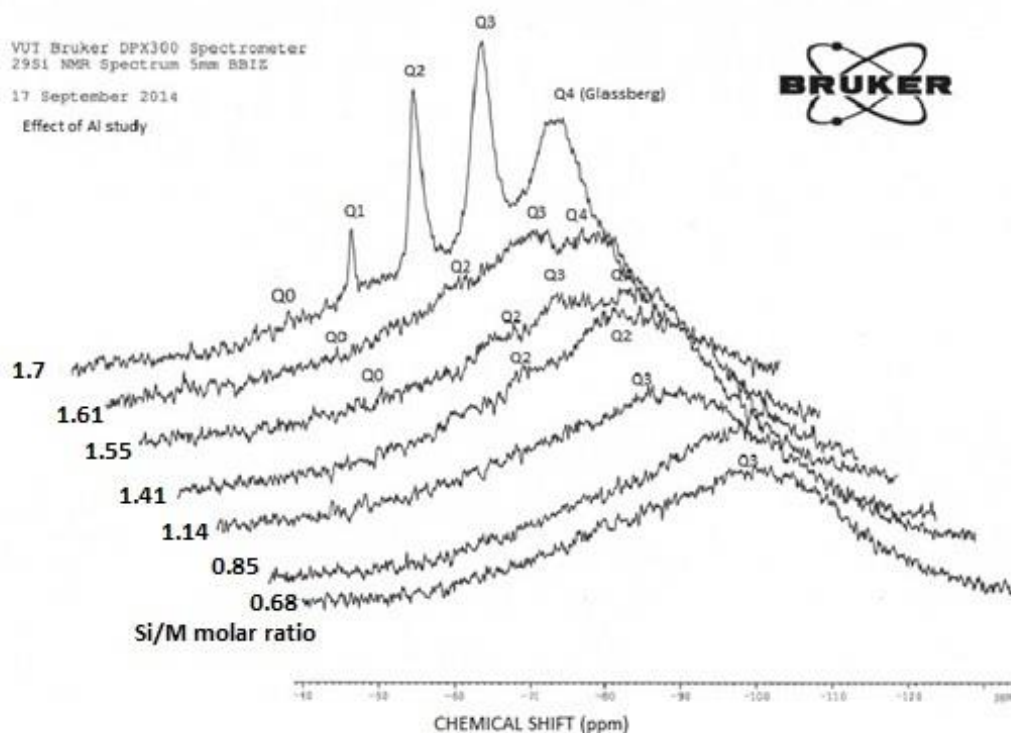


Figure 4.8 – Consolidated results of  $^{29}\text{Si}$  NMR spectrum ( $\text{Q}^0$ ,  $\text{Q}^1$ ,  $\text{Q}^2$ ,  $\text{Q}^3$  type surroundings) of the samples for the range of diluted silicate solutions with  $\text{AlCl}_3$  (130mg/L) (at Si/M molar ratio 0.68, 0.85, 1.14, 1.41, 1.55, 1.61, 1.7).

Continued addition of aluminium chloride showed  $\text{Q}^2$  type surroundings gradually disappeared at the 1.41Si/M molar ratio, presumably due to re-arranging polymeric silicate species and due to precipitation of silicate as aluminosilicate. It is known that  $\text{Al}^{+3}$  could break silicate polymeric structures and over time substitute O-Si-O unit (or  $\text{Q}^0$  type) from polymeric silicate. At the same time the loss of peaks for  $\text{Q}^1$ ,  $\text{Q}^2$ ,  $\text{Q}^3$  suggests that the number of possible atomic arrangements increases dramatically with the addition of aluminium, so there are no sharp peaks, but lots of little peaks that appeared as shown in Figure 4.9. Disappearance of  $\text{Q}^0$ ,  $\text{Q}^1$  type silica species were also

an indication that  $\text{Al}^{3+}$  affects hydrolysis reactions and the equilibrium between species. Addition of aluminium favours condensation processes probably because  $-\text{O}-\text{Si}-\text{O}-\text{Al}-$  bonds have higher reaction energy than  $-\text{O}-\text{Si}-\text{O}-\text{Si}-\text{O}-$  and are less mobile (Smolin 1978).

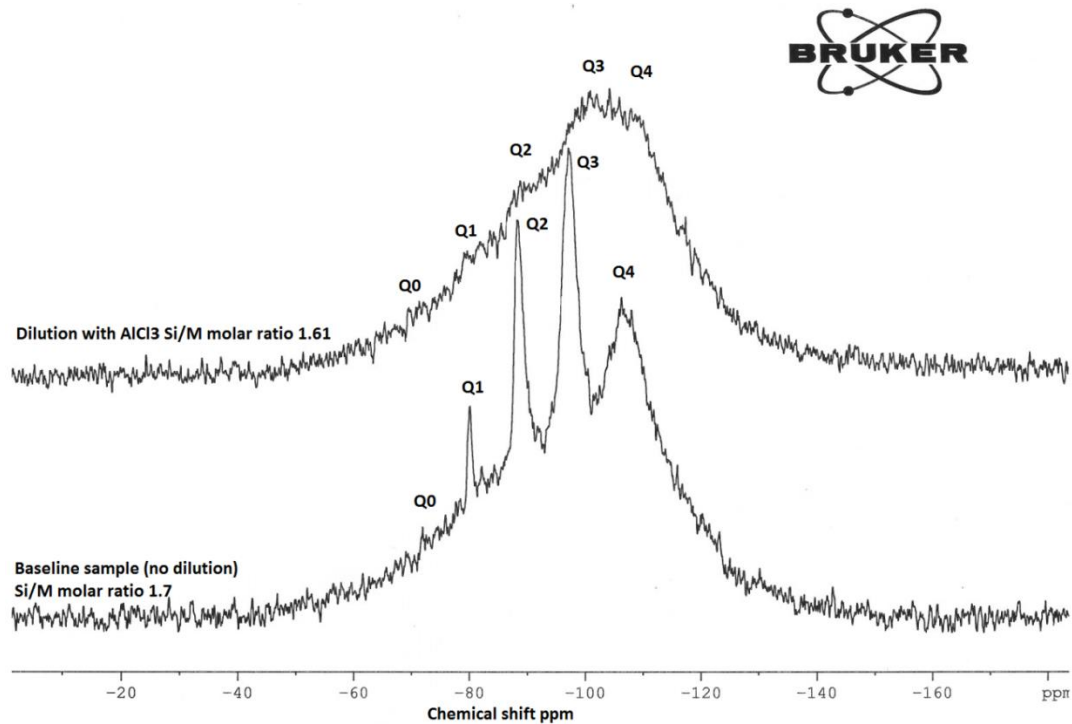


Figure 4.9 –  $^{29}\text{Si}$  NMR spectrum of baseline sample Si/M molar ratio 1.7 and of the sample diluted with  $\text{AlCl}_3$  (130mg/L) at Si/M molar ratio 1.61.

As a result, the equilibrium between hydrolysis and condensation shifts predominantly towards condensation. This explains rapid silicate and aluminium silicate precipitation on membrane surfaces when residual aluminium is present in RO feed solutions at elevated concentrations. In the case of RO desalination, this process predictably leads to scale formation.

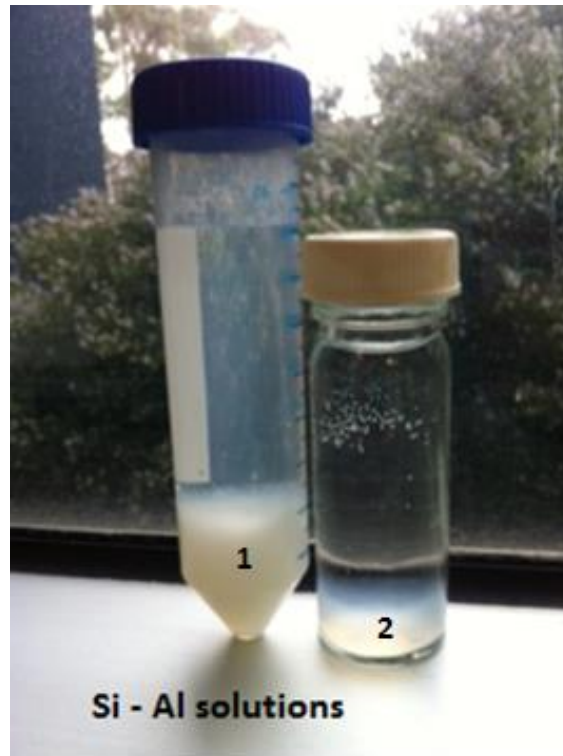


Figure 4.10 – The experimental solutions after 48 hours of  $^{29}\text{Si}$  NMR experiment: “1” is dilution with aluminium chloride at the 1.61 Si/M molar ratio and “2” is dilution with  $\text{H}_2\text{O}$  at the 1.61Si/M molar ratio.

Explicit characterisation of  $\text{Q}^n$  distributions by  $^{29}\text{Si}$  NMR is difficult in alkaline silicate solutions and even more difficult with a minor addition of aluminium. The reason for this increase in complexity is that, in contrast to dilution with deionised water or with a relatively low concentration of sodium chloride, with addition of aluminium even in very minor concentrations, it is no longer possible to match the observed  $\text{Q}^n$  distribution against the known stoichiometry of the sample. This is a result of the ill-defined aluminium coordination in these samples, Figures 4.8 and 4.9 due to multiply peaks.

When aluminium is added to sodium silicate solutions, aluminium hydroxide is formed and silicic acid polymerises on the aluminium hydroxide surface to form a layer of polysilicic acid. Once polysilicic acid is formed on the surface of aluminium hydroxide the growth of silica particles continue to the size 0.1nm (Dietzel 1999). Therefore, the Si:Al ratio in the solution decreases towards the deposit formed on the membrane

surface with the time as demonstrated in Figure 4.10, tube “1”, where significant precipitation was observed 24 hours after the experiment.

Two major observations can be drawn from these results, that the recorded chemical shifts moved into the region of Q<sup>3</sup> type spectra while Q<sup>0</sup>, Q<sup>1</sup> and Q<sup>2</sup> species are no longer seen in solution, (Figures 4.8, 4.9 and 4.10). Q<sup>3</sup> silica species is found in more amorphous type structures (Jong and Schramm and Parziale 1984), and is an indication that aluminium forces dissolved silicate species to precipitate quite rapidly.

## 4.6 Effect of pHs

### 4.6.1 High pH (9 – 11.5)

Figure 4.11 illustrates the silica <sup>29</sup>Si NMR spectrum documented in the sodium silicate solutions at the 0.5 Si/M molar ratio at pH9. As can be seen from Figure 4.11, the peak intensities recorded at pH9 were relatively weak for single peak areas.

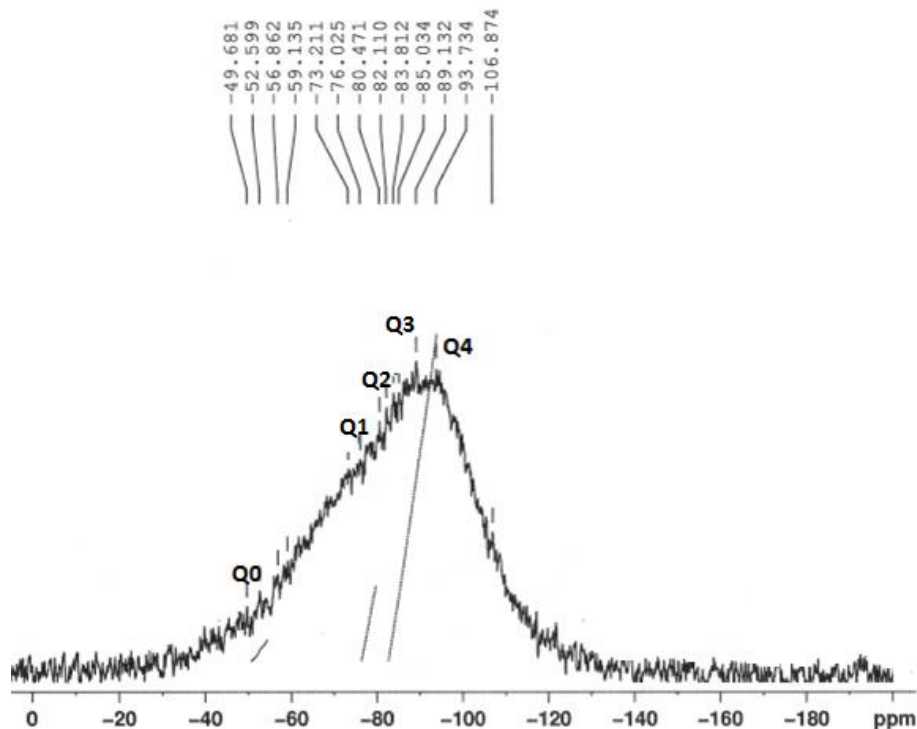


Figure 4.11 – <sup>29</sup>Si NMR spectrum of the sodium silica solution diluted with H<sub>2</sub>O at 0.5 Si/M molar ratio at adjusted pH9

However, various diluted sodium silicates solutions showed similar results – minor  $^{29}\text{Si}$  NMR peaks were recorded for 0.68, 0.85 Si/M molar ratios. Despite the noise,  $\text{Q}^0$ ,  $\text{Q}^1$ ,  $\text{Q}^2$ ,  $\text{Q}^3$  type surroundings were observed in relatively small proportions at pH 9.

Figure 4.12 shows the  $^{29}\text{Si}$  NMR spectrum recorded for pH10 at the 0.5 Si/M molar ratio indicating again a very small variations in peaks. Comparison of Figure 4.11 and Figure 4.12 shows a shift to the left for  $\text{Q}^1$ ,  $\text{Q}^2$ ,  $\text{Q}^3$  types peaks at pH 9 (Figure 4.11).

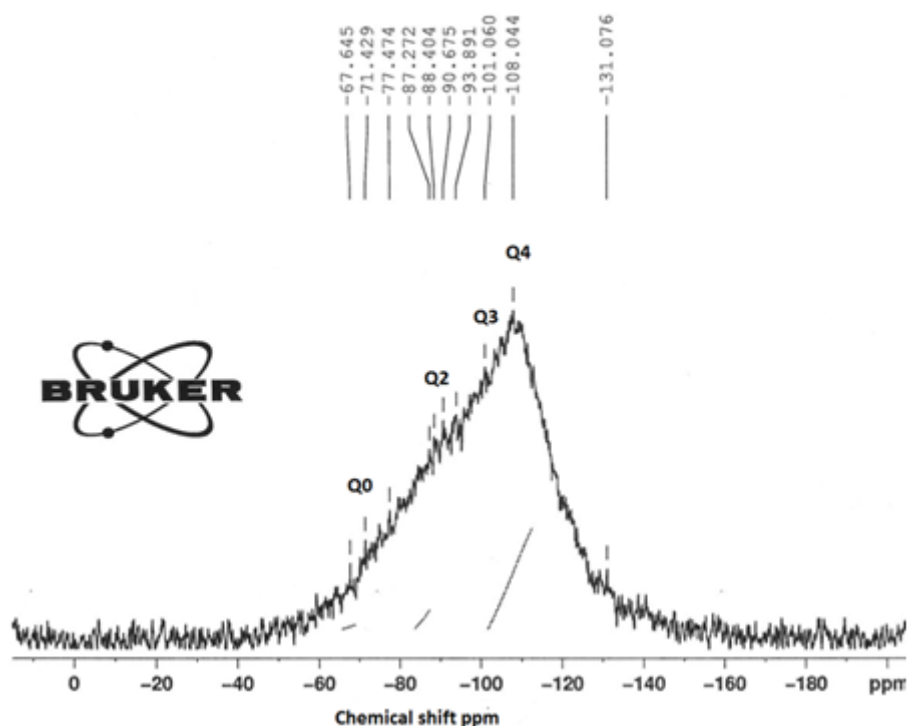


Figure 4.12 –  $^{29}\text{Si}$  NMR spectrum of the sodium silica solution diluted with  $\text{H}_2\text{O}$  at 0.5 Si/M molar ratio at adjusted pH10.

At high pH conditions, such as the range of pH 9 to 11.5, dissolved silica species are highly ionised and remain in solution without aggregating (Cornell 1996, De Jong 1984). However, a minor pH change could lead to slow rearrangement of silica structures due to increasing ionisation of some species. This may explain the relatively low detection of the five silicate species in the pH range 9 – 11.5. Iler (1976) identified that formation of silica oligomers at high pH proceeds via cyclic trimeric silicate anions which, at high pH values are more stabilised than the linear silicate anions. This cyclic trimeric anion plays a key role in oligomerisation reactions of aqueous silicate anions,

and the pH-value of the solution is a critical parameter concerning the formation of the ring structures, which leads to silica precipitation (Stoberg 1996).

#### 4.6.2 Low pH (2 – 3)

Coltrain and Kelts (2005) conducted a comprehensive literature review of the modern and past (prior Iler's) research and concluded that there are no monomer silicate species at low pHs (1 – 3), particularly  $Q^0$ . Yet, the experiments conducted in this research show relatively low proportions of silicate species such as  $Q^0$  and  $Q^1$  type surroundings at pH2 and at pH3 at the 0.50 Si/M molar ratio, Figures 4.13 and 4.14. The concentration of  $Q^0$  and  $Q^1$  types surroundings were analysed after various time periods (within 2 hours and 12 hours) following dilution. All samples were showed the presence of  $Q^0$  and  $Q^1$  silica species in relatively small proportions (1-3% of peaks area of the baseline sample).

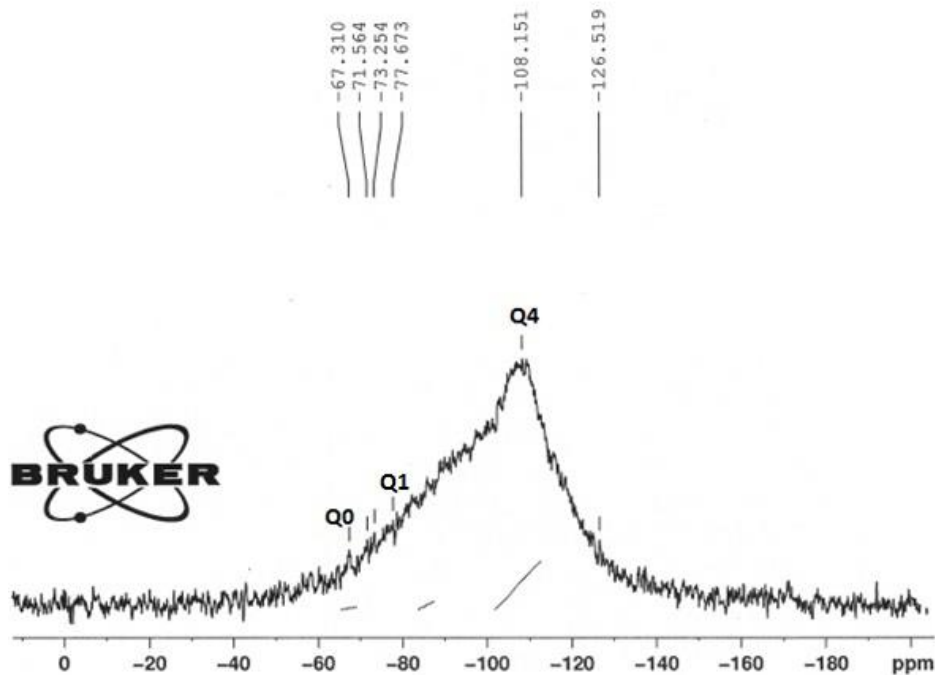


Figure 4.13 –  $^{29}\text{Si}$  NMR spectrum of the sodium silica solution diluted with  $\text{H}_2\text{O}$  at 0.5 Si/M molar ratio at adjusted pH2.

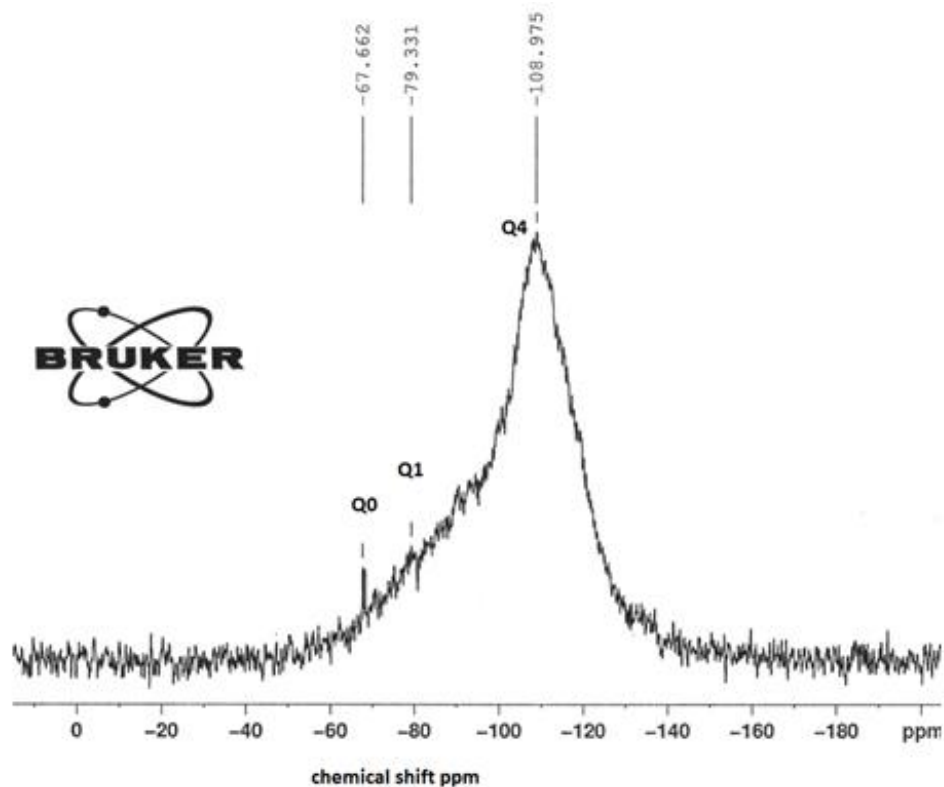


Figure 4.14 –  $^{29}\text{Si}$  NMR spectrum of the sodium silica solution diluted with  $\text{H}_2\text{O}$  at 0.5 Si/M molar ratio at adjusted pH3.

Lowering the pH-value of solutions causes the silica species to be less ionised resulting in an increased stability of the linear (oligomers) structures, which seem to be difficult to observe at pH2 – 3. Marshmann (1999) described two kinds of silicon compounds that are possible. The first kind, derived from divalent silicon  $[\text{Si}(\text{II})]$ , is normally thermodynamically unstable. However, a few are stable enough to be present at room temperature.

The majority of the  $^{29}\text{Si}$  NMR data reported involves derivatives of  $\text{Si}(\text{IV})$  as presented in this research. The chemical shift depends primarily on the coordination number of the silicon in such a way that a low number of substituents around the silicon leads to deshielding (13 to 175ppm) and a high coordination number gives high negative numbers (Marshmann 1999, Grenthe 1992).

In aqueous solutions at low pH, silica species condense to form gels (Harris 1982, Marsmann 1982), but the rate of this process is sufficiently slow that the kinetics can be

followed by  $^{29}\text{Si}$  NMR. The low-pH mechanism involves protonation of silicon atoms with electron-donating groups that hydrolyse more readily (Dietzel 2002, Smoli 1987). Because  $-\text{OH}$  and  $\text{OSi}$  groups are more electron withdrawing than  $-\text{O}-\text{Si}-\text{O}-\text{Si}-\text{O}-\text{Si}-\text{O}-$  groups, the reactions become more difficult with increasing hydrolysis as much slower transfer of electrons occurs between  $-\text{OH}$  and  $\text{OSi}$  groups. At low pH values, relatively low proportions of  $\text{Q}^1$ ,  $\text{Q}^2$ ,  $\text{Q}^3$  type surroundings still might be present at metastable conditions.

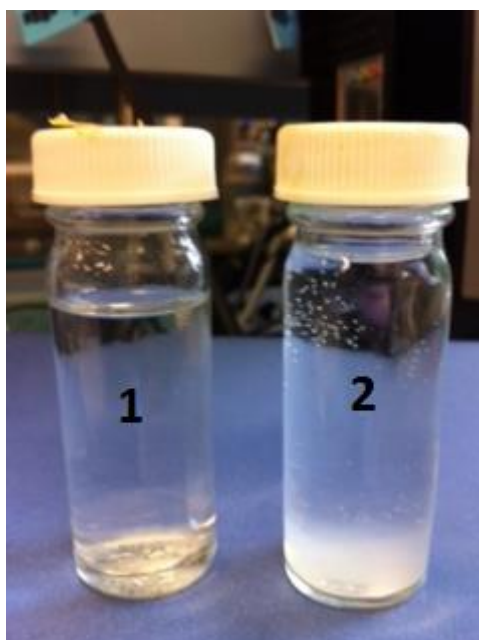


Figure 4.15 – The experimental solution at pH3 at Si/M molar ratio 0.5, “1” is the solution at pH3 immediate after pH adjustment, and “2” is the solution after 24 hours of  $^{29}\text{Si}$  NMR experiment, gel was observed at the bottom of sample 2.

Schmidt (1985) demonstrated that hydrolysis is enhanced under acidic conditions, but is retarded under basic conditions. Schmidt (1985) states that the monomeric silicate is less mobile in the interval pH 1-2.5 and as a result silica polymerisation is much slower at low pH conditions, but silica solubility is low at lower pHs. The results show relatively low proportions of dissolved silica species  $\text{Q}^0$  and  $\text{Q}^1$  types recorded at low pH 2 – 3. If hydrolysis is enhanced at low pH conditions, this would enhance the formation of monomeric silicate as shown in the results.

### 4.6.3 pH (5 – 8)

It was not possible to adjust pH of the sodium silica solutions in the studied dilution range to pH 5 – 8 conditions. All solutions within the pH range 5 – 8 immediately formed gels, figure 4.16. This illustrates that silicate polymerisation rates are very different for different pH conditions as expressed by Iler (1976) and Smolin (1986). In strong alkaline solution, monosilicic acid polymerises slowly, but polysilicic acid rapidly forms in neutral solution as was recorded in this experiment. In the pH range 5 to 8, monosilicic acid polymerises rapidly.

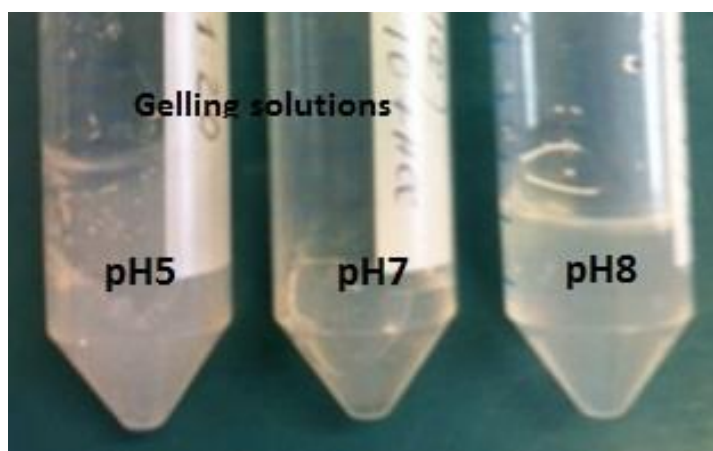


Figure 4.16 – Gelling solutions during the preparation of sodium silica solution at pH5, pH7 and pH8.

Colloidal silicate present in alkaline sodium silica solutions can also catalyse monomeric silica polymerisation, so that colloids present in the solution, or a gel that forms in solution, accelerate the polymerisation rate (Stoberg 1996, Fleming 1986). This perhaps explains rapid gelling of all solutions in these pH ranges.

### 4.7 Discussion

The results recorded in the dilution with H<sub>2</sub>O study illustrate that monomeric silicic acid may exist as isolated molecules, so called monosilicic acid Q<sup>0</sup> type surroundings or (Si(OH)<sub>4</sub>) and Q<sup>1</sup> type or Si<sub>2</sub>O<sub>3</sub>(OH)<sub>4</sub><sup>2-</sup>, (and as linked molecules, called polysilicic acid) and as Q<sup>2</sup>, Q<sup>3</sup> types. Polymers consist of silicate tetrahedrons that are linked via silicon-oxygen-silicon bonds. Addition of H<sub>2</sub>O to the solution immediately initiates

hydrolysis of monosilic acid groups and as a result adjustment of equilibrium between the rest of the silicate species.

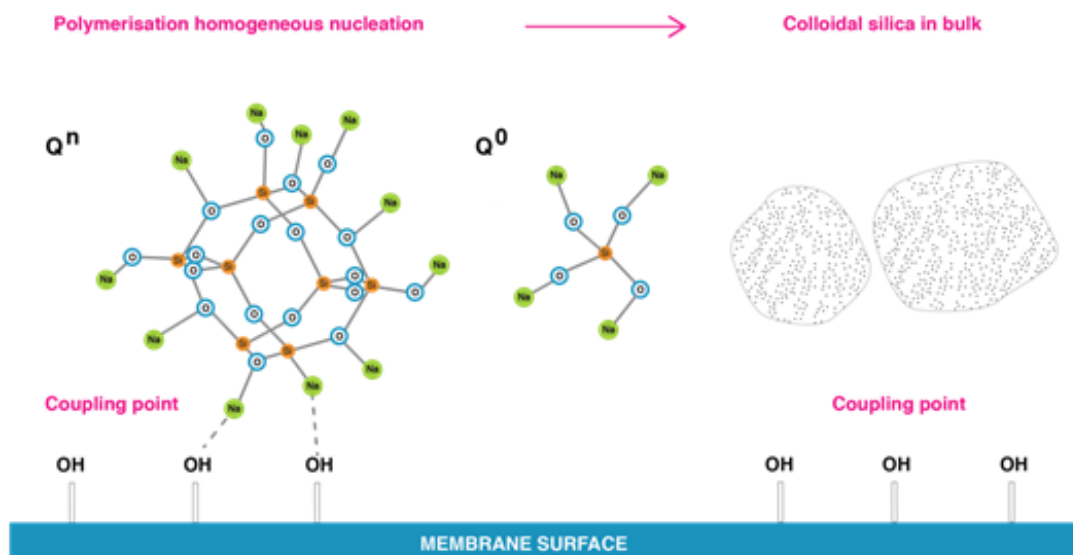


Figure 4.17 – Dissolved silicate polymerisation in CP layer on the membrane surface in medium and high salinity waters without presence of aluminium.

The results presented in Figures 4.4 and 4.5 clearly illustrate that the introduction sodium chloride into the mother sodium silicate solution impacts the sensitivity of  $^{29}\text{Si}$  NMR spectrum for  $\text{Q}^1$ ,  $\text{Q}^2$ ,  $\text{Q}^3$  types. The proportion of  $\text{Q}^3$  type was significantly reduced immediately after the first addition of sodium chloride at Si/M molar ratio 1.41, presumably due to shielding effect of sodium ions. As a result of further addition of sodium chloride,  $\text{Q}^1$  and  $\text{Q}^2$  type surroundings disappeared, and  $\text{Q}^3$  type also gradually decreased. This is consistent with the hypothesis that sodium ions tend to surround polymeric silica species, Figure 4.17, acting as a stabilising agent, protecting polymeric species from attack by water molecules.

The results with sodium dilution showed significant increased proportions of monomeric silicic acid ( $\text{Q}^0$ ) compare to similar dilutions with  $\text{H}_2\text{O}$ , Figure 4.5 (a), (b) and (c). This is a result of sodium ions attracting water shells, which initiate separation of monomeric silicic acid from polymeric silica groups.

When dissolved silicate exceeds its solubility limits the nucleation process will, in principle, be governed by interacting silanol groups that interact to form  $\text{-O-Si-O-Si-O}$  bonds (Bergna 2006, Smolin 1987). Under these conditions, the probability of interactions between neighbouring silanol groups to form  $\text{-Si-O-Si-}$  bonds is higher, and therefore intramolecular nucleation would be favoured (Iler 1979). During silicate precipitation the monomer groups  $[\text{SiO}_4]^{4-}$  and  $[\text{SiO}_6]^{4-}$  randomly pack and rapid growth results in a non-periodic structures, Figure 4.1. In medium to high salinity waters dissolved and polymerised silicate species will be surrounded by sodium ions as shown in Figure 4.17. Sodium ions attract to silicate, but also can interact with  $\text{-OH}$  groups present on the membrane surface (usually in abundance), Figure 4.17. However, the  $\text{Na-O-Si-O-Si-O-}$  bonds is stronger than  $\text{-O-H-O-Na}$  bonds (Stoberg 2001). According to Healy (1994), then more silicon atoms present in silicate polymeric structure the stronger the sodium binding layer attached to silicate. In this case, silicate polymerisation is likely to occur homogeneously in bulk solution. As can be seen from Figure 4.17, polymeric silicate species will aggregate into colloidal silica in bulk solution. The polymerised silicate is unlikely to deposit on the membrane surface due to sodium ions creating barriers between  $\text{-OH}$  groups and silicate. Monomeric silicic acid can potentially deposit solely on the membrane surface, but the reverse of this process will be apparent as it is likely dissolution (hydrolysis) process will dominate for monomeric silicic acid, Figure 4.17. It is known that monomeric silicic acid can coat natural organic matters presented on membranes, in this case silicate deposition on membrane surfaces is possible.

As expected a number of parallel and competitive reactions occurred in the solutions before dissolved silicate precipitated as a result of destabilisation of the equilibrium between silicate species. Healy (1994) suggests that sodium ions have a number of effects on silicate species. For instance  $\text{Na}^+$  ions in small concentrations ( $< 8\text{g/L}$ ) attract water molecules and sustain further dissolution (hydrolysis) of monosilicic acid increasing the concentration of  $\text{Q}^0$  type and at the same time preventing access to polymeric silicate structures such as  $\text{Q}^2$ ,  $\text{Q}^3$  types. Applying this knowledge to medium and high salinity CSG waters, dissolved silicate can be difficult to remove effectively due to sodium ions preventing access to silicate. Ultimately effective dissolved silicate

removal from CSG water by coagulation, for instance, might suggest that dissolved silicate was present in solely monomeric forms. Experimental and analytical observations by others frequently found high concentrations of monomeric silicic acid in high salinity groundwater in Tunisia, Egypt, Qatar, Oman where RO desalination present even bigger challenges due to extreme salinity of groundwater ( $\text{NaCl}=100 - 200 \text{ g/L}$ ) (El-Manharawy 2001).

The effect of aluminium ions on silicate species, shown in Figures 4.8 and 4.9, is reduced  $^{29}\text{Si}$  NMR spectra peak proportion due to silicate precipitation as aluminium silicates. As discussed in detail in chapter 2, aluminium ions can over time disassemble polymeric silicate structures due to  $(\text{AlO}_4)^{-5}$  having similar bonds to Si with oxygen  $\text{O}=\text{Al}-\text{O}=\text{Al}-\text{O}-$ , so Al can easily access polymeric silicate species. Once aluminium silicates are formed, aluminium will bond with  $-\text{OH}$  groups on membrane surfaces, leading to an irreversible process of scale formation on the membrane surface as shown in Figure 4.18.

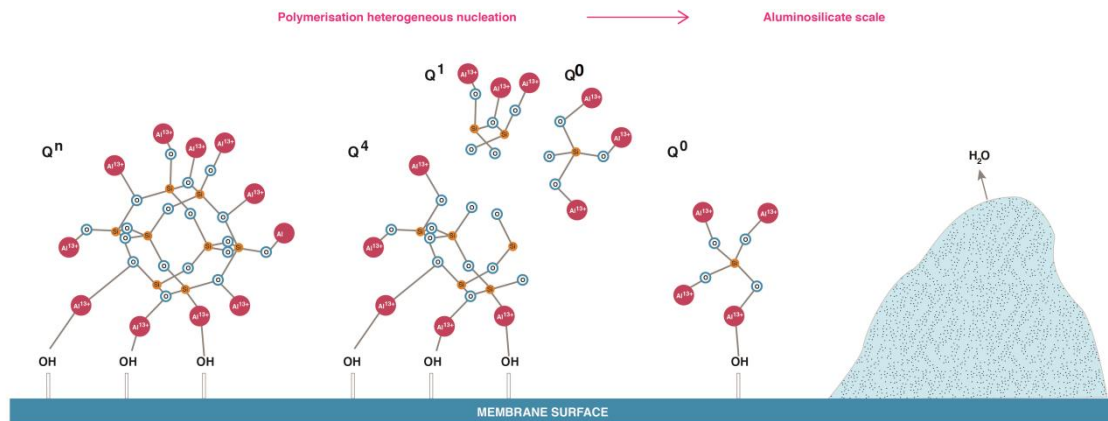


Figure 4.18 – Polymerised silicate under effect of aluminium and final deposition on the RO membrane surface.

Opposite to the effect of sodium ions on silicate species, aluminium ions force rearrangement of silicate species leading potentially to precipitation, Figure 4.18. This was clearly observed in Figure 4.9, when major peaks representing  $\text{Q}^1$ ,  $\text{Q}^2$ ,  $\text{Q}^3$  types transformed into small, multiple peaks. It appears that in presence of aluminium ions, monomeric silicic acid and other dissolved silicate species can deposit on the membrane

surface without following the classical polymerisation path ( $Q^0 \rightarrow Q^1 \rightarrow Q^2 \rightarrow Q^3 \rightarrow Q^4$ ). This is likely occurs in water when a number of conditions are present for silicate to deposit as monomeric silicate, such as elevated residual aluminium. Once silicate is fully polymerised and deposited on the RO membrane surface, dissolution of monomeric groups will depend on silicate concentration in the CP zone.

Silicate precipitation in solutions with low concentrations of cations and anions occurs via homogeneous nucleation leading to amorphous silicate scale formation, Figure 4.17. However, for CSG waters, solutions have various elevated concentrations of cations and anions such as aluminium for instance, which impact silicate precipitation patterns. Moreover, as can be seen from the comprehensive literature review conducted in this work, silicate has a special relationship with sodium and aluminium as discussed in chapter 2.

Most natural waters, including CSG water have a range cations and anions which influence polymeric structures of silicate species, which affect silicate precipitation patterns. The effect of aluminium on dissolved silica species recorded in this research showed that aluminium ions can interact with dissolved silicate species such as  $Q^2$ ,  $Q^3$  types forcing re-arrangement of species. Aluminium ions can serve as coupling points for polymerised silicate to deposit on the membrane surface as shown in Figure 4.17, leading to heterogeneous silicate polymerisation, Figure 4.18. Both sodium and aluminium are present in CSG waters and affect the speciation of silicates and precipitation patterns as can be concluded from the results recorded here.

The results obtained at different pHs conditions confirmed the silicate species recorded by Stumm and Morgan (1976) in the pH range 9.0 to 11.4. A detail not found in any previous works is the small proportions of monomeric silicate species recorded at pH 2 and pH3. Despite the noise recorded at low pH 2 – 3, relatively low (2-3%) proportions of  $Q^0$  and  $Q^1$  type surroundings were recorded. The relative proportion of silicate species, such as  $Q^0$ ,  $Q^1$ ,  $Q^2$  and  $Q^3$  type surroundings, is strongly pH-dependent (Applin 1987, Baes 1976, Baumann 1956) and controlled by different processes such as hydrolysis (dissolution), condensation (precipitation) and complexation (aggregation) (Alexander 1989, 1954). Structural bonding of the silicate species, or how many silicon

atoms are bound to other silicon atoms via oxygen, is complicated because diverse variables affect concurrent reactions in different ways. The hydrolysis of –O-Si-O-Si-O- linkages, however, is often considered as the key reaction dominating many geochemical processes. The bonds play a key role in many silicate transformations. The hydrolysis of this siloxane bond in the absence of defects has been studied by Walsh and Wilson (2000), Cypryk (2002), and Pelmentschikove (2000). These studies indicate that the high activation energy barrier effectively makes this kind of hydrolysis unlikely at ambient conditions.

## 4.8 Conclusion

In this chapter, results of a  $^{29}\text{Si}$  NMR study of dissolved silicate species are presented. For the first time a method was developed to evaluate the impact of sodium and aluminium cations on dissolved silicate species. The method provides a novel approach to study the impact of different cations on dissolved silicate species and shows that silicate polymerisation can be effected by different cations and as a result silicate precipitation needs to be understood for specific water systems. The main outcomes can be summarised as follows:

- As a result of dilution with deionised water, dissolved silicate species gain or lose monomeric silicic acid ( $\text{Q}^0$  type surroundings). A gradual decrease of  $^{29}\text{Si}$  NMR spectrum intensity or proportions of  $\text{Q}^0$  increased and  $\text{Q}^1$ ,  $\text{Q}^2$  and  $\text{Q}^3$  decreased, indicating that hydrolysis or dissolution of monomeric silicic acid occurred immediately. A consistent proportional decrease of  $^{29}\text{Si}$  NMR spectrum for each species indicates that there is an equilibrium between species at the Si/M molar ratio 1.7, which changed with further dilutions from the Si/M molar ratio 1.55 to 0.11.
- Here it is shown that addition of sodium chloride slightly increased the release of monomeric silicic acid ( $\text{Q}^0$ ) and decreased hydrolysis of more complex silicate species ( $\text{Q}^2$ ,  $\text{Q}^3$ ) compared to similar dilutions with deionised waters preventing water molecular to access  $\text{Q}^2$ ,  $\text{Q}^3$  types.
- The effect of sodium ions on silicate species suggests that  $\text{Q}^0$  type surrounding Si-OH is the preferred bond over Si-O-Na, while for  $\text{Q}^1$  and  $\text{Q}^2$  type surroundings Si-O-Na is preferred over Si-OH. For  $\text{Q}^3$  type both reactions with

$\text{Na}^+$  and  $\text{OH}^-$  may occur in combination and mix of bonds depending on the pH, and physical structures of more complex silicate species.

- Undoubtedly, a profound effect of aluminium ions was recorded on silicate species. The presence of aluminium on silicate species has three impacts: (a) aluminium ions connected to silicate, Al-O-Si-O, resulting in a loss of sensitivity of  $^{29}\text{Si}$  NMR spectrum, (b) aluminium forced re-arrangement of species perhaps into smaller groups, which are also lead to a loss sensitivity of  $^{29}\text{Si}$  NMR spectrum, and (c) it is likely some silicate species  $\text{Q}^1$ ,  $\text{Q}^2$  type precipitated as aluminium silicate. This was a clear indication structural shift of silicate species towards condensation (precipitation reaction) processes.
- A significant impact of minor concentrations of aluminium into relatively rich in silicon sodium silicate solutions is indicative that the Si:Al ratio can be quite low for aluminium to have a significant impact on dissolved silicate species.
- The chemical shifts recorded in low pH 2 and 3 illustrate the presence of monomeric silicic acid, have not been found in other studies (Stumm and Morgan (1976), Dietzel (2002)) probably due to rapid particle formation at these pH conditions and due to low interest in this experimental data from a practical application perspective.

## Chapter 5 Silica removal by coagulation

### 5.1 Introduction

#### 5.1.1 Objectives of experiment

The primary objective of this research was to identify the degree to which silica (as  $\text{SiO}_2$ ) could be removed by coagulation prior to RO process. The second objective was to study the effect of salinity on silica reduction by a range of coagulants. Six types of water quality (three CSG waters and three synthetic CSG waters) were used in the eighty seven coagulation experiments. The physical and chemical properties of CSG waters tested were described in chapter 2, and details of the collection of the field waters are outlined in chapters 3. Three coagulants - ACH, ferric chloride and aluminium sulphate were selected for the experiments as these reagents are commonly used in pre-treatment of natural waters priority to RO desalination. ACH is pre-polymerised coagulant and was selected in particular to evaluate its performance against as ferric salt and aluminium sulphate (alum).

Effective removal of suspended solids, colloidal matters, DOC as well as metals and silica during the pre-treatment stage is desired for successful operation of RO processes - to prevent fouling and scale deposition on the membrane surface in RO desalination. The coagulation process frequently results in a dramatic reduction in the total number of particles and colloids present, as well as metals and silica (Brant 2012, Bartman 2010). Yet, the simplicity of coagulation is offset by incomplete knowledge about the hydrolysis reactions of  $\text{Al(III)}$  and  $\text{Fe(III)}$ , the nature of colloids present in natural waters, silica species and the kinetics of competitive reactions that occur in complicated chemical systems. Selection of the correct coagulant to achieve effective silica removal remains challenging as effective silica removal is difficult to predict due to complex silica chemistry and its various possible silica forms, and the effect of other cations and anions present in the feed.

The coagulation experimental work was designed in two stages:

- First, different CSG waters were used to determine the silica removal efficiency and coagulation effectiveness of a set of coagulation conditions, and how the coagulation process would cope with changes in water quality.
- Second, the impact of salinity on coagulation efficiency, and turbidity and silica removals in low, medium and high salinity synthetic waters. The synthetic waters were similar to CSG water quality, and were used to identify the impact of salinity on coagulation performance to assist interpretation of the performance results for CSG water.
- In addition, in all the above experiments residual aluminium was recorded to evaluate the increase of aluminium concentration in post-coagulation waters compared to raw waters (CSG and synthetic).

### 5.1.2 Rational for salinity investigation

In practice, it is common for the salinity of CSG water to increase over the life-time of the project. The salinity can increase as a result of water table depression in the relevant aquifer; increase in the depth of production wells, and/or geology variations. In saline waters, however, coagulation behaviour may exhibit some distinctively different features compared to that for low salinity waters (Duan 2002, Healy 1994). Although coagulation has been used in CSG water pre-treatment for at least 10 years there is a lack of reported studies from field and research laboratories concerning the impact of salinity on coagulation efficiency. Nonetheless, the magnitude of ionic strength and relative sodium ion concentration in solution leads to a difference in the nature of coagulation mechanisms (Healy 1994), as depicted in Figure 5.1, and in particular for the hydrolysis of metal salts and silica removal mechanisms (Healy 1994). Figure 5.1 shows expected variations in the coagulation mechanism, developed by the author, for high salinity waters where sodium ions act as a stabilising agent. It was found that sodium cations in high salinity waters can create binding layers around dissolved silica species acting as a stabilising agent (Healy 1994, Bergna 1994). According to this hypothesis observed by Healy (1994), dissolved silica species aggregate into oligomeric-structures, such as  $Q^2$  or  $Q^3$  types surrounding in response to sodium binding layers. According to this theory, in high salinity water silica is surrounded by sodium

ions and in low salinity water sodium ions do not create bind layers around silica, Figure 5.1.

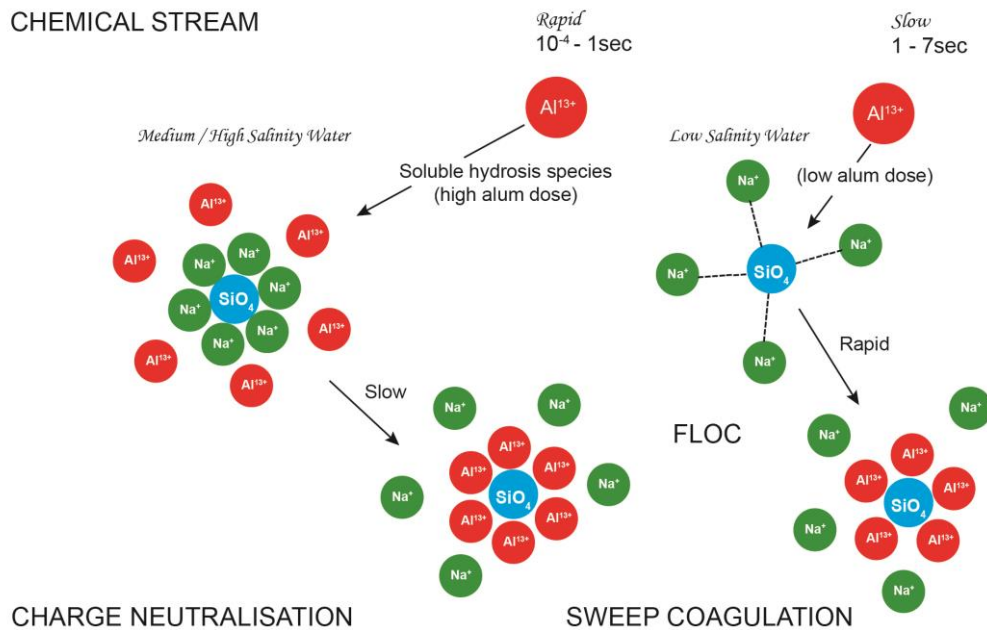


Figure 5.1 – Conceptual diagram of coagulation mechanism of silica (as  $\text{SiO}_4$ ) removal using ACH ( $\text{Al}^{13+}$  species) in low (0-8g/L), medium (12g/L) and high (30g/L) salinity waters.

Figure 5.1 illustrates that in medium-high salinity waters, silica removal by both charge neutralisation and sweep coagulation are inhibited by sodium ions filling the binding layers of silica species preventing ready access of aluminium to the hydrolysis species of silica. In low salinity water, silica is accessible for aluminium hydrolysis species enabling charge neutralisation and sweep coagulation to occur.

Based on the results obtained in this work, the hypothesis was proposed that sodium ions will be substituted by aluminium ions in the binding layers. A detail not found in any previous works illustrating the impact of salinity on silica removal efficiency by coagulation.

## 5.2 Results of jar tests

### 5.2.1 Coagulants and best doses

The primary focus of this set of experiments was to identify the best performing coagulant and its dose for effective turbidity, DOC, metals and silica reduction. The performance of the three coagulants was evaluated over a range of coagulation doses applied to two CSG waters sourced directly from the field in 2013 and 2014 (water quality described in Table 3.2 chapter 3).

#### 5.2.1.1 Turbidity removal (groundwater)

Figure 5.2 provides insight into the effect of three coagulants and coagulation doses required. Turbidity reduction increased from 0 to 86% for ACH when coagulation doses increased from 0 to 60mg/L.

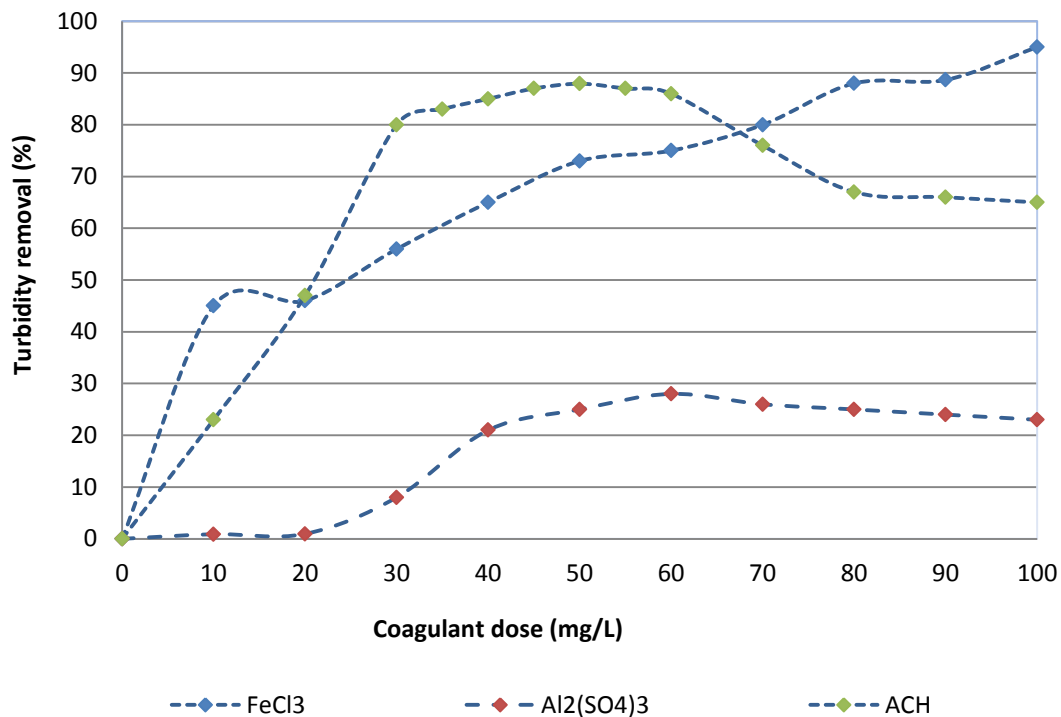


Figure 5.2 – Turbidity removal from groundwater composite samples (CSG water 2013) following coagulation with different doses of ACH, Al<sub>2</sub>(SO<sub>4</sub>)<sub>3</sub> and FeCl<sub>3</sub> pH =8.4 at initial turbidity 81.9NTU.

As can be seen from Figure 5.2, at the doses 30 to 60mg/L ACH maximum removal of turbidity occurred and achieved 88% removal at 50mg/L of ACH (as  $Al^{+3}$ ). Further increased ACH coagulation doses from 60 to 100mg/L did not show any further turbidity reduction, but rather a slight drop in efficiency to less than 70% occurred indicating overdosing of ACH. During coagulation with ACH at 30 – 50 mg/L doses, medium size floc formed immediately and the formed floc settled within a few minutes.

Measurements of floc size were determined by visual comparison. Measurements of floc size were recorded by observation of the floc size over the 45 minutes of monitoring time, Table 5.1. The observed clarity of the supernatant after decanting and effective floc formation and settling was an indication that effective charge neutralisation and inter-particle bridging reactions occurred within seconds of ACH addition.

Table 5.1 shows size formation during 45 minutes of mixing during jar tests. Size of floc were recorded after the first 2 minutes and then after each 5 minutes interval. Rate of floc formation takes 10 – 15 minutes; the floc was remained small in volume indicating relatively low sludge production by ACH. Progression of floc formation over the jar test is important because it provides an indication of the rate of flocculation, hydrolysis and charge neutralisation reactions and sweep coagulation (Stumm and Morgan 1976) taking place by careful observation of solution appearance, floc size, and settled sludge on the bottom of breaker. Coagulation with ACH did not create a large volume of floc at any dose, and Figure 3.8 in chapter 3 provides an example of this. As can be seen from Figure 3.8, sludge volume formed by coagulation with ACH for native pH8.4 and pH6.4 was relatively low compare to ferric chloride.

Figure 5.2 shows that aluminium sulphate was less effective for turbidity removal (~28%) than ACH and required higher dosing between 60 to 80 mg/L. Attempts at coagulation with aluminium sulphate produced no visible floc after the first fifteen minutes and very minor floc at the end the experiment prior to decanting, shown in Figure 3.10 (chapter 3).

Table 5.1 – The measurement of the sludge height between the top of the sludge and the bottom of the breaker. (Measurements of floc size during coagulation of CSG water (2013) with 50 mg/L ACH at pH8.23).

Time	Floc size					
	0mg/L	35mg/L	40mg/L	45mg/L	50mg/L	55mg/L
Minutes	mm	mm	mm	mm	mm	mm
2	<2	<2	<2	<2	<2	<2
5	<2	<2	<2	<2	<2	<2
10	<2	<2	<2	<2	<2	<2
15	<2	<2	2-2.5	2-2.5	2-2.5	2-2.5
20	<2	2-2.5	2-2.5	2.5-3	2.5-3	2.5-3
25	<2	2-2.5	2-2.5	2.5-3	2.5-3	2.5-3
30	<2	2-2.5	2-2.5	2.5-3	2.5-3	2.5-3
35	<2	2-2.5	2-2.5	2.5-3	2.5-3	2.5-3
40	<2	2-2.5	2-2.5	2.5-3	2.5-3	2.5-3
45	<2	2-2.5	2-2.5	2.5-3	2.5-3	2.5-3

Coagulation with ferric chloride was shown to be relatively effective for turbidity removal (95%), but required much higher doses of approximately 100 mg/L to achieve turbidity removals similar to ACH. The floc volume (Figure 3.10 chapter 3) generated by ferric chloride at higher dosage rates was significant, and it was 40% more than that

generated by ACH. The formation of higher floc volume was expected because of the higher coagulant dose. Overall the solubility of Fe(III) is much lower compared to aluminium sulphate, but higher than ACH (Pernitsky, 2003). For CSG waters ACH with lower solubility than ferric and higher aluminium content than aluminium sulphate was the best performing coagulant. Ferric chloride does not meet the conditions for effective floc formation and low coagulation dose for CSG waters, and was considered the second best performing coagulant behind ACH.

### 5.2.1.2 Effect of pH on turbidity removal

The effect of coagulation pH on turbidity removals is illustrated in Figure 5.3 for the three different coagulants at doses corresponding to their optimum effectiveness at pH 8.4 for ACH (35 mg/L  $Al^{3+}$ ) and  $Al_2(SO_4)_3$  (50 mg/L  $Al^{3+}$ ), and at an effective dose at pH 8.4 for  $FeCl_3$  (60 mg/L  $Fe^{3+}$ ) as no optimum was observed.

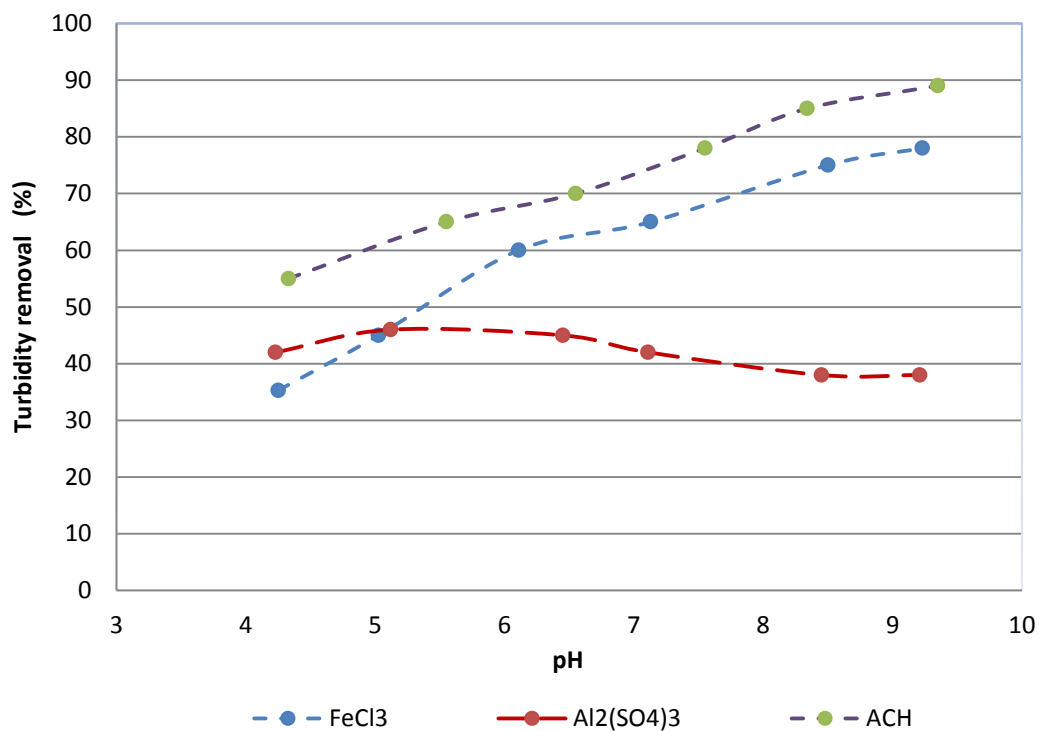


Figure 5.3 – Turbidity removal from the supernatant after sub-samples(groundwater composite) were treated with 35mg/L of ACH (as  $Al^{3+}$ ), 50 mg/L of  $Al_2(SO_4)_3$  (as  $Al_{+3}$ ) and 60 mg/L of  $FeCl_3$ , ( as  $Fe^{3+}$ ) respectively at initial turbidity 81.9 NTU.

At pH 5.8, near the pH of minimum solubility for ACH (Bertsch 1996) turbidity removal was <66% at a relatively low coagulation dose (35mg/L). At pH 7, 8 and 9, turbidity removals by ACH increased for the same dose, (35mg/L). It is evident that ACH was the most effective coagulant for turbidity removal over the pH range 5.5 to 9. These features are probably tied to the characteristics of different aluminium species present in the water at different pHs.

Ferric chloride was also effective with 60 - 78% turbidity removal for a 60mg/L dose over the pH range 6 to 9, but was less effective than ACH. Coagulation with aluminium sulphate at an optimal dose of 50mg/L (pH 8.4) achieved about 40% turbidity reduction. ACH and ferric chloride were found to be more effective for turbidity removal than aluminium sulphate over the tested pH range.

It can be seen that the best pH range for ACH and ferric chloride was already close to the native pH of the water (pH 8.4), and performance declined at lower pH for all of the coagulants. This can be explained by relatively high salinity of the waters especially seen in performance of ferric chloride and aluminium sulphate compare to pre-polymerised coagulant ACH. Overall trends were increasing turbidity reduction with increasing pHs for all CSG waters studied.

### **5.2.2 DOC removal (groundwater)**

Figure 5.4 shows the DOC removal efficiency by ACH, ferric chloride and aluminium sulphate for a range of doses at pH 8.4. Coagulation by ACH at a dose of 50mg/L showed about 50% DOC removal. Increasing the dose from 50 to 100 mg/L of ACH as  $Al^{3+}$  did not result in the further DOC reduction. Ferric chloride and alum were less effective for DOC removal than ACH at the native pH8.4. The trend in the results obtained by all three coagulants indicates that very low neutralisation of DOC substances occurred at the native pH, presumably due to the relatively high salinity of CSG water. It appears that metal hydrolysis species formed at native pH 8.4 or slightly lower pH (after addition of the coagulant) are not effective for neutralisation of organics present in this CSG water.

Figure 5.4 illustrates improved DOC removal at pH8.4 and pH6 with ACH, and that by lowering the pH more than 80% DOC removal could be achieved. ACH was again the most effective coagulant.

Low pH (pH5.5 – 6 ) is often recommended to maximise TOC/DOC removal by ACH, PACl, and alum, but effective turbidity removal does not require pH this low. Stumm and Morgan (1976) identified that turbidity and DOC removal do not overlap due to highly negative charge of DOC substances compared to turbidity. However, lowering pH of the solution lead to a reduction of negative charge on DOC so that neutralisation reaction can take place effectively with a lower coagulant dose.

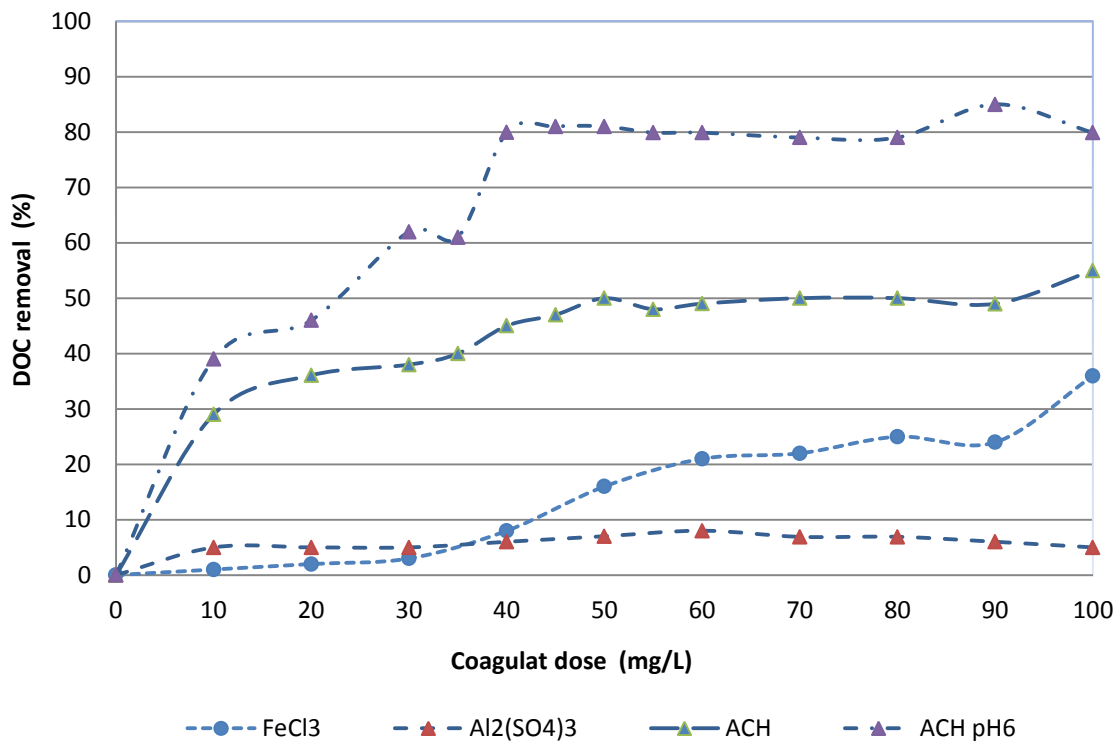


Figure 5.4 – DOC removal from groundwater composite samples treated at different doses of ACH (as Al<sup>3+</sup>) at pH6 and pH8.4, Al<sub>2</sub>(SO<sub>4</sub>)<sub>3</sub> (as Al<sup>3+</sup>) and FeCl<sub>3</sub> (as Fe<sup>3+</sup>) at pH 8.4 for initial DOC=19mg/L.

### 5.2.2.1 Effect of pH on DOC removal

As was expected, DOC removal increased dramatically with decreasing pH. At pH 6.4, DOC removal by ACH reached 84%, nearly two times higher than at the native pH8.4 for the same dose. The reduction of DOC by ACH at pH6.4 to 1.2 mg/L is sufficient for effective operation of RO systems.

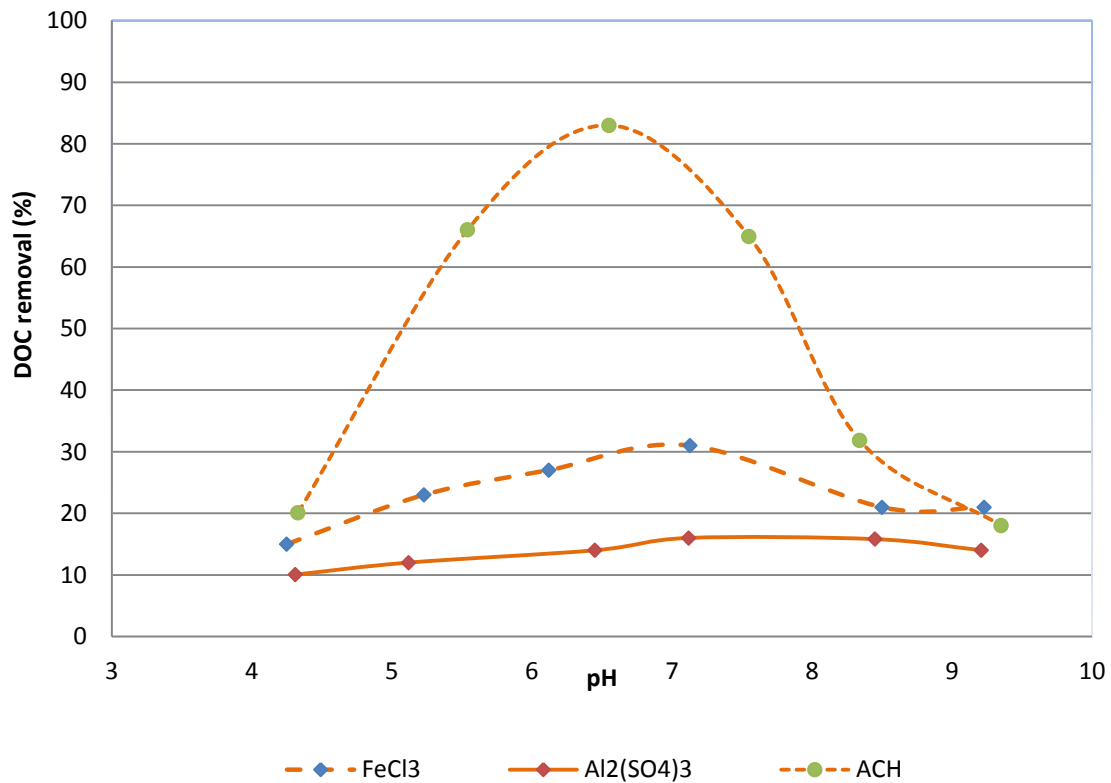


Figure 5.5 – DOC removal from the supernatant after sub-samples(groundwater composite) were treated with 45mg/L of ACH, 50 mg/L of  $Al_2(SO_4)_3$  and 60 mg/L of  $FeCl_3$ , respectively at initial DOC=19mg/L.

Figure 5.5 shows that at lower pH, DOC removal also improved for ferric and alum salts to 27% and 14% respectively, but the treated DOC concentrations were unlikely to prevent potential DOC deposition on the membrane surface. At pH7, DOC removal by ferric chloride was about 31%, much higher than at the native pH. Alum showed relatively poor DOC removal over the entire pH range with removals between 10 to 15%. Nevertheless, the results demonstrated that the trend of improved DOC removal for all CSG waters (2013 and 2014 samples) at lower pH.

### 5.2.3 Metals removal (groundwater)

Effective metals removal is also important for long term RO operation. Cations of Ca, Mg, Ba, Sr, Al attached as metal hydroxides on the membrane surface, both directly foul the membrane and serve as nucleation points for deposition of monomeric silica acids. Furthermore, they may also attract organic compounds, for instance Ca attracts alginates (El-Manharawy 2000, Gablich 2010). Previous studies have demonstrated that 10 – 12% membrane surface coverage by metal hydroxide species is sufficient to initiate scale formation on the RO membrane surface (Bremere 2000, Gablich 2010).

The results of metals removal by coagulation are shown in Figure 5.6, where the percentage removals of Ca(II), Mg(II), Ba(II), and Sr(II) are plotted against ACH dose applied. As ACH showed the best turbidity and DOC removal efficiency, and effective floc formation, the other two coagulants (ferric chloride and alum sulphate) were disregarded for this set of experiments.

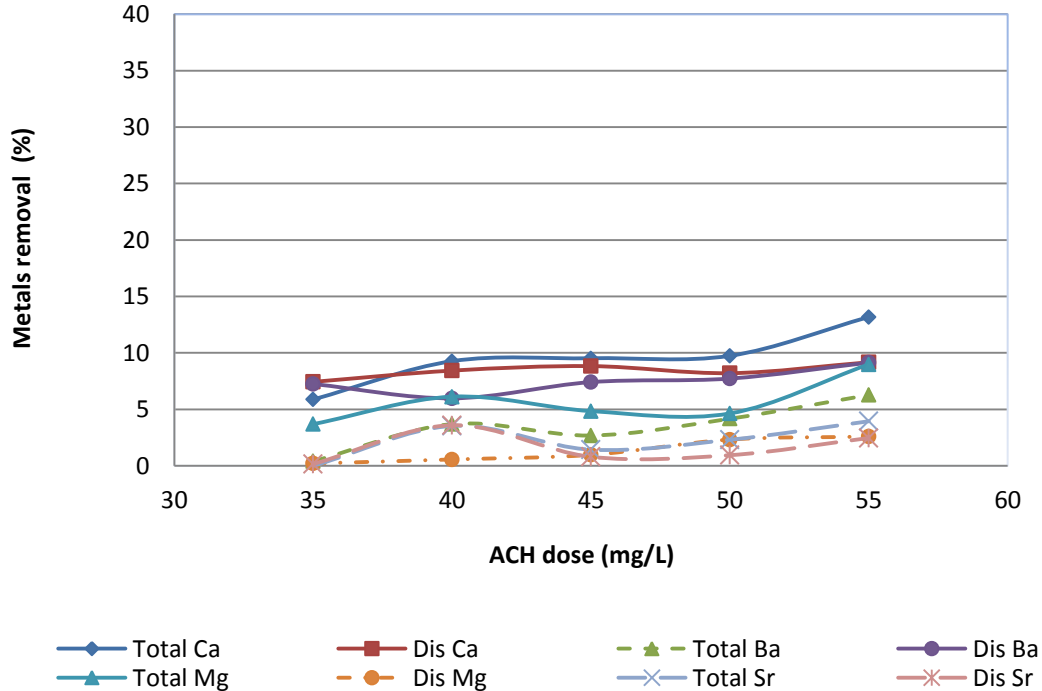


Figure 5.6 - Metals removal from the supernatant after sub-samples (groundwater composite 2013) were treated at various doses ACH.

On application of 55mg/L of ACH, the percentage metals removal were 13% of total and 9% dissolved calcium, 9% of total and 2.8% dissolved magnesium, 6.5% total and 4% dissolved barium, and 4.5% total and 2.5% dissolved strontium. These low removal results were expected given the relatively low initial concentrations of metals in CSG water and high salinity of CSG water. The mechanism of removal is precipitation and adsorption into the Al hydroxide. The results show that the removal efficiency slightly increased with an increased applied doses of ACH, Figure 5.6.

Maximum metal removal was at the 55mg/L dose by ACH. Total calcium reduction was from an initial 9.0mg/L to 7.74mg/L, and dissolved calcium from 4.23mg/L to 3.81mg/L. Total magnesium reduction was from 5mg/L to 4.31mg/L, and dissolved magnesium from 3.23mg/L to 2.91mg/L. Total barium reduction was from an initial 2.3mg/L to 2.1mg/L, and dissolved barium from 1.1mg/L to 0.91mg/L. Total strontium reduction was from an initial concentration of 2.1mg/L to 1.89mg/L, and dissolved strontium from 1.1mg/L to 1.01mg/L.

Medium to low efficiency removal for all metals arises from the pH at which the coagulation occurred being lower than that required for optimal metal precipitation. For each metal concentration there is a minimum solubility condition that corresponds to the maximum metal precipitation by chemical coagulation (Stumm and Morgan 1962, 1973). Because initial total and dissolved metals concentrations in CSG water (2013 ground sample) were relatively low, the results were considered to be satisfactory.

#### **5.2.4 Silica removal (groundwater)**

Figure 5.7 illustrates dissolved silica removal by each coagulant for the 2013 CSG water sample. Dissolved silica removal reached a maximum of 5% at 50mg/L ACH. Further ACH dose increases did not show any further silica removal. Less than 1% dissolved silica removal occurred by alum at doses of approximately 50 – 60 mg/L. Ferric chloride showed increasing silica removal up to 10% at 100mg/L, however, as discussed previously, the floc size was small and the sludge volume was quite significant. Ferric chloride was not considered for practical use because of its small floc size and hence, slows settling rate and its high sludge volume. The volume of sludge

generated by ferric chloride coagulation was about 40% higher than by ACH, as illustrated in Figure 3.10, chapter 3.

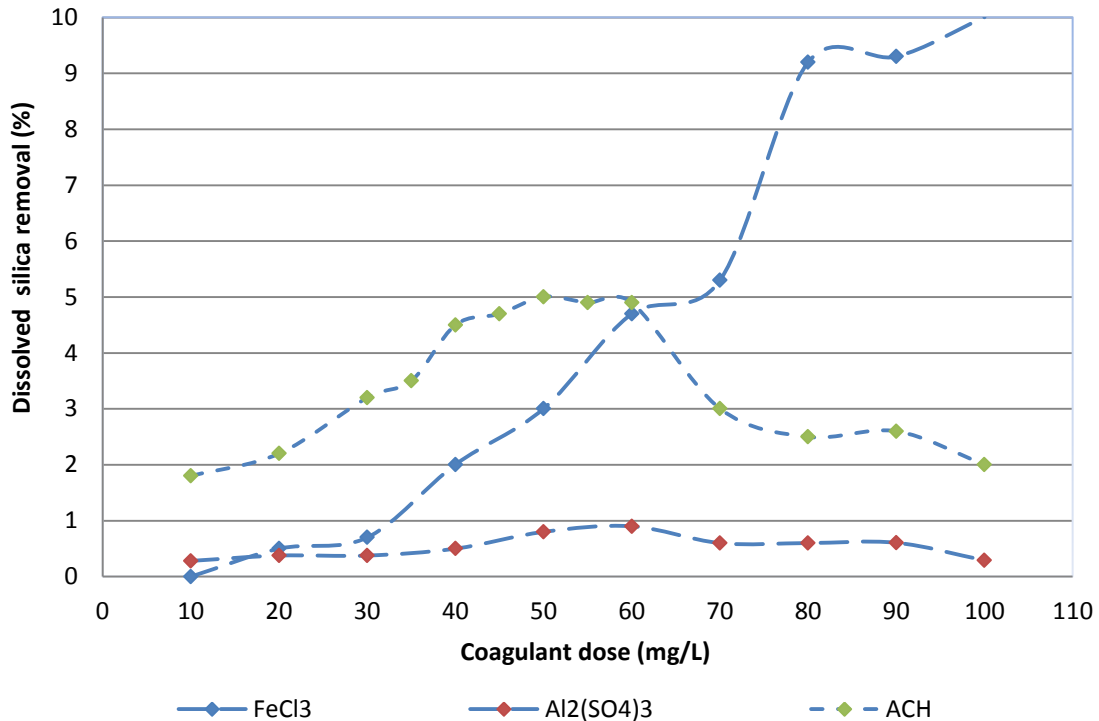


Figure 5.7 - Dissolved silica removal from the supernatant (groundwater composite CSG water collected in 2013 initial dissolved silica = 16 mg/L) at different doses of ACH, FeCl<sub>3</sub>, Al<sub>2</sub>(SO<sub>4</sub>)<sub>3</sub>.

Coagulation performance on CSG water collected in 2014 is shown in Table 5.2. Overall total silica removal by ACH was between 27 to 63% at 30 - 50mg/L doses. Dissolved silica removal by ACH was between 8 and 36% at the same dose 50mg/L. For aluminium sulphate, total silica removal was between 10 and 20% and dissolved silica removal was 1% for all experiments. Ferric chloride show total silica removal in the range of 15 – 20% and dissolved silica removals between 4 – 10%. Overall the trends were similar to the CSG water collected in 2013, except the dissolved silica removals were significantly higher for the 2014 water. Higher turbidity, DOC, total metals removals lead to better total and dissolved silica removal, as silica is frequently attached to particulate dispersed matter (metal hydroxides, clay).

Dissolved (reactive) silica in water is initially in the monomeric state as monosilicic acid ( $\text{Si}(\text{OH})_4$ ), and is mostly not ionised at the natural pH 8.5 (Sheikholeslami 2002). After addition of a coagulant, the native pH 8.5 of the water is slightly decreased. For the studied CSG sample, the pH decreased from pH 8.4 to pH 7.9 by applying 50mg/L of ACH, and from pH 8.4 to 7.1 by ferric chloride at the best doses. As the pH decreases, the degree of silicic acid ionisation decreases. At pH 8.5 only 10% of the monomeric silica is ionized, while at pH 9, 40% is ionised (Sheikholeslami 2002). As the pH (native pH) drops from pH 8.4 to 7.9, the ionised form of monosilicic acid decreases. As discussed in chapters 4 and 6, depending on the sodium chloride concentrations in water, dissolved silica species ( $\text{Q}^0$ ,  $\text{Q}^1$ ,  $\text{Q}^2$ ,  $\text{Q}^3$  type surroundings) can also be less accessible to the coagulant hydrolysis species due to stabilisation by sodium ions.

Table 5.2 – Summary of the coagulation by ACH, ferric chloride and aluminium sulphate for CSG water collected in 2014 (initial total silica =22.68 mg/L, initial dissolved silica = 11.88 mg/L).

Dose (mg/L)	Coagulant	Turbidity removal (%)	Total silica Removal (%)	Dissolved silica Removal (%)
<b>20</b>	ACH (as $\text{Al}^{+3}$ )	94	17	13
	Ferric (as $\text{Fe}^{+3}$ )	78	12	12
	Alum (as $\text{Al}^{+3}$ )	0	9	0
<b>30</b>	ACH (as $\text{Al}^{+3}$ )	95	63	36
	Ferric (as $\text{Fe}^{+3}$ )	75	20	13
	Alum (as $\text{Al}^{+3}$ )	85	45	1
<b>50</b>	ACH (as $\text{Al}^{+3}$ )	98	56	28.2
	Ferric (as $\text{Fe}^{+3}$ )	94	13	4.3
	Alum (as $\text{Al}^{+3}$ )	93	20	7.4

The  $\text{Al}^{3+}$  ion precipitates colloidal silica, but only in the pH range 4 to 5 (Sheikholeslami 2002, Exley and Birchall, 1993). Exley and Birchall (1993) have elucidated that silicic acid reacts with aluminium to form one of the two types of groups depending on the ratio of  $\text{Si}(\text{OH})_4$  to Al in solution. The reaction, however, is thought to involve only the condensation of  $\text{Si}(\text{OH})_4$  across hydroxyl groups on adjacent Al atoms which are part of an aluminium hydroxide ( $\text{Al}(\text{OH})_{3(s)}$ ) framework, but does not directly

engage free Al ions (Exley and Birchall 1993). This probably explains why dissolved silica removal was significantly improved with ACH, as it contains aluminium hydroxides that may directly associate with silica. For aluminium sulphate and ferric, the metals ions are unable to directly associate with the silicate and must first form aluminium or iron hydroxides. Low removal efficiency by ferric chloride and aluminium sulphate suggest that the formation of these aluminium and iron hydroxides was inhibited presumably due the high salinity of CSG waters.

### 5.2.5 Turbidity removal (storage dam water)

CSG water pumped from production wells is frequently stored in temporary evaporation ponds (5 – 30 days volume) prior to RO desalination. Pre-treatment of this water is commonly applied to prevent organic and inorganic fouling of the membrane.

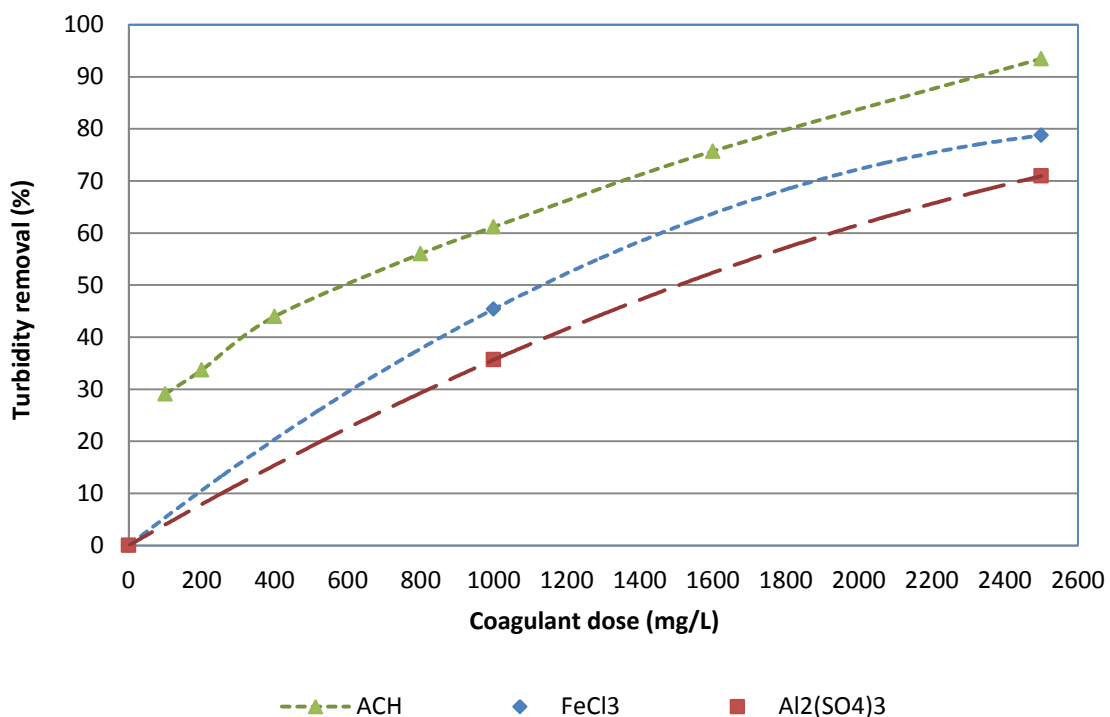


Figure 5.8 - Turbidity removal from dam water composite treated with different doses of ACH,  $Al_2(SO_4)_3$  and  $FeCl_3$  at initial turbidity 60mg/L.

Removal of silica by coagulation is also beneficial to this CSG water, as elevated concentrations of silica in combination with organic contaminants can lead to

significant membrane fouling. CSG water quality from a storage dam is summarised in Table 3.2 in chapter 3.

Figure 5.8 demonstrates the results of coagulation on turbidity removal. As can be seen, much higher coagulant doses were required by all of the coagulants. ACH achieved 34% turbidity removal at a dose of 200mg/L (as  $Al^{+3}$ ). At a dose of 1000mg/L ACH only 60% turbidity removal was obtained. Further significant increases in ACH dose showed turbidity removal up to 92% for a dose of 2500mg/L.

During the coagulation of the storage dam composite sample, the effluent (pH9.4) and conductivity (14200  $\mu$ S/cm) changed notably from its feed values to lower pH (7.1) and higher conductivity (18300  $\mu$ S/cm), indicating that the aqueous background matrix reacted with aluminium hydroxyl species. Ferric chloride showed less turbidity removal than by ACH at all doses studied. 80% turbidity removal was attained by applying ferric chloride at a dose of 2500mg/L. During coagulation with  $FeCl_3$ , the effluent (pH9.4) and conductivity (14200  $\mu$ S/cm) changed to from its feed values to pH(6.5) and conductivity (19100  $\mu$ S/cm) indicating that the aqueous background matrix have reacted with ferric hydroxyl species. Aluminium sulphate had lower efficiency for turbidity removal than ACH and  $FeCl_3$  at coagulation dose 1000mg/L, with only 33% turbidity removal achieved at 1,000 mg/L  $FeCl_3$ .

The volume of floc produced by coagulation (and especially by ferric chloride) when treating the storage dam water was significantly higher than that from the groundwater, and the floc was so thick that individual flocs could not be differentiated from the general sludge. This was because of the high coagulant doses used and due to water quality of the storage dam water, and in particular the high TOC concentration (121mg/L). The high density of the floc had the effect of making the floc settle as a thick sludge, so that very little floc remained in the supernatant. When the 2000 mg/L dose of ferric chloride was used, the sample contained approximately 40% volume of settled floc (sludge volume) underlying 60% clear supernatant after 30 minutes of settling. In practice, if the volume of floc increases with higher doses of coagulant, it is

likely that this will lead to problems extracting clean supernatant and require a large sludge treatment facility. Such a process would be impractical.

### 5.2.6 Silica removal (storage dam water)

Silica concentration in the storage dam sample was slightly higher than water directly sourced from production wells. This might be a result of evaporation of water and/or release of silica by diatoms or their remains in the storage dam. Algae are often a major problem for CSG water desalination plants in Queensland. Many RO plants in Queensland are located in areas subject to algae blooms (according to DERM algae blooms occurred each 4 years period), where concentrations may exceed  $10^3$  cells per mL (DERM, 2014). Two extensive reviews of algae in freshwaters by Henderson et al., (2008) and Ghernaout (2010) cover algal properties, dissolved organic matter excreted by algae, and coagulation of algae.

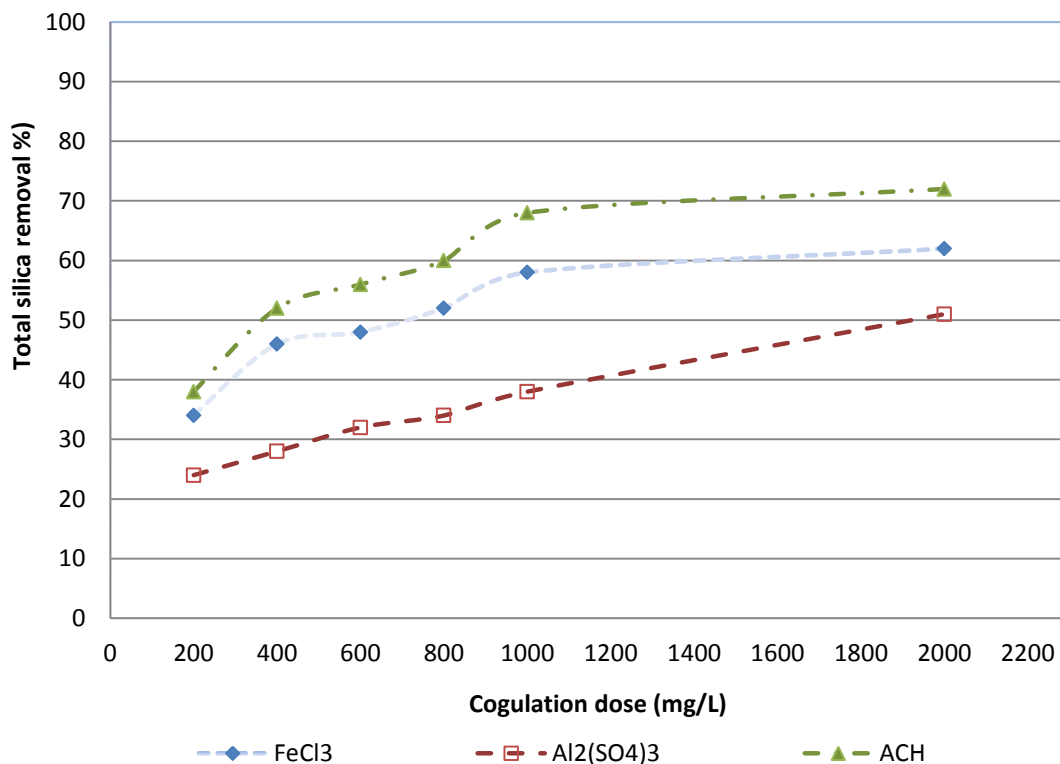


Figure 5.9 – Total silica (as SiO<sub>2</sub>) removal from storage dam water treated at different doses of ACH, Al<sub>2</sub>(SO<sub>4</sub>)<sub>3</sub> or FeCl<sub>3</sub> at initial total silica concentration 25mg/L.

Unlike mineral particles, algae remain suspended while undergoing growth and do not coagulate until they are in the later stage of their growth cycle (Henderson 2008, Ghernaout 2010). In the later phase of growth they can, however, release silica (Henderson 2008, Ghernaout 2010). If this occurs then the silica (as SiO<sub>2</sub>) concentration in solution will suddenly increase.

The results for total silica removal from the storage dam sample show 38% silica removal by ACH at 200mg/L, and that silica removal continues to increase with an increase of dose to 2,000 mg/L ACH for 72% maximum removal, Figure 5.9. Ferric chloride removed about 36% of silica (SiO<sub>2</sub>) at 200mg/L and maximum removal was 61% at 2000mg/L. Aluminium sulphate again showed relatively low removals, with removals of 31% at 600mg/L and 50% at 2,000mg/L as shown in Figure 5.9 and Table 5.3. ACH was again the best performing coagulant, producing less sludge. Table 5.3 summarises the result of pre-treatment of CSG sample collected from the storage dam.

Table 5.3 – Summary of silica (as SiO<sub>2</sub>) removal by coagulation using ACH, ferric chloride and aluminium sulphate for dam water at 200, 400 and 600mg/L doses at initial total silica concentration 25mg/L and dissolved silica 20mg/L.

Dose (mg/L)	Coagulant	Turbidity removal (%)	Total Silica removal (%)	Dissolved Silica removal (%)
<b>200</b>	ACH (as Al <sup>+3</sup> )	30	38	15
	Ferric (as Fe <sup>+3</sup> )	10	36	13
	Alum (as Al <sup>+3</sup> )	7	22	1.3
<b>400</b>	ACH (as Al <sup>+3</sup> )	43	51	21
	Ferric (as Fe <sup>+3</sup> )	19	46	4.5
	Alum (as Al <sup>+3</sup> )	15	51	2.3
<b>600</b>	ACH (as Al <sup>+3</sup> )	50	56	39.5
	Ferric (as Fe <sup>+3</sup> )	30	47	13.2
	Alum (as Al <sup>+3</sup> )	20	31	3.4

The extremely high doses required for good turbidity removal for all three coagulants make coagulation treatment of this water impractical. The very high chemical consumption leads to high sludge volumes as shown in Figure 3.8 (ferric chloride coagulation) that will contribute significantly to the cost.

### 5.2.7 Aluminium residual

Control of residual aluminium becomes increasingly important as post-precipitation of aluminium residuals in the RO system, particularly in the presence of silicon, is possible. As discussed in chapter 2, residual aluminium can cause a significant decrease in the capacity of RO membranes by precipitating in the RO system. Table 5.4 summarises the results of residual aluminium concentrations in the post-coagulation treated CSG waters. Coagulation by ACH, generally, led to lower residual aluminium increases than coagulation by aluminium sulphate. The extremely high coagulation doses (> 200mg/L) used for the storage dam water also showed significant increases of residual aluminium.

Table 5.4 – Residual aluminium recorded in raw CSG waters and in post-coagulated treated CSG waters at various coagulation doses by ACH and aluminium sulphate.

Type of CSG water	Alum (as Al <sup>3+</sup> ) in raw CSG water (mg/L)	Best coagulation dose by ACH (mg/L)	Best coagulation dose by Alum (mg/L)	Al <sup>3+</sup> in treated water post-coagulation (mg/L)
Groundwater	7.5	45	-	23.4
Dam storage	11.5	200	-	34.7
Groundwater	7.5	-	60	27.7
Dam storage	11.5	-	200	68.9

A recent survey by Letterman and Driscoll (2003) indicated that the high total Al concentrations in the treated water (post-coagulation) were associated with (1) high source water total Al concentration as was found for CSG waters in Australia, (2) high treated water turbidity, and (3) aluminium as a contaminant in the lime used for post MF/UF filtration for pH adjustment.

The most common strategy to reduce residual aluminium levels in RO feed is to use alternative coagulants such as iron, or reduce the aluminium dose by using pre-polymerised aluminium products (such as ACH), and to ensure effective removal of

particulate matter during filtration to reduce floc carry over. Nevertheless coagulation of CSG water with ferric chloride was found to generate a significant volume of sludge which the industry tries to avoid because of significant additional investment into sludge treatment and disposal facilities. ACH or similar pre-polymerised reagents seem to be better suited for high recovery RO plants operating on CSG water. However, reduction of residual aluminium concentrations in post-coagulation water remains a key of concern. The effect of elevated concentrations of residual aluminium in CSG waters (post-coagulation water quality) was investigated and is discussed in detail in chapters 4 and 6.

### **5.2.8 Effect of salinity**

#### ***5.2.8.1 Experimental***

The impact of salinity on silica removal by the three coagulants was investigated by applying the best coagulation dose to three different salinity synthetic waters, Table 3.2. Preparation of the solutions was described in detail in chapter 3. Each sample was prepared twice and each sample analysed by the ICP six times. Supplementary data for floc characterisation was collected, including the colour and turbidity of clarified water, percentage sludge volume, floc settling rate, and sludge volume. Table 5.1 Sludge settling conditions were classified as two possible cases: (1) classified as diffused layer, when each particle deposits as if it was alone with some settling faster and others slower, and (2) classified as a sludge layer, when sedimentation involves all the flocculated particles, creating a layer of clear liquid above a sludge layer inside the breaker. The effect of sodium concentrations on coagulation reactions and silica removal efficiency are discussed in subsequent sections.

#### ***5.2.8.2 Effect of sodium***

Figure 5.10 illustrates the results of total and dissolved silica removal by ACH, ferric and alum salts. The impact of salinity on silica removal plotted in Figure 5.10 clearly illustrates the impact of sodium concentration on silica removal efficiency. Increasing the salinity of the synthetic water from 5 to 45g/L leads to decreasing efficiency of total

silica (TS) removal by ACH from 72.3% to 38%, and for dissolved silica (DS) removal from 68 to 35.6%, TS removal by ferric from 67 to 26% and DS removal from 62 to 23%, and by alum for TS removal from 11 to 3% and DS removal from 10 to 3%.

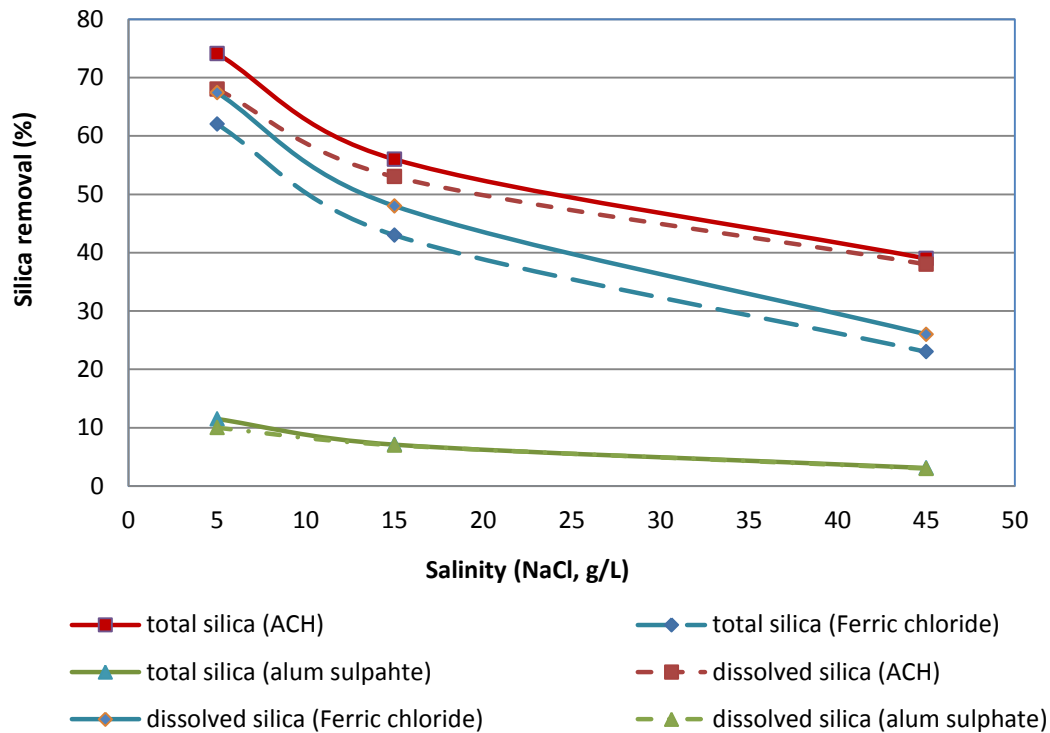


Figure 5.10 – Total (TS) and dissolved (DS) silica removal by ACH, ferric chloride and alum at 45mg/L dose and for various salinity waters at initial total silica concentration 21mg/L and dissolved silica 16.8mg/L.

While reduction of silica (total and dissolved) by coagulation is readily achieved in relatively low salinity water, it seems a very different coagulation mechanism is involved in medium (< 8g/L of NaCl) and high (> 15g/L) salinity waters.

In low salinity water, floc formation during coagulation with ferric chloride was observed after 10 minutes, and the flocculated solution was allowed to rest. During the coagulation experiment with alum, the first appearance of floc was observed after 5 minutes of monitoring time and floc size slightly increased during 45 minutes of slow mixing. The small sludge volume inside the breaker created a distinctive layer with clear liquid above.

In medium salinity water, floc formation with ferric salt was less visible compared to the low salinity water coagulation. Alum sulphate achieved 7.1% removal of total and 3% dissolved silica. No floc formation was observed in this salinity water by aluminium sulphate, and similar trends were observed in medium salinity CSG waters. ACH was effective for total silica removal of 56% and dissolved silica removal of 53%. Floc was formed immediately after the first 2 minutes of monitoring time (as described in Table 5.1) and final sludge volume was less than 10%.

In high salinity water, ACH showed 39% total and 38% dissolved silica removals. Floc was observed after 5 minutes of coagulation mixing and the final supernatant was very clear demonstrating good coagulation performance by ACH at this high sodium chloride concentration. As ACH is pre-hydrolysed coagulant, it shows that aluminium species formed as result of hydrolysis in high salinity water was able to overcome interference of sodium ions.

In low salinity waters (0 – 8 g/L of Na<sup>+</sup>) silica species (reactive silica) and colloidal silica are dispersed between water molecules and well separated from Na<sup>+</sup> ions. In this type of aqueous solution, water molecules provide a homogeneous environment for cations and anions to interact freely, and for charge neutralisation of particles arising from addition of the coagulant. Once a coagulant is introduced into the solution, hydrolysis takes place within seconds, Figure 5.1. The pH of the solution will define the quantities of different hydrolysis species. Positively charged ionised species attack negatively charged contaminants including silica. In this case, the coagulation reactions follow standard patterns (neutralisation, bridging, precipitation, co-precipitation and adsorption) as shown in Figure 5.1.

In the presence of elevated concentrations of Na<sup>+</sup> ions (0.15M of Na<sup>+</sup> and higher), however, Na<sup>+</sup> ions act as a stabilising agent towards dissolved silica species. This hypothesis was introduced by Healy (1994) during his work on the development of silica coating criteria.

It is hypothesised that when metal salts, for example ACH, are introduced into the solution, some aluminium species (product of coagulant hydrolysis) will substitute for sodium in the binding layers. The  $^{29}\text{SiNMR}$  study in chapter 4 demonstrated that aluminium ions have higher reactivation energy than sodium ions when binding to silicate, and that the Al-O-Si-O-Al bonds have stronger connectivity than Na-O-Si-OH bonds. In medium high salinity waters (8 – 30 g/L) aluminium species will substitute for sodium ions in the binding layers of silicate to create –Al-O-Si-O- structures.

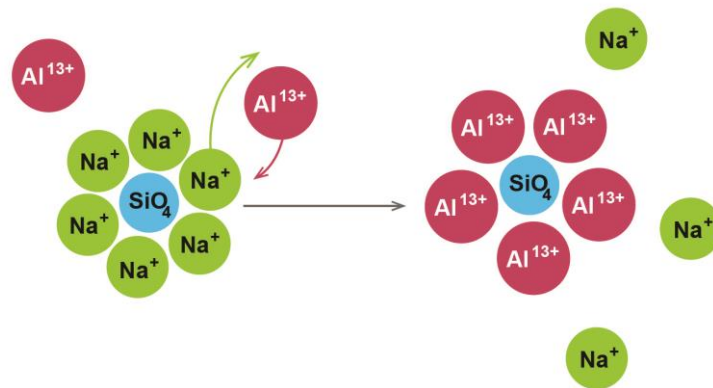


Figure 5.11 – Sodium binding layer surrounding silica species and substitution of sodium ions from these binding layers by aluminium ( $\text{Al}^{13+}$  species) in solutions with NaCl concentrations of  $< 8\text{g/L}$ .

The substitution reaction, however, will depend on the concentrations of sodium, silica, aluminium or ferric within the coagulant applied, pH and likely other cations and anions present in the solution. Thus, the more strongly hydrated the cations in the poly-silicate exchange layer, the lower the binding energy and the lower the extent of exchange between layers (i.e. the lower the ion exchange between poly-silicate layer and sodium stabilising layer), the thicker the layer at any given pH and salt molarity, and the more effective the electro-steric barrier (Healy 1994). As a result of all these effects, silica coagulation can proceed in two possible ways:

- by part substitution of sodium for aluminium in aluminium hydrolysis species;
- by full substitution of sodium from binding layer by aluminium hydrolysis species, Figure 5.11.

For CSG water pre-treatment by coagulation, this means increasing salinity can lead to higher dose requirements for silica removal. Monitoring the post-coagulation water quality and residual silica and aluminium will be necessary to prevent membrane fouling.

### 5.3 Discussion

Coagulation involves a complex mechanism of neutralisation, bridging of neutralised particles, precipitation and co-precipitation, and frequently the chemical reactions are not complete. The coagulation results illustrated that total and dissolved silica reduction depends on the water matrix, pH, silica concentrations (total and/or dissolved), salinity and coagulant dose. At the best dose for the CSG groundwater sample, based on turbidity and DOC removal rates, was between 35 and 55 mg/L ACH. DOC removal efficiency was relatively high (80%) at the adjusted pH of 6.4 at 35mg/L ACH. Ferric chloride showed higher total silica removal than ACH and was an effective coagulant for low and medium salinity waters, but required higher coagulant doses (100mg/L) and produced much higher sludge volumes than ACH and aluminium sulphate.

Treatment of waters by coagulation is a traditional water treatment process, particularly for mining waters when coagulation and clarification is often the only treatment process applied. However, silica removal by coagulation is not a straight forward process and according to Iler (1976) and Healy (1994) it is still not well understood. Generally, coagulation has been considered to be the results of van der Waals attraction which draws two particles together at the moment of collision, unless opposed by a hydration barrier or by electrostatic repulsive forces between similarly charged particles, or both. There are, therefore, two factors that retard coagulation of silica: one being the “hydration” of the surface of the particles by a layer of water molecules hydrogen-bonded to SiOH groups, and the surrounding cloud of positive counter ions such as Na<sup>+</sup>, forming a double layer” (Sjoberg 2010, Bergna and Healy, 1994). The coagulation process is important for silica removal, but silica is “hydrophilic”, although under some conditions where salts cause coagulation it has become classed as somewhat hydrophobic (Sheikholeslami 2002, 2003).

These characteristics of silica affect silica removal coagulation patterns and effect silica precipitation patterns as also discussed in chapter 6 of this research. Den *et al* reported using coagulants for high salinity waters (brine) containing silica, with a silica removal efficiency of up to 80%. They concluded that the optimum dose depended on the silica concentration and the background water composition, as well as the extent of silica removal required (Den 2007, Stumm and Morgan 1962). The higher the silica concentration then the higher expected removal efficiency. They demonstrated that coagulants were particularly effective in removing colloidal silica because the colloidal particles carry strong negative charges in the neutral pH range. Cheng *et al* used a jar test to show that colloidal silica and soluble silica can be effectively removed with alum, with a dose of 30 mg/L alum for a 30 mg/L SiO<sub>2</sub> feed removing up to 50% of the silica at pH 7.1 (Cheng, 2009). All of the evidence thus indicates that it is feasible to remove both colloidal silica and dissolved silica using coagulation.

The best performing coagulant was ACH. It is thought that ACH exhibited the best removal efficiencies in CSG waters in respect of suspended solids, turbidity and DOC, metals and silica removal because of the high neutralisation capacity of Al<sup>13+</sup> species. Theoretically, ACH consists almost entirely of the thermodynamically stable polymer Al<sub>13</sub>(OH)<sub>7</sub><sup>32+</sup>, allowing these pre-formed flocs to neutralise colloidal particles immediately. Its dissolution, however, is slow (Dirk, 1981). ACH is pre-hydrolysed coagulant and contains significant amounts of highly charged and stable poly-nuclear alum hydrolysis products, which are less affected by the pH of the raw water than the more traditional coagulants aluminium sulphate and ferric chloride (Van Benschoten 1990).

ACH has also been shown to be a better coagulant than ferric chloride for high pH and the range of salinity conditions found in CSG waters. It is noted in this context, however, that the removal of DOC from CSG waters is improved by a decrease in pH, although the use of ACH needs to be balanced by the need to maintain low Al residuals (Sheikholeslami, 2002). The presence of aluminium cations or aluminium hydroxide can impact on silica polymerisation and lead to silica precipitation as silicate, discussed in detail in chapters 4 and 6. While aluminium hydroxide species formed from

dissolution of ACH, silica species can create stable silicate groups that would be expected to precipitate from solution during coagulation. Because of this, a significant concentration of natural organics in the form of humic species can control the coagulation doses required for effective coagulation and alter the sweep coagulation zones. The coagulation tests conducted by Amirtharaja and Mills (1982) and others (Stumm and Morgan 1996) have reported a significant increase in coagulation doses by aluminium coagulants when DOC increased by even minor concentrations (Hossain 1996).

The second best performing coagulant was ferric chloride resulting in total silica removal of about 20 to 40% and much less of dissolved silica being less than 5%. Ferric coagulants seem to be the best choice for seawater coagulation (Edzwald and Benschoten 1999, Haarhoff 2011), however, for CSG water ferric chloride is used in very limited applications in the CSG industry in Australia. As mentioned previously, ferric chloride (salt) requires high doses to be effective and subsequently generates a substantial volume of sludge in treatment of CSG water. Therefore, it is considered not to be suitable. It is recognised that ferric chloride is very insoluble, reportedly leaving very little residual dissolved Fe in the water after pre-treatment and this of-course, reduces scaling problems. However, ferric is not right for the high pH CSG water. Metal hydroxide species, which are product of hydrolysis of ferric chloride, are a function of pH. For pH 8 and 9 and ambient temperature (15 – 25 degree) there would be relatively low fractions of positively charged Fe as  $\text{Fe}(\text{OH})^{+2}$  available for charge neutralisation reactions (Carlson 1981, Bernal 1959). In addition, ferric chloride showed relatively low efficiency for total and dissolved silica removal in high salinity water when compared to ACH coagulation.

Coagulation with aluminium sulphate resulted in low total and dissolved silica removal (~40%) across all pHs, and salinity conditions, perhaps due to the impact of the relatively high pH of CSG waters. Coagulation with all three reagents at native pH8.4 of CSG waters has shown relatively low DOC removal, with all three coagulants removing less than 36%. However, improving DOC removal from CSG water was important for reducing membrane fouling in downstream processes such as UF and RO. A second

series of coagulation experiments was performed to find a best pH condition for DOC reduction. It was found that DOC removal was increased to 80% at pH6.4 with ACH. Ferric chloride and alum sulphate again showed relatively low efficiencies for DOC removal. It is likely that higher salinity inhibits the initial coagulation processes. The effect of increasing coagulation performance by ACH with decreasing pH is associated with a systematic decrease in the zeta potential of the coagulated humic acid with decreasing pH (Stumm and Morgan 1962, Hundt 1988). These results suggest that pH had a stronger effect on the rate of precipitation (bridging and adsorption) than on the rate of flocculation. Hundt and O'Melia (1988) tested this mechanism to coagulate humic acid with aluminium salts at pH greater than 5.0 and obtained more than 80% DOC removal (cited in Hossain, 1996). Edwards (1990) and Amirtharajah (1982) observed that at pH ranges of approximately 5.75 or more, the humic acid alum interaction appears to be related to the physical attachment to aluminium hydroxide precipitate.

Removal of dissolved (reactive) silica species is a key for silica scale mitigation on the RO membrane surface. Silica species present as monomeric acids can coat organic deposits on the membrane surface, serving as nucleation sites for other inorganic and organic compounds (Brant 2012, Bremere 2000). The solubility of these spherical units (very small particles) depends on the particles size, and the resultant radius of curvature of the surface. It also depends on the completeness of the dehydration of the internal solid phase (Kiselev 1974, Iler, 1976). Because small particles are more soluble than large particles, and since not all the small particles are the same size, the larger particles grow in size and the smaller particles dissolve with the silica deposited upon the large ones. This process is known as Oswald ripening. Above pH 6 and 7, and up to 10.5 where silica begins to dissolve as silicate, the silica is negatively charged and repels each other. Therefore they do not collide, so that particles grow continuously without aggregation. Bigger silica groups are more difficult to neutralise until they attach to clay or other suspended matters, which could be partly coagulated and settled by gravity separation.

Coagulation of silica in low, medium and high salinity waters seems to follow slightly different coagulation mechanisms. It is proposed, that sodium ions present in the solution can act as stabilising agents for silica, restricting access to water molecules and metal hydrolysis species.

As was discussed in chapter 2, while some references on salinity are available, the impact of sodium ion concentration on different silica forms in aqueous solutions is lacking fundamental studies. The experimental results presented in this chapter were aimed at developing a better understanding of how different salinity waters affect silica removal by coagulation. Floc size, structure and strength play a significant role in suspended and dispersed matter separation, including both total and dissolved silica removal in water treatment. Observation of the supernatant and floc formations showed a distinctively different trend in respect to the impact of sodium chloride concentration on coagulation reactions. It was observed that the removal efficiency was strongly influenced by the salinity of the solution.

Based on the coagulation results and  $^{29}\text{Si}$  NMR study impact of aluminium (discussed in chapter 4) a new hypothesis proposed in this research is that the high neutralisation capacity of  $\text{Al}^{13+}$  species can substitute for sodium ions from the silica sol binding layer resulting in more effective removal of total and dissolved silica. Sodium ions present in solution create barriers for metal hydrolysis species required for effective neutralisation and bridging reactions. A comparison of the results of the coagulation tests in low, medium and high salinity waters show that all the coagulants seemed to show a similar decreasing trend for silica removal with salinity.

The decrease in coagulant performance with increased salt content by all coagulants studied is due to a lower interaction between the positively charged coagulant and the negatively charged sample suspended matter due the shielding effect of the high electrolyte concentration. It appears sodium ions can shield silica and reduce the effect of neutralisation and bridging reactions necessary for effective coagulation. Sodium ions tend to form a binding layer around silica sol to prevent it from hydration. This is similar to the way silicon atoms is surrounded by four oxygen atoms is the silica

moiety, which actually protects silicon atom from being destroyed by water molecules (Smolen 1964). In a similar way, sodium atoms tend to surround silica when sodium concentrations reach to 0.15M of  $\text{Na}^+$  (Bergna and Roberts 2006). For these layers to stabilise the sol under these conditions, they must extend further than 2nm (Bergna 1994, Healy 1994). The hypothesis proposed by Healy (1994) is, therefore, that a 2 nm steric silicate oligomeric – polymer barrier protects a silica sol at pH8.0 in 0.15 M salt. When additional salt is added to the solution, the increasing concentration of sodium ions lead to further binding of  $\text{Na}^+$  to the stabilising layer, Figure 5.12. Aluminium species produced as a result of the introduction of coagulant (ACH) to the solution will be less ionised in high salinity water than in lower salinity environment.

As ionisation of aluminium species is slightly less in high salinity waters, substitution of sodium ions with aluminium ions in the sodium binding layer is more difficult, Figure 5.12. If this is the case, it might lead to relatively poor silica coagulation (adsorption, precipitation), as it was observed in this work for high salinity water, Figure 5.10.

Healy (1994) highlights that “*the silica sol coagulation behaviour with respect to the  $\text{Na}^+$  is not simple*”. As discussed, in low salinity water sodium ions tend to attract water molecules (this phenomenon can be easily observed in practice when dry salt adsorbs moisture from a high humidity environment). For salt exposed to the natural environment for some time, the moisture coefficient could reach 1.8 – 2. A similar effect takes place in low sodium concentrations solutions. This reaction mechanism between the water shell and sodium cations can affect coagulation patterns and affect silica solubility. Comparison of coagulation conducted in deionised and low salinity waters (Duan 2001) showed that a much lower dose of alum was required to achieve effective coagulation for turbidity and DOC removals. The effect was also observed in  $^{29}\text{Si}$  NMR study and was discussed in details in chapters 4.

For additional metals removal to mitigate potential mineral scale formation on the membrane surface, ion exchange system is commonly used in CSG water desalination prior to RO process. This pre-treatment is targeted to remove undesirable cations (Ca, Mg, Ba, Sr, Al, Si) that can deposit or couple as hydroxide groups to the membrane

surface, and act as nucleation sites. The combination of coagulation, clarification, ultrafiltration and ion exchange treatment, Figure 2.10, can achieve nearly zero metals in the RO feed (Brant 2012). Other pre-treatments for total and dissolved metals removal such as lime addition are found to be not practical for CSG water desalination. As the most of the CSG RO desalination plants operate with large flowrates, any additional sludge waste involves high capital and operating costs, as well as post-remediation cost to remediate the land if tailing dams were used.

The coagulation results clearly demonstrated that treatment of the CSG water sample collected from the storage dam required much higher doses (200 to 1000mg/L) by all three coagulants due to high TOC/DOC and higher salinity. Approximately five times more coagulant dose was required to be able to effectively remove silica. However, total silica removal by ACH was higher than from CSG groundwater samples collected in 2013 and 2014. This may be due to different silica species present in this dam storage water, as some silica potentially can be released by algae. In practice, this sort of CSG water will be pre-treated via coagulation, clarification and might be recycled a number of times via the same pre-treatment processes (coagulation, clarification, and filtration) priority to be pumped for RO purification.

Coagulation process for silica reduction in particular as pre-treatment of CSG waters can be effective, but increasing salinity of CSG water over the life time of the project as a result of aquifer depression can reduce the efficiency of silica removal by coagulation as a result of sodium ions binding (preserving) to silica. The use of pre-polymerised coagulant such as ACH can improve silica removal in high (~ 30g/L) salinity waters. Careful monitoring of residual aluminium, however, in post-coagulation water is necessary to prevent aluminium silicate deposition of the membrane surface.

## 5.4 Conclusion

In light of the results described in this chapter, it is clear that simultaneous charge neutralisation and sweep coagulation of silica is a complex process that requires consideration of more than just the mechanisms of collision and particle growth. It was shown that the concentration of sodium chloride in solution inhibits reduction of silica

by coagulation. Having tested three salinity waters, a new hypothesis was introduced indicating that aluminium ( $\text{Al}^{13+}$ ) can substitute for sodium ions to neutralise and bridge silica sol. The relationships between  $\text{Si}(\text{OH})_4$  and  $\text{Al}^{3+}$  and  $\text{Na}^+$  seems to play key roles in effective silica removal by coagulation, a detail not found in any previous works.

In conclusion, these findings can be framed in terms of the implication for the operation of a full-scale coagulation pre-treatment process in RO plant as follows:

- Coagulation can reduce silica concentrations in raw CSG water from initial concentrations 20 – 80mg/L to 12 – 23 mg/L.
- Pre-hydrolysed coagulant as ACH (PACI) is an effective coagulant in silica removal; however, residual aluminium concentrations can slightly increase and required careful monitoring of the downstream concentrations.
- Increasing salinity of CSG water demands higher coagulant dose.
- Storage of CSG water in open evaporation ponds for prolonged period time is not recommended as water quality degrades as a result of evaporation (salinity increase), algae growth, and potential significant increase of TOC/DOC contents. The changes result in substantially increased coagulant doses being required for effective coagulation and very large sludge volumes will result.
- The best turbidity reduction shown by ACH was at native pH8.4 – 9.2 of CSG waters.
- For effective DOC removal, pH adjustment was required to pH6-6.4. However, lowering the native pH of CSG water has shown to be not practical as a large amount of acid is required.

## Chapter 6 RO silica fouling

### 6.1 Introduction

#### 6.1.1 Experimental

The experimental objective of this work was to develop relationships between silica precipitation and the effects of pH, feed water salinity, and residual aluminium (post-coagulation water quality) using synthetic and natural CSG waters.

The first series of experiments investigated silica solubility limits identified by Hamrouni (2001) in various sodium chloride concentrations solutions at pH8. Then silica precipitation was studied in deionised water at three pH (pH3, 9, 11) conditions to record the impact of increasing silica concentrations on flux decline. Then silica fouling profiles were studied at three similar salinities and silica concentrations for three pHs conditions in synthetic and natural CSG waters. The impact of residual aluminium on silica precipitation patterns on medium salinity (12.5g/L) synthetic and natural CSG water was also investigated.

Prior to RO experiments, a 2 litre batch of CSG water was pre-treated with ACH coagulant followed by ultrafiltration. The RO feed water quality had turbidity less than 1 NTU in all RO experiments.

### 6.2 Data analysis

#### 6.2.1 Types of silica fouling

Figure 6.1 shows four types of identified silica fouling. The type's one, two and three were previously briefly described by Semiat (2001, 2003). Type four was first recorded and described in this research. The type of silica fouling is related to precipitation of silica and is dependent on silica concentrations, salinity, pH and presence of other cations and anions, and combinations of these factors. Type one is applicable for low

salinity waters and relatively high pH (pH 9 – 11) where the silica concentrations follow the theoretical concentration curve that gradually increases with water recovery in accordance with the concentration factor summarised in Table 6.1 (assumes no precipitation). In this type silica precipitated at the end of RO experiments when a relatively high (~ 85%) water recovery reached. For the type two residual silica concentrations follow the theoretical concentration curve until the dissolved silica concentration exceeds its solubility limit.

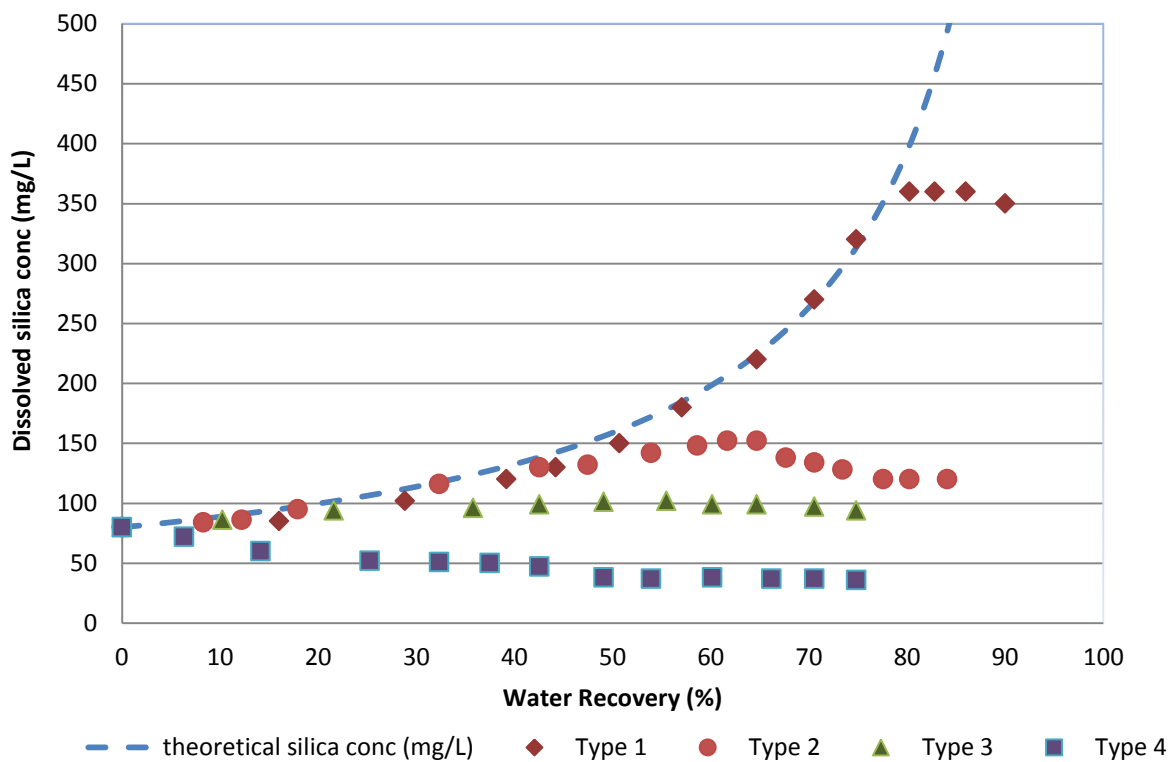


Figure 6.1 – Four types of RO silica fouling in the initial range of salinity 12.5g/L (0.4mol/L) to 30g/L to final salinity 59.6g/L (1Mol/L) plotted against silica concentrations vs water recovery.

Type two normally has maximum and stable residual silica concentrations, with the stable residual silica concentration normally equal to the silica solubility limit at this condition. Type three is relevant for medium to high salinity RO feeds (> 12.5g/L) when silica solubility is depressed by high concentrations of sodium chloride. For these conditions, flux is relatively low (due to high salinity) and silica fouling occurs at relatively low concentrations (80-100mg/L). Due to the low flux and more prolonged

time of the RO experiment, silica fouling curves show stable silica concentrations due to consistent precipitation. Type three fouling was observed for medium to high salinity waters for pH7, 9 and 3.

Table 6.1 – Recovery rate vs concentration factors

Water recovery rate (%)	Concentration factor (CF)
50	2
75	4
80	5
90	10

The type four (silica precipitation) occurs when silica solubility is depressed by high salinity (24 - 30g/L) and the initial silica concentration at the start of the run is at the solubility level or close to “practical solubility” level. In addition, other factors can depress silica solubility, for instance the presence of non-ionised silica species (low pH conditions), which could catalyse silica polymerisation and precipitation. This was recorded for pH3 conditions with relatively high initial silica concentrations (80 – 90 mg/L). As can be seen from Figure 6.3, the type 4 silica fouling curve does not follow the theoretical concentration, but instead gradually declines in concentration. This phenomenon was not noted for similar silica concentrations processed in deionised waters. No previous research describes this type of silica fouling.

### 6.2.2 Normalised flux

In the recycling technique used in RO experiments, permeate is continuously withdrawn and as a result the recycling solution is gradually concentrated. Continuous withdrawal of permeate leads to an increase in the osmotic pressure, causing a flux decline. Figure 6.2 illustrates the typical flux decline for the three salinity waters (synthetic and CSG waters). The deleterious effect of scale deposit on the membrane is the decline in permeate flux due to flow obstructions. The permeate flux decline curves, shown in Figure 6.2, however, do not distinguish between flux decline due to scaling and decline simply due to the increase in osmotic pressure.

Duration of RO experiments in low salinity water was approximately 8 – 10 hours, in medium salinity waters is was approximately 12 - 16 hours and in high salinity waters is was up to 42 hours. The longest RO run was for the high salinity waters as the osmotic

pressure was high and the flux was low, so it normally took a long time to process this type of water.

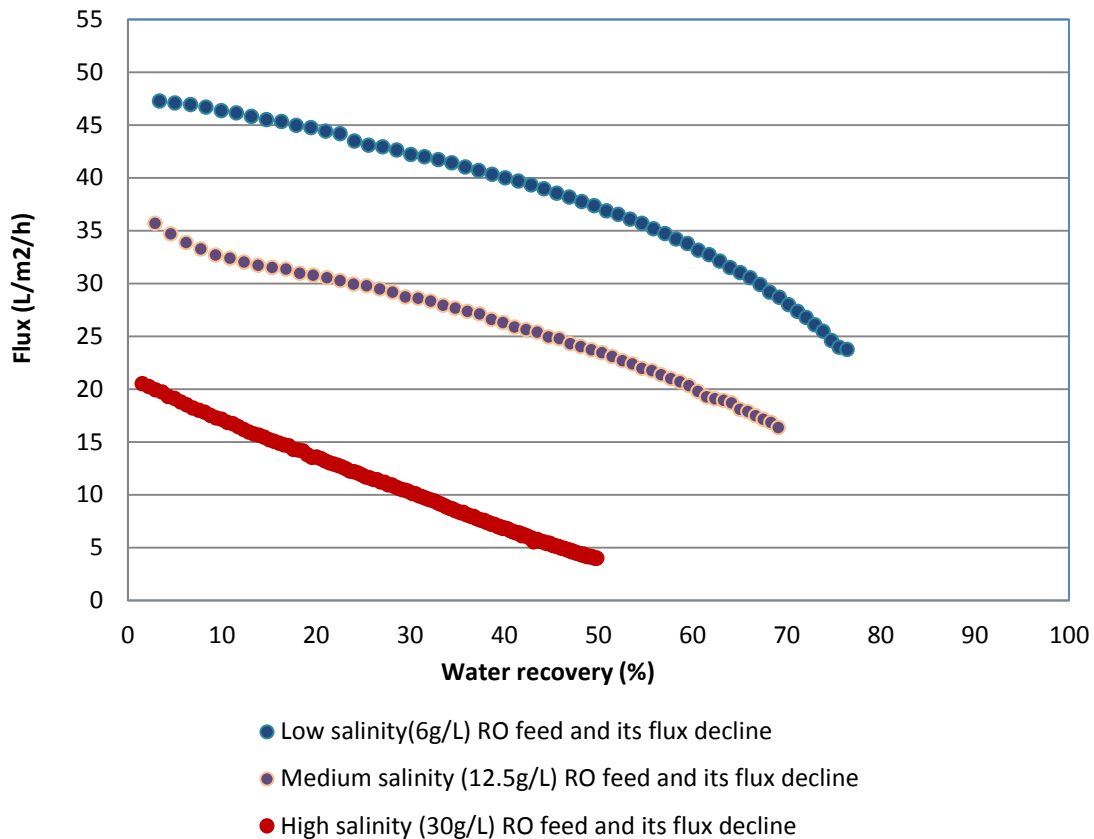


Figure 6.2 – Flux decline trends for low(6g/L), medium(12.5g/L) and high(30g/L) salinity waters vs water recovery at initial silica concentrations ( $\text{SiO}_2=70\text{mg/L}$ ) at pH9 condition. (Low salinity RO runs were 8 – 10hours, medium salinity RO runs were 12 – 14 hours, high salinity RO runs were 36 – 42 hours).

The data monitored during each run included the weight of the recovered permeate, pressure, temperature, run time, pH, turbidity, conductivity and dissolved silica concentrations in the concentrate. The data calculated include the permeate flow rate, flux, water recovery, and salt rejection. Samples for ICP analysis were taken during RO experiments for each 2% of permeate recovery and were analysed immediately by ICP to track changes in the silica concentration of the recycling stream that may be indicative of RO fouling. As described in chapter 3, all samples for dissolved silica concentrations for ICP analysis were filtered via 0.2 $\mu\text{m}$  filter paper. Silica precipitation was monitored by the flux decline as a function of water recovery, and silica

concentration in the concentrate stream. The normalised flux with respect to pressure in the RO system as a function of the water recovery is summarised in Table 6.2 for an operating temperature of 15.5°C.

Table 6.2 – Salinity vs normalised flux

Salinity of synthetic and CSG waters (as NaCl (g/L))	Normalised initial flux (L/m <sup>2</sup> /H/bar @ 15.5°C)	Water recovery (average) (%)
6	1.02 - 1.11	82 - 92
12.5	0.78 - 0.81	74 - 78
30	0.45 - 0.47	50 - 66

To avoid the influence of operational variables on flux decline, fouling outcomes, operation conditions such as pressure, temperature, the storage volume (related to filtration time rate of water recovery), were kept the same for all experiments. The precision of the pH control was pH3-pH11+/-0.05. The amount of acid added was 2.7 – 4.6mL of 10% HCl for pH3 filtration, and 0.8 – 1.4mL of 10% NaOH for pH11 correction.

In all, one hundred and eighty one (181) RO runs were performed, and the focus of these experiments was on the dissolved residual silica concentration profiles in the RO concentrate stream as a function of the RO feed composition. The focus of the experiment was limited to the chemistry of silica fouling and silica scale deposition on the membrane surface.

## 6.3 Results

### 6.3.1 Stable and maximum silica concentrations

Silica precipitates when dissolved silica concentration exceeds its solubility limit. Though, due to slow precipitation reactions (slow kinetics) dissolved residual silica concentrations can vary. For this reason the concept of maximum and stable residual silica concentrations was introduced in this research to capture potential variations in silica fouling patterns. Figure 6.3 shows a typical silica fouling response for medium (12.5g/L) salinity synthetic waters for an initial silica (as SiO<sub>2</sub>) concentration of 70mg/L

recorded during the RO experiments. A maximum residual silica concentration above the solubility limit indicates that super-saturation of dissolved silica occurred in the RO system. This silica concentration is frequently named a “pseudo-solubility” state when silica concentrations significantly exceed theoretical silica solubility concentration prior to precipitation occurring. Once silica precipitates, the silica concentration settles to the solubility limit for the particular water composition and conditions, and stabilises as filtration proceeds.

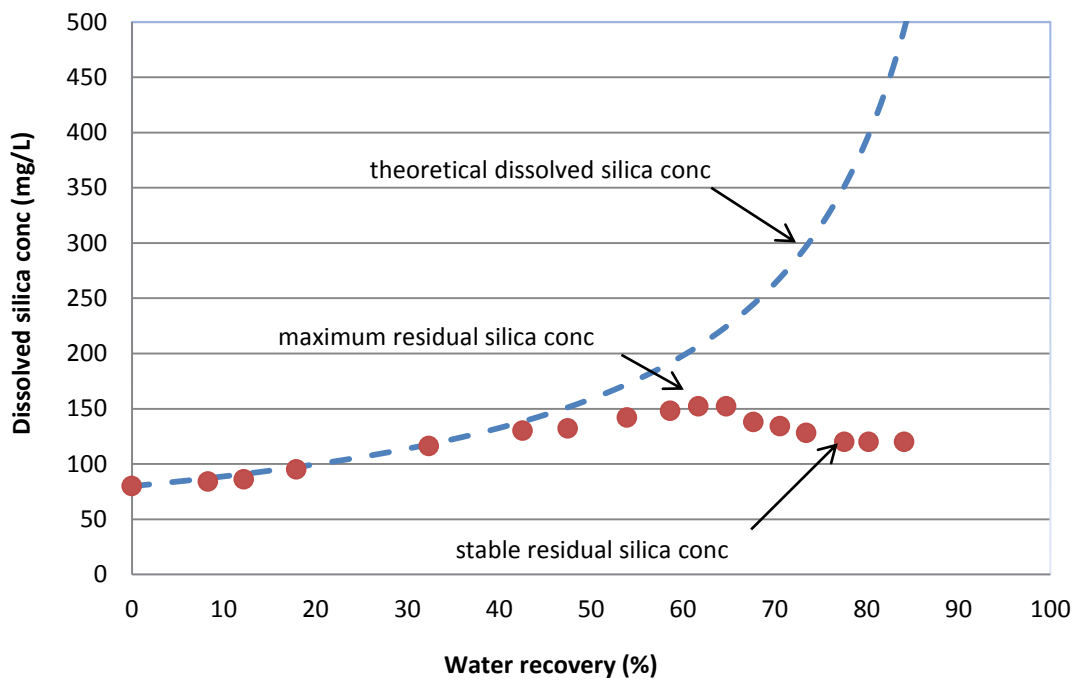


Figure 6.3 – Dissolved silica (as SiO<sub>2</sub>) concentrations (RO residual silica concentrations in the recycled stream) vs water recovery - maximum and stable residual silica concentrations recorded in medium salinity (NaCl=12.5g/L) synthetic waters with initial silica concentration 70mg/L at pH9.

As can be seen from Figure 6.3, the residual silica concentration departs from the theoretical curve, but continues to increase to the maximum residual concentration before stabilising at a lower concentration. Stable silica concentrations arise when silica concentration leaves the theoretical curve and remains at the stable residual silica concentrations for some time. A stable silica concentration is usually a concentration close or equal to the theoretical silica solubility concentration, but as the results will

show, can vary with the specific water matrix and the kinetics of precipitation for specific conditions.

In this work, experimentally recorded stable and maximum silica concentrations are presented and kinetics of silica precipitation was discussed in the subsequent sections. Effect of variables such as pH, salinity, aluminium concentrations on maximum and stable silica concentrations was analysed. The experimental maximum and stable silica concentration data was then correlated with the silica solubility data of Hamrouni (2001) and Gorrepati (2010).

### **6.3.2 Practical silica solubility**

Silica precipitation (fouling) in RO desalination, like all other precipitation processes, involves two stages: super-saturation in liquid followed by nanoparticle aggregation within the super-saturation zone, most likely near the membrane surface where the silica concentration will be highest. Exact knowledge of the solubility limit of silica in saline waters is vital since the solubility determines whether the solution is saturated or not. It is necessary, however, to investigate the “practical solubility” limit relevant to the particular water matrix (Hamrouni 2001). “The solubility limit is defined as the total amount of solute species that can be retained permanently in solution under a given set of conditions (sodium chloride concentrations, fixed temperature, pressure, etc.) in the presence of an excess of undissolved material of definitively known composition and crystal structure from which the solute is derived. This practical solubility limit is similar to the definition of solubility limits except the impact of all components of the water matrix of the equilibrium silica concentration is unknown. For instance, we can predict the solubility limit of silica in saline water from the data of Hamrouni (2001) but for CSG water, the effect of minor components such as aluminium, calcium and magnesium are unknown and can only be determined by experimentation. As such, characterisation of each experiment involved measuring parameters that characterised the two steps of dissolved silica concentration in the recycled stream, and elemental examination of solids on the membrane surface for selected experiments. The membrane surface examination was performed via SEM and EDS as described in chapter 3. The “practical silica solubility” concept was introduced by Hamrouni (2001)

when it was shown that theoretical silica solubility concentrations vary and depend on sodium chloride concentrations, pH, other physical and chemical conditions of waters, Figure 6.4.

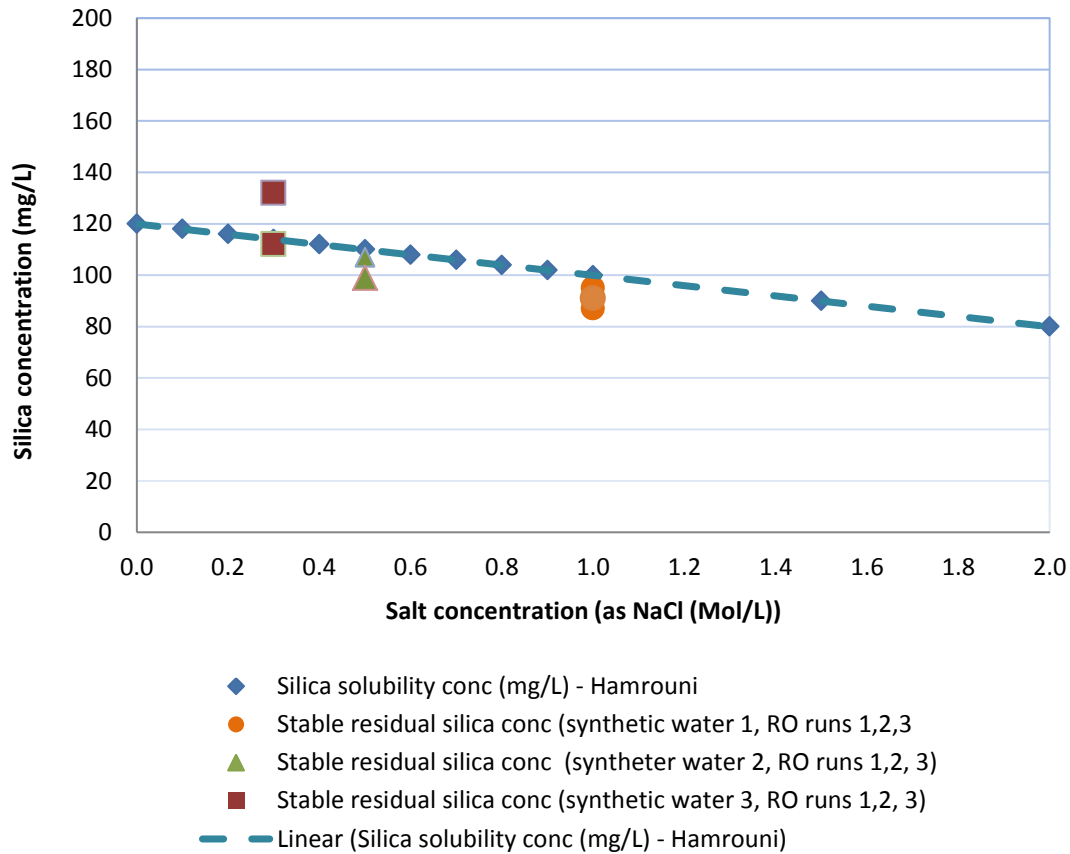


Figure 6.4 – Stable residual silica (as SiO<sub>2</sub>) concentrations at pH 8.5-9 (sodium chloride concentration for synthetic water 1 - NaCl=59.6g/L, synthetic water 2 – NaCl=29.5g/L, synthetic water 3 – NaCl=17.5g/L) and the Hamrouni et al (2001) silica solubility plotted against salt concentration.

Hamrouni (2001) investigated silica solubility using three analytical methods: standard gravimetric method, atomic adsorption spectroscopy and spectrophotometric determination to measure the optical density of siliconmolybdic acids. Figure 6.4 illustrates silica solubility in various sodium chloride solutions documented by Hamrouni (2001). Prior to undertaking silica precipitation studies for RO systems this diagram was tested to confirm the relevance of silica solubility limits for the RO systems studied in this research. Residual silica concentrations are plotted with silica

solubility determined by Hamrouni (2001) in Figure 6.4. The residual stable and maximum silica concentrations recorded for various salinity synthetic and natural CSG waters were compared to the silica solubility by Hamrouni (2001). In addition, the silica solubility results recorded at pH3 for various salinity synthetic and CSG waters were compared to the results recorded for various salinity waters and specifically the pH3 condition of Gorrepati (2010). During the RO runs, the silica concentration increases as a result of permeate withdrawal and hence the concentration level on the membrane surface also increases. The concentration effect also increases the bulk osmotic pressure and reduces membrane flux. As a result, any silica precipitation on the membrane surface acts to reduce the degree of super saturation and concentration polarisation. Different patterns (types) of silica fouling were observed in the subsequent sections. Table 6.3 summarises stable and maximum residual silica concentrations recorded to verify silica solubility's limits obtained by Hamrouni (2001).

Table 6.3 – RO feed compositions, flux and permeate recovery, stable and maximum residual silica solubilities

RO feed salinity as NaCl, (g/L)	Initial silica conc, (as SiO <sub>2</sub> ) (mg/L)	pH	RO initial flux, (L/m <sup>2</sup> /h)	Permeate recovery (%)	Stable residual silica conc., (as SiO <sub>2</sub> ) (mg/L)	Maximum residual silica conc., (as SiO <sub>2</sub> ) (mg/L)
12.5	50	8 - 9	27 - 28	78	120	132
17.5	50	8 - 9	24 - 25	76	110	128
30	50	8 - 9	21 - 23	55	81	100
12.5	60	8 - 9	27 - 28	78	116	127
17.5	60	8 - 9	24 - 25	76	113	134
30	60	8 - 9	21 - 23	55	89	102
12.5	70	8 - 9	27 - 28	78	123	147
17.5	70	8 - 9	24 - 25	76	121	134
30	70	8 - 9	21 - 23	55	91	107

NF = non fouling conditions.

### 6.3.3 SiO<sub>2</sub> - HO<sub>2</sub> system

#### 6.3.3.1 Silica precipitation at pH3, pH9 and pH11

In order to understand patterns of silica precipitation (gelling) in more complex systems (synthetic and CSG waters), silica precipitation was first studied in deionised water. The SiO<sub>2</sub>-HO<sub>2</sub> system is essential for explaining silica polymerisation and precipitation

reactions since silica hydrolysis and condensation processes depend on the amount of water molecules in the solution.

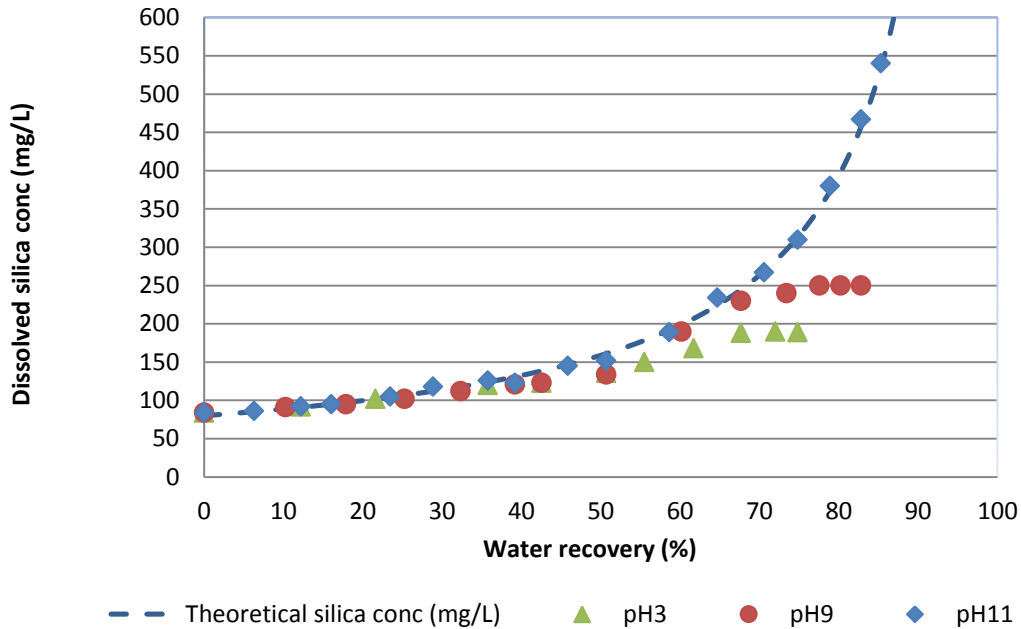


Figure 6.5 – Dissolved silica concentration vs water recovery in deionised water for an initial silica concentration of 84mg/L at pH3, pH9 and pH11 (Figure 6.6).

Consequently, water molecules or –OH groups attack O-Si-O bonds forcing silica to hydrolyse. It was expected that this data would provide base line data to benchmark more saline waters against, and in particular the effects of increasing silica concentration, sodium ions and aluminium ions on silica fouling.

Figure 6.5 illustrates silica fouling trends for pH3, pH9 and pH11 conditions against the theoretical calculated values in accordance with concentration factors, Table 6.2. At pH3, dissolved silica concentration leaves the theoretical curve at approximately 152-160 mg/L (as SiO<sub>2</sub>) at 57% water recovery. At pH9 silica leaves the theoretical line at 230mg/L (water recovery 81%) and still gradually increased to 250mg/L at which concentration it stabilised. At pH11, experimental residual silica concentrations follow the theoretical concentration curve indicating there was no silica precipitation in the recycled stream, Figure 6.5.

The results recorded at pH3 condition, Figure 6.5, shown gradual depletion of dissolved silica concentration in the recycled stream as a result of particle formation. This result is consistent with the results obtained by Gorrepati et al., (2010) who demonstrated that at pH3 silica precipitation proceeds through two distinct steps. First, monomeric silica is quickly depleted from solution as it polymerizes to form primary particles ~5 nm in diameter. Second, the primary particles formed then flocculate into bigger silica structures. An autocatalytic effect of silica is also well known. Increasing silica concentration in the recycled stream with increasing permeate recovery lead to further particle formation and subsequent particle flocculation become exponentially faster with increasing silica concentrations. These primary particles are very easy to filter out via 0.2µm filter which is required for preparation of ICP samples.

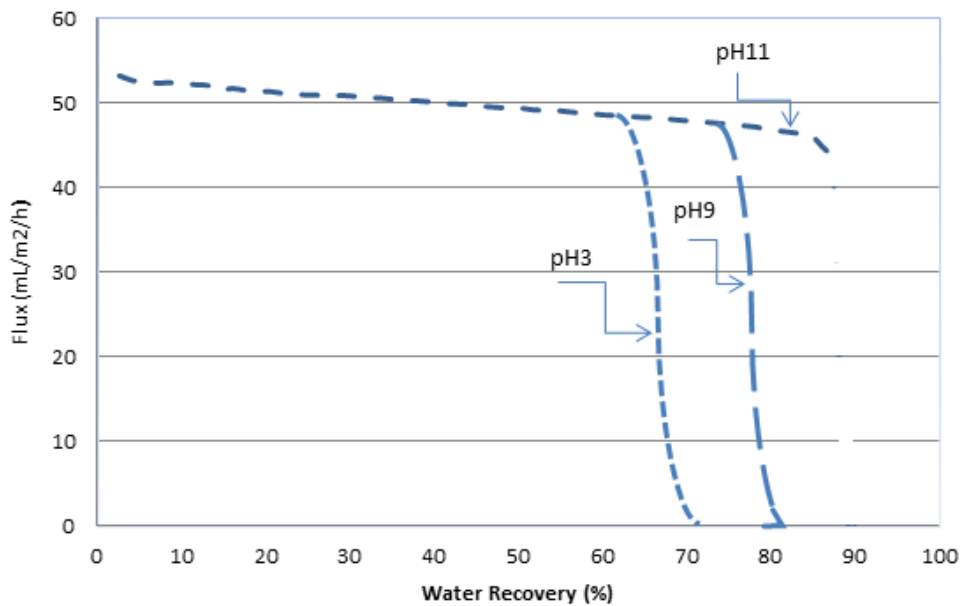


Figure 6.6 – Flux decline trends vs water recovery in deionised water at an initial silica concentration 84mg/L at pH3, pH9 and pH11 (Figure 6.5).

Figure 6.6 shows the flux decline trends for the experiments described in Figure 6.5. Working in deionised water can be challenging because altering pH affects the ionic strength. However, as can be seen from the diagrams presented in Figure 6.6, no change in initial flux was observed due to variations in salinity arising from the pH correction.

The effect of osmotic pressure was practically eliminated so the impact of increasing silica concentration can be recorded on flux decline. For pH3, the dramatic flux decline occurred at approximately 73% water recovery, and for pH9 at 82%. As mentioned the above, for pH11 the RO experiments were terminated once full permeate recovery was reached as no feed was left.

The initial turbidity in all solutions was 0.4 – 0.5 NTU and was constantly measured in the recycling stream. It was recorded that turbidity did not change (+/- 0.02) with increasing silica concentrations in the recycling stream and silica deposited on the membrane surface. The recycled solutions remain relatively clear until the end of RO experiments.

### 6.3.3.2 Membrane surface examination

The flux decline for pH3 and pH9 conditions occurred as a result of silica deposition on the membrane surface.

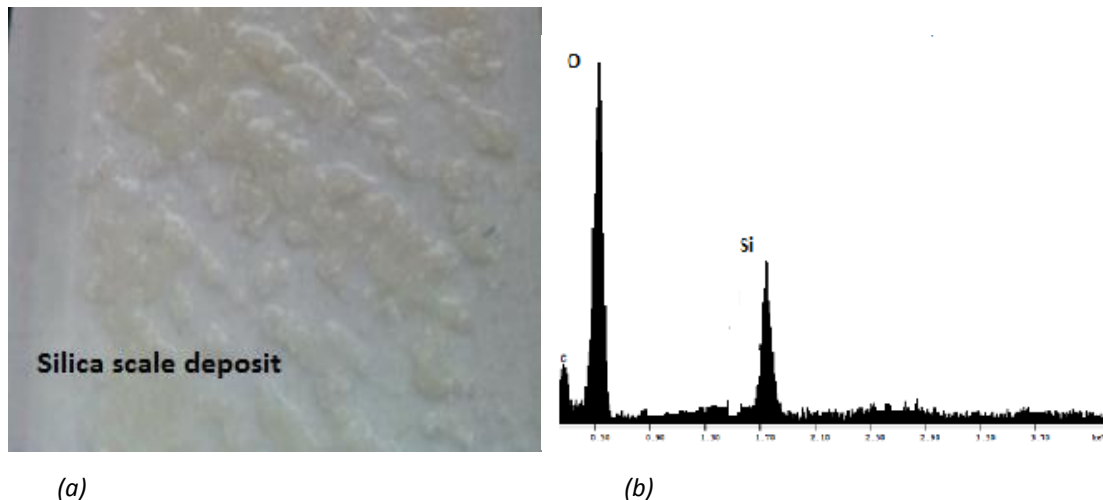


Figure 6.7 (a) Silica scale deposit on the RO membrane surface at initial concentration  $\text{SiO}_2=84\text{mg/L}$  diluted in deionised water, pH9 and (b) EDS membrane surface elemental analysis.

After the membranes were carefully removed from the RO unit, visible silica gel (amorphous silica) was seen as shown in Figure 6.7 (a) for pH9. Similar deposition of amorphous silica was found at pH3. Visual examination of the membrane surface following RO filtration of silica in deionised water at pH9 showed a significant

amorphous silica deposition, Figure 6.7 (a). It was observed that well after silica deposition occurred on the membrane surface, the membranes were permeable enough to allow continuous permeate recovery. It is presumed that the deposit had porosity that was sufficient for permeate to filter through.

### 6.3.4 Synthetic water

#### 6.3.4.1 RO residual silica concentration

Figures 6.8, 6.9, and 6.10 summarise the silica precipitation trends recorded for synthetic waters. Figure 6.8 shows residual silica concentration results in low salinity water illustrating that the residual silica concentration followed the theoretical concentration curve. The relatively low salinity of this water resulted in high flux and comparatively short run times. Figures 6.9 and 6.10 demonstrate silica fouling results in the medium and high salinity waters, where silica fouling is shown for both pH9 and pH3 conditions.

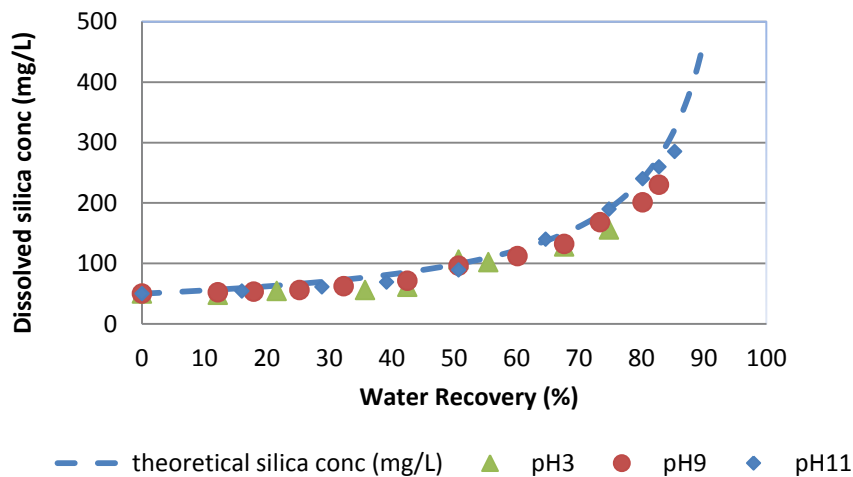


Figure 6.8 – Silica fouling trends in synthetic water at pH3, pH9 and pH11 vs water recovery in low salinity feed (NaCl=6g/L). Initial RO feed dissolved silica concentration = 50mg/L.

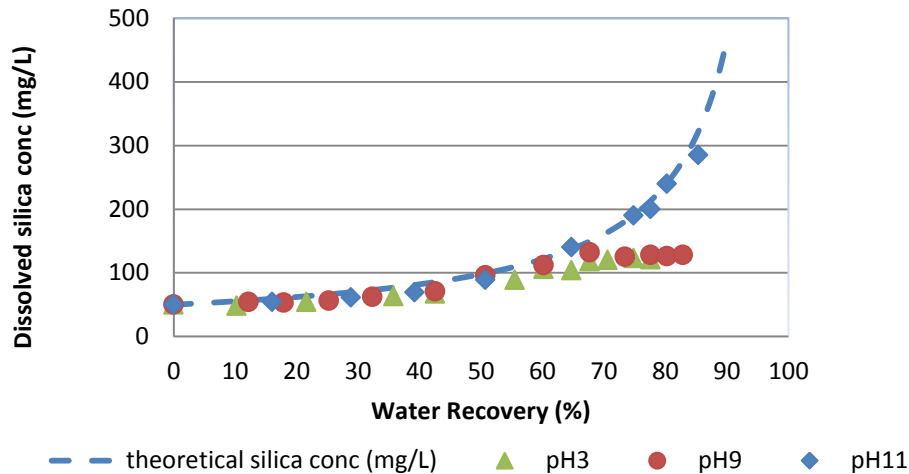


Figure 6.9 – Silica fouling trends in synthetic water at pH3, pH9 and pH11 vs water recovery in medium salinity feed (NaCl=12.5g/L). Initial RO feed dissolved silica concentration = 50mg/L.

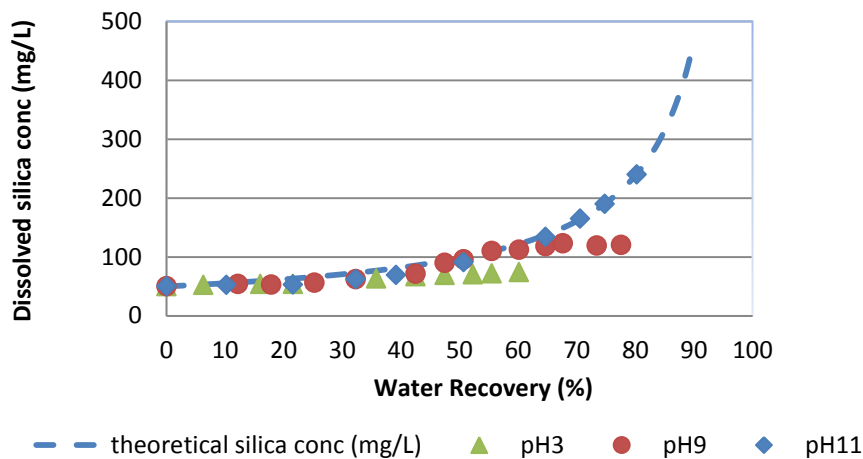


Figure 6.10 – Silica fouling trends in synthetic water at pH3, pH9 and pH11 vs water recovery in high salinity feed (NaCl=30g/L). Initial RO feed dissolved silica concentration = 50mg/L.

In medium salinity synthetic water, Figure 6.9, the silica concentration curve leaves the theoretical silica curve at around 60% water recovery for pH9 and at about 52% for pH11. Figure 6.10 shows the typical silica fouling trends recorded for high salinity waters. At pH3 residual silica concentration leaves the theoretical concentration at 41%

water recovery and at pH9 at 56% water recovery. No silica precipitation occurred at pH11 for medium and high salinity waters as was expected because of the higher silica solubility at this pH. Stable and maximum residual silica concentrations recorded in the synthetic waters are summarised in Table 6.3. The results for the medium and high salinity synthetic waters showed a spread of maximum and stable silica concentrations that varied from 104 to 145mg/L. This is due to the kinetics of silica precipitation and the variation in filtration times between low and high salinities.

Table 6.4 – Summary of silica precipitations for synthetic waters

RO conditions				Residual silica concentration	
RO feed (NaCl), (g/L)	RO feed dissolved silica conc., (as SiO <sub>2</sub> , mg/L)	Water recovery (average) (%)	pH	Stable residual silica conc., (average) (mg/L)	Maximum residual silica conc., (average) (mg/L)
Synthetic waters					
6	50	85	9	NF	NF
6	50	82	3	NF	NF
6	50	87	11	NF	NF
12.5	50	76	9	125	142
12.5	50	75	3	123	148
12.5	50	76	11	NF	NF
30	50	60	9	96	112
30	50	60	3	94	113
30	50	67	11	NF	NF

NF = non fouling conditions.

As can be seen from Table 6.1, the normalised flux for medium salinity water was 1.7 times higher than for high salinity water. For high salinity water, the duration of the RO run was nearly 2.5 times longer than for medium salinity. The spread of stable concentrations was insignificant for variations in pH at a given salinity, and the maximum concentrations were also very similar for runs with the same salinity. The exception is at pH 11, where there was no fouling. Kinetics may explain the lower maximum silica concentration for high salinity waters, as the filtration was conducted over a longer time and the rate of increase in water recovery was slower Table 6.4.

### 6.3.4.2 Effect of salinity

Figure 6.11 shows the effect of salinity on stable residual silica concentrations. As can be seen, silica solubility decreased as the salinity of water increased. For salinity at about 59-60g/L (NaCl) or 1Mol NaCl, stable residual concentrations were 84-88mg/L. This was slightly lower than the silica solubility limit recorded by Hamrouni (2001).

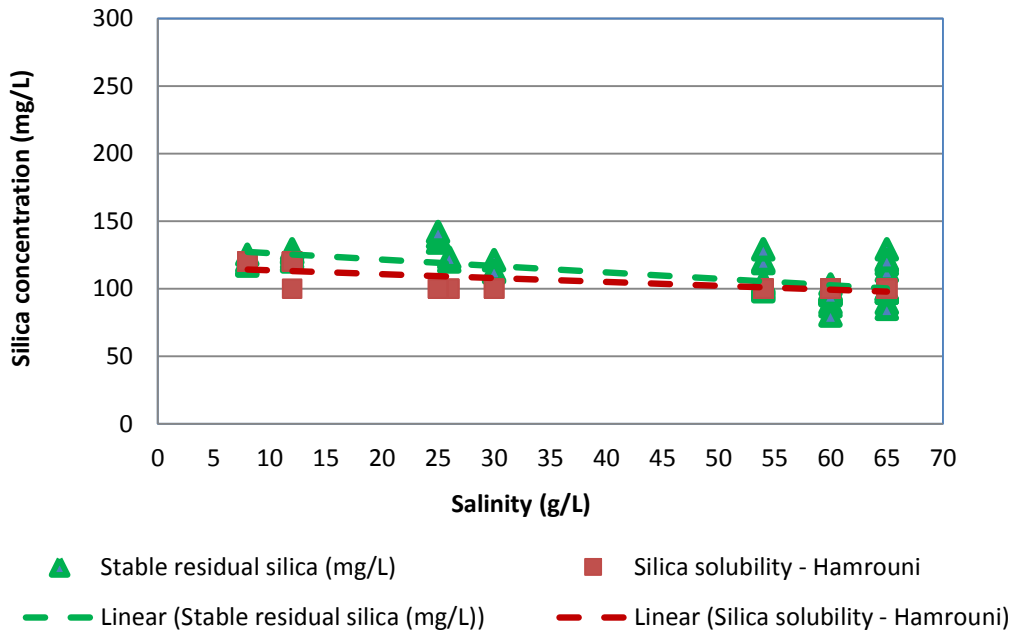


Figure 6.11 – Effect of salinity on stable residual silica concentrations plotted against silica solubility by Hamrouni (2001) in synthetic waters at pH 8-9.

The effect of salinity on the experimental maximum silica values is plotted in Figure 6.12, illustrating that maximum silica concentrations were also affected by sodium chloride concentrations and were decreasing from 150mg/L for medium salinity waters (12.5g/L) to 100mg/L at very high salinity (60g/L). Overall, maximum residual silica concentrations in synthetic waters were 10-12% higher than stable concentrations and about 12-15% higher than silica solubility by Hamrouni (2001).

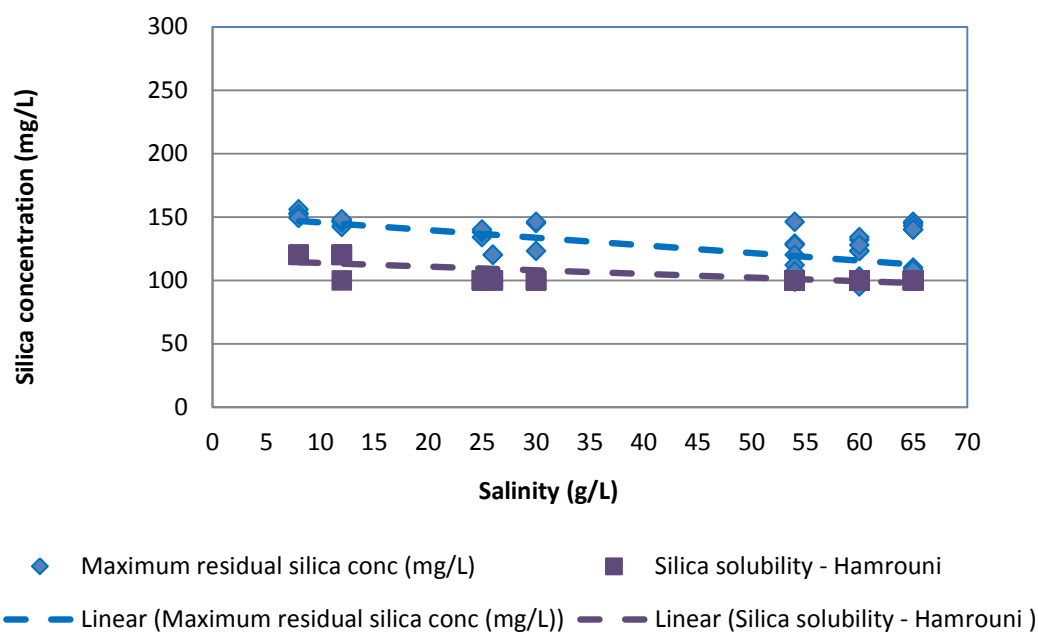


Figure 6.12 – Effect of salinity on maximum residual silica concentrations plotted against silica solubility by Hamrouni (2001) in synthetic waters at pH8-9.

### 6.3.3.3 Effect of pH

Figures 6.13 illustrate the effect of low pH conditions on stable and maximum residual silica concentrations.

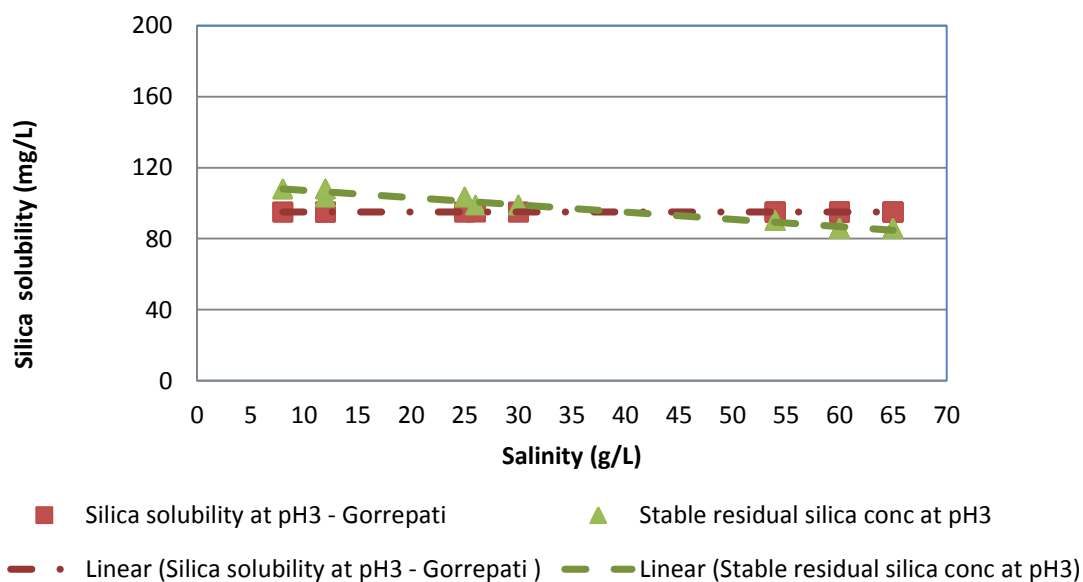


Figure 6.13 – Stable residual silica concentrations for medium, high salinity synthetic waters at pH3 and silica solubility at pH3 (Gorrepati (2010)) vs salinity.

The results in both graphs are plotted against the results obtained by Gorrepati at pH3 in medium and high salinity waters. As can be seen, the stable residual silica concentrations (86 – 96mg/L) were slightly lower than the silica concentrations (98 – 102mg/L) recorded by Gorrepati (2010), however, overall the results were in relatively good agreement with the silica solubility limits recorded by Gorrepati (2010), Figure 6.13. At pH3 dissolved silica can form polymers, which are less than critical nucleating size (Weres, Yee and Tsao, 1981). Depending on the salinity and total silica concentrations, these very small unionised dissolved silica (gel) initiate gelling of silica. It was observed that silica polymerisation in the RO feed solutions starts immediately after pH-adjustment from the native pH9.2 to pH3 as slightly clear white floc appeared in the recycled solution. The total mass of silica precipitate increased at the lower pH3 probably as a result of gel particle formation in the bulk solution during the pH adjustment, which later can act as nucleation centres for silica sol structures.

Maximum residual silica concentrations at pH3 recorded in this research were slightly higher (86 – 112mg/L) than the silica solubility (98 – 102mg/L) recorded by Gorrepati (2010) at pH3 probably due to analytical technique. Gorrepati used dissolved silica minerals in acid solutions over time periods at about 5 - 7 hours while in the current experiments, silica glass was dissolved and then silica precipitated as the concentration increased due to RO filtration over a period of >8 hours.

Figures 6.14 and 6.15 illustrate effect of pH on stable and maximum residual silica concentrations. As can be seen slightly lower stable and maximum residual silica concentrations were observed at pH3, however, a slight increase in solubility at high pH is possible but this trend is within the variation of the experimental results.

This research reveals that silica solubility in acidic solutions has lower solubility than at pH9 for instance. According to Gorrepati (2010), and Fogler (2009), silica precipitation at low pH follows a two-step process – formation of 5 nm primary particles followed by particle flocculation – which becomes exponentially faster with increasing HCl concentration and with salts accelerating the process. The majority of the research

completed on silica scale formation recognises that silica precipitation is not a simple function of pH (Thomas 1992, Semiat 2003, Damakis 2007).

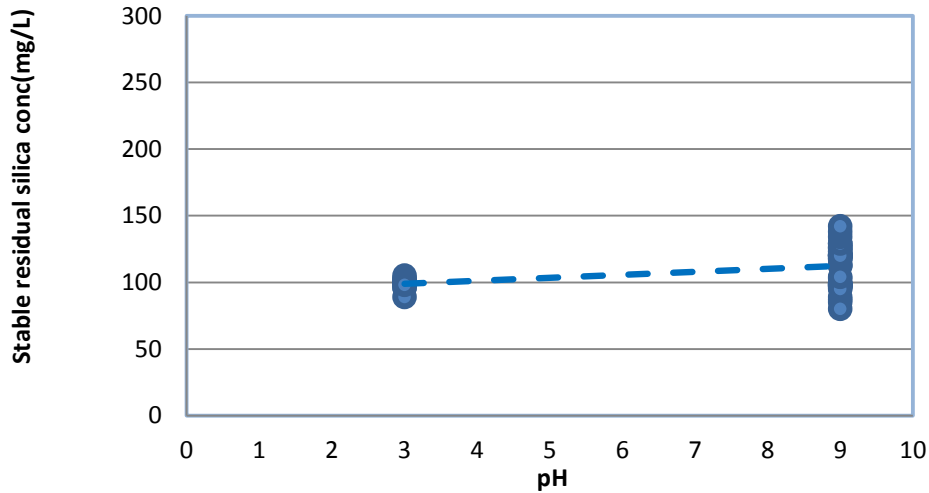


Figure 6.14 – Effect of pHs on stable residual silica concentrations in medium (12.5g/L) and high (30g/L) salinity synthetic waters.

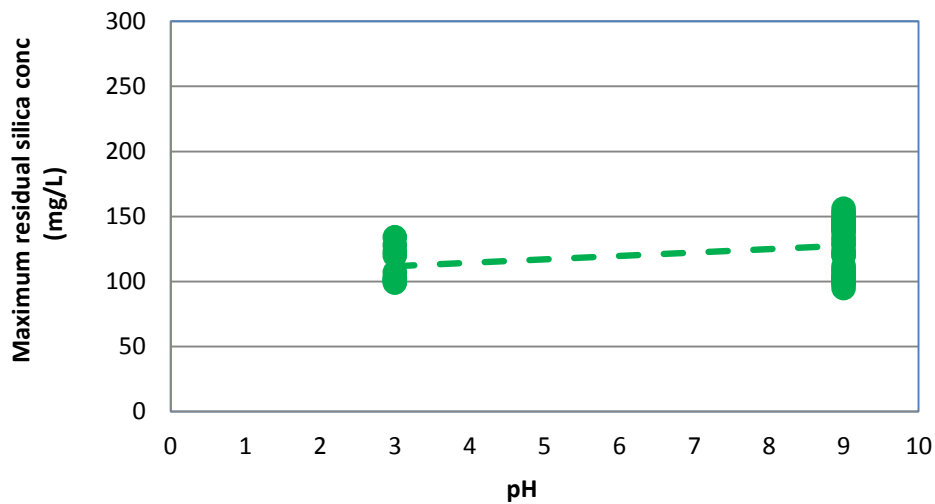


Figure 6.15 – Effect of pH on maximum silica solubility in medium and high salinity synthetic waters.

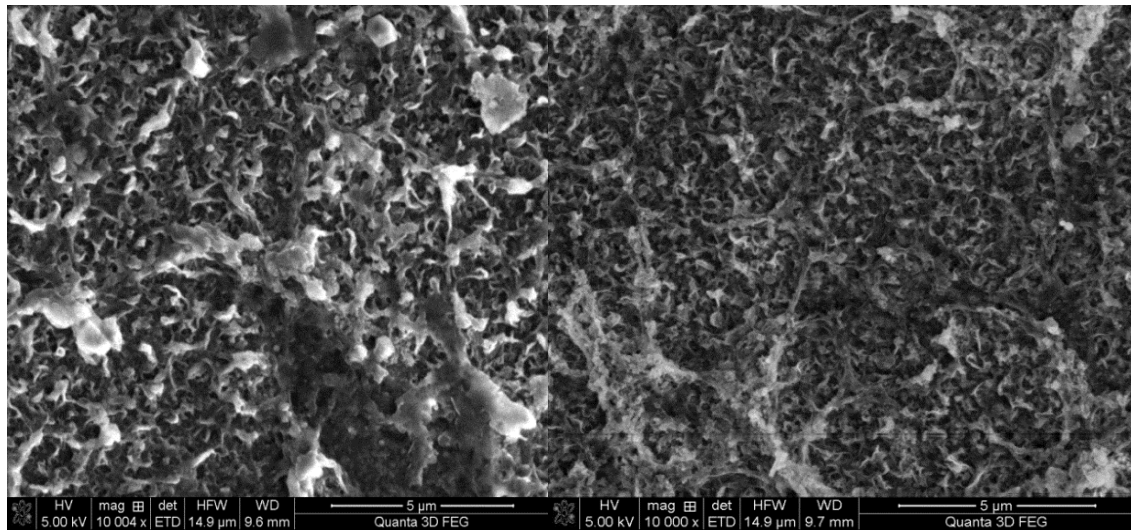
At relatively high concentrations, silica could skip a precipitation step to form a gel or monomeric silica acid (such as  $Q^0$  type silica species), which could be perceived as monomer silica acid (Dietzel 2001). On the other hand, it is well known that kinetics of

silica precipitation increases with increasing pH (Stumm and Morgan, 1996, Healy 1994). However, at low pH conditions, silica polymerisation proceeds via proton initiated gelling and as a result silica sol agglomeration via –O-Si-O- bonds occurs immediately once pH 3.2 - 3.5 is reached (Smolin 1976). At this point silica species remain as a gel (Smolin 1976).

#### ***6.3.4.4 Membrane surface examination***

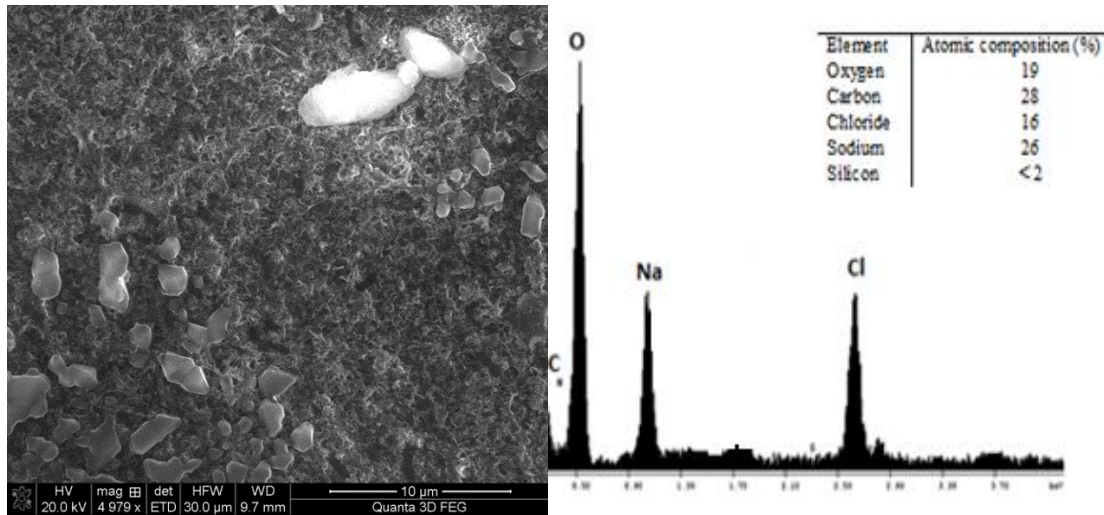
To determine the nature of the deposits on RO membranes following desalination experiments, autopsies were performed. The autopsy consisted of two methods – microscopic examination of the fouled surface and the deposited layer from the membrane to determine the elemental composition of the deposit.

Figures 6.16 (a), (b), (c) and (d) show the membrane surface examination images by SEM and EDS spectra for membranes fouled by synthetic water with an initial silica concentration  $\text{SiO}_2=50\text{mg/L}$ . The morphological images of the membrane surface using SEM at different magnifications indicated that surface particles were occasionally sodium chloride crystals probably formed after the membrane was removed from the RO unit. No silica deposition was detected on the RO membrane surfaces in medium and high salinity waters. EDS elemental analysis of each membrane showed low detectable silica deposition on the membrane surface for each water studied. This result suggests that perhaps sodium ions were preventing precipitated silica from bonding to the membrane surface. It is likely silica aggregated into colloidal structures, which remained in the recycled stream until the experiment terminated. These results are consistent with the hypothesis proposed by Healy (1994) and others (Gorrepati 2010, Demakis 2007), that in the solutions with relatively high concentrations of sodium ions ( $> \text{NaCl}=8\text{g/L}$ ), sodium ions create binding layers around silica preventing it from deposition or preventing silica from attack of water molecular and specially –OH groups, which link to homogeneous silica deposition on the membrane surface.



(a)

(b)



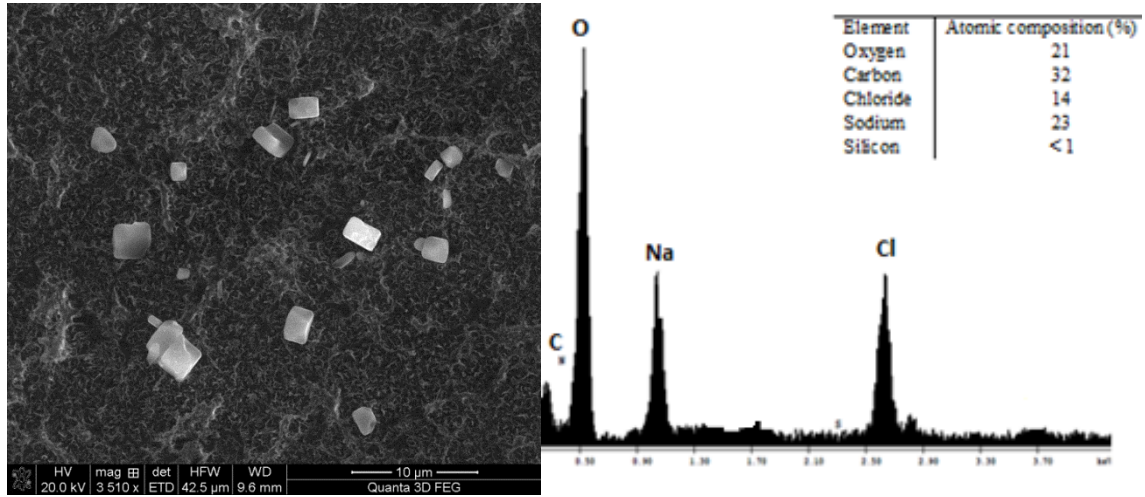
(c)

(d)

Figure 6.16 - Membrane surface EDS examination (a) low salinity synthetic water  $\text{SiO}_2=50\text{mg/L}$  at pH9, (b) medium salinity synthetic water  $\text{SiO}_2=50\text{mg/L}$  at pH9, (c) high salinity synthetic water  $\text{SiO}_2=50\text{mg/L}$  at RO feed at pH9, (d) EDS elemental analysis of the membrane surface (high salinity).

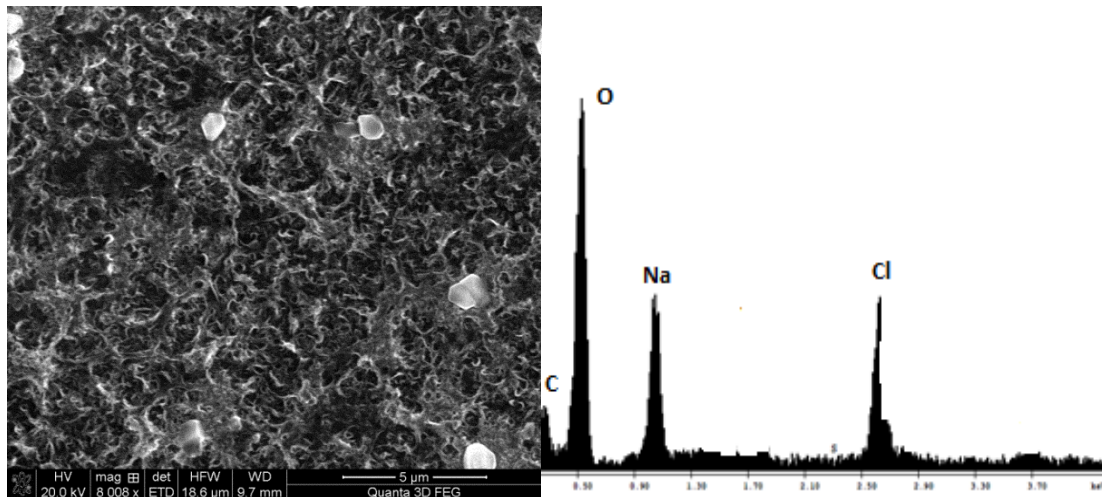
Figures 6.17 (a) and (b) illustrate the membrane surface following filtration at pH3 and the EDS spectra of deposited particles. At pH3 slightly less sodium chloride particles were observed. EDS elemental analysis also confirmed that silicon was < 1% (undetectable level) on the membrane surface, Figure 6.17 (b). This is probably due to slight contamination of the membrane surface upon drying, but not to silica deposition. It should be noted that the concentration of carbon in both cases, pH3 and pH9, was

high due to the polyamide RO membrane, which contained substantial amounts of carbon and oxygen functional groups (COO-groups). Figures 6.17 (c) and (d) show the membrane surface at pH11 condition for the similar high salinity waters. No silicon was observed again for pH11 RO experiments as was expected. As can be seen, single sodium chloride particles were observed as a result of formation during drying of the membrane samples.



(a) pH3

(b)



(c) pH11

(d)

Figure 6.17 – Membrane surface and EDS analysis (a) high salinity synthetic water  $\text{SiO}_2=50\text{mg/L}$  at pH3, (b) EDS elemental analysis for the pH3 experiment, (c) high salinity synthetic water  $\text{SiO}_2=50\text{mg/L}$  at pH11, (d) EDS elemental analysis of the membrane surface (high salinity) for the pH11 experiment.

### 6.3.5 CSG water

#### 6.3.5.1 RO residual silica concentration

Figure 6.18 illustrates the results of residual silica concentrations plotted against the theoretical values recorded for medium salinity natural CSG water at native pH9. As can be seen in Figure 6.18, residual silica concentrations followed the theoretical concentration curve between 0%-50% water recovery. The silica concentrations leave the theoretical curve and indicate precipitation occurs when the recycled feed reaches 128 to 137mg/L silica. Both stable and maximum silica concentrations values were recorded. Turbidity increased from an initial 0.8NTU (after coagulation with ACH and UF filtration) to 4NTU by the end of the RO run.

Figure 6.19 demonstrates residual silica concentrations at pH3. Dissolved silica concentrations follow the theoretical silica curve up to 56% water recovery, where silica fouling occurred at approximately 110-120 mg/L silica and the dissolved silica data points leave the theoretical silica concentration line. The residual silica concentration stabilised at approximately  $\text{SiO}_2=121\text{mg/L}$  (three consistent ICP samples). This was a slightly lower residual silica concentration than was recorded for a similar salinity and dissolved silica concentration in the synthetic water ( $\text{SiO}_2=127\text{mg/L}$ ).

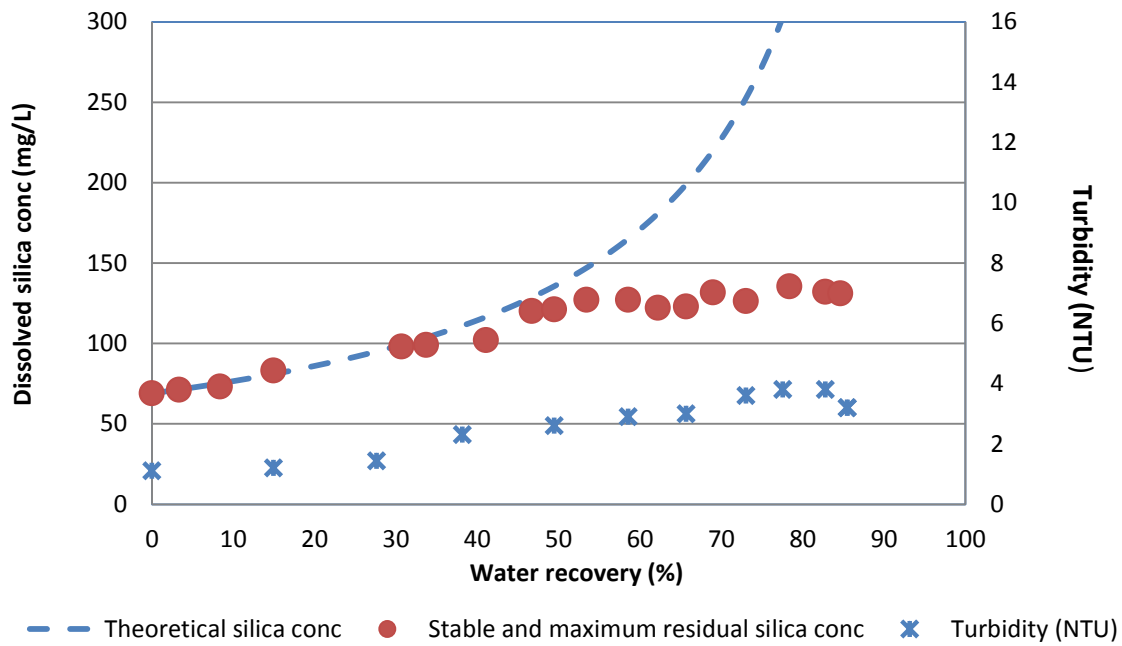


Figure 6.18 – Silica fouling and turbidity results measured in the recycle stream in medium salinity (12.5g/L) CSG water, initial silica concentration  $\text{SiO}_2=70\text{mg/L}$  at pH9 vs water recovery.

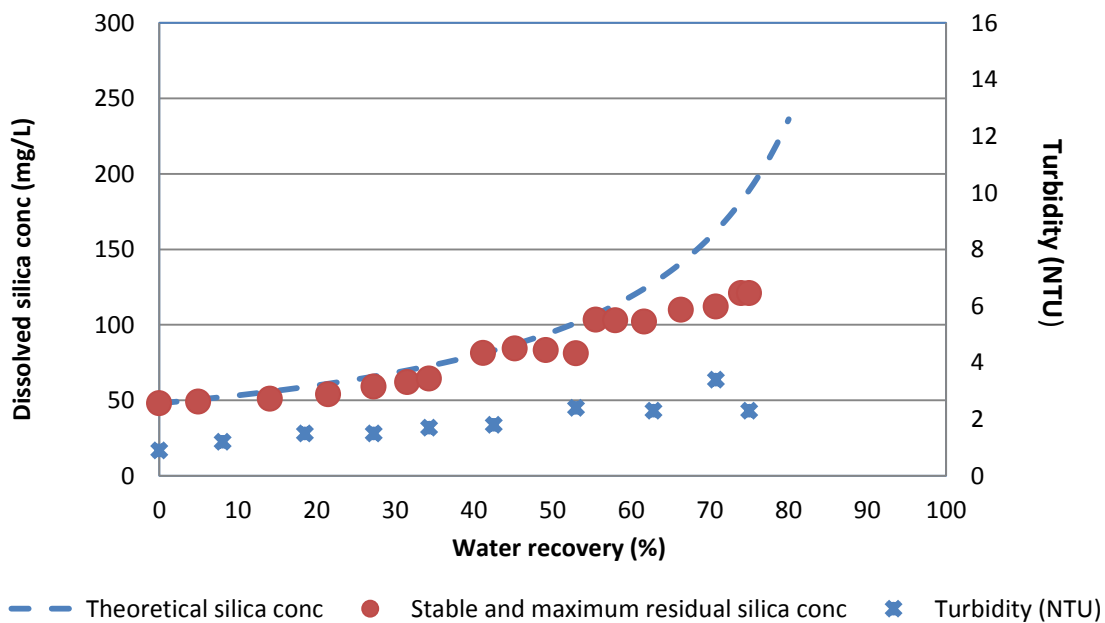


Figure 6.19 – Silica fouling and turbidity results measured in the recycled stream in medium salinity (12.5g/L) CSG water, initial silica concentration  $\text{SiO}_2=50\text{mg/L}$  at pH3 vs water recovery.

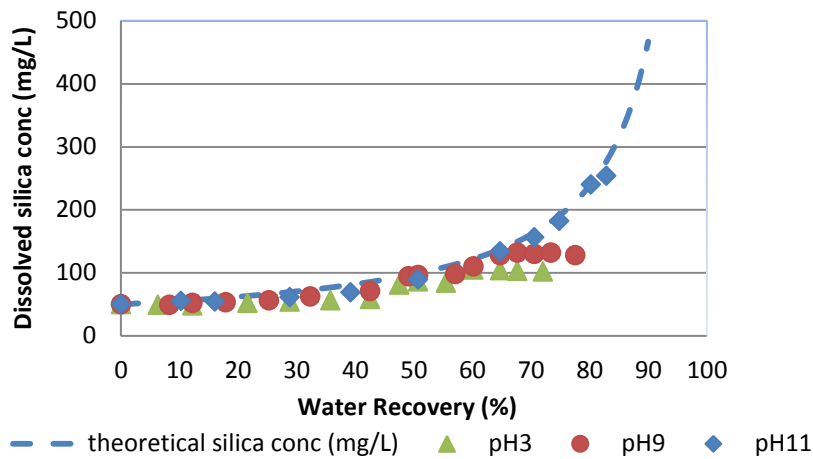


Figure 6.20 – Silica fouling trends in CSG water at pH3, pH9 and pH11 vs water recovery in low salinity (NaCl=6g/L) RO feed and dissolved silica concentration 50mg/L.

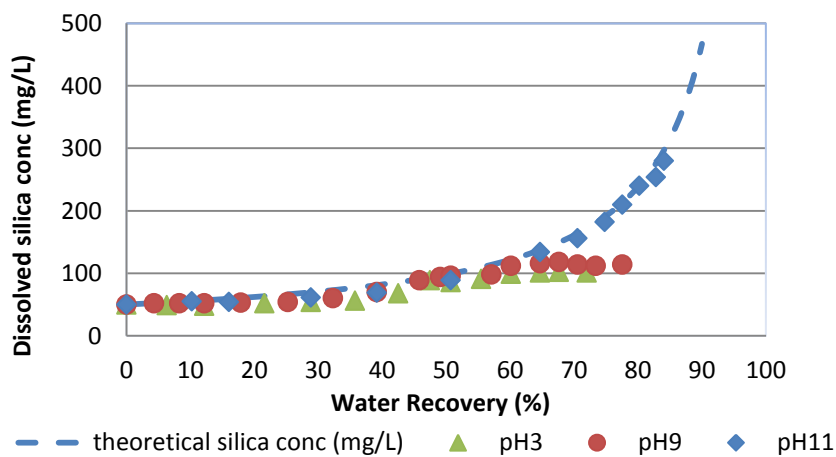


Figure 6.21 – Silica fouling trends in CSG water at pH3, pH9 and pH11 vs water recovery in medium salinity (NaCl=12.5g/L) RO feed and dissolved silica concentration 50mg/L.

Consistent silica fouling trends were recorded for CSG waters, as presented in Figures 6.20, 6.21 and 6.22. Figures 6.20, 6.21 and 6.22 show a decline of stable silica concentrations with lowering pH indicating silica polymerisation in bulk solution or on membrane surface or both. At relatively low initial salinity (>6 g/L), silica fouling

occurred at about 126mg/L maximum reading at pH9 and 127mg/L maximum at pH3, Figure 6.22.

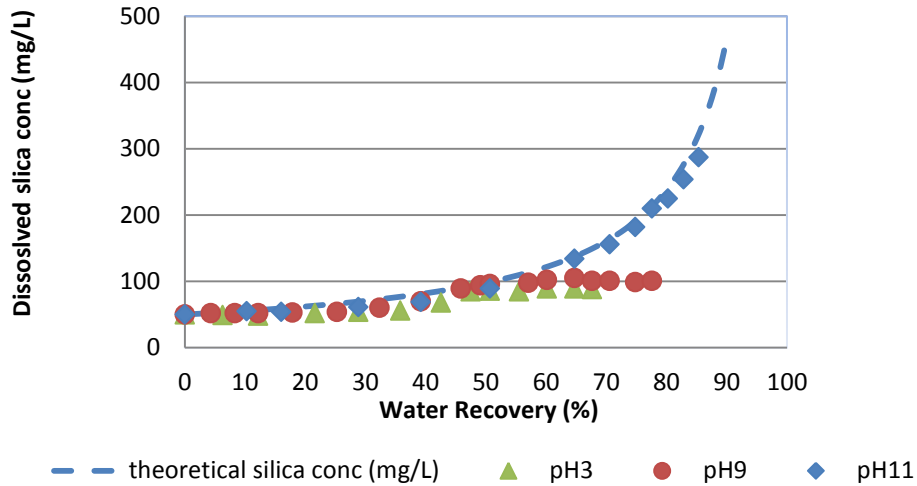


Figure 6.22 – Silica fouling trends in CSG water at pH3, pH9 and pH11 vs water recovery in high salinity (NaCl=30g/L) RO feed and dissolved silica concentration 50mg/L.

Table 6.5 summarises the average stable and maximum silica concentrations recorded in the natural CSG waters.

Table 6.5 – Summary of silica precipitations for CSG waters

RO conditions				Residual silica concentration	
RO feed (as NaCl), (g/L)	RO feed dissolved silica conc., (as SiO <sub>2</sub> , mg/L)	Water recovery (maximum) (%)	pH	Stable Residual silica conc., (average) (mg/L)	Maximum Residual silica conc., (average) (mg/L)
CSG waters					
6	50	85	9	123	127
6	50	82	3	120	126
6	50	78	11	NF	NF
12.5	50	76	9	120	121
12.5	50	75	3	114	123
12.5	50	78	11	NF	NF
30	50	64	3	91	94
30	50	62	9	81	84
30	50	68	11	NF	NF

NF = non fouling conditions.

In medium salinity (>12.5g/L) silica fouling commenced when the concentration in the brine reached a maximum of 120mg/L for pH9 and 114mg/L maximum at pH3, Figure 6.24. In high initial salinity (30g/L) fouling occurred at about 84 mg/L maximum residual silica concentrations for pH9 and about 94mg/L (maximum reading) dissolved silica concentration for pH3, Figure 6.25.

### 6.3.5.2 Effect of salinity

Figure 6.23 shows the effect of sodium chloride concentrations on stable residual silica concentrations. Similar to synthetic waters, elevated concentrations of sodium chloride depressed silica solubility. In low salinity CSG water silica precipitation occurred at 120 – 134mg/L residual stable concentrations. The stable silica concentration in the high salinity CSG water after 60% water recovery was around 81 - 90 mg/L. As can be seen from Figure 6.23, stable silica concentrations gradually decreased with increasing salinity. The results illustrate the stable residual silica concentration was approximately followed the silica solubility by Hamrouni (2001), but slightly higher than documented by Gorrepati (2010).

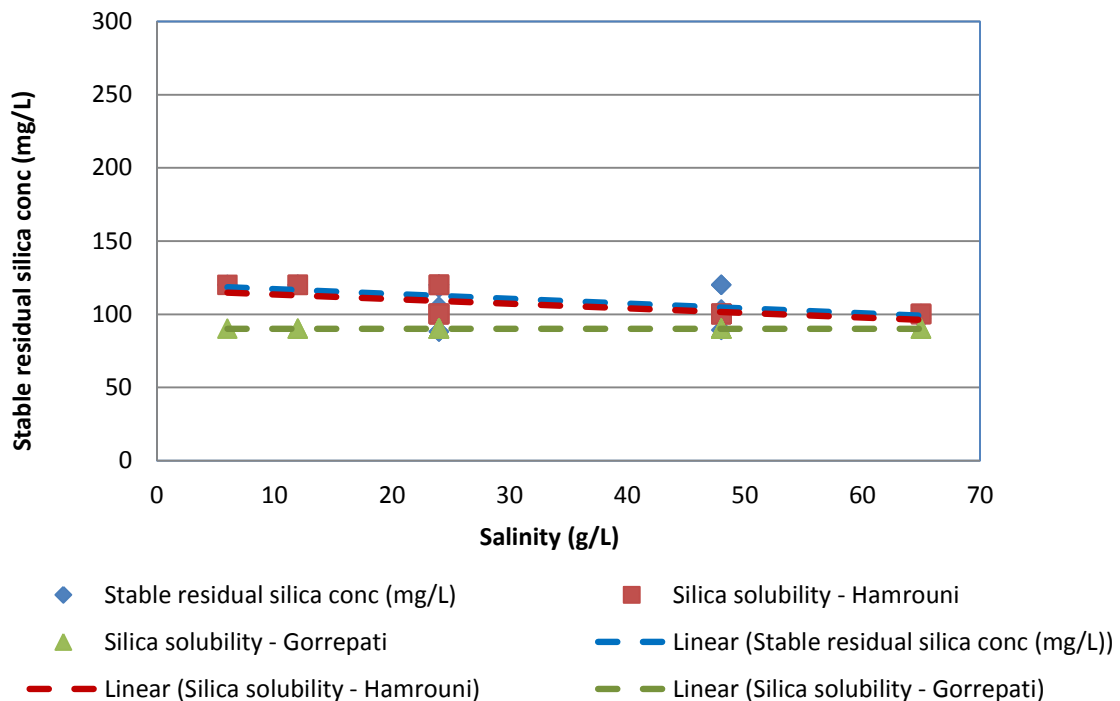


Figure 6.23 – Effect of salinity on stable residual silica concentrations in CSG waters.

The effect of salinity on maximum residual silica concentrations is shown in Figure 6.24 and illustrates that the effect of salinity on maximum values were similar to the effect of stable silica concentrations. The spread of maximum residual silica concentrations was less compared to the maximum residual silica concentrations recorded for similar salinity synthetic waters, Figures 6.8 and 6.10. Overall the difference between stable and maximum residual silica concentrations documented for CSG waters were insignificant or less than 2 - 5%. It appeared that silica precipitation in natural CSG waters occurred due perhaps to other cations and anions present, and perhaps as a result of slightly elevated concentrations of aluminium in raw waters.

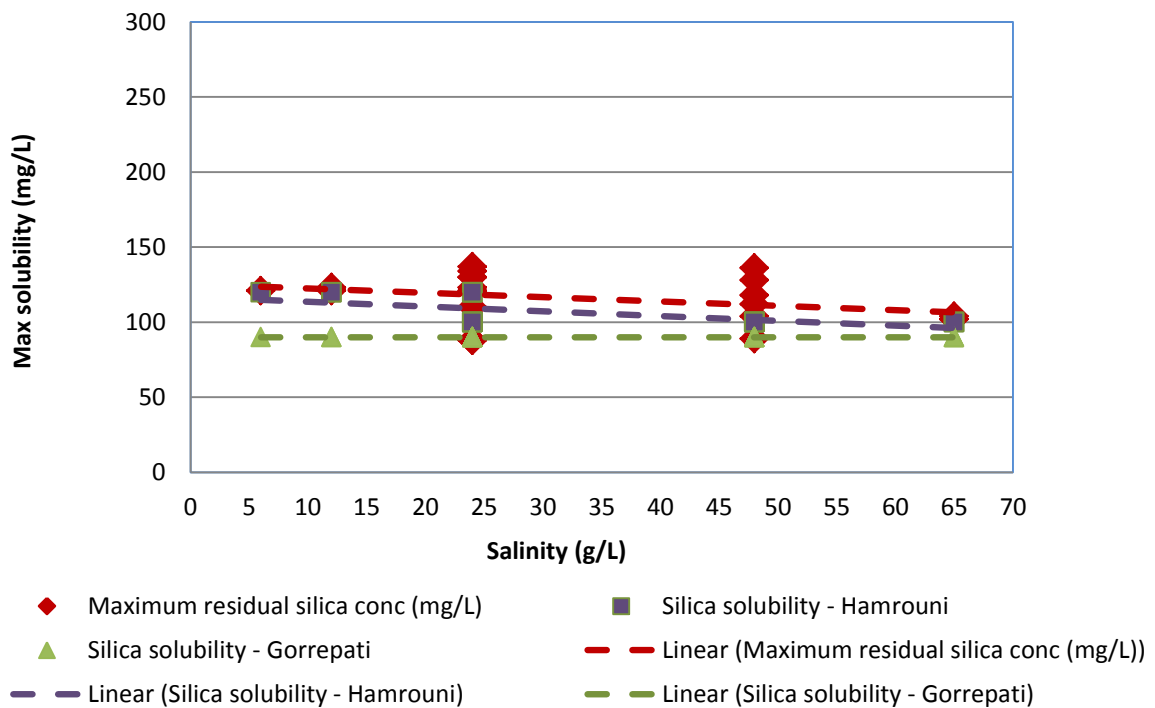


Figure 6.24 – Effect of salinity on maximum residual silica concentration in CSG waters.

### 6.3.5.3 Effect of pH

Figures 6.25 and 6.26 demonstrate minor effect of pHs on stable and maximum residual silica concentrations.

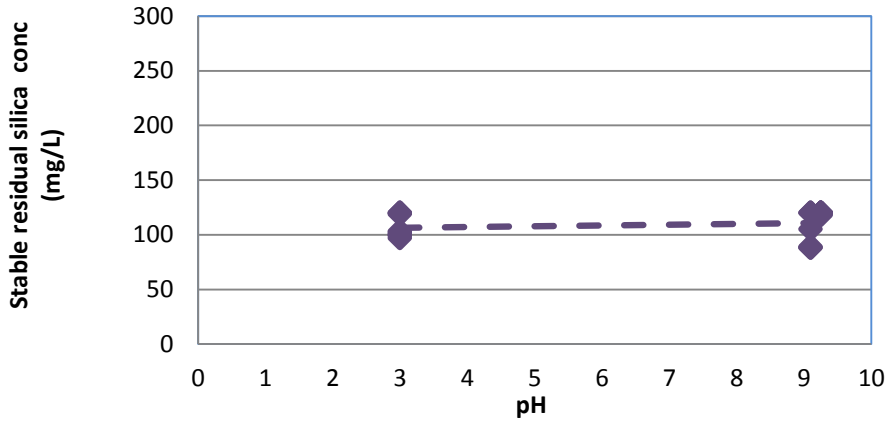


Figure 6.25 – Effect of pH on stable solubility in medium and high salinity CSG waters.

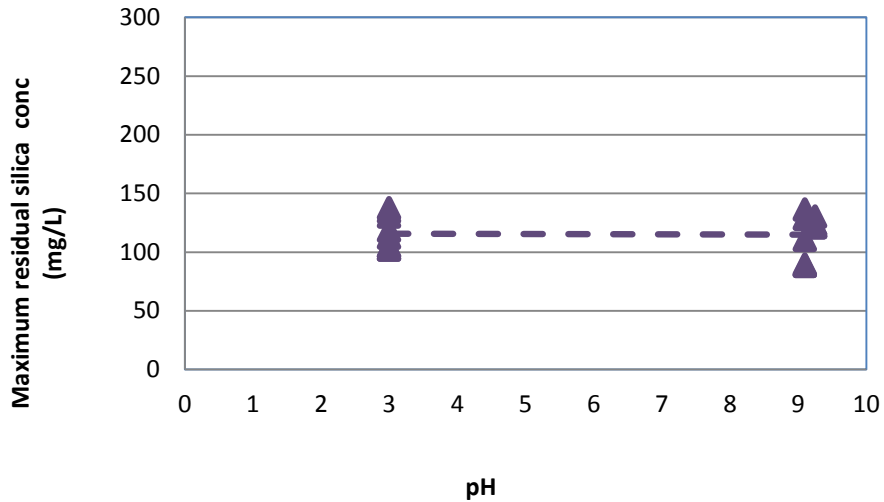


Figure 6.26 – Effect of pH on maximum solubility in low, medium and high salinity CSG waters.

Silica fouling occurred in CSG waters at slightly lower (4 - 5%) residual silica concentration. For example, at pH 3, high salinity the stable residual silica concentration was 85mg/L for CSG water compared 91 mg/L for the synthetic water with similar initial silica concentration. Similarly, silica fouling occurred at a stable

residual concentration 90mg/L in CSG water compare to the residual silica concentration in the synthetic water 96mg/L at pH9 and high salinity. Maximum silica solubility recorded for the CSG water was 130 – 145mg/L at pH9, Figure 6.25 compared to maximum silica residual concentrations of 137 – 147 mg/L at pH9 in the medium salinity synthetic water. This is due to different water matrix in synthetic and CSG waters. The presence of even minor concentrations of calcium (1-3.5mg/L), magnesium (1-4.7mg/L), barium (1-2.3mg/L), strontium (1.3-4.3mg/L), aluminium (7-11mg/L) alter silica fouling patterns as demonstrated by the results recorded with CGS waters.

Stable and maximum residual silica concentrations recorded in CSG waters have smaller variations between stable and maximum readings compared to the stable and maximum values recorded in the similar salinity and pH conditions for synthetic waters. Table 6.5 shows a summary of silica residual concentrations recorded in natural CSG waters.

Table 6.5 – Summary of silica precipitations in different salinity CSG waters

Salinity, (g/L)	Silica (as SiO <sub>2</sub> ) (mg/L)	WR (%)	pH	Turbidity (final) NTU	Turbidity (final) NTU	Stable silica fouling (mg/L)	Maximum silica fouling (mg/L)
6	24	84	3	0.91	11.2	NF	NF
6	24	86	9	0.93	11.5	NF	NF
6	24	86	11	0.81	12.1	NF	NF
6	50	81	3	0.51	14.23	128	130
6	50	83	9	0.51	14.11	127	136
6	50	85	11	0.53	5.67	NF	NF
12.5	50 - 70	78	3	0.98	12.23	130	138
12.5	50 - 70	79	9	1.1	11.45	136	142
12.5	50 - 70	80	11	1.1	6.93	NF	NF
30	50 - 70	55	3	1.12	12.1	85	105
30	50 - 70	60	9	1.11	13.2	90	111
30	50 - 70	65	11	1.01	9.87	NF	NF

NF = non fouling conditions.

### 6.3.5.4 Membrane surface examination

Figure 6.28 shows SEM images and EDS elemental analysis of the membrane surface after the RO run with CSG water spiked with sodium chloride (30g/L), silica (50mg/L), native aluminium concentration (7.5mg/L) and low DOC (7mg/L) at native pH9.2.

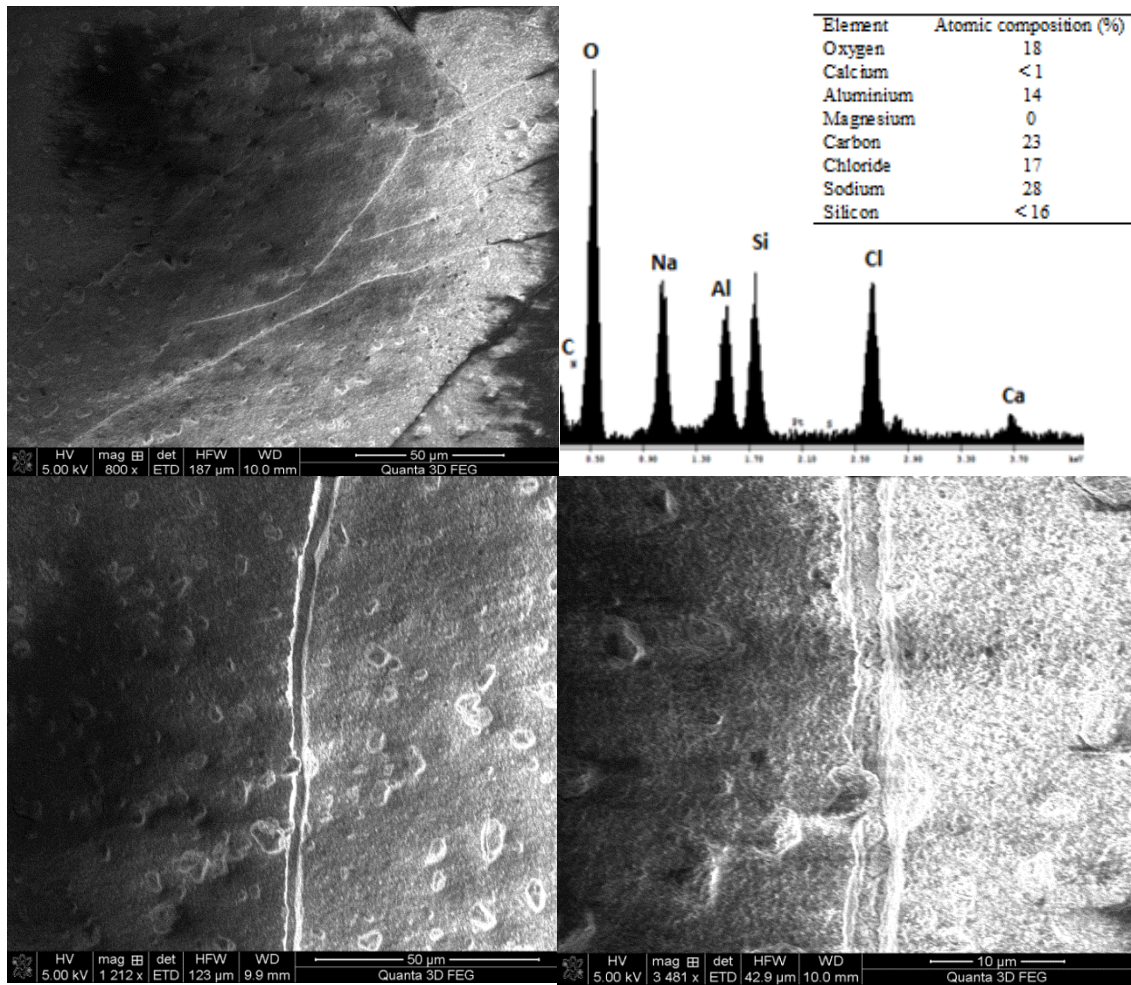


Figure 6.27 – Membrane surface of RO experiment with CSG water spiked with sodium chloride (30g/L) and silica (50mg/L) at pH9.2 - SEM (7000 x magnification) and EDS elemental analysis of the membrane surface.

As can be seen from the images presented, the membrane surface was covered with a complex and thick foulant material. EDS of the foulant layer along with atomic composition of the foulant layer showed a high percentage of silicon (<16%) and aluminium (14%).

The flux decline data collected during the each RO experiments showed that deposition of foulant layer on the membrane surface formed much faster in higher salinity and higher silica concentration waters. The presence of a low concentration of DOC (post-coagulation) could stimulate cake formation on the RO membrane surface. DOC matter even in small concentration in RO feed is considered the most serious and troublesome foulant, because it is the most difficult to remove via conventional pre-treatment processes (Potts et al., 1981, Safaric and Phipps, 2005). According to Brant (2012) DOC is capable of forming chemically resistant bridges between surfaces of two or more colloidal particles. The multitude of chemical bonds formed with DOC matters leads to the limited mass transport of cleaning agents through the foulant structure to the membrane surface. Membrane fouling by DOC has proven to be a significant problem for RO membranes because of diversity of organic molecules which are present in DOC matter.

### **6.3.6 Effect of aluminium**

#### **6.3.6.1 Flux decline**

This set of RO experiments was performed with natural medium salinity CSG waters, which had elevated residual aluminium concentrations (post-coagulation quality). Residual aluminium concentrations were specified in chapter 3, Table 3.5. Simple monitoring of the recycling stream during the RO experiment showed that the concentrated solution changed colour after the water recovery reached approximately 30%. The solution became slightly white coloured, and some fine dispersed particles appeared in the recycled stream (RO feed) as the experiment continued. This probably was a result of aluminium-silicate formation in the recycled stream and on the membrane surface. Figure 6.28 shows turbidity increased from the initial 0.5NTU to 6.8NTU at 20-30% water recovery and reached 6.3NTU at the end of the experiment. After minor permeate withdraw (20 – 30%) the recycled stream slightly changed in colour from a relatively clear solution into a cloudy beige colour probably due to heterogeneous nucleation. Figure 6.29 also illustrates typical fragmented deposition observed on the membrane surface.

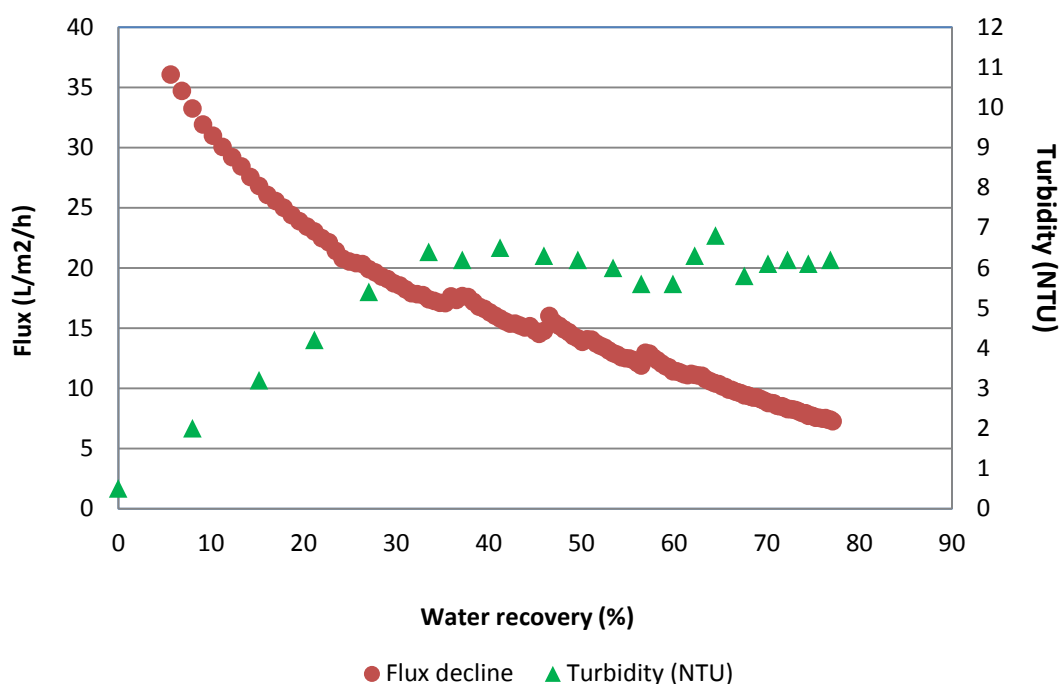


Figure 6.28 – Flux decline and turbidity results at silica concentration  $\text{SiO}_2=40\text{mg/L}$ , medium salinity (12.5g/L) CSG water and  $\text{Al}=27.7\text{mg/L}$  at pH9.

Figure 6.28 illustrates the typical flux decline for the range of RO experiments with elevated residual aluminium. The flux declined sharply from 0% to approximately 20% water recovery and then declined more slowly after 20% water recovery until the experiments was stopped at 76% water recovery as shown in the Figure 6.28. At approximately 35% water recovery the pressure started to drop for few seconds and then returned back to the designed pressure. This was an indication of gradual scale deposition on the membrane surface, and when the membrane was carefully removed from the RO unit for visual observation a deposit was observed. 76% permeate recovery was possible even with ongoing aluminium-silicate scale formation.

Examination of the membrane surface, shown in Figure 6.29, for the 55 % water recovery showed a thin scale deposit. Salt rejection (calculated value between initial and final TDS values) was slightly less than in the previous experiments (99.1 – 99.4 %), but still relatively high at 97.8%.

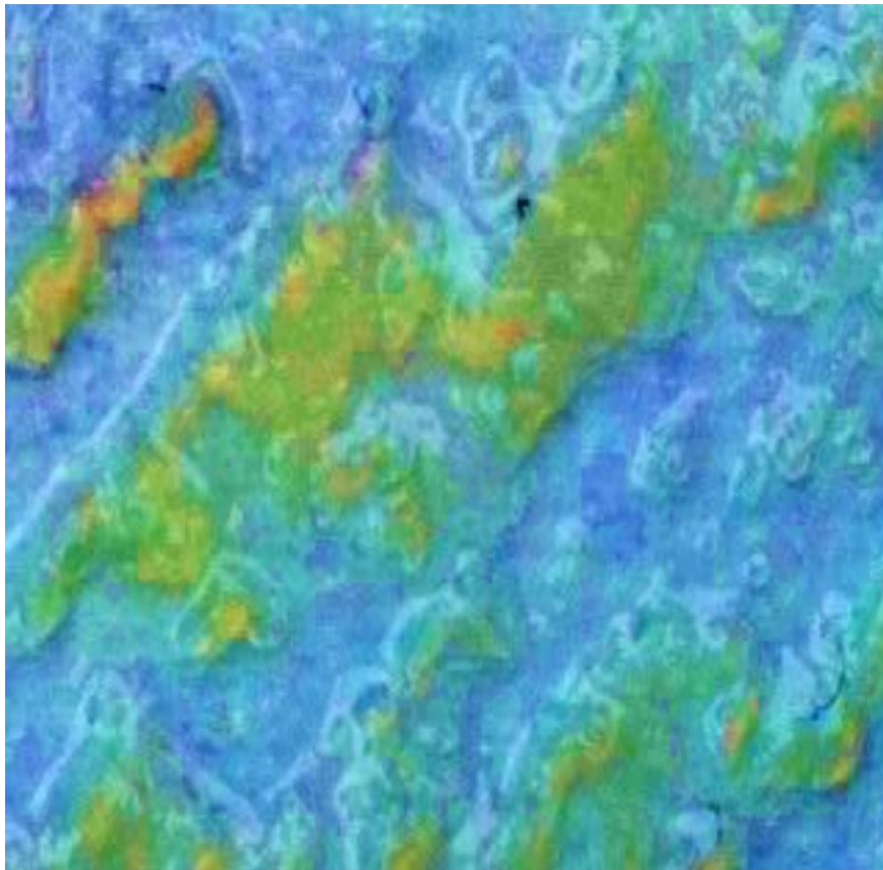


Figure 6.29 – Aluminosilicate scale deposition on the RO membrane surface at 55% water recovery in medium salinity CSG with an initial silica concentration (as  $\text{SiO}_2$ ) of 80mg/L and aluminium concentration (as  $\text{Al}^{+3}$ ) of 27.7mg/L at pH9. (Blue is silicate, Green is aluminosilicate).

#### ***6.3.6.2 Aluminium-silicate fouling***

Figure 6.30 illustrates typical silica fouling in medium salinity CSG water spiked with silica at initial concentrations of 40, 80 and 120mg/L, and with aluminium at 27.7mg/L silicon at native pH9. Figure 6.30 shows that dissolved residual silica concentrations did not follow the theoretical concentration curves, instead silica concentrations gradually declined.

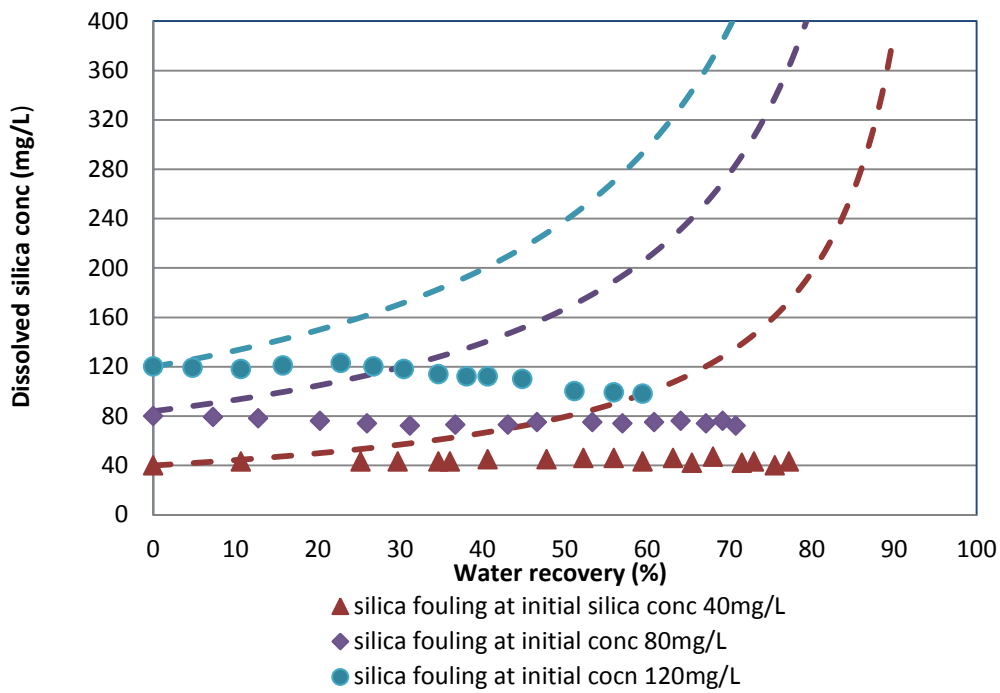


Figure 6.30 – Aluminium-silicate fouling at silica concentration  $\text{SiO}_2=40\text{mg/L}$ ,  $80\text{mg/L}$  and  $120\text{mg/L}$  in medium salinity ( $12.5\text{g/L}$ ) CSG water and  $\text{Al}=27.7\text{mg/L}$  at pH9.

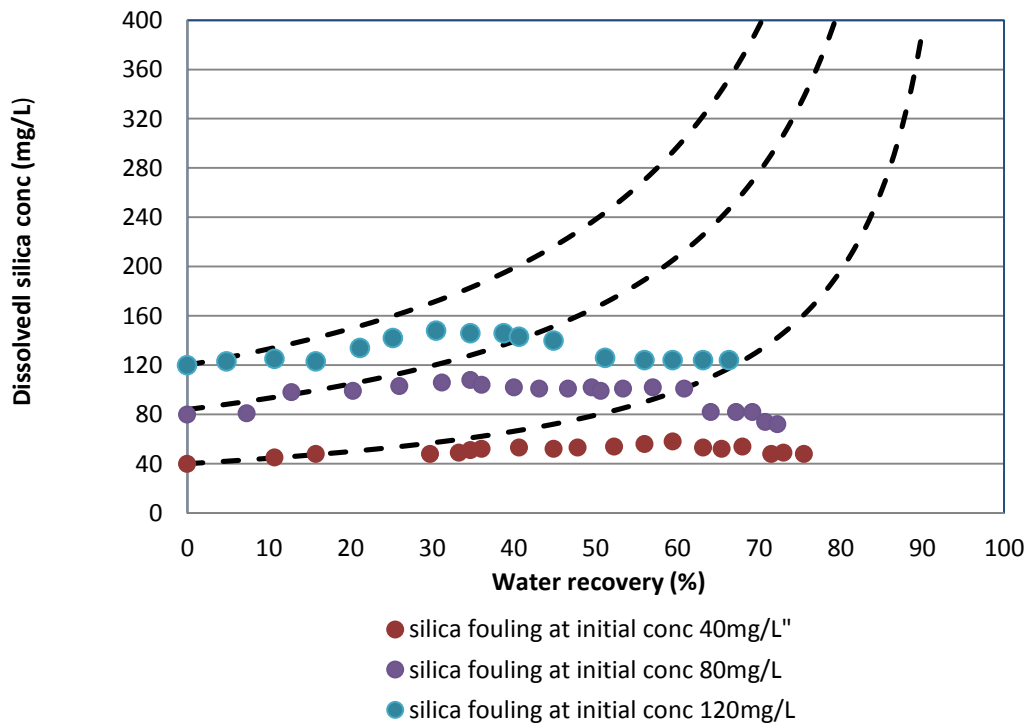


Figure 6.31 – Aluminium-silicate fouling at silica concentration  $\text{SiO}_2=40\text{mg/L}$ ,  $80\text{mg/L}$  and  $120\text{mg/L}$  in medium salinity ( $12.5\text{g/L}$ ) synthetic water and  $\text{Al}=27.3\text{mg/L}$  at pH9.

The dissolved silica concentration remained at approximately the same concentration or slightly higher than the initial concentration of 80mg/L. At about 27% permeate recover the silica concentration was 89 mg/L and then slowly declined. As can be seen, the residual silica concentration for initial silica concentrations of 40, 80 and 120mg/L followed the similar trends – silica solubility was depressed perhaps by elevated residual aluminium, which was in abundance on the membrane surface.

For comparison Figure 6.31 presents the results of silica fouling in medium salinity synthetic water. In this water matrix silica concentrations followed the theoretical concentrations until ~30% water recovery before repeating the similar trends recorded in the CSG water, Figure 6.30. This suggests that silica solubility was depressed by salinity and aluminium concentrations.

In this experiment silica fouling occurred in accordance with type four silica precipitation, discussed in the data analysis section, and suggested for the first time in this research work, when dissolved silica concentrations decline from the start of theoretical curve when precipitation occurs immediately after RO filtration commences for the water close to their saturation limit or “practical solubility limit”. The type four silica fouling can occur as a result of depression of silica solubility arising from salinity, other cations present and pH conditions.

#### ***6.3.6.3 Membrane surface examination***

It was recorded that a minor addition of aluminium, for instance from initial 7mg/L to 27.7mg/L appears to show an increase in scaling thickness. The membrane sample for SEM and EDS examinations was taken each time from the same middle location on the RO membrane. Figure 6.32 shows the typical membrane deposit formed during this study. EDS examination shown that aluminium peak was always consistent with the silicon peak indicative of aluminosilicate formation on the membrane surface. At pH condition (8.5 – 9.0) it was expected to see aluminium hydroxide precipitation. A potential fouling pathway is through the creation of an aluminium foulant that originally precipitates onto the membrane surface, with these foulants then serving as nucleation sites for subsequent aluminium silicate formation.

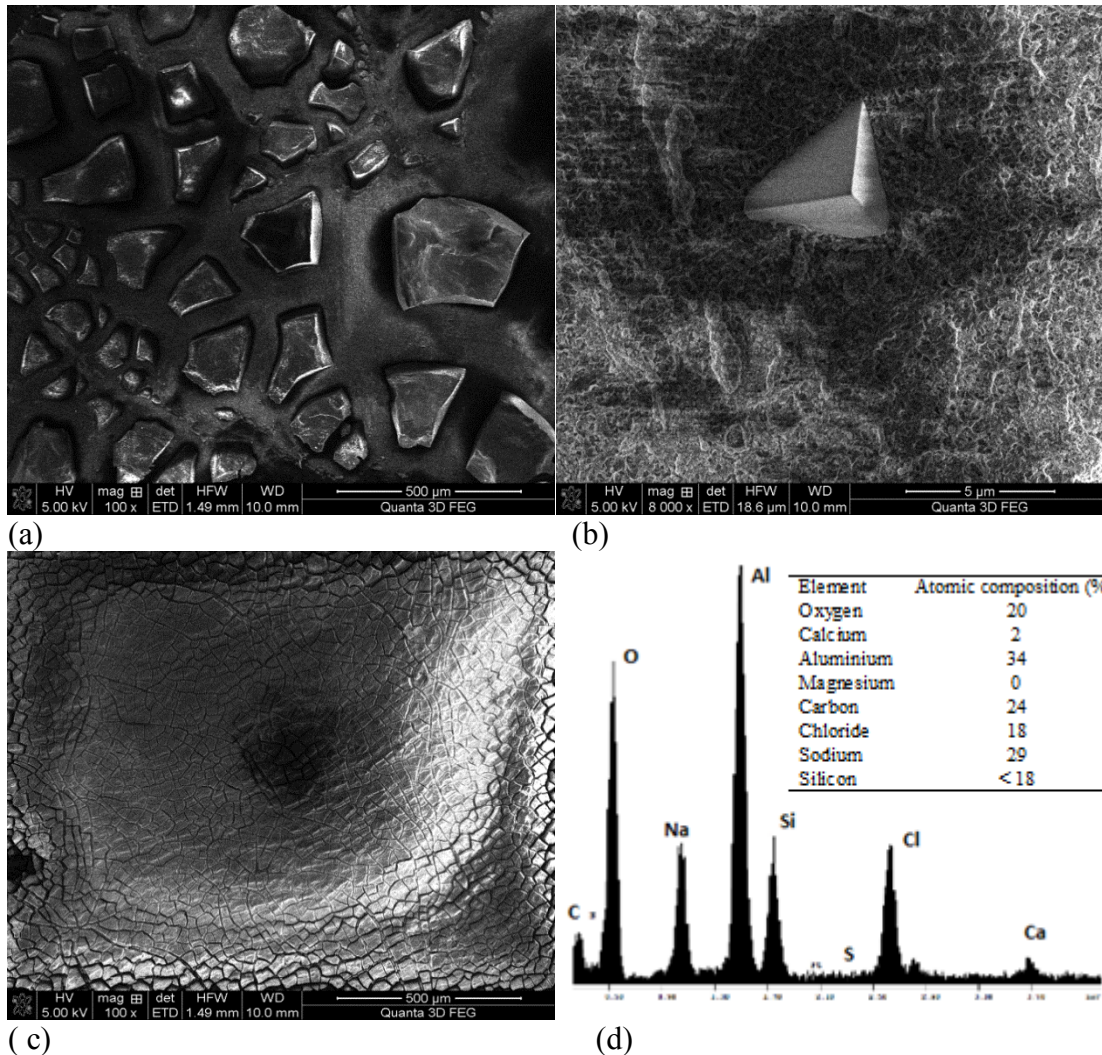


Figure 6.32 – (a), (b) SEM images of the RO membrane surface at 76% water recovery in medium salinity CSG water with an initial silica concentration (as  $\text{SiO}_2$ ) of 50mg/L and aluminium concentration (as  $\text{Al}^{+3}$ ) of 27.5mg/L at pH9 (c) SEM image of the RO membrane surface at different magnification and (d) EDS elemental mapping of the RO membrane surface.

## 6.4 Discussion

The results recorded for silica precipitation profiles in deionised water showed that increasing silica concentrations in the recycling stream had relatively little impact on flux decline, Figure 6.6 (the interval of 0 – 70% water recovery), until silica concentrations in the recycled stream reached ~250mg/L when the membrane surface was significantly covered by gel (amorphous silica). At both pH3 and pH9 conditions it

was possible to recover 70-80% permeate. This is perhaps due to high permeability of cake (gel) formed on the membrane surface. Silica concentrations reached 130 – 250 mg/L showing that dissolved silica can remain in dissolved forms at concentrations much higher than the known silica solubility limits. This is due to different forms of silica being present, such as dissolved reactive silica and dissolved non-reactive silica. It seems the kinetics of silica polymerisation at pH3 is slower than at pH9 condition. The results obtained in this research are consistent with the research by Gorrepati et al., (2010) and Healy (1994) illustrating that under very acidic conditions silica forms particles in ~ 5nm diameter. At low pHs (1-3) these particles form in a two-step process. “First, the monomeric form of silica is quickly depleted from solution as it polymerizes to form primary particles ~5 nm in diameter. Second, the primary particles formed initiate flocculation of other particles” Gorrepati et al., (2010). The results documented in this research show that at pH3 dissolved silica concentration depleted within 4 – 5 hours of the RO experiment, presumably due to nanoparticle formation described by Gorrepati (2010) and Healy (1994). It would be expected that in this acidic condition the rate of formation of particles (~5nm) will increase due to increasing silica concentration in accordance with concentration factor and reduction of water volume in the recycled stream. The hydrolysis reaction that “breaks” a Si-O bond in low pH (1-3) involves simultaneous electrophilic attack by H<sup>+</sup> from the water molecule on a bridging oxygen atom and nucleophilic attack on the Si atom by the O<sup>2-</sup> atom from that water molecule (Smolin 1976). It was observed that in low pHs conditions, dissolved silica tended to gel at much lower concentrations than at pH9. This is also due to lack of –OH groups on the silicate, as the kinetics of silica polymerisation and precipitation reactions are impacted by –OH groups and proton exchange between different interconnected silica species (Smolin 1976).

As discussed in chapter 4, the presence of sodium cations in the solution sustains a significant number of monomeric silicic acid (Q<sup>0</sup> type surrounding), which potentially lead to a high concentration of dissolved silica species in medium and highly salinity waters. The results, Figure 6.4, 6.9 and 6.10 show that NaCl in relatively high concentrations (8 – 60g/L) greatly reduced the silica solubility limits from expected concentrations of 120 – 140mg/L (see Table 2.1) to 90 – 80mg/L when residual

aluminium (< 7mg/L) is present. The silica precipitation trends documented (Figures 6.4, 6.9, 6.10, 6.20, 6.21, 6.22) in this research were consistent with the silica solubility data obtained analytically by Hamrouni (2001), except at high salinity (30 – 60g/L as NaCl) for both synthetic and CSG waters were the stable residual silica concentrations were lower than documented by Hamrouni (2001). The maximum and stable silica residual concentrations recorded in this research are summarised in Table 6.6.

Table 6.6 – Maximum and stable residual silica concentration for different salinity waters at pH9 (20°C).

RO feed salinity (as NaCl, g/L)	RO feed silica conc., (as SiO <sub>2</sub> , mg/L)	Stable residual silica conc., (as SiO <sub>2</sub> , mg/L)	Maximum residual silica conc., (as SiO <sub>2</sub> , mg/L)
Synthetic waters			
6	50 – 70	NF	NF
12.5	50 - 70	110 - 100	110 - 120
30	50 - 70	100 - 95	105 - 110
CSG waters			
6	50 - 70	120 - 125	120 - 125
12.5	50 - 70	105 - 100	105 - 100
30	50 - 70	85 - 90	85 - 90

NF = non fouling conditions.

The silica polymerisation path, as shown in the results described in this chapter and in the results discussed in chapter 4, is affected by presence of sodium ions and sodium concentration. The results obtained on high salinity synthetic and CSG waters confirmed a significant decrease of silica solubility from 120 – 140mg/L to 80 – 81 mg/L for approximately 1Mol sodium chloride concentration RO feed solutions (recycled stream). It has been found that silica (as SiO<sub>2</sub>) has a special affinity with sodium ions (Bergan 1994, Healy 1994). It seems sodium ions have two effects on silica and silica species. First, in solutions with high concentrations of sodium ions (> 8g/L) binding layers of sodium surround silica species acting as a stabilisation agent and protecting silica from attack from water molecules. Second, however, sodium ions

interact with water shells and attract water molecules. The attraction between sodium ion and water molecules impacts the silica hydrolysis process and polymeric silica can release monomeric silicic acid as a result of excess of –OH groups. The effect of sodium ions on monomeric silicic acid is also demonstrated and discussed in detail in chapter 4. As can be emphasised here relationships between **sodium – silica – aluminium** have a significant impact on the RO desalination process and must be understood for the specific water matrix to evaluate the effect of sodium and aluminium ions on silica fouling.

The impact of aluminium on silica fouling seemed to be quite dramatic as shown here, Figures 6.30 and 6.31. The presence of residual aluminium in synthetic and CSG waters depressed silica solubility to 45-60mg/L. In the presence of 27.7mg/L of residual aluminium in the RO feed, silica fouling was recorded after 20 – 30% permeate recovery. Higher aluminium and silica concentrations in the recycled stream, in accordance with concentration factors for the higher water recoveries (table 6.1), dramatically increase the flux decline, Figure 6.28. Deposition of aluminium silicate on the membrane surface was detected after 30% permeate recovery. As can be concluded from the results, silica solubility is depressed by the presence of the elevated concentrations of aluminium and therefore silica precipitates as aluminosilicate on the membrane surface as demonstrated in this research.

When aluminium chloride is added to the water, aluminium hydroxide will form. Monomeric silica present in the solution will gradually adsorb on aluminium hydroxide. Once silica is adsorbed on the aluminium hydroxide, more monomeric silicic acids will be adsorbed into this structure. Silica polymerisation via mono – dimer – trimer – tetramer pathway is out competed by Al-O-Si-O-Si-O-Al reaction, which dominates over OH-O-Si-O-Si-OH pathways. As shown in chapter 4, the presence of aluminium reduces the conversion of silica species into polymer-oligomer species (such as Q<sup>2</sup>, Q<sup>3</sup> type surroundings) which are required polymerisation. Monomeric acid silica species, as Q<sup>0</sup> and Q<sup>1</sup> type surrounds, react with aluminium hydroxide and precipitate as aluminium silicates. Absorption characteristic of mono-silicic acid on metal hydroxides has been studied (Diagaku 1981, Jepson 1991, Tarutani and Kato, 2001). Yet, few

reports have been published on the formation of polysilicic acid layers formed by polymerisation of silicic acid on the aluminium hydroxide surface indicating a significant silica solubility decrease. In the results obtained in this research, the membrane surface examination by EDS clearly shown the presence of aluminosilicate layers (cement like structures) covered the membrane surface. Moreover, after drying the membrane, the deposit was not washable from the surface as in the case with other silica deposition.

Cumulative effect of sodium and aluminium ions on silica precipitation involves complex reactions. Sodium ions depress silica solubility at the same time preventing silica from deposition on the membrane surface. The majority of dissolved silica polymerised in the bulk solution and discharged in the reject stream of the RO system. According to Healy's hypothesis then higher salinity then more sodium ions create binding layers to surround silica sol. In response to sodium binding layers, however, dissolved silica species will aggregate into polymeric-oligomer structures and as a result silica aggregates into colloidal structures and remains in the brine stream rather than depositing on the membrane surface. This was a key finding of the synthetic water study of the impact of salinity on silica precipitation in the RO experiments.

Aluminium ions depress silica solubility at the same time react with silica to form aluminium silicates which immediately deposit on the membrane surface. As can be concluded here, aluminium ions can break the sodium layer surrounding silica species and silica polymeric structures, allowing the formation of aluminosilicate. However, silica deposition as silicate or aluminium silicate on the membrane surface depends on several factors, such as the presence of silica gel that catalyses continued silica precipitation, and the presence of nucleation coupling points that provide a favourable environment for silica to precipitate. It is known that aluminium hydroxide groups can serve as nucleation points for silica deposition on the membrane surface (Cob 2012).

Silica polymerisation leading to silica precipitation is a much more complex mechanism and also pH dependent. Considering that silica precipitation reaction is usually initiated by neutral monomeric silicic acid ( $Q^0$  type), low ionisation species seem to be not

important. Nevertheless, silica polymerisation in particular is initiated by low ionised species so it seem silica precipitation in low pH conditions could occur as dramatic as in any high pH conditions assuming enough silica is present for precipitation reactions. The mechanism seems to be more understood in the literature for higher pH conditions.

In natural CSG waters silica precipitated in low, medium and high salinity waters probably due to many factors - elevated concentrations of aluminium, salinity, and minor concentrations of calcium and magnesium. Total and dissolved barium and strontium were present in very low concentrations, table 3.2. Depressed silica solubility by medium and high concentrations of sodium forced silica to precipitate at 90 – 81 mg/L concentrations at approximately 1Mol sodium chloride concentration in the recycled stream. Presence of residual aluminium contributed to silica deposit formation on the membrane surface for all CSG water salinities studied. Figure 6.32 shows a significant aluminosilicate deposition on the membrane surface. It was discovered that sodium ions were not able to prevent silica deposition on the membrane surface as was the case with synthetic waters were no membranes showed silica scale deposition. It confirmed that sodium ions were not able to overcome the affinity between silica and aluminium. Formation of aluminosilicate on the membrane surface was slightly visible on the membrane surface after the membranes were removed from the RO unit. The flux declines, Figure 6.28, were quite dramatic after first 20 – 30 % permeate recovery and this was also an indication that the membrane was losing permeability due to aluminium-silicate formation on the membrane surface. In the presence of elevated concentrations of aluminium in the CSG water spiked with sodium chloride (different concentrations), silica precipitation occurred in concentrations 47 – 68mg/L. It is clear that silica solubility reduced in the presence of aluminium because of the lower solubility limits for aluminosilicate.

Figure 6.33 summarises residual silica concentrations recorded in natural and altered CSG waters, which are also compared to silica solubility documented by Hamrouni in various salinity waters (2001). In CSG waters, the spread of maximum and stable residual silica concentrations was less broad indicating silica precipitation occurred close to theoretical solubility values. First, the dissolved silica precipitated in high

salinity CSG waters was slightly below the solubility of amorphous silica known in the literature. This probably is due to depression of silica solubility by high sodium concentration and the presence of other cations and anions, which serve as nucleation points for monomeric silica groups to precipitate.

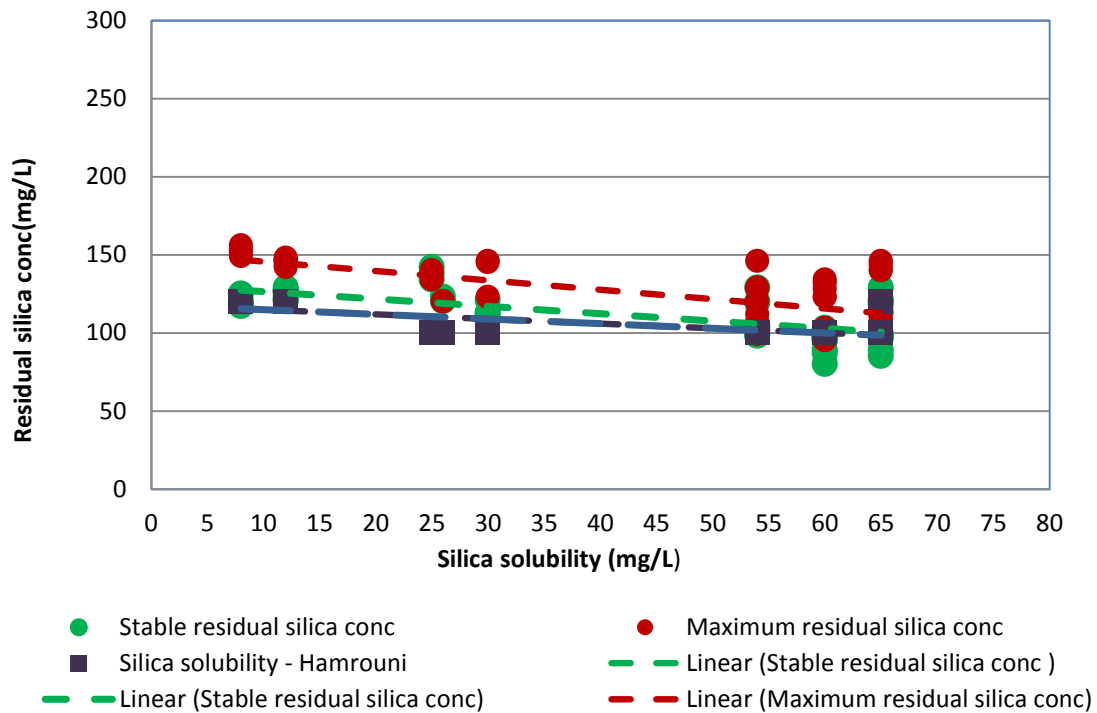


Figure 6.33 – Maximum and stable residual silica concentrations at initial RO silica concentrations 50 - 70mg/L and silica solubility by Hamrouni (2001) vs salinity at pH9.

The other condition for silica precipitation is the native pH 9.2 of CSG water, when dissolved silica groups present in more ionised forms as discussed above. Therefore, it has been found that CSG water had all four criteria for formation of silica deposits on the membrane surface. These include: (1) medium to high salinity which depress silica solubility forcing silica polymerisation. The medium and high salinity groundwater also often contains a high proportion of monomeric silica acid which could initiate silica deposition particular at pH9 (2). It is known that at pH9, ionised silica species exhibits strong coating characteristics (Bergna 2005, Healy 1994) which may also lead to silica coatings on RO desalination. (3) Presence of residual aluminium found in CSG water in Australia at concentrations 5 – 11 mg/L, creates favourable conditions for silica fouling. Further increase of residual aluminium concentrations to 27.7mg/L showed a significant increase in flux decline and aluminium silicate deposition on the membrane surface. (4)

CSG waters in Australia have medium (10 – 30mg/L) to high (30 – 140mg/L) silica concentrations, which normally will be reduced by coagulation before RO processing. However, the increase of residual aluminium in post-coagulation RO feed remains a significant concern for the industry. It is expected that 0.1 µm cartridge filter will be able to remove all particulate aluminium and iron. However, monitoring of RO feed quality remains a key requirement for RO desalination without silica deposition, especially for the high recovery (94 – 96%) permeate recovery systems.

## 6.5 Conclusion

Practical silica solubility or the solubility defined empirically is a key for prevention of silica polymerisation in RO desalination systems. What has been done in this study is to better define what this means for RO processes and how water chemistry affects this. Soluble or dissolved (reactive) silica contains different silica species; monomer, dimers, trimers and other polymers of silicic acid in different solutions. These dissolved silica species can be presented in various ionisation states which depend on the pH of solutions and silica concentrations. Chemical reactions between these silica species and cations and anions often present in the CP layer in super-saturation conditions are commonly lead to irreversible silica scale formation on the membrane surface. Contrarily, not all highly super-saturated silica streams lead to scaling of membrane surfaces as it was shown in this research. The new knowledge created from this work can be summarised as follow:

- i. Silica precipitation profiles studied in deionised water showed that increasing silica concentrations in the recycled stream had little impact on flux decline until majority of the membrane surface was covered by gel (amorphous silica). After silica gel deposition the membranes were able to maintain high permeability.
- ii. The results documented in this research show that NaCl in relatively high concentrations (8 – 60g/L) depress silica solubility limits leading silica fouling at 90 – 81 mg/L, but no silica deposition or single silica bonding to the membrane surface was found on the membrane surface illustrated that precipitated silica remained in the recycled stream.

- iii. The maximum and stable residual silica concentration concepts were introduced to highlight potential theoretical silica solubility deviations in different water matrices and recorded pseudo – silica solubility. Residual silica concentrations can increase above the silica solubility limit, to form super-saturated solutions, especially for low salinity and high flux conditions where silica concentrations increase rapidly in accordance with the RO concentration factor. The kinetics of precipitation is slow due to the requirement for nucleation to occur and the relatively short time of the desalination experiments.
- iv. The presence of minor (7 – 11mg/L) to moderate (27.7mg/L) concentrations of aluminium in CSG waters increased silica fouling and deposition as aluminium silicate on the membrane surface. The deposit formed on the membrane surface was much harder to dissolve compare to other silica deposit found in this research.
- v. Silica precipitation occurred at pH3 condition in both synthetic and natural CSG waters. Stable and maximum residual silica concentrations reached at pH3 were slightly lower to stable and maximum residual silica concentrations recorded at pH9. Overall little effect of pH (between 3 and 9) was observed on silica fouling trends in both synthetic and CSG waters.

The practical implications of the new knowledge obtained here can be summarised as follows:

- vi. The presence of moderate to high concentrations of silica in CSG waters can result in rapid rates of silica precipitation in lower thresholds limits as low as 85-90mg/L dissolved silica concentration (the current RO industry is 100mg/L). Minor concentrations of calcium, magnesium, strontium, barium, aluminium adversely impact on silica solubility and promote silica scaling rather than precipitation in the bulk water.
- vii. CSG water pre-treated with coagulants (such as ACH or aluminium sulphate) has slightly high residual aluminium concentrations (20 – 32mg/L) in post-coagulation water quality compared to initial aluminium concentrations (7 – 11mg/L in raw CSG waters). Silica present in medium concentrations (20 –

45mg/L) in CSG waters increased scale formation on the membrane surface, and therefore residual aluminium concentrations need to be minimised in the RO pre-treatment stages.

## Chapter 7 Conclusion and future research

### 7.1 Summary

The primary aim of this research was to improve the understanding of silica fouling (polymerisation and precipitation processes) in RO desalination of CSG water. The research was undertaken in three prolonged phases. First, the effect of sodium, aluminium, and pH on dissolved silica species was studied by  $^{29}\text{Si}$  NMR spectroscopy. Second, the effect of salinity on silica removal efficiency by three coagulants was investigated, and third, silica fouling patterns were studied in multiple RO experiments.

The specific objectives of the research were to:

- (1) Develop a conceptual silica polymerisation model using  $^{29}\text{Si}$  NMR data and silica solubility results to explain silica polymerisation on RO membrane surfaces.**
- (2) Review potential silica removal efficiency of coagulation and the influence of salinity on silica removal by a range of coagulants.**
- (3) Identify CSG water components and coagulation residuals that influence silica solubility, and in particular lowering of silica solubility, using synthetic and field CSG waters.**
- (4) Develop relationships between pH, silica concentration, and silica species present for the polymerisation of silica (silica scale formation).**

### 7.2 Conclusion

Based on the results presented and discussed in this research and comparison of the results obtained by different techniques on the effect of sodium, aluminium and pH on silica polymerisation and silica precipitation patterns the following conclusions can be drawn as follows, specifically from the  $^{29}\text{Si}$  NMR study described in the chapter 4:

- a) As a result of dilution with deionised water, dissolved silicate species gain or lose monomeric silicic acid ( $\text{Q}^0$  type surroundings). A gradual decrease of  $^{29}\text{Si}$  NMR spectrum intensity, increased proportions of  $\text{Q}^0$  and decreased  $\text{Q}^1$ ,  $\text{Q}^2$  and  $\text{Q}^3$ , indicates that hydrolysis or dissolution of monomeric silicic acid occurred

immediately. Overall a consistent proportional decrease of  $^{29}\text{Si}$  NMR spectrum for  $\text{Q}^1$ ,  $\text{Q}^2$ ,  $\text{Q}^3$  indicated that there was an equilibrium between species at the Si/M molar ratio 1.7, which changed with further dilutions from the Si/M molar ratio 1.55 to 0.11.

- b) Here it is shown that addition of sodium chloride slightly increased the release of monomeric silicic acid ( $\text{Q}^0$ ) and decreased hydrolysis of more complex silicate species ( $\text{Q}^2$ ,  $\text{Q}^3$ ) compared to similar dilutions with deionised waters. It suggests that sodium prevents water molecule access to  $\text{Q}^2$ ,  $\text{Q}^3$  types, thus stabilising silicate structures.
- c) The effect of sodium ions on silicate species suggests that  $\text{Q}^0$  type surrounding Si-OH is the preferred bond over Si-O-Na, while for  $\text{Q}^1$  and  $\text{Q}^2$  type surroundings Si-O-Na is preferred over Si-OH. For  $\text{Q}^3$  type both reactions with  $\text{Na}^+$  and  $\text{OH}^-$  may occur in combination and mix of bonds depending on the pH, and physical structures of more complex silicate species.
- d) Certainly, a profound effect of aluminium ions was recorded on silicate species. The presence of aluminium on silicate species has three impacts: (a) aluminium ions connected to silicate, Al-O-Si-O, resulting in a loss of sensitivity of  $^{29}\text{Si}$  NMR spectrum, (b) aluminium forced re-arrangement of species perhaps into polymerisation and precipitation, which are also lead to a loss sensitivity of  $^{29}\text{Si}$  NMR spectrum, and (c) it is likely some silicate species  $\text{Q}^1$ ,  $\text{Q}^2$  type precipitated as aluminium silicate. There was a clear indication of a structural shift of silicate species towards condensation (precipitation reaction) processes.
- e) A significant impact of minor concentrations of aluminium into relatively rich in silicon sodium silicate solutions is indicative that low aluminium concentrations have a significant impact on dissolved silicate species.
- f) The chemical shifts recorded at low pH 2 and 3 illustrate the presence of monomeric silicic acid, have not been found in other studies (Stumm and Morgan (1976), Dietzel (2002)) probably due to rapid particle formation at these pH conditions and due to low interest in this experimental data from a practical application perspective.

In light of the results described in the chapter 5, it is clear that simultaneous charge neutralisation and sweep coagulation of silica is a more complex process than just incorporating the mechanisms of collision and particle growth. It is obvious that the concentration of sodium chloride in solution inhibits removal of silica by coagulation. Having tested three different salinity waters, a new hypothesis was introduced indicating that aluminium ( $\text{Al}^{13+}$ ) can substitute for sodium ions to neutralise and bridge silica sol. The relationships between  $\text{Si}(\text{OH})_4$  and  $\text{Al}^{3+}$  and  $\text{Na}^+$  seems to play a key role in effective silica removal by coagulation, a detail are not found in any previous work. Furthermore, the new hypothesis proposed the substitution of sodium ions by aluminium ions in the sodium layer surrounding silica species can potentially introduce a new field research, where sodium – silica - aluminium relationships are key to understanding the chemical reactions.

In conclusion, these findings can be framed in terms of the implication for the operation of a full-scale coagulation pre-treatment process in a RO plant as follows:

- g) Coagulation can sufficiently reduce total silica concentrations in raw CSG water via removal of particulate matters overall from initial concentrations 20 – 80mg/L to 12 – 23 mg/L. Reduction of dissolved silica by coagulation can be also relatively effective treatment via precipitation and precipitation mechanisms of dissolved silica species if an effective coagulant is selected.
- h) Pre-hydrolysed coagulant as ACH (PACI) is an effective coagulant in silica removal; however, residual aluminium concentrations can slightly increase and required careful monitoring of the downstream concentrations.
- i) Increasing salinity of CSG water demands higher coagulant dose.
- j) Storage of CSG water in open evaporation ponds for prolonged period time is not recommended as water quality degrades as a result of evaporation (salinity increase), algae growth, and potential significant increase of TOC/DOC concentrations. The changes result in substantially increased coagulant doses being required for effective coagulation and very large sludge volumes result.
- k) The best turbidity reduction shown by ACH was at native pH8.4 – 9.2 of CSG waters.

- l) For effective DOC removal, pH adjustment was required to pH6-6.4. However, lowering the native pH of CSG water has shown to be not practical as a large amount of acid is required.

The new knowledge created from the results discussed in the chapter 6 can be summarised as follow:

- m) Silica fouling profiles studied in deionised water showed that increasing silica concentrations in the recycled stream had little impact on flux decline until the majority of the membrane surface was covered by gel (amorphous silica). Silica gel deposited on the membrane surface was allowed water to filter through the membrane without an impact of flux.
- n) The results documented in this research show that NaCl at relatively high concentrations (8 – 60g/L) depressed silica solubility limits leading to silica fouling at 90 – 81 mg/L silica. However, no silica deposition or single silica bonding to the membrane surface was found on the membrane surface, illustrating that precipitated silica remained in the recycled stream.
- o) The maximum and stable residual silica concentration concepts were introduced to highlight potential theoretical silica solubility deviations in different water matrices and recorded pseudo – silica solubility limits. Residual silica concentrations can increase above the silica solubility limit, to form super-saturated solutions, especially for low salinity and high flux conditions where silica concentrations increase rapidly in accordance with the RO concentration factor. The kinetics of precipitation is slow due to the requirement for nucleation to occur and the relatively short time of the desalination experiments.
- p) The presence of minor (7 – 11mg/L) to moderate (27.7mg/L) concentrations of aluminium in CSG waters increased silica fouling and deposition as aluminium silicate on the membrane surface. The deposit formed on the membrane surface was much harder to dissolve compared to other silica deposits found in this research.
- q) Silica precipitation occurred at pH3 condition in both synthetic and natural CSG waters. Stable and maximum residual silica concentrations reached at pH3 were slightly lower than stable and maximum residual silica concentrations recorded

at pH9. Overall little effect of pH (between 3 and 9) was observed on silica fouling trends in both synthetic and CSG waters.

The practical implications of the new knowledge obtained here can be summarised as follows:

- i. The presence of moderate to high concentrations of silica in CSG waters can result in rapid rates of silica precipitation at thresholds limits as low as 85-90mg/L dissolved silica concentration (the current RO industry assumption is 100mg/L). Minor concentrations of aluminium adversely impact silica solubility and promote silica scaling rather than precipitation in the bulk water.
- ii. CSG water pre-treated with coagulants (such as ACH or aluminium sulphate) has slightly higher residual aluminium concentrations (20 – 32mg/L) in post-coagulation water quality compared to the initial aluminium concentrations (7 – 11mg/L in raw CSG waters). Residual aluminium presents in medium concentrations (20 – 45mg/L silica) in CSG waters increased scale formation on the membrane surface, and therefore residual aluminium concentrations need to be minimised in the RO pre-treatment stages.

#### 7.4 CSG water

It was found in this research that the combination of the five following conditions in a RO feed can potentially lead to significant silica deposition on the membrane surface. These five conditions frequently found in CSG water in Australia include:

- Silica precipitation is recorded at 84 – 94mg/L at 80% water recovery when initial silica concentration (RO feed) was 50 to 60mg/L
- High proportion of total silica that is dissolved silica (as  $\text{SiO}_4=$  60 - 80%)
- Native the pH9
- Medium to high sodium chloride concentrations (8 – 45g/L)
- Elevated residual aluminium concentration (post-coagulation water quality) (as  $\text{Al}^{13+}=27.7\text{mg/L}$ ).
- The research found there was no impact of residual aluminum on silica precipitation when dissolved residual aluminum concentrations were less than

11.7mg/L. At this condition, silica solubility was affected by high salinity rather than the presence of low concentrations of dissolved aluminum. The silica fouling trends in CSG waters were similar to synthetic waters. Depending on permeate recovery required (80 – 90 – 92%), however, it is advisable to reduce silica concentrations to < 10mg/L regardless of residual aluminum.

Understanding of practical silica solubility for specific water matrix is a key for prevention of silica fouling on RO membrane surface. Interactions between these silica species and cations present in elevated concentrations in super-saturation conditions on the membrane surface frequently lead to irreversible silica scale formation as demonstrated in Figures 4.17 and 4.18. Other important key considerations for silica scale deposition is the percentage of coupling points present on the membrane surface serving as a nucleation points for precipitation to occur. This research showed that the presence of elevated concentrations of aluminium (post-coagulation water quality) in synthetic and CSG waters leads to significant scale deposition on the membrane surface. Silica precipitation in super-saturated conditions, as shown in these results, did not always lead to full silica precipitation and deposition, but it depended on residual aluminium present.

In this research, silica coating characteristics have been considered. As this unique characteristic of silica to coat surfaces to extend the life-time of many materials by providing a hard, wear resistant surface in case of membrane works against us. At suitably high pH, if  $\text{Al}(\text{OH})_3$ ,  $\text{Ca}(\text{OH})_2$  and  $\text{Mg}(\text{OH})_2$  are present, these hydroxides readily participate in the copolymerisation resulting complex anhydrous silicate structures. The strong tendency of aluminium hydroxide to react with silica, even in the monomeric state, is shown by the fact that increasing aluminium concentration from 7.5mg/L to 27.7 mg/L led to a significant flux decline and silicate deposition on the membrane surface. At slightly elevated concentrations of aluminium, silica solubility was depressed leading to silica precipitation at 85 – 90 mg/L as shown in this study. In the absence of aluminium ions silica surrounded by sodium layers or super-saturated silica did not scale the membrane surface in the medium and high salinity synthetic waters as found in this research.

## 7.5 Significance

From the conclusions stated above, it is clear that the primary objective of silica fouling in CSG water in RO desalination was accomplished well. The silica fouling and scale deposition trends identified in the RO experimental investigation, in relationships between pH, silica concentration, and silica species present, were consistent with a conceptual silica polymerisation model using  $^{29}\text{Si}$  NMR data. Previously, silica solubility trends for RO desalination could not be explained using available silica precipitation data. The final result of this research is a silica precipitation model under the effect of sodium ions (Figure 4.17) and under the effect of aluminium ions (Figure 4.18) that accounts for the mechanisms of hydrolysis and condensation of silica species in the CP zone on the membrane surface. The model accounts for practical silica solubility arising on the membrane surface not only as a result of super-saturation conditions, but also due to the presence of sodium shown in Figure 4.17 and aluminium shown in Figure 4.18.

Based on the findings of this research, several recommendations can be made regarding engineering practice such as the design and RO desalination of CSG water. As discussed in chapter 6, the majority of CSG water in Australia requires desalination. Critical parameters of CSG water such as pH9.2, medium silica concentrations, aluminium and relatively high salinity lead to silica precipitation on the membrane surface, mostly because silica solubility is depressed by salinity and aluminium ions. Aluminium leads to scale formation on the membrane surface. All these critical parameters affect silica polymerisation – silica forms scale readily on the membrane surface as aluminumsilicate, which is hard to wash from the membrane surface. In light of these findings, it is clear that removal of silica in the pre-treatment stage is the most desirable option. Nevertheless, this study has demonstrated that coagulation pre-treatment is not always effective for silica and metal removals. Lowering of the native pH is required to achieve a good DOC removal and lowering and/or increasing pH is necessary to achieve an effective silica removal. In addition for coagulation to be effective during long term-operation of RO system, residual aluminium (post-coagulation water) must not be exceed 5 -7 mg/L in RO feed to avoid the effect of aluminium on silica precipitation on the RO membrane surface. Silica precipitation on

the membrane surface was not observed in low salinity synthetic water in the absence of aluminium.

As salinity and silica concentrations can vary in CSG waters as result of water table decrease within the aquifer, it is paramount for the industry to understand the impact of salinity and water composition on silica precipitation patterns. In fact, silica concentrations of the bore water increase continuously from the Earth's surface to a depth of 300 meters (Anderson 2013).

RO systems can be designed in four stages with an additional coagulation pre-treatment step between the third and fourth stages of RO to remove colloidal silica from the brine. Practically some RO plants, especially the plants combined with a brine treatment facility, will operate in this arrangement. However, remote operation is not suitable for four stage RO with coagulation between stages 3 and 4, as the industry frequently prefers to have non-manned operation facilities and to monitor the plant remotely. Furthermore, in recent time CSG resources have been found in Brazil, Canada, and China, so this research will be a valuable reference for good environmental management practice of CSG waters.

## 7.5 Recommendation for future research

The current research has led to in a vastly improved ability to predict the changes in the silica scale formation, which occurs as a result of depressed silica solubility. However, the effect of other factors on silica scale formation such as iron, cumulative effect of iron and aluminium, is also needs to be investigated to better predict depression of silica solubility and critical silica concentrations within the RO system. In addition, it would beneficial to use  $^{29}\text{Si}$  NMR method developed in this research to study the impact of other cations and anions on dissolved silica species. Recommendations for specific research tasks include:

- Performing silica solubility experiments using more complex synthetic waters with minor iron residual concentrations (7 – 30mg/L) to determine the effects on silica solubility and silica scale formation nature on the membrane surface and

specifically the effect of iron on silica – sodium – aluminium reactions. Work in this area would allow validation of the trends identified in the present research at a more specific and realistic set of conditions relevant to groundwater which has different forms of iron present.

- Confirm the new hypothesis of the substitution of sodium ions by aluminium ions from the sodium binding layer by combination of  $^{29}\text{Si}$  NMR and Al NMR spectroscopy and potentially other complimentary techniques to further develop an understanding of the chemical reaction mechanism between silica – sodium – aluminium and the reactivation energy involved to substitute sodium ions.
- Research into an aluminium sensing for monitoring of residual aluminium in RO feed is necessary to prevent elevated concentrations of aluminium after coagulation being fed to the RO membrane. Such sensing could help to prevent aluminosilicate scale formation.
- Research is necessary to improve membrane materials which support dissolution or inhibit scaling by amorphous silica from the membrane surface. The material which is able to reject deposition of silica or silicate from the membrane surface would discharge silica to the brine (reject) stream. It seems hydrolysis and condensation processes of dissolved silica species will remain key chemical reactions in research of this type of material. This could prevent aging of membrane material, reduce chemical consumption on RO plants, and simplify operation of the plant by reducing man-hours at the facilities particular at remote plants.
- The impact of DOC on silica scale formation in CSG water is worthy of future study.
- The method developed in the  $^{29}\text{Si}$  NMR study could be used to investigate effect of other common cations such as iron, calcium, magnesium, barium; strontium on the five thermodynamically stable silica species and any chemical shift that occurs as result of these impurities. The current method developed as part of this research work, however, provides a solid foundation from which to build.

Understanding the properties of CSG waters, potential variations of the water quality over the lifetime of the CSG development and selection of an effective coagulant is key

for effective pre-treatment and silica removal. Coagulation enables physical and chemical elements to be removed at an early stage of the water treatment process. Nevertheless, the introduction into the desalination sequence of pre-treatment by coagulation could create a major new waste stream. In its untreated form, this sludge is rarely suitable for discharge into the natural environment (relatively high concentrations of chemicals after the coagulation used). It is essential, therefore, that this waste stream be properly managed and the coagulation process optimised by minimising coagulant dose and minimising sludge volumes produced.

In this study, removal of total and dissolved silica from the CSG waters by coagulation in an attempt to prevent silica fouling in RO desalination process was investigated. The process frequently resulted in a dramatic reduction in the total number of particles and colloids present, including metals and silica. Yet, the simplicity of coagulation is compounded by incomplete knowledge about the hydrolysis reactions of Al(III) and Fe(III), the nature of colloids present in natural waters, silica species and the kinetics of competitive reactions that occur in complicated chemical systems. Selection of the correct coagulant to achieve the most effective silica removal remains challenging as effective silica removal is difficult to predict due to complex silica chemistry and its various possible silica forms.



## Reference

- Alexander, J. Vega, George W. Scherer, 1989, Study of structural evolution of silica gel using  $^1\text{H}$  and  $^{29}\text{Si}$  NMR, *Journal of Non-Crystalline Solids*, Volume 111, Issues 2–3, 1, Pages 153-166
- Alexander, G.B, W.M. Heston and R.K. Iler, 1954, The solubility of amorphous silica in water, *Journal of Physical Chemistry*, v. 58, 453-455
- Alexander, K.L., Owens, E., Patel, M., McGovern, L., 2003, In low fouling reverse osmosis membranes: evidence to the contrary on micro filtered secondary effluent, *American Water Works Association Membrane Technology Conference*, Atlanta, Georgia, pp34-45
- Allen, L. and Matijevic, 1971, Stability of colloidal silica: II. Effect of hydrolysable cations, *Journal of Colloidal Science*, volume 35, no. 1, 66-76
- Alvarez, R. and Sparks D. L., 1985, Polymerization of silicate anion in solutions at low concentrations, *Nature* 318, Pages 649-651
- American Water Works Association, 2001, *Reverse Osmosis and Nano-filtration*, American Water Works Association, viewed 20 June 2014
- Amirtharajah, A. and K.M. Mills, 1982, "Rapid-mix design for mechanisms of alum coagulation", *Journal of the American Water Works Association* 74(4): 210-216
- Amjad, Z., 1992, *Reverse Osmosis: Membrane Technology, Water Chemistry, and Industrial Applications*, Ed., Chapman & Hall, New York
- Applin, K. R., 1987, The diffusion of dissolved silica in dilute aqueous solution. *Geochim. Cosmochim. Acta* 51(9), Pages 2147-2151
- ASTM (American Society for Testing and Materials), 1989, *Standards Practice for Calculation and Adjustment of Silica ( $\text{SiO}_2$ ), Scaling for Reverse Osmosis*. ASTM Designation D 4993-89, ASTM, Philadelphia, viewed 23 January 2013.
- Anick, D., J, Ives, J., 2007, The silica hypothesis for homeopathy: physical chemistry, *Journal of Homeopathy*, 96, 189-195
- Baes C. F., Mesmer R. E., 1976, *The hydrolysis of cations*. Wiley-Interscience, New York, 1976, Page 489
- Bartman A. R, Lyster, W. E, Rallo, G. R, Christofides, P., Cohen, Y., 2010, Mineral scale monitoring for reverse osmosis desalination via real-time membrane surface image analysis, *Journal of Desalination*, 234, 40-41 pp
- Baldyga, J., Jasinka, K, Petelski, P., 2012, Precipitation of amorphous colloidal silica from aqueous solutions – aggregation problem, *Journal of Chemical engineering science*, 77, 207-216
- Baoxia, M., Elimelech, M., 2013, Silica scaling and scaling reversibility in forward osmosis, *Journal of Desalination*, 312, 75-81
- Baumann H., 1959, Polymerisation and Depolymerisation der Kieselsaure unter verschiedenen Bedingungen *Kolloid Zeitschrift* 162(1), Pages 28-35
- Behrman A., Gustafson, H., 1940, "Removal of silica from water", *Journal of Industrial Engineering Chemistry*, 32(4), pp468-472
- Bergna and Roberts 2006, *Colloidal Silica: Fundamentals and Applications*, CRC Press, 131-128 pp
- Bergna H., 1994, *The Colloid Chemistry of Silica*, American Chemical Society, Washington, DC
- Bernal J. D., Dasgupta D. R. Mackay A. L., 1959, The oxides and hydroxides of iron and their structural interrelationship, *Clay Min. Bull.* 4, Pages 15-30

- Bertsch P. M. & Parker, D. R., 1996, "Aqueous Polynuclear Aluminum Species: The Environmental Chemistry of Aluminum. CRC Press, Boca Raton, FL, pp. 117–168
- Bertsch P. M., 1987, "Conditions for Al<sub>13</sub> Polymer Formation in Partially Neutralized Aluminium Solutions:", *America Journal of Soil Science Society*, 51: 825-828
- Berz L., Noll, and Maquire, J., 1941, "Adsorption of Soluble Silica from Water", *Industrial and Engineering Chemistry*, 33, 6, pp 814-821
- Benefield, L. D., J. F. Judkins, and B. L. Weand, 1982, *Process CHEMistry for Water and Wastewater Treatment*, Prentice- Hall, Inc., New Jersey
- Bing-Ru Zhang Yu-Ning Chen, Feng-Ting Li, 2011, Inhibitory effects of poly(adipic acid/amine-terminated polymether D230/diethylenetriamine) on colloidal silica formation, *Colloids and Surfaces A: Physicichem. Eng Aspects* 385, 11-19
- Birchall, D., *Silicon-aluminium interactions and biology*, Keele University, Department of Chemistry, CRC Press
- Bohme G., Dietzel M., Heinrichs H., Heydemann A., Schlabach S., Usdowski E., 1999, Wechselwirkungen zwischen Losungen und Festrkorpem in offenen systemen und stromenden Medien. In: *Wechselwirkungen an geologischen Grennzflachen - SFB 468 Arbeits - und Ergebnisbericht*, Universitat Gottingen, 1999, Pages A4-1 - A4
- Bottero J. Y., 1980, "Study of partially neutralized aqueous aluminium chloride solutions: identification of aluminium species and relationship between the composition of the solutions and their efficiency as a coagulant", *Journal of Progress in Water Technology*. 12, 601–612
- Bouguerra, W., Ali, B., Hamrouni, B., Dhahbi, M., 2007, Equilibrium and kinetics studies of adsorption of silica onto activated alumina, *Journal of Desalination*, 206, 141-146
- Brady P. V., House W. A., 1996, Surface controlled dissolution and growth of minerals. In: *Physics and Chemistry of Mineral Surfaces* (eds.: Brady, P.V.) Chapter 4. CRC Press. Boca Raton New Your London Tokyo, Pages 225-305
- Brant J., Kwan, P., 2013, *State-of-the Science Review of Membrane Fouling: Organic, Inorganic and Biological*, Bureau of Reclamation, California Department of Water Resources
- Brauer G., 1982, *Handbuch der preparativen anargoanischen Chemie. Band 3*, Enke, Stuttgart
- Braun G, Hater, W, 2010, "Investigation of silica scaling on reverse osmosis membranes", *Journal of Desalination*, volume 250, 982-984
- Brevard P. Granger; 1981, "Handbook of High Resolution Multinuclear NMR" John Wiley & Sons, Chichester
- Bremere, I., Kennedy, M., Mhyio, S., Jaljuli, A., Witkamp, Schppers, J., 2000, Prevention of silica scale in membrane system: removal of monomeric and polymeric silica, *Journal of Desalination*, 132, 89-110
- Buhrs T and Bartlett, R. 1993, "The Role of the State: From: State vandalism" Towards a "Market-led" Environment", In *Environmental Policy in New Zealand*, Oxford University Press, Auckland. P90-112
- Busey R. H., Mesmer R. E., 1977, Ionization equilibria of silicic acid and polysilicate formation in aqueous sodium chloride solutions to 3000C. *Inorganic Chemistry* 16(10), Pages 2444-2450

- Carlson L., Schwertmann U., 1981, Natural ferrihydrites in surface deposits from Finland and their association with silica. *Geochim. Cosmochim. Acta* 45(3), Pages 421-429
- Cary L. W., De Jong B. H. W. S., Dibble W. E., 1982, A  $^{29}\text{Si}$  NMR study of silica species in dilute aqueous solution. *Geochim. Cosmochim. Acta* 46(7), Pages 1317-1320
- Cary L., de Jong B.H.W.S and Dibble, 1978, Walter, A  $^{29}\text{Si}$  NMR study of silica species in dilute aqueous solution
- Casey W. H., Westrich H. R., Banfield J. F., Ferruzzi G., Arnold G. W., 1993, Leaching and reconstruction at the surfaces of dissolving chain-silicate minerals, *Nature* 366, 1993, Pages 253-256
- Cha C., 1994, Controlling silica/silicate deposition using phosphonate combinations, U.S. Patent 5,300,231
- Chappex, T., Scrivener, K., 2012, The effect of aluminium in solution on the dissolved of amorphous silica and its relation to cementations systems, *Journal of American Ceramic Society*, 1-6
- Cheng H., Chen, S., Yang, S., 2009, “In-line coagulation/ultrafiltration for silica removal from brackish water as RO membrane pre-treatment”, *Journal of Separation and Purification Technology*, 70, 112 – 117
- Christopher T.G. Knight, Stephen D. Kinrade, 2001, Chapter 4 A primer on the aqueous chemistry of silicon, *Studies in Plant Science*, Volume 8, 2001, Pages 57-84
- Cob, S., Beaupin, C., Nederlof, M., Harmsen, D., Cornelissen, E., Zwijnenburg, Guner, G., Witkamp, 2012, Silica and silicate precipitation as limiting factors in high-recovery reverse osmosis operations, *Journal of Membrane Science*, 423-424, 1-10
- Cohen Y., Gabelish C., Williams M., Rahardianto A., Franklin J., 2007, High-recovery reverse osmosis desalination using intermediate chemical demineralization, *Journal of Membrane Science*, 301, 131-141
- Cornell R. M., Giovanoli R., 1987, The influence of silicate species on the morphology of goethite (a  $\text{FeOOH}$ ) grown from ferrihydrite ( $5\text{Fe}_2\text{O}_3 \cdot 9\text{H}_2\text{O}$ ), *Journal of Chemical Society, Chem. Commun.*, Pages 413-414
- Cornell R. M., Schwertmann U., 1996, *The iron oxides. Structure, properties, reactions, occurrence and uses*, VHC Verlagsgesellschaft mbH, Weinheim, 1996, Page 573
- Coronell B, Marinas, B. Watanabe, L, Cahill, D. Petrov, I., 2006, “Physico-chemical characterisation of NF/RO membrane active layer by Rutherford backscattering spectroscopy”, *Journal of Membrane Science* 282, 71-81
- Darton, E., Fazel, M., A Statistical review of 150 membrane autopsies. <http://www.derwentwatersystems.co.uk/chemical-treatments/paper-four.pdf> (accepted July 2011), viewed July 2014
- Davies S., Silica in streams and ground water. 1964, *American Journal of Science*, 1964, Pages 870-876
- Davis J.A., Kent D. B., 1990, Surface complexation modelling in aqueous geochemistry. In: *Mineralwater interface geochemistry* (eds.: Hochella, M.F., White, A.F.) Chapter 5. *Rev. Min*, 23, Pages 177-260
- De Jong B., Charles M. Schramm, Victor E. Parziale, 1984, Polymerization of silicate and aluminate tetrahedra in glasses, melts, and aqueous solutions—V. The polymeric structure of silica in albite and anorthite composition glass and the

- devitrification of amorphous anorthite, *Geochimica et Cosmochimica Acta*, Volume 48, Issue 12, Pages 2619-2629
- Decker A.D., Klusman, R., Horner, D.M., 1987, Geochemical techniques applied to the identification and disposal of connate coal water. *Proceedings – International Coalbed Methane Symposium*, 1987:229-242
- Demadis K., K. Pachis, A. Ketsetzi, A. Stathoulopoulou, 2009, Bio inspired control of colloidal silica in vitro by dual polymeric assemblies of zwitterionic phosphomethylated chitosan and polycations or polyanions, *Advanced Colloid Interface Science* 151, 3
- Demadis K., Neofotistou, N., 2007, Synergistic effects of combinations of cationic polyaminoamide dendrimers/anionic polyelectrolytes on amorphous silica formation: a bioinspired approach, *Chem. Mater.* 19, 581
- Demadis K., Stathoulopoulou, A., 2005, Novel, multifunctional, environmentally friendly additives for effective control of inorganic foulants in industrial water and process applications, *Mater. Performance* 45, 40
- Demadis K., Stathoulopoulou, A., 2006, Solubility enhancement of silicate with polyamine/polyammonium cationic macromolecules: relevance to silica-laden process waters, *Ind. Eng. Chem. Res.* 45
- Dempsey B., 2006, Chapter 2: Coagulation characteristics and reactions, *Journal of Interface Science in Drinking Water Treatment*, volume 34
- Den W., Wang, C., 2008, Removal silica from brackish water by electrocoagulation pre-treatment to prevent fouling of reverse osmosis membranes, *Journal of Separation Purification Technology*, 59, 318-325
- Dennis F. Evans, Jonathan Parr, Chih Y. Wong, 1992, Nuclear magnetic resonance studies of silicon (IV) complexes in aqueous solution—II. Tris-tropolonato and tris-3-hydroxypyridin-4-onato complexes, *Polyhedron*, Volume 11, Issue 5, Pages 567-572
- Depasse J., 1997, Coagulation of Colloidal Silica by Alkaline Cations: surface Dehydration or Interparticle bridging? *Journal of Colloidal and Interface Science*, 541, vol 194
- Depasse, J., Watillion, A., 1970, The stability of amorphous colloidal silica, *Journal of colloid interface science*, 33, 430-438
- Dietzel M., 1993, Depolymerisation von hochpolymerer kieselsaure in waBriger Losung. Dissertation, Universitat Gottingen, Germany, Page 93
- Dietzel M., 1998, Geloste polymere und monomere Kieselsauren und die Wechselwirkung mit Gibbsit und Fe-O-OH-Festphasen. *Habilitations - Schrift*, , Universitat Gottingen, Germany, Page 93
- Dietzel M., 2000, Dissolution of silicates and the stability of polysilicic acid. *Geochim. Cosmochim. Acta* 64(19), Pages 3275-3281
- Dietzel, M., Bohme G., 1997, Adsorption und Stabilitat von polymerer Kieselsaure, *Chem. Erde* 57, Pages 189-203
- Dietzel, M., Usdowski E., 1995, Depolymerization of soluble silicae in dilute aqueous solutions. *Colloid Polymeric Science.* 273, Pages 590-597
- Dietzel, M.B., 2002, Interaction of monosilicic and polysilicic acids with mineral surfaces: *Water-Rock Interactions*, Springer, 6, 217-223 pp
- Dirk, L., Teagarden, Stanley, L. and White, J., 1981, Conversion of aluminium chlorohydrate to aluminium hydroxide, Presented at the SCC Annual Scientific Meeting, New York, NY, Dec. 11-12

- Dove, P. M., Rimstidt J. D., 1994, Silica-Water Interactions. In: Silica (eds.: Heaney P.J., Prewitt C. T., Gibbs G.V.) Chapter 8. Rev. Min. 29, Pages 259-308
- Drever, J., 1988, The geochemistry of natural waters, Prentice-Hall, Englewood, NY
- Duan, J., Wang, J., 2001, Coagulation of humic acid by aluminium sulphate in saline water conditions, *Desalination* 150, 1 – 14
- Dzombak, D. A., Morel F. M. M., 1993, Surface complexation modeling. Hydrous ferric oxide, Wiley-Interscience, New York, Page 393
- Eckenfelder, WW, 2000, Industrial Water Pollution Control, 3rd edition, McGraw Hill, London
- Edwards, J. K. and Van Benschoten, J. E. 1990, Aluminium coagulation of natural organic matter. In: in Hahn, H. H. & Klute, R. (eds) Chemical Water and Wastewater Treatment. Springer-Verlag, New York, pp. 341–359
- Eikenberg, J., 1990, On the problem of silica solubility at high pH. Nationale Genossenschaft für die Lagerung radioaktiver Abfälle, Baden (Switzerland). Technical Report 90-36, page 54
- El-Manharawy, S., Hafez, A., 2000, Technical management of RO system, Nuclear Geochemistry department, Nuclear Materials Corporation, Cairo, Egypt, *Desalination* 131, 173-188
- El-Manharawy, S., Hafez, A., 2002, Study of seawater alkalization as a promising RO pre-treatment method, *Journal of Desalination*, 153, 109-120
- El-Manharawy, S., Hafez, A., 2001, Water types and guidelines for RO system design, *Journal of Desalination*, 139, 97-113
- El-Manharawy, S., Hafez, A., 2001, Dehydration model for RO-membrane fouling: a preliminary approach, *Journal of Desalination*, 153, 95-107
- Elimelech, M., Bhattacharjee, S., 1998, A novel approach for modelling concentration polarization in crossflow membrane filtration based on the equivalence of osmotic pressure model and filtration theory, *Journal of Membrane Science*, 145, 223-241
- Elimelech, M., 2005, Chemical cleaning of organic-fouled reverse osmosis membranes, US Bureau of Reclamation: Denver, CO, p72
- Exley, J., D., and Birchall, 1993, A mechanism of hydroxyaluminosilicate formation, *Polyhedron* 12, 1007-1017
- Fattahpour, I., Dedeh, Sjöberg, S., Lars-Olof Öhman, 1993, Equilibrium and structural studies of silicon (IV) and aluminium (III) in aqueous solutions. 31. Aqueous complexation between silicic acid and the catecholamines dopamine and L-DOPA, *Journal of Inorganic Biochemistry*, Volume 50, Issue 2, 1, Pages 119-132
- Fleming B.A., 1986, Kinetics of reaction between silicic acid and amorphous silica surfaces in NaCl solutions, *Journal of Colloidal and Interface Science*, v. 110, 40-64
- Freeman, S., Majerle, R., 1995, Silica fouling revisited, *Journal of Desalination*, 103, 113-115
- Fourier R. 1988, The solubility silica in hydrothermal solutions: practical applications, US Geological Survey, Mento Park, California, December 1988
- Fuchtbauer H., 1988, Sediment - Petrologie Teil II. Sedimente und Sedimentgesteine, Schweizerbart sche Verlagsbuchhandlung, Stuttgart, Page 1141
- Gabelich C, Chen, W, Bradley Y, Coffey, M, Suffet, M, 2005, The role of dissolved aluminium in silica chemistry for membrane processes, *Journal of Desalination* 180, 307 – 319

- Gabelich, C., Yun, T., Coffey, B., Suffet, I., 2002, Effect of aluminium sulphate and ferric chloride coagulant residuals on polyamide membrane performance, *Journal of Desalination*, 150, 15-30
- Gao B., Yue, Q., Wang, B., Chu, Y., 2003, "Poly-aluminum-silicate-chlorite (PASiC) – a new type of composite organic polymer coagulant", *Journal of Colloids and Surfaces*, 229, 121 – 127
- Gekas, V. and B. Hallström, 1990, *Journal of Desalination*, 77:195
- Gill J.G. 1993, Inhibition of silica-silicate deposit in industrial waters, *Colloids Surface A Physicochemical, Engineering Aspects* 74, 101-106 pp
- Gorrepati E., Wongthahan, P., Sasanka Raha and H. Scott Fogler, 2010, Silica Precipitation in Acidic Solutions: Mechanism, pH Effect, and Salt Effect, Department of Chemical Engineering, University of Michigan, American Chemical Society, *Langmuir*, 26 (13), pp 10467–10474
- Gray, S., Ritchie, C., Tran, T., Bolto, B., 2007, Effect of NOM characteristics and membrane type on microfiltration performance. *Water Resources*, 41, 3833-3841
- Grenthe, I., Fuger J., Konings R. J. M., Lemire R. J., Muller A. B., Nguyen-Trung Cregu C., Wanner H., 1992, *Chemical Thermodynamics of Uranium*, Chemical Thermodynamics 1. Nuclear Energy Agency, North-Holland Elsevier, Page 750
- Hamawand I., Yusaf, T., Hamawand, S., 2013, "Growing algae using water from coal seam gas industry and harvesting using an innovative technique: A review and a potential", *Journal of Fuel*, 23, 45 - 56
- Hamawand I., Yusaf, T., Hamawand, S., 2013, "Coal seam gas and associated water", A review paper, *Journal of Renewable and Sustainable Energy Reviews* 22 (2013) 550-560
- Hamrouni B., Dhahbi, M., 2001, "Analytical aspect of silica in saline waters – application to desalination of brackish waters", *Journal of Desalination* 136, 225-232
- Harris T., 1999, *Chemical structure of silicates in solutions*, John Wiley, New York, 630-760
- Hann W., Bardsley, J.H., Robertson, S.T., Shulman, J.E., 1997, Method for inhibiting the deposition of silica and silicate compounds in water systems, U.S. Patent 5,658,465
- Hann W.M., J.H. Bardsley, S.T. Robertson, J.E. Shulman, 1994, Silica scale inhibition, U.S. Patent 5,277,823
- Hansen H. C. B., Wechte T. P., Raulund-Rasmussen K., Borggaard O. K., 1994, Stability constants for silicate adsorbed to ferrihydrite. *Clay Min.* 29, Pages 341-350
- Healy T., 1994, *Stability of Aqueous Silica Sols*, School of Chemistry, The University of Melbourne, Australia
- Hem J. D., 1970, Study and interpretation of the chemical characteristics of natural waters. *Geol. Sur. Water-Supply Paper* 1473, Page 363
- Hiemstra T and Van Riemsdijk, W. H., and Bolt, G. H, 1989, *Journal of Colloidal Interface Science*, 133 (1)
- Hingston F. J., Psner A. M., Quirk J. P., 1972, Anion adsorption by goethite and gibbsite. 1. The role of the proton in determining adsorption envelopes, *Journal of Soil Science*, 23(2), Pages 177-192
- Hossain D., 1996, "Mechanism of coagulation of coloured water with aluminium sulphate", *Journal of Civil Engineering*, vol., CE 24, no 2

- Hundt T. R. and O'Melia, C. 1988, "Aluminium-Fulvic Acid Interactions: mechanisms and applications". *Journal of the American Water Works Association* 80(4): 176-186
- Hunt J., Kavner, A., Schauble, E., Snyder, D., Manning, C., 2011, "Polymerisation of aqueous silica on H<sub>2</sub>O-K<sub>2</sub>O solutions at 25-200 degree and 1 bar to 20 Kbar", (2011) *Journal of Chemical Geology*, 283, 161-170
- Iler R. K., 1976, *The chemistry of silica - Solubility, Polymerization, Colloid and Surface Properties, and Biochemistry*, Wiley-Interscience, New York, Page 866
- Jones B. F., Retting S. F., Eugster H. P., 1967, Silica in alkaline brines, *Science* 158, Pages 1310-1314
- Kallala M. Jullien, R., and cabane, B, 1992, *Journal of Physics*, II, France, 2, 7
- Katarachia S.D., 2005, Inorganic foulants in membrane systems: chemical control strategies and the contribution to "green chemistry", *Desalination* 179 (2005) 281
- Kenneth R. Applin, 1987, The diffusion of dissolved silica in dilute aqueous solution, *Geochimica et Cosmochimica Acta*, Volume 51, Issue 8, August 1987, Pages 2147-2151
- Kiselev, A. V., Yashin, Ya, 1969, *Gas-absorption chromatography*, Russia, Plenum Press, New York, 1969
- Kiselev, A. V., *Intermolecular interactions in adsorption and chromatography*, Vysshaya Shkola, Moskow, 1986
- Klohn Crippen Berger, 2012, *Healthy Head Waters, Coal Seams Gas Water Feasibility Study, Forecasting coal seam gas water production in Queensland's Surat and southern Bowen basins*, technical report, Klohn Crippen Berger, prepared for the Department of Natural Resources and Mines, pp23-98
- Knollmann S., 2001, *Korrosionsprodukte in Trinkwasserrohren: Geloste Kieselsaure und die Stabilitat von Goethit*. Bachlorarbeit, Universitat Gottingen, Page 44
- Kleinstreuer, C., and G. Belfort, 1984, *Mathematical Modelling of Fluid Flow and Solute Distribution in Pressure-Driven Membrane Processes*, in *Synthetic Membrane Processes* (ed G.Belfort) Academic Press, Orlando, Florida, pp98-123
- Koo, T., Lee, Y., Sheikholeslami, 2001, Silica fouling and cleaning of reverse osmosis membranes, *Journal of Desalination*, 139, 43-56
- Legrand A., 1999, *The surface properties of silicas*, John Wiley & Sons
- Lerman S.I., Scheerer, C.C., 1988, "The Chemical Behaviour of Silica," *ULTRAPURE WATER*, December 1988
- Liss P. S., Spencer C. P., 1970, Abiological processes in the removal of silicate from sea water. *Geochim. Cosmochim. Acta* 34(10), Pages 1073-1088
- Loucaides S. Koning, E. Cappellen, Ph, 2013, Effect of pressure on silica solubility of diatom frustules in the oceans: Results from long-term laboratory and field incubations, *Journal of Marine science*, volume 2
- Lovgren L., Sjoberg S., Schindler P. W., 1990, Acid/base reactions and Al(III) complexation at the surface of goethite. *Geochim. Cosmochim. Acta* 54(5), Pages 1301-1306
- Lumdsdom D. G., Evans L. G., 1994, Surface complexation model parameters for goethite (α-FeOOH). *J. Colloid Interface Sci.* 164, Pages 119-125
- Luo, F., Dong, B., Xie, J., Jiang, S., 2012, Scaling tendency of boiler feedwater without de-siliconization treatment, *Journal of Desalination*, 302, 50-54

- Lyster E., and Y. Cohen., 2007, Numerical study of concentration polarization in a rectangular reverse osmosis membrane channel: Permeate flux variation and hydrodynamic end effects, *Journal of Membrane Science*, 303, 140-153 pp
- Marshall C, and Fairbridge, W., 2010, *Encyclopaedia of Geochemistry*, Klumer Academic Publishers, London
- Marshall W.L., 1980, Amorphous silica solubilities – III. Activity coefficient relations and predictions of solubility behaviour in salt solutions, 0-350degree, *Journal of Geochimic, Cosmochim Acta*, v.44, 925-931
- Marshall W.L., 1980, Amorphous silica solubilities - I. Behavior in aqueous sodium nitrate solutions; 25-3000C, 0-6 motal, *Geochimica et Cosmochimica Acta*, Volume 44, Issue 7, Pages 907-913
- Marshall W.L., 1980, Amorphous silica solubilities - III. Activity coefficient relations and predictions of solubility behavior in salt solutions, 0 - 3500C, *Geochimica et Cosmochimica Acta*, Volume 44, Issue 7, Page 925-93
- Marshall W.L., Chen-Tung A. Chen, 1982, Amorphous silica solubilities IV. Behavior in pure water and aqueous sodium chloride, sodium sulfate, magnesium chloride, and magnesium sulfate solutions up to 3500C, *Geochimica et Cosmochimica Acta*, Volume 46, Issue 2, Pages 279-287
- Marshall W.L., Chen-Tung A. Chen, 1982, Amorphous silica solubilities V. Predictions of solubility behavior in aqueous mixed electrolyte solutions to 3000C, *Geochimica et Cosmochimica Acta*, Volume 46, Issue 2, Pages 289 - 291
- Marshall W.L., John M. Warakowski, 1980, Amorphous silica solubilities - II. Effect of aqueous salt solutions at 250C, *Geochimica et Cosmochimica Acta*, Volume 44, Issue 7, Pages 915-917, 919-924
- Marsmann H. C., Uhlig H. F.; 2001 <sup>29</sup>Si NMR Database System (PC based, see also <http://www.silicium-nmr.de>) reviewed on January 2013
- Marsmann H. C., 1999, <sup>29</sup>Si NMR, Reference Module in Chemistry, Molecular Sciences and Chemical Engineering, from *Encyclopaedia of Spectroscopy and Spectrometry* (Second Edition), Pages 2539-2549
- Masaaki M., Kazuhiko Y., 1997, Correlation between the average particle diameter of porous silicas and <sup>29</sup>Si NMR spectra, *Progress in Organic Coatings*, Volume 31, Issues 1–2, Pages 153-156
- McKeague J. A., Cline M. G., 1963, Silica in soil solutions. II. The adsorption of monosilicic acid by soil and by other substances. *Canadian Journal of Soil Science* 43, Pages 83-96
- Moran C., Vink, S., 2012, Centre for Water in the Minerals Industry, Sustainable Minerals Institute, The University of Queensland, Assessment of impacts of the proposed coal seams gas operations on surface and groundwater systems in the Murray-Darling Basin, pp 120-230
- Morel F. M. M., Hering J. G., 1993, Principles and applications of aquatic chemistry. Wiley-Interscience, New Yourk Toronto, Page 588
- Moroni S, 2004, Towards a reconstruction of the public interest criterion, SAGE Publications (London, Thousand Oaks, CA and New Delhi) volume 3(2):151-171
- Mott C. J. B., 1969, Sorption of Anions by Soils. S. C. I. Monograph 37, Pages 40-53
- Muller G., Sigg L., 1992, Adsorption of lead (II) on the goethite surface; voltametric evaluation of surface complexation parameters, *Journal of Colloid Interface Sci.* 148, Pages 517-532

- Multon R.F. 1951. Estimation of silica in water, *Journal of Applied Chemistry (London)* 1: (Supplement No 2)126
- Ndiaye P., Moulin, P., Domínguez, L., Millet, J., Charbit, F., 2004, Treatment of silica effluents: ultrafiltration or coagulation-decantation. *Journal of Hazardous Materials B116*, 75-81
- Nghiem L.D., Ren, T., et al., 2011, Treatment of coal seam gas produced water for beneficial use in Australia: a review of best practices. *Desalination and Water Treatment* 32 (1-3)
- Ning, R., 2002, Discussion of silica speciation, fouling, control and maximum reduction, *Desalination* 151, pp67-73
- Ning, R., Tarquin, A., Balliew, J., 2010, Seawater RO treatment of RO concentrate to extreme silica concentrations, *Journal of Desalination and Water treatment*, 22, 286-291
- Ning, R., Troyer, T., 2007, Colloidal fouling of RO membranes following Mf/UF in the reclamation of municipal wastewater. *Journal of Desalination*, 208, 232-237
- Norihiro N., Kozo H., Tetsuo A., 1989, Adsorption behaviour of a silane coupling agent onto a colloidal silica surface studied by <sup>29</sup>Si NMR spectroscopy, *Journal of Colloid and Interface Science*, Volume 129, Issue 1, April 1989, Pages 113-119
- Obihara C. H., Russell E. W., 1972, Specific adsorption of silicate and phosphate by soils, *J. Soil Sci.* 23, 1972, Pages 103-117
- Ontiveros G., 1988, Polymerisation and deposition of silica in aqueous solutions, *Journal of Geochemical, Cosmochim. Acta*, UMI Dissertation Information Service
- Pang F., Teng, Sh., Teng, T., Omar, A., 2009, Heavy metals removal by hydroxide precipitation and coagulation-flocculation methods from aqueous solutions, *Water Qual*, vol 44, No 2
- Parekh B.S., 1988, *Reverse Osmosis Technology: Applications for High-Purity-Water Production*, Edt., Marcel Dekker, New York, pp120-140
- Parfitt R. L., 1978, Anion adsorption by soils and soil materials. *Dep. Argon. Ser. Pap.* 1225
- Parfitt R. L., Van der Gaast S. J., Childs C. W., 1992, A structural model for natural siliceous ferrihydrite, *Clays and Clay Minerals* 40(6), 1992, Pages 675-681
- Parks G. A., 1990, Surface energy and adsorption at mineral interface: An introduction, *Mineral-water interface geochemistry* (eds.: Hochella, M. F., White, A. F.) Chapter 4. *Rev. Min.* 23, 1990, Pages 133-176
- Peairs D., 2001, *Silica Over-Saturation, Precipitation, Prevention and Remediation In Hot Water Systems*, Cal Water, Technical Director
- Penitsky D., 2003, *Coagulation 101*, the Conference 2003, Associated Engineering, Calgary, Alberta
- Pernitsky D., Edzwald, K., 2006, Selection of alum and polyaluminium coagulants: principles and applications. *Journal of Water Supply: Research and Technology – AQUA* 56.2
- Perry, C., Keeling-Tucker, T., 2000, Model studies of the precipitation of silica in the presence of aluminium; implication for biology and industry, *Journal of Inorganic Biochemistry* 78, 331-339
- Rautenbach R., 1989, *Membrane Processes*, Wiley, New York, 1989
- Reynolds J., 2007, Thermodynamic evaluation of a partial charge model assumption for the dissolved silica system, *Silicon Chemistry*, vol 3, issue 5, pp267-269

- Richard O., Wang-Hong Y., Kirkpatrick, R., Richard L Hervig, Alexandra Navrotsky, Ben Montez, 1987, High-resolution  $^{23}\text{Na}$ ,  $^{27}\text{Al}$  and  $^{29}\text{Si}$  NMR spectroscopy of framework Aluminosilicate glasses, *Geochimica et Cosmochimica Acta*, Volume 51, Issue 8, Pages 2199-2209
- Rimstidt J. D., Barnes H. L., 1980, The kinetics of silica-water reactions, *Geochim. Cosmochim. Acta* 44(11), Pages 1683-1699
- Robert O. Fournier, William L. Marshall, 1983, Calculation of amorphous solubilities at 250 to 3000C and apparent cation hydration numbers in aqueous salt solutions using the concept of effective density of water, *Geochimica et Cosmochimica Acta*, Volume 47, Issue 3, Pages 587-596
- Robin K. Harris, James Jones, Christopher T.G. Knight, David Pawson, 1980, Silicon- $^{29}\text{Si}$  NMR studies of aqueous silicate solutions: Part II. Isotopic enrichment, *Journal of Molecular Structure*, Volume 69, Pages 95-103
- Rosen M.R., and Institute of Geological & Nuclear Sciences Limited., 1999, New Zealand guidelines for the collection of groundwater samples for chemical and isotopic analysis. Institute of Geological and Nuclear Sciences, Lower Hutt, N.Z
- Rowe J. J., Fournier R. O., Morey G. W., 1973, Chemical analysis of thermal waters in Yellowstone National Park, Wyoming, 1960-1965., *Geological Survey. Bull.* 1303, Page 31
- Sancilo, P., Milne, N., Taylor, K., Mullet, M., Gray, S., 2014, Silica scale mitigation for high reverse osmosis of groundwater for a mining process, *Journal of Desalination*, 340, 49-58
- Saint-Michel F., F. Pignon, 2003, "Fractal behaviour and scaling law of hydrophobic silica in polyol" *Journal of Colloid and Interface Science* 267(2): 314-319
- Samuel L. Papendick, Kajda R. Downs, Khang D. Vo, Stephanie K. Hamilton, Grant K.W. Dawson, Suzanne D. Golding, Patrick C. Gilcrease, 2011, Biogenic methane potential for Surat Basin, Queensland coal seams, South Dakota School of Mines & Technology, Rapid City, United States
- Schecher W. D., McAvoy D. C., 1998, MINEQL+: A chemical equilibrium modelling system, Version 4.0 for Windows, User's manual. Environmental Research Software, Hallowell, Maine, Page 318
- Schwertmann U., Thalmann H., 1976, The influence of Fe(II), Si and pH on the formation of lepidocrocite and ferrihydrite during oxidation of aqueous  $\text{FeCl}_2$  solutions, *Clay Min.* 11, Pages 189-200
- Semiati R., Bramson, D., Hasson, D., 1996, International Membrane Science and Technology Conference, No 7, University NSW, Sydney, Australia, pp271-273
- Semiati, R., Sutskover, I., Hasson, D., 2003, Scaling of RO membranes from silica supersaturated solutions, *Journal of Desalination*, 157, 169-191
- Semiati, R., Sutskover, I., Hasson, D., 2001, Technique for evaluating scaling and its inhibition in RO desalinating, *Journal of Desalination*, 140, 181-193
- Smolin Y., 1967, Structure of water soluble silicates with complex cations, Institute of silicate chemistry of the USSR Academia of Science, Leningrad
- Seward T. M., 1975, Determination of the first ionization constant of silicic acid from quartz solubility in borate buffer solutions to 3500C, *Geochimical. Cosmochim. Acta* 38(11), Pages 1651-1664
- Sheikholeslami J. Bright, 2002, Silica and metal removal by pre-treatment to prevent fouling of reverse osmosis membranes, *Journal of Desalination* 143, 255-267

- Sheikholeslami R., Al-Mutaz, I., Ko, T., Young, A., 2001, "Pre-treatment and the effect of cations and anions on prevention of silica fouling", *Journal of Desalination* 143, 83-95
- Sheikholeslami R., Al-Mutaz, I., Tan, S., Tab, D., 2002, "Some aspects of silica polymerisation and fouling and its pre-treatment by sodium aluminate, lime, and soda ash", *Journal of Desalination*, 150, 85-92
- Siever R., 1972, Silicon-abundance in natural waters, 14-I, In: *Handbook of Geochemistry II-2* (ed.: Wedepohl, K.H.) Springer, Berlin Heidelberg New York
- Siler, J. L., 1987, "Reverse Osmosis Membranes, Concentration Polarization and Surface Fouling: Predictive Models and 33 Experimental Verification", PhD Dissertation, University of Kentucky.
- Sigg L., Stumm W., 1981, The interaction of anions and weak acids with the hydrous goethite (α-FeOOH) surface, *Colloids and Surfaces* 2, 1981, Pages 101-117
- Sigg L., Stumm W., 1994, *Aquatische Chemie: eine Einführung in die Chemie wässriger Lösungen und natürlicher Gewässer*. 3., Aufl. Zurich, Verl. Der Fachvereine, Stuttgart, Teubner
- Sjöberg S., Hagglund Y., Nordin A., Ingri N., 1983, Equilibrium and structural studies of silicon (IV) and aluminium (III) in aqueous solutions: V. Acidity constants of silicic acid and the ionic product of water in the medium range 0.05-2.0m Na(Cl) at 250C, *Mar. Chem.* 13, Pages 35-44
- Sjöberg S., Nordin A., Ingri N., 1981, Equilibrium and structural studies of silicon (IV) and aluminium(III) in aqueous solution. II. Formation constants for the monosilicate ions  $\text{SiO}(\text{OH})^{3-}$  and  $\text{SiO}_2(\text{OH})_2^{2-}$ . *Mar. Chem.* 10, Pages 521-532
- Sjöberg S., Ohman L. O., Ingri N., 1985, Equilibrium and structural studies of silicon (IV) and aluminium (III) in aqueous solution. II. Polysilicate formation in alkaline aqueous solution. A combined potentiometric and  $^{29}\text{Si}$  NMR study, *Acta Chemical Scand. A* 39, Pages 93-107
- Sjöberg S., 1996, Silica in aqueous environments, *Journal of Non-Crystalline Solids*, Volume 196, March 1996, Pages 51-57
- Sjöberg S., Agneta Nordin, Nils Ingri, 1981, Equilibrium and structural studies of silicon(IV) and aluminium(III) in aqueous solution. II. Formation constants for the monosilicate ions  $\text{SiO}(\text{OH})^{3-}$  and  $\text{SiO}_2(\text{OH})_2^{2-}$ . A precision study at 25°C in a simplified seawater medium, *Marine Chemistry*, Volume 10, Issue 6, December 1981, Pages 521-532
- Sjöberg S., Nils Ingri, Ann-Marie Nenner, Lars-Olof Öhman, 1985, Equilibrium and structural studies of silicon(IV) and aluminium(III) in aqueous solution. 12. A potentiometric and  $^{29}\text{Si}$ -NMR study of silicon tropolonates, *Journal of Inorganic Biochemistry*, Volume 24, Issue 4, Pages 267-277
- Standard Methods, 1975, *For the Examination of Water and Wastewater*, 14th Edition, 1975, APHA-AWWA-WPCF
- Steven S., Anderson, B., 2007, Coal petrology and coal seam gas contents of the Walloon Subgroup – Surat Basin, Queensland, Australia, *International Journal of Coal Geology* 70 (2007) 209-222
- Sjöberg S., 1996, Silica in aqueous environments, *Journal of Non-Crystal. Solids*. 196 (1996) 51
- Stumm W., 1992, *Chemistry of the solid-water interface*, Wiley-Interscience, New York, Page 428

- Stumm W., Morgan J. J., 1996, Aquatic chemistry - Chemical equilibria and rates in natural waters, 3rd ed. Wiley-Interscience New York, Page 1022
- Stumm W., and Morgan, J., 1962, "Chemical aspects of coagulation:" Journal of AWWA 54, p 971
- Suciu D., Miller, R., 1980, Removal of Silica from RAFT River Geothermal Water, US Department of Energy, Idaho Operation Office
- Sullivan J. J. and Singley, J.E, 1968, "Reactions of metal ions in aqueous solutions; hydrolysis of aluminium" Journal of AWWA, 60, p 1280-1287
- Taulis M., Milke, M., 2013, "Chemical variability of groundwater samples collected from a coal seam gas exploration well", Maramarua, New Zealand, Water Research 47(2013) 1021-1034
- Taulis M., Milke, M., 2012, Department of Engineering, University of Canterbury, Christchurch, New Zealand, Coal seams gas water from Maramarua, New Zealand: Characterisation and Comparison to US Analogues
- Teagarden D., Stanley, L., and White, J., 1981, Conversion of aluminium chlorohydrate to aluminium hydroxide, Presented at the SCC Annual Scientist Meeting, New York, NY, 11-12
- Thomas D., 1992, Silica recovery and control in Hawaiian geothermal fluids, US grant No. DE-FGO7-881D12741, Hawaii Institute of geophysics, school of Ocean and earth Science and Technology, University of Hawaii
- Thurman E.M. 1985, Organic Geochemistry of Natural Waters. Martinus Nijhoff/Dr. W. Junk Publishers, Dordrecht, The Netherlands
- Tognonvi, M. T., Massiot, D., Lecomte, A., Rossignol, S., Bonnet, J., 2010, Identification of solvated species present in concentrated and diluted sodium silicate solutions by combined <sup>29</sup>Si NMR and SAXS studies, Journal of Colloid and Interface Science, 352, 309-315
- Tognonvi, M. T., Soro, J., Rossignol, S., 2011, Physical-chemistry of alkaline silica interactions during consolidation. Part 1: Effect of cation size, Journal of non-crystalline solids, 358, 81-87
- Vail J.G. 1952. The Soluble Silicates, Their Properties and Uses. Reinhold Publishing Corp., New York, N.Y Vol, 1, pp 95-97, 100-161
- Van Voast W.A., 2003, Geochemical signature of formation waters associated with coalbed methane. AAPG Bulletin, 87(4): 667-676
- Hann W.M., Bardsley, J.H., Robertson, S.T. Shulman, J.E., 1994, Method for inhibiting scale formation and/or dispersing iron in reverse osmosis systems, U.S. Patent 5,358,640
- Wang X., Ozdemir, O., Hampton, M., 2013, The effect of zeolite treatment by acids on sodium adsorption ration of coal seams gas water. Water Research 46 (2012) 5247-5254
- Weisner M. R. and Klute, R., 1997. Properties and measurements of particulate contaminants in water. In Treatment process selection for particle removal, J.B. McEwen, Denver, AWWARF: 35-72
- Weres, O., Yee, A., Tsao, L., 1981, Kinetics of silica polymerisation. Journal of Colloidal interface science, 84, 379-402
- White D. E., Brannock W. W., Murate K. J., 1956, Silica in hot-spring waters, Geochim. Cosmochim. Acta 10(1), Pages 27-59
- Whitehouse F.W., 1955, The geology of the Queensland portion of the Great Artesian Basin: Appendix G in Artesian water supplies in Queensland. Department of the

- Co-ordinator General of Public Works, Queensland Parliamentary Papers, vol. A56
- Wijnen P.W.J.G., Beelen, T.P.M., J.W. de Haan, C.P.J. Rummens, L.J.M. van de Ven, R.A. van Santen, 1989, Silica gel dissolution in aqueous alkali metal hydroxides studied by  $^{29}\text{Si}$ -NMR, *Journal of Non-Crystalline Solids*, Volume 109, Issue 1, Pages 85-94
- Wijnen P.W.J.G., T.P.M. Beelen, J.W. De Haan, L.J.M. Van De Ven, R.A. Van Santen, 1990, The structure directing effect of cations in aqueous silicate solutions. A  $^{29}\text{Si}$ -NMR study, *Colloids and Surfaces*, Volume 45, Pages 255-268
- Williams L. A., Crerar D. A., 1985, Silica diagenesis, II. General mechanisms, *J. Sed. Pet.* 55(3), Pages 312-321
- Yuan W., Kocic A., Zydney A., Analysis of humic acid fouling during microfiltration using a pore blockage–cake filtration model, *Journal of Membrane Science*, 2001
- Yan M., Wang, D., Qu, J., Ni, J., Chow, Ch., 2008, enhanced coagulation for high alkalinity and micro-polluted water: The third way through coagulant optimisation. *Journal of Water Research*, 42, 2278 – 2286
- Yates D. E., 1975, The structure of the oxide/ aqueous electrolyte interface, Ph.D. Thesis University Melbourne. Australia
- Yokoyama T., Y. Takahashi, C. Yamanaka and T. Tarutani, 1989, “Effect of aluminium on the polymerisation of silicic acid in aqueous solutions and the deposition of silica”, *Journal Geothermics*, v.18, no. ½, 321-325
- Zhang, B., Xin, S., Chen, Y., Li, F., 2012, Synergetic effect of polycation and polyanion on silica polymerisation, *Journal of Colloidal and Interface Science*, 368, pp181-190
- Zhuravlev L. T., 1993, *Journal of Colloids Surface*, 74(1), 71
- Zhu, X., Elimelech, M. 1997, Colloidal fouling of reverse osmosis membranes: Measurements and fouling mechanisms. *Journal of Environmental Science and Technology*, 31, 3654-3662
- Zhu, A., Christofides, P., Cohen, Y., 2009, On RO membrane and energy costs and associated incentives for future enhancements of membrane permeability, *Journal of Desalination*, 344, 1-5

## Appendix A – CSG water quality typical parameters (Surat basin, Queensland, Australia)

Analyte	LOR	Units	Descriptive statistics							Calculated Concentrations Min
			No. Samples	No. Non Detects	No. Detects	Minimum	Maximum	Average	Standard Deviation	
<b>Alkalinity</b>										
Bicarbonate Alkalinity as CaCO3	1	mg/L	57	0	57	611	1640	1118.474	315.721	5194
Carbonate Alkalinity as CaCO3	1	mg/L	57	25	32	4	174	54.688	47.359	34
Hydroxide Alkalinity as CaCO3	1	mg/L	57	57	0	0	0	-	-	0
Total Alkalinity as CaCO3	1	mg/L	57	0	57	611	1690	1149.316	332.988	5194
										0
Bromide	0.02	mg/L	57	1	56	0.96	11.2	6.104	2.728	8
Chloride	1	mg/L	57	0	57	1220	4240	2226.316	1073.764	10370
Fluoride	0.1	mg/L	57	0	57	1.4	2.6	2.002	0.344	12
Silicon	0.05	mg/L	57	0	57	6.98	10.4	8.376	0.844	59
Sulfate as SO <sub>4</sub> <sup>2-</sup>	1	mg/L	57	34	23	1	2	1.304	0.470	9
Sulfide as S <sup>2-</sup>	0.1	mg/L	57	57	0	0	0	-	-	0
<b>Major Cations</b>										0
Calcium	1	mg/L	57	0	57	3	43	11.193	10.232	26
Magnesium	1	mg/L	57	0	57	2	14	5.509	4.548	17
Potassium	1	mg/L	57	0	57	4	12	7.368	2.193	34
Sodium	1	mg/L	57	0	57	1280	2870	1876.491	497.800	10880
<b>Major Ions</b>										0
Ionic Balance	0.01	%	57	0	57	0.03	4.74	2.315	1.285	0
Total Anions	0.01	meq/L	57	0	57	58.4	132	85.753	24.779	496
Total Cations	0.01	meq/L	57	0	57	56.2	128	82.846	22.532	478
<b>Metals (Dissolved)</b>										0
Aluminium	5	µg/L	53	41	12	5	50	14.833	12.074	43
Arsenic	0.2	µg/L	57	37	20	0.3	2	0.640	0.382	3
Barium	0.5	µg/L	57	0	57	870	4440	1936.333	1297.672	7395
Beryllium	0.1	µg/L	57	57	0	0	0	-	-	0

Analyte	LOR	Units	Descriptive statistics							Standard Deviation	Calculated Concentrations Min
			No. Samples	No. Non Detects	No. Detects	Minimum	Maximum	Average			
Boron	5	µg/L	53	0	53	219	590	363.000	95.630	1862	
Cadmium	0.05	µg/L	57	40	17	0.08	0.19	0.128	0.033	1	
Chromium	0.2	µg/L	57	45	12	1	6	3.500	1.883	9	
Cobalt	0.1	µg/L	57	54	3	0.2	0.2	0.200	0.000	2	
Copper	0.5	µg/L	57	25	32	0.6	4	1.872	1.023	5	
Ferric Iron	0.05	mg/L	57	41	16	0.05	0.67	0.146	0.149	0	
Ferrous Iron	0.05	mg/L	57	55	2	0.06	0.49	0.275	0.304	1	
Hexavalent Chromium	0.01	mg/L	57	57	0	0	0	-	-	0	
Lead	0.1	µg/L	57	51	6	0.1	0.5	0.300	0.141	1	
Manganese	0.5	µg/L	57	0	57	2	78.8	17.211	21.434	17	
Mercury	0.0001	mg/L	57	57	0	0	0	-	-	0	
Molybdenum	0.1	µg/L	53	25	28	0.1	10	2.289	3.150	1	
Nickel	0.5	µg/L	57	42	15	0.5	2	1.120	0.489	4	
Selenium	0.2	µg/L	53	37	16	0.2	1.3	0.488	0.369	2	
Strontium	1	µg/L	57	0	57	1450	9970	3871.404	3146.980	12325	
Trivalent Chromium	0.01	mg/L	57	57	0	0	0	-	-	0	
Vanadium	0.2	µg/L	57	16	41	0.4	20	6.854	5.879	3	
Zinc	1	µg/L	57	11	46	1	43	12.087	10.885	9	
<b>Metals (Total)</b>										0	
Aluminium	5	µg/L	57	1	56	7	7480	1597.625	1826.762	60	
Arsenic	0.2	µg/L	57	34	23	0.3	9	1.239	1.764	3	
Barium	0.5	µg/L	57	0	57	1020	4820	2101.053	1339.334	8670	
Beryllium	0.1	µg/L	57	57	0	0	0	-	-	0	
Boron	5	µg/L	57	0	57	220	600	373.895	103.139	1870	
Cadmium	0.05	µg/L	57	38	19	0.1	0.2	0.147	0.037	1	
Chromium	0.2	µg/L	57	7	50	0.3	156	5.854	21.779	3	
Cobalt	0.1	µg/L	57	32	25	0.1	13	2.112	2.882	1	
Copper	0.5	µg/L	57	3	54	0.5	67	6.972	10.956	4	
Lead	0.1	µg/L	57	9	48	0.1	16	3.496	4.161	1	
Manganese	0.5	µg/L	57	0	57	7	337	47.561	52.738	60	
Mercury	0.0001	mg/L	57	57	0	0	0	-	-	0	
Molybdenum	0.1	µg/L	57	39	18	0.2	16	1.383	3.670	2	

Analyte	LOR	Units	Descriptive statistics							Calculated Concentrations Min
			No. Samples	No. Non Detects	No. Detects	Minimum	Maximum	Average	Standard Deviation	
Nickel	0.5	µg/L	57	25	32	0.5	32	3.991	7.029	4
Selenium	0.2	µg/L	57	41	16	0.2	1.1	0.450	0.263	2
Strontium	1	µg/L	57	0	57	1660	10300	4057.544	3205.523	14110
Vanadium	0.2	µg/L	57	33	24	0.5	20	4.825	6.781	4
Zinc	1	µg/L	57	13	44	2	67	17.409	17.421	17
<b>Microbiological</b>										0
Coliforms	1	CFU/100mL	47	46	1	4	4	4.000	-	
Heterotrophic Plate Count (21°C)	1	CFU/mL	47	13	34	1	190	18.882	38.573	
Heterotrophic Plate Count (22°C/72hrs)	1	CFU/mL	7	1	6	10	30	25.000	8.367	
Heterotrophic Plate Count (36°C)	1	CFU/mL	47	14	33	2	240	28.788	54.330	
Heterotrophic Plate Count (37°C/48hrs)	1	CFU/mL	7	7	0	0	0	-	-	
Hydrocarbon Utilising Bacteria	1	CFU/mL	40	37	3	10	170	63.333	92.376	
Sulphate-reducing bacteria	2	MPN/100mL	40	1	39	4	4300	582.769	1206.055	
Total Coliforms (Colilert)	1	MPN/100mL	7	7	0	0	0	-	-	0
<b>Nutrients</b>										0
Ammonia as N	0.01	mg/L	57	0	57	0.71	1.7	1.084	0.243	6
Nitrate as N	0.01	mg/L	57	10	47	0.01	0.27	0.039	0.043	0
Nitrite + Nitrate as N	0.01	mg/L	57	10	47	0.01	0.27	0.039	0.043	0
Nitrite as N	0.01	mg/L	57	57	0	0	0	-	-	0
Reactive Phosphorus as P	0.01	mg/L	57	16	41	0.01	0.04	0.026	0.009	0
Total Kjeldahl Nitrogen as N	0.1	mg/L	57	0	57	0.8	1.8	1.305	0.253	7
Total Nitrogen as N	0.1	mg/L	57	0	57	0.8	1.8	1.316	0.266	7
Total Phosphorus as P	0.01	mg/L	57	3	54	0.02	0.36	0.087	0.075	0
<b>Organic Carbon</b>										0
Dissolved Organic Carbon	1	mg/L	57	4	53	2	40	11.868	7.447	0
Total Organic Carbon	1	mg/L	57	0	57	2	40	17.368	8.859	0
<b>Physico-Chemical</b>			0	0	0	0	0	-	-	0
Electrical Conductivity @ 25°C	1	µS/cm	57	0	57	6170	13200	8373.509	2375.867	51000
pH Value	0.01	pH Unit	57	0	57	8.04	8.77	8.320	0.176	9

Analyte	LOR	Units	Descriptive statistics							Calculated Concentrations Min
			No. Samples	No. Non Detects	No. Detects	Minimum	Maximum	Average	Standard Deviation	
Suspended Solids (SS)	5	mg/L	57	0	57	7	885	214.737	212.778	0
Total Dissolved Solids @ 180°C	5	mg/L	57	0	57	3530	7340	4985.439	1329.119	30005
Turbidity	0.1	NTU	57	0	57	4.2	550	106.149	138.717	0
<b>Polynuclear Aromatic Hydrocarbons</b>										0
Acenaphthene	1	µg/L	57	57	0	0	0	-	-	0
Acenaphthylene	1	µg/L	57	57	0	0	0	-	-	0
Anthracene	1	µg/L	57	57	0	0	0	-	-	0
Benz(a)anthracene	1	µg/L	57	57	0	0	0	-	-	0
Benzo(a)pyrene	0.5	µg/L	57	57	0	0	0	-	-	0
Benzo(b)fluoranthene	1	µg/L	57	57	0	0	0	-	-	0
Benzo(g,h,i)perylene	1	µg/L	57	57	0	0	0	-	-	0
Benzo(k)fluoranthene	1	µg/L	57	57	0	0	0	-	-	0
Chrysene	1	µg/L	57	57	0	0	0	-	-	0
Dibenzo(a,h)anthracene	1	µg/L	57	57	0	0	0	-	-	0
Fluoranthene	1	µg/L	57	57	0	0	0	-	-	0
Fluorene	1	µg/L	57	57	0	0	0	-	-	0
Indeno(1,2,3,cd)pyrene	1	µg/L	57	57	0	0	0	-	-	0
Naphthalene	1	µg/L	57	57	0	0	0	-	-	0
Phenanthrene	1	µg/L	57	57	0	0	0	-	-	0
Pyrene	1	µg/L	57	57	0	0	0	-	-	0
Sum of polycyclic aromatic hydrocarbons	0.5	µg/L	57	57	0	0	0	-	-	0
<b>Silica</b>										0
Reactive Silica	0.1	mg/L	57	0	57	14.3	20.2	17.016	1.599	122
Silica	0.1	mg/L	57	0	57	15	22.3	17.939	1.806	128
<b>Total Petroleum Hydrocarbons</b>										0
C10 - C14 Fraction	50	µg/L	57	57	0	0	0	-	-	0
C10 - C36 Fraction (sum)	50	µg/L	57	53	4	50	50	50.000	0.000	425
C15 - C28 Fraction	100	µg/L	57	57	0	0	0	-	-	0
C29 - C36 Fraction	50	µg/L	57	57	0	0	0	-	-	0

Analyte	LOR	Units	Descriptive statistics							Calculated Concentrations Min
			No. Samples	No. Non Detects	No. Detects	Minimum	Maximum	Average	Standard Deviation	
C6 - C9 Fraction	20	µg/L	57	57	0	0	0	-	-	0
<b>Total Recoverable Hydrocarbons</b>										0
>C10 - C16 Fraction	100	µg/L	57	57	0	0	0	-	-	0
>C10 - C40 Fraction (sum)	100	µg/L	57	52	5	100	100	100.000	0.000	850
>C16 - C34 Fraction	100	µg/L	57	56	1	100	100	100.000	-	850
>C34 - C40 Fraction	100	µg/L	57	57	0	0	0	-	-	0
C6 - C10 Fraction	20	µg/L	57	57	0	0	0	-	-	0